Thesis/
Reports
Yokelson,
R. J.

Residual Smoldering Combustion: The Effects of Moisture Content On Smoke

Final Report: RMRS-99508-RJVA

To:
USDA Forest Service
Rocky Mountain Research Station
Intermountain Fire Sciences Laboratory
Missoula, MT 59807

By:

Robert J. Yokelson
Associate Research Professor, Department of Chemistry, University of Montana

March 31, 2003

Residual Smoldering Combustion: The Effects of Moisture Content On Smoke

Final Report: RMRS-99508-RJVA

To:
USDA Forest Service
Rocky Mountain Research Station
Intermountain Fire Sciences Laboratory
Missoula, MT 59807

By:

Robert J. Yokelson
Associate Research Professor, Department of Chemistry, University of Montana

March 31, 2003

Executive Summary

Rationale for and scope of work. Biomass burning has a strong influence on atmospheric chemistry, but characterization of this influence is challenging because of the complex, rapidly changing, and difficult-to-measure composition of smoke. Fourier transform infrared (FTIR) spectroscopy is well-suited for continuous, low-interference, measurement of a broad range of reactive and stable gases. Thus, FTIR can contribute significantly to our knowledge of smoke composition. The major goals of this work were to test the accuracy of FTIR, use FTIR to investigate how emissions depend on different fuel types and the condition of those fuels, and how emissions change downwind from fires. In this report, we describe our research activities from January 7, 1999 to March 31, 2003 that were supported by **RMRS-99508-RJVA**. This work includes some of the most significant results obtained in biomass burning research to date. We start with an aside: the title is perhaps unfortunate. It was modified to a specific topic at the last minute by Dr. Darold Ward. However, the objectives were always broad and one of the earliest results was that fuel moisture does not necessarily have a strong effect on emissions.

Major results. Much previous research on how the condition of wildland fuels influences fire propagation identified fuel moisture as a key variable governing the extent and occurrence of flaming combustion (Albini, Anderson et al, etc). This was an important result for predicting the ease of fire suppression. In contrast, a major goal of this investigation was to develop an ability to predict total smoke production by residual smoldering combustion (RSC). We began with the hypothesis that fuel moisture would play a large role in determining the extent of RSC. However, early on, we found that fuel moisture mostly influences whether fuel continues to burn after a brief ignition source is removed, but fuel moisture has little effect on total smoke production once independent combustion is initiated. Since fuel moisture varies widely on typical field sites during the burning season, combustion can be initiated on a drier part of the site and RSC can then propagate largely independent of fuel moisture. Our exploratory work in the laboratory showed that fuel geometry (heat transfer) was the major influence on fuel consumption and smoke production. This was later confirmed in field observations by Forest Service scientists. Another hypothesis when we started this research was that smoke production from residual smoldering combustion (RSC) would follow an exponential decay. In fact, we found that smoke production from RSC in laboratory fires can follow an unlimited number of trajectories. This was also later confirmed in the field by Forest Service

scientists. For instance, an increase in windspeed caused accelerated duff consumption. These early, key findings made it clear to the PI and the Forest Service collaborators that: (1) Total smoke production by RSC depends in complex fashion on a number of interrelated environmental variables (fuel moisture, fuel geometry, bulk density, recent weather, etc.). (2) Developing models of smoke production requires a more comprehensive approach than was originally anticipated. To move the science forward, an international workshop was convened, which brought together the critical mass of scientists and support personnel required to perform the greatly-needed multivariate field study of RSC. Unfortunately, due in part to uncertainty in Forest Service research funding, the experiment was abandoned after the workshop.

On the other hand, our laboratory measurements, supplemented by field data, did provide the first temporal profiles in real-time of the emissions by RSC, the first RSC-average emission factors, and the first quantitative study of the difference between airborne and ground-based fire-emissions measurements. We found that RSC emissions can change dramatically over the course of RSC, which could lead to large errors if the emissions were measured by a few intermittent grab samples. Thus, only methods capable of sustained, nearly continuous real-time measurements are capable of characterizing overall emissions due to RSC. Most of the published data on fire emissions is from airborne studies. We investigated the likely error in airborne studies due to the fact that aircraft cannot sample RSC emissions because they are not entrained in a lofted plume. We found that proper inclusion of RSC emissions can change the fire-average emission factors by as much as a factor of six.

On a global scale, cooking fires account for almost one-third of biomass burning. As part of this work, we made (and reported) the first detailed measurements of the emissions from cooking with biofuels. A major surprise was that for most smoldering compounds the annual emissions from cooking fires greatly exceed those from savanna fires for a typical African country. In fact, even during the dry, savanna-fire season, cooking fires are the main source of most smoldering compounds from biomass burning.

As part of this RJVA, we have now reported the first broad overview (i.e. including reactive species) of the emissions from boreal, temperate and tropical-savanna fires, an impressive variety of fuel-types. In addition, we obtained external funding (from NSF) to make the first comprehensive measurements of tropical forest fire emissions. For the fuel types investigated to date, we found that previously ignored oxygenated organic compounds account for 70-80% of the organic emissions. This has a major impact on

ozone production in smoke plumes. This is an important result for the Forest Service because it greatly improves our ability to predict the ozone production from wild and prescribed fires. We also made the first time-resolved measurements ever of the post-emission destruction of primary smoke species and the formation of secondary products (including ozone). Our measurements agree well with new photochemical models for smoke that have been enhanced by addition of the oxygenated compounds we discovered (as mentioned above). We have made these field measurements in both Alaska and Africa.

We performed intensive, collaborative laboratory work with the Max Planck Institute, which provided a new type of trace gas measuring instrument for our joint work. This project resulted in: (1) The most comprehensive measurements to date of the emissions from fires in domestic fuels prone to RSC and African fuels. (2) The first detailed measurements ever of the emissions from burning Indonesian fuels (including peat, which burns by RSC). (3) The first intercomparison of FTIR, proton-transfer reaction mass spectrometry, and canister sampling followed by GC. These are the three leading trace gas measurement techniques. (4) The first application of a novel technique to test for sampling artifacts relevant to enclosed instruments in real smoke was applied to our airborne FTIR system. Overall the project with Max Planck essentially doubled our knowledge of the trace gas emissions from RSC and other fires and it also clarified the preferred instrumentation for characterizing various fire emissions.

Organization of this report. In Part 1 of this report, the entire set of the objectives and associated deliverables of **RMRS-99508-RJVA** is quoted verbatim from the agreement and amendments. Next, we summarize the progress to date in addressing each task. (Note that, as expected in a research environment, we were not successful on some tasks.) Throughout the task summaries, we provide cross-references to appended publications that fully describe how we studied the task and the results. Part 2 is a partial list of publications resulting from this work. It does not include approximately 5 papers that are in advanced stages of writing, but have not been submitted yet. We anticipate that these publications will be included in the progress reports and final report for 03-JV-11222049-046. Part 3 provides copies of six of the most relevant publications listed in Part 2. The six publications that are provided give full details on how some of the specific research objectives of this RJVA were addressed.

1a. Overview of the Research Objectives/Deliverables of RMRS-99508-RJVA.

The Objectives/Deliverables from the Original Agreement and Subsequent Amendments:

A. The overall objective of this agreement is to develop models for the residual smoldering combustion phase of fires describing the rate of decrease in smoke production over time (for periods of time ranging from hours to days). In addition through this research, the change in composition of smoke emissions will be characterized, thus making it possible to develop smoke management guidelines for residual smoldering combustion and the potential for ameliorating this problem.

B. Specific objectives are as follows:
   1. In the RMRS Combustion Laboratory:
      a. To characterize samples of selected important wildland fuels with respect to fuel moisture, resin content, and degree of decomposition.
      b. To burn samples of the fuel at several different fuel moistures and develop fuel consumption decay rate algorithms for a few different classes of fuel burned under a range of moisture content conditions.
      c. To complete the development of methods for quantifying the rate of release of carbon described above.
      d. To measure high-accuracy emission factors, in real time, throughout the fires described above for the initially selected "test fuel."
      e. To develop a more complete chemical characterization of the trace gas and particle emissions from fuels prone to RSC through a joint deployment/inter-comparison of FTIR and PTR-MS as provided by the Max Planck Institute. To analyze FTIR spectra and determine the emissions factors for trace gases emitted from fires burned in RSC-type fuels in the Fire Sciences Laboratory. To combine and compare this data with the results from the Max-Planck Institute PTR-MS measurements on the same fires. To prepare the combined dataset for publication.
   2. The field component will be:
      a. To assist in developing and testing a portable lightweight measurement system for quantifying the flux of CO and CO_2 from RSC.
      b. To assist in developing and testing a portable particulate matter sampling system for measuring the production of PM2.5 before and during RSC and assist in having the PM2.5 samples analyzed for cations, trace elements, and carbon content.

c. To use the FTIR open-path system for making comprehensive measurements of smoke composition on several sits before and during RSC for the purpose of verifying laboratory findings and the possibility of other compounds produced under field conditions.
d. To develop a probe for use with the FTIR that will be compatible with the University of Washington CV-580 Aircraft and will minimize production of artifacts. To test the aircraft sample inlet for passing efficiency for several important reactive species. Develop an improved probe if necessary. Determine method for in-flight calibration or performance verification.
e. To make high-quality emission factor measurements for an experimental fire in Oregon during fall 2001 and conduct research fires as available in spring 2002. These measurements will strongly complement simultaneous measurements of pre-fire environmental variables, fuel consumption by RSC, and smoke dispersion. To develop a rapid deployment open-path FTIR system (similar to that used in Africa) for use in measuring trace gases emitted by RSC during the collaborative research fire (Sept. – Oct. 2001) in the Blue Mountains in eastern Oregon. The system would be deployed during spring RSC burns in Montana if they become available. To analyze the spectra and calculate emission factors for the RSC portion of the fire. To help combine the emission factors with other data for publication.

3. Objectives for Southern Africa Fire Atmosphere Research Initiative (SAFARI 2000) that highly compliment the ongoing RSC study and include:
   a. To characterize oxygenated compounds and nitrogen compounds for a range of African savanna ecosystems and especially the RSC using both airborne and ground-based sampling methodology.
   b. To accomplish B.3.a. above for other sources including cooking fires and charcoal-making following SAFARI 2000 experiments.
   c. To measure biogenic emissions for a few selected vegetation types relative to the pyrogenic emissions released. IE explore fire-induced changes in vegetative emissions.

C. (From this point on added as part of amendment No. 2.)To investigate the importance of fuel moisture, geometry, and lignification in determining fuel emissions from fires and consumption of the fuels under spring and fall conditions. To plan and execute a series of fires and associated measurements of fuel characteristics, fuel consumption, and emissions in collaboration with scientists from the Missoula Fire Sciences Laboratory.

D. The Forest Service requests that the Principal Investigator attend the October 2002 Safari 2000 meeting in Charlottesville, VA to present data gathered as part of this RJVA and to plan future work and publications with collaborators at the meeting.

1b. Summary of the Progress on the Research Objectives/Deliverables of RMRS-99508-RJVA by Task.

A. The overall objective of this agreement is to develop models for the residual smoldering combustion phase of fires describing the rate of decrease in smoke production over time (for periods of time ranging from hours to days). In addition through this research, the change in composition of smoke emissions will be characterized, thus making it possible to develop smoke management guidelines for residual smoldering combustion and the potential for ameliorating this problem.

We note that we adopted a working definition of RSC as combustion that produces emissions that are not lofted by strong convection. This relates conveniently to the expected dispersion of the emissions and the smoke management aspects of this work. Under this definition, there is actually no such thing as an RSC "phase." RSC can occur on one part of a fire while the emissions from another part of the same fire are being entrained into a convection column. We did observe, and extensively measure, a gradual decrease in smoke production for laboratory fires burning small samples of duff or other fuels. These data are available from the author. However, we do not include these data in the report, as we are not convinced that they are highly relevant to real fires. For instance, in our simulation of a larger, more natural fuel complex that included a stump and surrounding duff, a spontaneous shift in fuel geometry due to natural settling occurred some 20 hours after ignition as can be seen in *publication 9*. This was accompanied by a sudden, large increase in combustion that nearly burned the FTIR. In later field-work in the southeastern US, our Forest Service collaborator (Dr. Darold Ward) confirmed non-exponential behavior on several occasions. Dr Ward observed that an increase in windspeed greatly accelerated duff consumption. He also observed that RSC consumption of logs was more extensive near the intersections of logs or when logs were close together, than along isolated sections of logs. In fact, the importance of fuel geometry was recognized in the "Burnout" model developed by Albini. The Burnout model predicts that flaming combustion persists longer near the intersection of logs. Our combined laboratory and field work seems to indicate that the relative importance of fuel geometry/fuel moisture is greater for RSC than for flaming. Thus, modeling fuel consumption as an exponential decay probably has some value, but we feel it is equally important to stress that actual smoke production from real fires may not decay exponentially. In fact, smoke production may not decrease! In retrospect, we probably should have modified the tasks of the agreement, but instead we modified the research activity in two ways. We planned an integrated field experiment of smoke production and we expended relatively more effort on some other objectives.

We were quite successful in measuring the change in emission factors over time for isolated fuel elements as shown in detail in *publication 9*. However, we stress that these temporal profiles are for isolated fuel elements and the real site-average, temporal progression may be different in the field where fresh fuel is available for a much longer time. Nevertheless, we expect that the emissions of those compounds observed near the end of the combustion of isolated elements (i.e. hydrocarbons, ammonia, etc…) could be relatively suppressed if real fires are terminated within 2-10 hours. We assumed that each fuel element in the field would go through the same progression as an isolated fuel

element in the lab. Thus, our fuel element average emission factors should be close to the site-average emission factors for that fuel-type. These are the first EF ever measured explicitly for RSC and we think they can be coupled with data on fuel consumption by RSC to confidently estimate trace-gas specific, site-average emissions due to RSC. In addition, we observed that "complete combustion" of duff left a large residual mass of ash and that the EFPM2.5 for duff were lower than average for forest fuels. This suggests that PM emissions from duff would be overestimated if the entire mass of duff above mineral soil was assumed to burn with a typical PM emission factor. *Publication 9* also describes a detailed procedure for combining our RSC EF with airborne measurements of EF in appropriate ecosystems to derive "real" fire average EF. We show the real EF can be as much as a factor of six higher than the airborne measurements indicate.

B.1.a. Characterize samples of selected important wildland fuels with respect to fuel moisture, resin content, and degree of decomposition.
B.1.b. Burn samples of the fuel at several different fuel moistures and develop fuel consumption decay rate algorithms for a few different classes of fuel burned under a range of moisture content conditions.
B.1.c. Complete the development of methods for quantifying the rate of release of carbon described above.

We measured the fuel moisture on a typical spring afternoon (two days after gentle rain) for a large variety of RSC-prone fuel components on a logged site near Seeley Lake, Montana. They varied as expected from very low (5-10%) for loosely-packed dead needles to very high (~200%) for the underside of rotting logs or the interior of stumps. (This data is not unique, but it is available from the author.) The main point is that there is no such thing as a single fuel moisture that characterizes a real site. This has considerable relevance as explained next. An early lab experiment showed that one end of a log could be soaked in water until it had an overall fuel moisture of 70%, which is well above the 20% level that some authors have claimed prevents combustion. This log was ignited on the drier end and it burned slowly, but completely. Thus, the oft-published statement that fires cannot burn above 20% fuel moisture is misleading. Another related experiment measured the total consumption of wooden blocks resulting from a standard, weak ignition pulse and any subsequent combustion. When the blocks were 1 cm apart, ~50% of the mass of the blocks was consumed by RSC after the ignition pulse, regardless of whether they were wet or dry. When similar blocks (wet or dry) were placed 7 cm apart, combustion ceased as soon as the ignition pulse was over. It was found that dry duff (~10% moisture) and dry rotten wood continued to burn after a small ignition pulse. However, wet duff and sound dry wood did not continue to burn after the same ignition pulse. The implication is that low duff fuel moisture and decomposition of wood promote the initiation of independent combustion. However, in the field, decomposed wood tended to have higher fuel moisture. In addition, independent combustion of wood required fuel geometry that promoted efficient heat transfer to fresh fuel. The above experiments are also described in *publication 9*.

In summary, it was not clear that a single fuel descriptor would be an effective predictor of fuel consumption. Rather, a variety of factors interact to control this with the most important variable likely being fuel geometry. This would be very difficult to

quantify for a real field site. With this in mind, we hosted a large international workshop to plan a detailed, multi-investigator field experiment at Lubrecht Forest in which a series of similar sites would be burned over the course of varying spring and fall conditions. The plan was to measure many of the important fuel variables identified in the lab for these fires. Unfortunately, perhaps due mostly to uncertainty in Forest Service research funding, our Forest Service partners eventually declined to commit to support of this large-scale project and it was abandoned. Appendix A includes the agenda of the experiment-planning workshop and a post-workshop report. The PI still retains maps of potential sites etc.., which are available upon request. Cancellation of the project essentially halted the PI's progress on tasks A, B1a, B1b, B1c, and C.

B.1.d. Measure high-accuracy emission factors, in real time, throughout the fires described above for the initially selected "test fuel."

This aspect of the work was very successful. Therefore, it was expanded to include most of the RSC-prone fuel types as described in detail in *publication 9*. The key findings are also summarized above.

B.1.e. Develop a more complete chemical characterization of the trace gas and particle emissions from fuels prone to RSC through a joint deployment/inter-comparison of FTIR and PTR-MS as provided by the Max Planck Institute. Analyze FTIR spectra and determine the emissions factors for trace gases emitted from fires burned in RSC-type fuels in the Fire Sciences Laboratory. Combine and compare this data with the results from the Max-Planck Institute PTR-MS measurements on the same fires. Prepare the combined dataset for publication.

This task was addressed quite successfully. *Publication 1* presents detailed results for PM2.5 and trace gases for 47 fires involving a large number of RSC-prone fuels. With the combined instrumentation and high concentrations encountered in the lab, we were able to measure almost 30 of the most abundant trace gas emissions and the EF for PM2.5, black carbon, organic carbon, Cl, S, and K for these fires. These data represent the first EF for Indonesian fires (including Indonesian peat) and the most comprehensive measurements of fire emissions ever made. We could not convince our German partners to continue measurements throughout the entire RSC period for some of the longer fires. Thus, the data from these fires were not representative of the fire average and they are not included in *publication 1*. However, we present these data in this report and a method for utilizing them. Table 1 (page 11) shows the EF obtained for spot measurements of RSC (along with the published peat measurements for comparison). Our suggested utilization of this data is as follows. One should use the RSC-average EF from *publication 9* for all the compounds in *publication 9* for each fuel type. The EF for compounds that were only measured in *publication 1* should be scaled by the most similar compound in *publication 9* to get improved RSC average EF for the new compound. For example, the acetol/methanol ratio for cottonwood logs in Table 1 is 16.45/12.09 or 1.36. Multiplication of the methanol EF for cottonwood logs in *publication 9* (10.80 g/kg) by 1.36 gives 14.7 g/kg, which we recommend as an estimate of the acetol EF for complete RSC of a cottonwood log. Analogously the benzene/ethylene ratio in Table 1 is 0.53,

which can be multiplied by the ethylene EF in *publication 9* (2.36 g/kg) to estimate a benzene EF for complete RSC of cottonwood logs of 1.25 g/kg. Note that for the cottonwood log, the adjusted EF are within about 10% of the values from the spot measurement. This is consistent with our observation in *publication 9* that logs produce a fairly stable mix of emissions and thus, for this fuel only, spot measurements should be close to RSC-average values. In contrast, the early-fire, spot EF for oxygenated compounds from burning duff samples in Table 1 are 2-5 times larger than the fire-integrated EF in *publication 9*.

The intercomparison between FTIR, can sampling, and PTR-MS is described in full detail in *publication 2*. In summary the agreement varied by compound from excellent to poor. The overall agreement for hydrocarbons between FTIR and GC/FID was excellent (within 1%). Good agreement between FTIR and PTR-MS was obtained for methanol and other alcohols but major disagreements occurred for acetone and propylene. The sum of acetic acid and glycolaldehyde measured by FTIR agreed well with the PTR-MS mass 61 signal. Likewise, the FTIR isoprene+furan agreed well with PTR-MS mass 69. PTR-MS agreed well with GC/MS for methylethylketone and methylvinylketone, but not for acetone. Because *publication 2* is appended in full, we refer the reader to this for full details. A major conclusion is that much more work is needed to enable reliable speciation of oxygenated organic compounds at sub-ppb levels. This will be a critical need if we are to progress in understanding the atmospheric chemistry of smoke in the future.

Table 1. Spot emission factors[a] for RSC-type fuels[b]. See text for explanation of use.

	Cottonwood (1)		Fir duff (1)		IndoPeat (1)		NWT duff (1)		Pine Fir duff (1)	
	OP-FTIR	PTR-MS	OP-FTIR	PTR-MS	OP-FTIR	PTR-MS	OP-FTIR	PTR-MS	OP-FTIR	PTR-MS
CO2	1423		1543		1703		1631		1371	
CO	124.5		184.7		210.3		282.7		237.2	
CH4	13.17		11.91		20.80		11.61		25.50	
C2H4	2.94		1.83		2.57		0.99		3.28	
C2H2	0.82		0.12		0.06				0.05	
C3H6	1.27	4.55	0.00	3.64	3.05	3.71	3.07	2.07	3.12	6.65
Benzene		1.56		0.65		3.19		0.57		1.66
Toluene		0.80		0.86		1.55		1.00		2.46
HFo	3.06	1.03	3.17	1.10	0.79	0.30	1.09	0.59	2.82	0.93
HAc	13.21		18.17		8.97		7.59		18.17	
GA	1.51		1.44		1.59				0.10	
mass 61 [c]		21.59		19.88		11.04		7.31		22.99
HCHO	2.46		0.39		1.40		0.78		1.99	
CH3CHO		2.61		4.30		3.27		1.43		5.41
MeOH	12.09	12.17	10.93	10.22	8.69	8.23	2.55	2.76	11.66	10.21
Phenol	7.57	6.99	3.46	1.04	3.62	3.37	3.26	1.03	6.26	4.76
Acetol	16.45	12.74	10.21	5.62	4.28	2.21	3.68	0.92	18.71	10.45
MEK		2.37		2.96		2.25		1.13		4.81
Acetone [d]	0.57	3.66	2.34	3.94	1.25	2.69	1.68	2.76	2.50	6.01
MVE	0.15		0.45		0.85		0.22		0.74	
Furan	0.69		0.80		1.91		0.81		1.15	
Isoprene	0.52		0.51		1.38		0.92		1.73	
mass 69 [e]		2.28		2.04		1.05		1.15		4.77
NH3	0.25		4.22		19.92		1.64		8.23	
HCN	0.35		2.19		8.11		3.82		2.64	
NO	0.46		0.71		1.00				0.38	
CH3CN		0.08		1.23		4.91		0.66		1.72
C3H5N [f]										
C3H3N [g]										

[a] g/kg dry fuel (ash free), CO and CO2 by TECO and LICOR

[b] number in parentheses following fuel type denotes maximum number of fires sampled

[c] HAc + GA

[d] PTR-MS acetone values are PTR mass59 minus FTIR MVE

[e] Furan + Isoprene

[f] Propanenitrile

[g] Propenenitrile

B.2.a. Assist in developing and testing a portable lightweight measurement system for quantifying the flux of CO and CO_2 from RSC.

The PI proposed measuring the rate of buildup of carbon-containing gases in a chamber placed over RSC, as a method of measuring the fuel consumption rate. The PI also recommended the use of a chamber-mixing fan, a chamber window (to visually check on mixing), a chamber volume of 1 cubic meter (to simplify calculations), and the use of a Licor and canister GC/FID for redundant carbon measurements. Finally, the PI suggested co-deploying the chamber in the field with time-resolved fuel consumption measurements and The Forest Service partners largely adopted these suggestions, but substituted inexpensive glass bottles for canisters and eventually did not opt for a window. The final system was tested with the PI's help during the stump fire simulation in the Fire Sciences lab. It was then used successfully throughout the US, especially in the Southeast. Ron Babbitt of the US Forest Service has the detailed results, which he has presented at numerous meetings.

B.2.b. Assist in developing and testing a portable particulate matter sampling system for measuring the production of PM2.5 before and during RSC and assist in having the PM2.5 samples analyzed from cations, trace elements, and carbon content.

To our knowledge, the Forest Service did not develop such a system and thus the PI did not assist in development. However, we did perform detailed characterization of PM2.5 collected during our laboratory fires as summarized above and discussed in detail in *publication 1*. We found that about 1/3 of the fuel chlorine was incorporated in the particles and the very low MCE fires (typical of RSC) produced very little black carbon.

B.2.c. Use the FTIR open-path system for making comprehensive measurements of smoke composition on several sites before and during RSC for the purpose of verifying laboratory findings and the possibility of other compounds produced under field conditions.

We measured the RSC emission factors for dead/downed logs in the deciduous miombo woodlands of Zambia. This fuel type is responsible for most of the RSC in the tropics where most biomass burning occurs and duff is rare. Logs are also an important RSC fuel in the US, especially in harvested or blow-down areas. We did not detect any "new" compounds that were not previously observed in the laboratory fires. In fact, the RSC field measurements for logs were in remarkable agreement with laboratory measurements of RSC for hardwood logs made before (*publication 9*) and after (*publication 1*) the field experiment. We compared the EFRSC for the miombo logs to the EF we measured in a plume above a miombo fire. In addition, Dr. Ward and collaborators had determined that about 10% of the fuel consumption on the miombo fire sampled from the air was RSC of logs. Consideration of the RSC emissions raised the fire-average EF for CH_4 by a factor of 2.5. Smaller, but significant changes in the fire-average EF for other compounds were also determined as discussed in *publication 9*.

B.2.d. Develop a probe for use with the FTIR that will be compatible with the University of Washington CV-580 Aircraft and will minimize production of artifacts. Test the aircraft sample inlet for passing efficiency for several important reactive species. Develop an improved probe if necessary. Determine method for in-flight calibration or performance verification.

We tested our inlet and Pyrex cell extensively for acidic (acetic acid), basic (NH_3), and neutral sticky compounds (i.e. methanol) in simple mixtures at room and reduced temperature. These compounds were then retested by a novel methodology in well-mixed smoke. The inlet coating (halocarbon wax) had excellent performance and can be highly recommended for sampling the above compounds. Small, temporary NH_3 losses were observed due to passivation of the Pyrex cell. A method to overcome this artifact with the current system was determined. External funding (NSF) was obtained to build a Teflon-lined cell that may eliminate the NH3 passivation losses. The results are described in detail in *publication 4*.

B.2.e. Make high-quality emission factor measurements for an experimental fire in Oregon during fall 2001 and conduct research fires as available in spring 2002. These measurements will strongly complement simultaneous measurements of pre-fire environmental variables, fuel consumption by RSC, and smoke dispersion. Develop a rapid deployment open-path FTIR system (similar to that used in Africa) for use in measuring trace gases emitted by RSC during the collaborative research fire (Sept. – Oct. 2001) in the Blue Mountains in eastern Oregon. The system would be deployed during spring RSC burns in Montana if they become available. To analyze the spectra and calculate emission factors for the RSC portion of the fire. To help combine the emission factors with other data for publication.

We did develop a more portable open-path FTIR system and deploy it on the Oregon fire. (Our African system relied on vehicle power, whereas the Oregon system required only a single automotive battery.) Unfortunately, it began to rain shortly after our Oregon deployment. In fact, we essentially were "pinned down" under a hastily-erected wedding canopy provided by a Forest Service collaborator. We have obtained external funding (from NSF) to build a much lighter, and more easily protected, open-path FTIR system. (NSF funding is 400K in all.) It may be possible to retrieve useful information from the collected spectra and if so, we anticipate including the results in a future report.

B.3. Objectives for Southern Africa Fire Atmosphere Research Initiative (SAFARI 2000) that highly compliment the ongoing RSC study and include:
B.3.a. Characterize oxygenated compounds and nitrogen compounds for a range of African savanna ecosystems and especially the RSC using both airborne and ground-based sampling methodology.

We measured the nascent emissions from 11 savanna fires located in a variety of savanna ecosystems: dambo (pure grassland), miombo (open hardwood forest), highveld (brush), lowveld (scrub forest), open coastal forest, etc. These were the first

comprehensive measurements of the emissions from African fires. Oxygenated compounds accounted for 70% of the non-methane organic compounds emitted by savanna fires. Ammonia and HCN emissions were much higher than previously claimed for African savanna fires. We also made the first measurements of photochemistry in post-emission smoke plumes in Africa, the first estimate of OH in a biomass burning plume, and the first measurements anywhere of cloud-scavenging of trace gases in smoke. The results are described in detail in *publications 5, 6, and 11*. Two more manuscripts on the cloud-processing observations are at advanced stages. We note that the cloud-processing observations have some intriguing smoke-management implications. Scheduling a prescribed fire just before an impending rainstorm could reduce smoke emissions in multiple ways: (1) Particles are removed by clouds and precipitation as previously observed by Dr. Ward. (2) Trace gases are removed at a much higher than expected rate, even by non-precipitating clouds, as we observed for the first time. (3) Rain could reduce the total duration of smoke production.

B.3.b. Accomplish B.3.a. above for other sources including cooking fires and charcoal-making following SAFARI 2000 experiments.

We made the first comprehensive measurements of the emissions from tropical biofuel use on wood and charcoal cooking fires and on a charcoal kiln as described in *publication 10*. About 70-80% of the NMOC were oxygenated compounds. HCN was not emitted by cooking fires or RSC (which involved wood combustion), but it was emitted by savanna fires. This suggests a way to separate the signals from woody and herbaceous fuel types involved in global biomass burning. The data in Table 1 of this report also suggest that acetonitrile is also emitted by grass and litter, but much less by wood. Our intercomparison (*publication 2*) found that acetonitrile is measured sensitively, accurately, and rapidly by PTR-MS (unlike HCN, which has too low a proton affinity). Thus acetonitrile may be a useful tracer for grass-fire smoke.

B.3.c. Measure biogenic emissions for a few selected vegetation types relative to the pyrogenic emissions released. I.E. explore fire-induced changes in vegetative emissions.

We built a Teflon chamber to place over our open-path FTIR cell so that we could measure the buildup of biogenic emissions. We brought the chamber with us to Zambia. Unfortunately, due to a misunderstanding between NASA and the Zambian military we were asked to leave Zambia before we could attempt this measurement. The chamber should be tested in the future in the US. There are literature reports that young vegetation emits more trace gases per unit mass than mature vegetation. One expects fires to replace mature vegetation with young vegetation and thus, fires could potentially impact trace gas emissions on a time-scale much longer than the fire itself. This remains an interesting and unexplored issue, which we hope we can address in the future.

C. Investigate the importance of fuel moisture, geometry, and lignification in determining fuel emissions from fires and consumption of the fuels under spring and fall conditions. To plan and execute a series of fires and associated

measurements of fuel characteristics, fuel consumption, and emissions in collaboration with scientists from the Missoula Fire Sciences Laboratory.

As discussed above, the PI organized a large international workshop in Missoula to plan a major, field experimental effort in this respect (See appendices A.1. and A.2.). The workshop was attended by participants from the US Forest Service, INPE (Brazilian Space Agency); U of Sao Paulo, Oregon State U; Montana State U; U of Washington; U of Montana Departments of Chemistry, Forestry, and Lubrecht Experimental Forest; the Nature Conservancy; BLM, and NOAA. The plan was to monitor/measure the many environmental variables that effect smoke production and the trade-offs of spring vs. fall prescribed burning in a holistic fashion. Thus, we needed to assemble/involve a critical mass of researchers. Due, we think, primarily to funding uncertainty, the project was cancelled by the Forest Service.

D. The Forest Service requests that the Principal Investigator attend the October 2002 Safari 2000 meeting in Charlottesville, VA to present data gathered as part of this RJVA and to plan future work and publications with collaborators at the meeting.

The PI attended the workshop and presented a talk entitled "*Recommended Trace Gas Emission Factors for African Savanna Fires & Post-Emission Transformations*," and a poster entitled "*Recommended Trace Gas Emission Factors for the Production and Use of Biofuels*." The PI was the discussion leader for the fire "breakout group." The PI presented a report on the discussion to a plenary session and a written report suitable for publication in a "synthesis" book to the meeting convener. All these documents are available upon request.

The PI engaged in a great deal of discussion about collaborative projects including:

1) With Chris Justice's MODIS group: we are doing a joint paper on the seasonal trends in savanna fire EF and the resulting effect on the seasonal profile of emissions. This paper is underway and includes 4 Fire Laboratory scientists.

2) The above is being used in a second paper to make an improved estimate of total, annual savanna fire emissions from southern Africa for 2000 and 2001. This is an issue of great concern to the modeling community.

3) With Tobi Landmann (CSIR South Africa): we are writing a paper to produce a highly accurate estimate of emissions from a specific, well-characterized sub-region of South Africa. This can be used as a benchmark for less-detailed approaches.

4) Joyce Penner's postdoc, Akinori Ito, requested and received a full set of our measurements of EF from around the globe, which he plans to incorporate in their global model.

5) Daniel Jacob requested/received a copy of our African biomass burning EF for "immediate use in their TRACE-P modeling."

6) We have set up a team including Dr. Ward to compare the CO/CO_2 ratio we measured by airborne sampling of Zambian fires to the CO/CO_2 ratio that can be derived from the simultaneous MODIS determination of flaming versus smoldering.

7) Sherri Mason (SUNY Fredonia chemistry department) is using our detailed, African smoke-plume evolution paper (*publication 7*) to test her smoke model.

8) Joerg Trentmann (MPI) is using the same paper to validate their independently developed smoke model.

9) Ryan Boger (UM graduate student): is developing a cloud model to interpret our unique observations of cloud-processed smoke.

10) Azadeh Tabazadeh, Hanwant Singh (NASA Ames), and the PI have developed a smaller-scale cloud model to be submitted to *Nature* soon.

11) In the course of measuring EF, we also measure regional trace gas vertical profiles in background air. The profiles are of great value to compare to trace gas vertical profiles measured or predicted by other platforms for example:

11a) With Wallace McMillan (U Maryland) we published a nice comparison of our in-situ CO profile with their column CO that was remotely-sensed from the ER2 on Sept 7, 2000. (*publication 8*)

11b) Similar to above, but for much different conditions on Sept 6. (Will be submitted soon).

12) With Peter Hobbs, an interpretation of regional trace gas profiles in the context of regional meteorology (*publication 3*) .

APPENDIX A.1. RSC WORKSHOP AGENDA

Date: THURSDAY MAY 24TH 2001
Location: MISSOULA, MT.
Venue: Rooms 326-327 at University of Montana University Center

Statement of Purpose: Appended at end of agenda

8:30 AM
Hao/Yokelson
Welcome/Intro

PART 1. Overview of Conceptual Framework for RSC

8:40 AM
Sam Sandberg
Overview of the current smoke management modeling system including fuel models, emissions production models (CONSUME/EPM), dispersion forecasting (NFSPUFF). Summary of the new, global, fuel classification scheme under development at PNW. What type and format of results are needed to support/improve these systems.

9:10 AM
Roger Ottmar
Overview of the type of fuel loading and fuel consumption measurements that are compatible with the new fuel classification scheme and recent field results in the Pacific NW. Recommendations for future research on: format of fuel measurements and the environmental variables that may be useful in predicting whether RSC will occur.

PART 2. Measurements of RSC Smoke and Sites for Continuing Field Research

9:40 AM
Dr. Joao Andrade de Carvalho Jr.:
"Field and laboratory experiments on smoldering combustion of tropical biomass in Amazonia."

10:00 - 10:15 AM
Break

10:15 AM
Sue Ferguson
CO and particulate measurements from several prolonged smoldering events around the US.

10:45 AM
Steve Baker
Summary of recent field measurements of the multiday "smoke production rate" for fuel elements (stumps, logs, duff, etc…) in the Northwest and SE.

11:00 AM
Isaac Bertschi
Summary of preliminary laboratory studies of the ignition probability for duff and rotten and sound logs, fuel geometry interaction with fuel consumption, and the burning rate for large diameter, sound or rotten fuels, and organic soils. Presentation of the first comprehensive quantification of the major trace gas and particulate emissions from RSC. Description of some significant temporal progressions in the trace gas and particle emission factors during RSC.

11:30 AM
Frank Maus
Brief description of the types of sites available at Lubrecht for paired plots burned in spring or fall. Recommendations considering **safety**, homogeneity, accessibility, and relevance to the nation-wide situation.

11:45 AM
Lunch

PART 3. Relevant "New" Models and Additional Perspectives.

1:00 PM
Fernando Costa:
"Simplified Models of Smoldering Logs"

1:15 PM
Jim Reardon
Description of an ignition probability model for organic soils and the practical interpretation of the model predictions for land managers. How to obtain the field fuel moisture measurements needed for model input. Thoughts on the potential for extending the model framework to other fuel types.

1:30 PM
Stu McKeen
Regional-continental impacts of summertime smoke. Brief, preliminary thoughts on the impacts of spring/fall smoke relative to summer and the treatment of dispersion of smoke emitted into the boundary layer by NOAA and ECMWF models.

1:40 PM
Dick Field
Time scale for, and description of, the major post-emission photochemical changes in the composition of smoke.

1:50 PM
Gary Achtemeier / John Stanturf / Dale Wade
Overview of problem in Southeastern US (where most of the US burning is done) and key contrasts and similarities to the situation in Northwestern US. Summary of proposed RSC research in the Southeastern US. Dispersion modeling in the nighttime boundary layer and the Southeastern US in general.

2:30 PM
Break

2:40 PM
Open Discussion led by Darold Ward focused on optimizing upcoming research
Option to break into smaller groups if needed.

4:00 PM
Adjournment. Evening, informal working/social/dinner gathering to follow. Details announced at meeting.

Background on the Purpose of the Workshop

The air quality impacts of recent wildfire events and other undesirable ecological effects have increased because of fuel buildup resulting partly from fire exclusion. The controlled burning of "commercially-worthless" logging slash is now often delayed due to air quality concerns, which also leads to a fuel buildup in wildlands. A practical method to restore or maintain fuel loading at ecologically-sound and safe levels for many landscapes is prescribed burning. A major challenge is to implement these burns without negative impacts on air quality. The usual approach is to burn so that the emissions are entrained in an intense convection column, lifted, and well-diluted before, potentially, advecting back to the ground and impacting public health. The occasional, undesired air quality impacts that do result from prescribed fire are often due to "residual smoldering combustion" (RSC). We loosely define RSC as that combustion (usually smoldering) that continues after flame-induced convection from a site has ceased. Concentrated emissions from RSC can drift into nearby communities causing multiple problems such as increased pollution and decreased visibility. RSC also simply increases total duration and amount of smoke production. In fact, on a global scale, this largely uncharacterized phenomenon may contribute a large fraction of the total tropospheric trace gas input.

We hope to learn more about the environmental factors that control whether RSC occurs and better characterize the emissions in an upcoming field experiment planned for Lubrecht Forest. The proposed design for the experiment is to burn a series of small plots within a homogeneous site under varying conditions in both spring and fall. Key environmental variables would be monitored and fuel consumption by RSC, if it occurs, would be quantified. The temporally-resolved composition and amount of smoke produced would also be determined. We hope that the experimental results will be of practical value to land managers and compatible with an emerging system of fuel classification and smoke management models. (Ultimately, if both the environmental variables that control extent of combustion and the transport of smoke can be monitored by satellite it could result in improved understanding of regional to global atmospheric chemistry.) We welcome presentations focused on optimizing the upcoming field campaign and we gratefully thank all the participants in advance for their energy and contributions.

APPENDIX A.2. Informal Report on Residual Smoldering Combustion Workshop

Overview:

On Thursday May 24th 30 researchers from around the US and Brazil gathered to discuss issues related to fuel consumption by residual smoldering combustion (RSC) during wildland fire and the resulting impacts on air quality. The venue was a workshop held at the University of Montana and organized by the Fire Chemistry Project of the Missoula Fire Laboratory. Institutions represented included the Missoula Fire Lab, UM Chemistry, UM Forestry, UM Lubrecht Forest, USFS PNW Research Station, USFS Southern Research Stations at Athens and Auburn, BLM Fire and Aviation Management, NOAA Aeronomy Lab, NASA Goddard, INPE (Brazilian Space Agency), and USGS. Twelve presentations, each followed by lively discussion, focused on ignition probability models, fuel loading and consumption measurements, emission factors for residual smoldering combustion, smoke production rates and dispersion, post emission chemistry in smoke, and future research. Among other things the results will be used to help plan an upcoming field experiment on RSC.

A brief summary of the speaker's comments and the ensuing/interspersed discussion follows.

Sam Sandberg. Described the CONSUME2.3 model, which is used to predict fuel consumption as a function of time from various important types of wildland sites based largely on experimental results from clear-cut slash. CONSUME2.3 underpredicts the measured emissions for residual smoldering combustion, which Sam defines operationally as independent smoldering not requiring an external flame heat input. Sam notes that this definition differs from the working definition adopted in the workshop statement of purpose, which is combustion continuing after flame-induced convection from the site has ceased. More precisely, the original workshop definition could be combustion at a point that continues after the "convection envelope" associated with flaming fronts no longer includes the point. In discussion multiple definitions are determined to be useful, but care should be taken to define how one is using the term. By Sam's definition up to 85% of the fuel consumption at Frostfire was by RSC even though it was nominally a "crown fire." Sam describes a new fuel classification scheme under development at PNW designed to improve estimates of fuel consumption globally. The model recognizes 6 different major fuel classes that create distinct combustion environments. They are canopy, shrubs, low vegetation, woody fuel, litter, and ground fuel. Each major category can be further subdivided and then also grouped by whether it contributes mainly to flaming or smoldering combustion. In addition sites can be assigned FCC numbers, which are like Cartesian coordinates: 0-9 based on packing ratio and surface area of fuels, 0-9 crowning potential based on the continuity of aerial fuels, and 0-9 effects potential based on the potential residence time of the heat source.

Roger Ottmar. Previous research suggested that the main source of error in emissions estimates for many compounds is the uncertainty in fuel consumption. Roger described efforts to reduce the uncertainty in fuel loading and fuel consumption by combustion type. A photo series has been developed to help US land managers accurately estimate

fuel loading. The volume for the Rockies (NFES 2629) is published, but an improved photo series for interior west P-pine sites is also being developed. A new version of CONSUME (3.0) will be available in 2003, which is designed for natural fuels rather than activity fuels. Their work on RSC had focused on the following fuel elements: rotten logs, snags, stumps, organic layers, and basil accumulation. Duff pins, heat sensitive paint, and wire-based and ocular estimates were used to quantify the fuel consumption every six hours on many sites. Also, as a qualitative probe, in one study the "number of smokes" as a function of days after ignition was noted. Duff moisture was strongly correlated with the amount of RSC. During discussion Colin Hardy suggested that surface wind speed should also effect duff consumption. It was emphasized that the fuel consumption measurements at Lubrecht should be compatible with the PNW reporting format. Roger offered to help train a UM grad student to make fuel measurements according to their scheme.

Fernando Costa. Experiments were carried out in the Amazon "crescent of destruction" in Brazil to simulate fires associated with shifting cultivation. Primary forest sites were slashed and the subsequent total fuel loading was measured. Most of the fuel (~84%) was large diameter woody material. About 50% of this fuel was consumed on average sites with higher consumption (~60%) at a site that had dried an extra year. Visual estimation was that most of the fuel was consumed in the presence of flaming combustion. Near the edges of the cleared, slashed areas non-typical results were obtained.

Sue Ferguson. Described experiments where CO monitors and nephelometers had been placed on the perimeters of several multi-day fires. A pattern of lofting during the day and downslope drainage at night was clearly documented. In the case of Frostfire this pattern continued for weeks despite 15-20 inches of rain falling on the site. On Frostfire balloon and LIDAR measurements showed that RSC also caused the development of elevated, thick smoke layers. The sheer scale of possible dispersion scenarios and rapid changes in wind speed, RH, etc. complicate data analysis in this type of experiment.

Steve Baker. The rate of carbon consumption as a function of time since ignition was measured from numerous fuel elements prone to RSC in Montana and the Southeast. A one-meter cubic, well-mixed chamber was placed over the fuel elements and the rate of increase of carbon-containing gases was measured. From this a fuel consumption rate can be accurately estimated. In this set of observations the duration of RSC (2-40 hours) was generally shorter and at lower combustion efficiency in the Southeast as compared to Montana.

Isaac Bertschi. In a series of laboratory experiments dry duff and dry rotten wood were more easily ignited than wet duff and dry sound wood. Once ignited fuel consumption seemed to be more strongly related to fuel geometry than fuel moisture. In the field rotten wood tended to be wetter than sound wood. In laboratory experiments only about one-half of the mass of material in dry duff above the mineral soil layer was consumed before natural extinction. In addition, for duff, the fire-integrated emission factors for PM2.5 were much lower than is typical for aboveground biomass and the fire-integrated emission factors for CO and ammonia were much higher. Therefore, it is likely that the

PM2.5 emissions from RSC of duff are much lower than would be inferred from multiplying an EFPM2.5 appropriate for aboveground biomass times the mass/area of the organic layer. Large diameter downed woody material had higher than "normal" emission factors for PM 2.5 and oxygenated organic compounds. These measurements were the first comprehensive measurements of the emissions from residual smoldering combustion and the emissions were related to the specific processes that produce them (distillation, low temperature pyrolysis, high temperature pyrolysis, and gasification).

Frank Maus. Described some of the opportunities for research sites at Lubrecht Experimental Forest. This includes 28,000 acres of varied, inventoried forest with summary descriptions by stand in a searchable database, fireline construction capabilities, a student fire crew, capacity for custom pretreatment of sites, lodging facilities on site, etc. Legal requirements for conducting research and cooperating with other uses (such as grazing and hunting) were also described.

Fernando Costa. Described a model to calculate the consumption rate for smoldering logs. The model is similar to earlier models developed for smoldering cigarettes with a major difference being that the log is not porous. The model calculates a velocity at which a smoldering (gasification) front preceded by a pyrolysis front will advance along a log. The results are in good agreement with several experimental laboratory measurements. In discussion, Fernando mentions that field observations of the burning rate of logs, the density of the char and wood, and the thickness of the char layer would be helpful for continued model development.

Jim Reardon. Described a two-variable model for probability of ignition of the organic layer in the Pocosin ecosystem of North Carolina. The model is a simplified version of an earlier model and requires as input fuel moisture and inorganic content, but does not require measurement of bulk density. Development of an improved handheld duff moisture meter in collaboration with Campbell Scientific is described. In discussion the possibility of fuel moisture measurements by both time domain reflectometry (TDR) and microwave-based instruments is raised. An aspect of the work at Lubrecht could be to compare these methods to gravimetric methods.

Stu McKeen. Presented evidence that an unusually large area burned by wildfires in Northern Canada in 1995 could have contributed 10-30 ppb of additional ozone in the Eastern US (out of 60-100 ppb total). The unusual meteorological transport conditions and the plume chemistry causing this were described. This reminds land management agencies of the impacts that can be associated even with well-dispersed smoke and is relevant to the tradeoffs between wild vs prescribed fire and burning in different seasons. In subsequent discussion Stu suggests that some measure of the larger scale dispersion from the experimental fires at Lubrecht would be desirable.

Dick Field. Described a comprehensive, state-of-the-art smoke chemistry model. In a typical simulated smoke plume, ozone destruction followed by significant ozone production occurs within a few hours. The initial NO_x/CO ratio and the presence of oxygenated organic compounds can strongly affect plume chemistry. In particular the

NO_x lifetime (which is less than one hour) and the distribution of nitrogen reservoir species are sensitive to initial conditions. Other scenarios being explored with the model include the transport of VOC-rich smoke to NOx-rich urban areas.

Gary Achtemeier. Described aspects of the RSC problem in the southeastern US. Originally > 90 million acres of longleaf pine savanna dominated the area with a 2-3 year fire return interval. Today some 6 million acres a year of pine/hardwood, second-growth forest are subject to prescribed fire, which is much less than optimum especially in the Piedmont. Much of the smoke produced is due to non-traditional fuels. The high humidity and flat terrain present problems not typical in the Western US. For example super-dense smoke/fog can form; possibly due to interactions between the CCN in smoke and the high water content of smoke driven from wet organic layers. This is problematic given the high density of roads in the southeast. In fact road cuts and vegetation may dominate the topography in some cases and, along with intense nighttime inversions, channel smoke into sensitive areas. Some 40% of US forest is located in the southeast and 70% is privately owned. This suggests that the results of our experiment at Lubrecht will be most relevant nationally if they are relevant to pine forests and if the methods and guidelines are accessible to "smallholders."

Don Despain. Found that a burned site was "missing" wood density values below a threshold value compared to an adjacent unburned site. Possibly the insulating properties of sound wood prevent large amounts from being consumed in isolated logs. Suggests that measurements of the distribution of bulk density on a site could help predict fuel consumption for large diameter woody debris.

Darold Ward/Discussion

Due to the spirited discussion accompanying each talk the anticipated, lengthy, post-presentations discussion was not possible. Instead, Bob Yokelson, Darold Ward, and Ron Babbitt made concluding remarks.

Bob read a list of field measurements taken from the presentations that seemed to be important for the Lubrecht study. Darold summarized the presentations and made some key points for future research. 1. Fuel classification should use Sam's new classification scheme. 2. Much more needs to be learned about the fate of smoke in the non-convective scenario. This may be 1/2 the smoke produced and we don't know anything, for instance, about it's interaction with and possible removal by vegetation. 3. A result of future research should be guidelines for land managers to avoid RSC. Ron Babbitt summarized the scope and schedule for implementing the upcoming field campaign at Lubrecht.

Partial List of Attendees and email addresses (not everyone signed the sheet, contact info for other participants is available by consulting the distribution list for this message):

Bob Yokelson	U of M Chemistry	byok@selway.umt.edu
Ron Wakimoto	U of M Forestry	wakimoto@forestry.umt.edu
Don Despain	USGS-BRD	don_despain@usgs.gov
Melanie Miller	BLM-Fire and Aviation	melaniemiller@fs.fed.us
Wei Min Hao	USFS-Fire Sciences Lab	whao@fs.fed.us

Frank Maus	U of M Lubrecht Forest	frank@forestry.umt.edu
Isaac Bertschi	U of M Chemistry	isaacpb@selway.umt.edu
Ted Christian	U of M Chemistry	theo@selway.umt.edu
Sherri Mason	U of M Chemistry	arrieta@selway.umt.edu
Dick Field	U of M Chemistry	ch_rjf@selway.umt.edu
Kereen Monteync	U of M Chemistry	kereen@selway.umt.edu
Charles McMahon	USFS- S. Res. Stat. Auburn	cmcmahon@fs.fed.us
Gary Achtemeier	USFS- S. Res. Stat. Athens	gachtemeier@fs.fed.us
Ron Babbitt	USFS-Fire Sciences Lab	rbabbitt@fs.fed.us
Janice Peterson	USFS-Region 6	jlpeterson@fs.fed.us
Colin Hardy	USFS-Fire Sciences Lab	chardy01@fs.fed.us
Darold Ward	Independent	pyrward@aol.com
John Stanturf	USFS- S. Res. Stat. Athens	jstanturf@fs.fed.us
Dale Wade	USFS- S. Res. Stat. Athens	rxfire@ix.netcom.com
Jim Reardon	USFS-Fire Sciences Lab	jreardon@fs.fed.us
Stephen Baker	USFS-Fire Sciences Lab	sbaker03@fs.fed.us
Ron Susott	USFS-Fire Sciences Lab	rsusott@fs.fed.us
Rick Shea	USFS-Fire Sciences Lab	rshea@fs.fed.us
Daniel Guthrie	USFS-Fire Sciences Lab	dguthrie@fs.fed.us
Dan Jimenez	USFS-Fire Sciences Lab	djimenez@fs.fed.us
Stu McKeen	NOAA Aeronomy Lab	stu@al.noaa.gov

2. Partial List of Publications supported by RMRS-99508-RJVA.

(Italicized number indicates that the publication is appended in part 3)

1. Christian, T.J., B. Kleiss, **R.J. Yokelson**, R. Holzinger, P.J. Crutzen, D.E. Ward, B.H. Saharjo, and W.M. Hao, Comprehensive laboratory measurements of biomass-burning emissions: I, The emissions from Indonesian, African, and other fuels, to be submitted to *J. Geophys. Res.* during April **2003**.

2. Christian, T.J., B. Kleiss, **R.J. Yokelson**, R. Holzinger, P.J. Crutzen, J. Williams, W.M. Hao, and T. Shirai. Comprehensive laboratory measurements of biomass-burning emissions: II, First intercomparison of open-path FTIR, PTR-MS, GC-MS/FID/ECD, to be submitted to *J. Geophys. Res.* during April **2003**.

3. Sinha, P., P.V. Hobbs, **R.J. Yokelson**, D.R. Blake, S. Gao, and T.W. Kirchstetter, Distributions of Trace Gases and Aerosols during the Dry Biomass Burning Season in Southern Africa, submitted to *J. Geophys. Res.*, **2003**.

4. **Yokelson, R.J.**, T.J. Christian, I.T. Bertschi, and W.M. Hao, Extractive sampling of ammonia, acetic acid, methanol, and other atmospheric trace gases, submitted to *J. Geophys. Res.* 2003JD003549, **2003**.

5. Sinha, P., P.V. Hobbs, **R.J. Yokelson**, T. J. Christian, T.W. Kirchstetter, and R. Bruintjes, Emissions of trace gases and particles from two ships in the southern Atlantic Ocean, in press *Atmospheric Environment.*, **2003**.

6. Sinha, P., P.V. Hobbs, **R.J. Yokelson**, I.T. Bertschi, D.R. Blake, I.J. Simpson, S. Gao, T.W. Kirchstetter, and T. Novakov, Emissions of trace gases and particles from savanna fires in southern Africa, *J. Geophys. Res.*, *108*, 8487, doi:10.1029/2002JD002325, **2003**.

7. Hobbs, P.V., P. Sinha, **R.J. Yokelson**, T.J. Christian, D.R. Blake, S. Gao, T.W. Kirchstetter, T. Novakov, and P. Pilewskie, Evolution of gases and particles from a savanna fire in South Africa, *J. Geophys. Res.*, *108*, 8485, doi:10.1029/2002JD002352, **2003**.

8. McMillan, W.W., M.L. McCourt, H.E. Revercomb, R.O. Knuteson, P. Antonelli, T.J. Christian, B. Doddridge, P.V. Hobbs, J. Lukovich, P. Novelli, S. Piketh, L. Sparling, D. Stein, R.J. Swap, and **R.J. Yokelson**, Tropospheric carbon monoxide measurements from the Scanning High-Resolution Interferometer Sounder on 7 September 2000 in southern Africa during SAFARI 2000, *J. Geophys. Res.*, *108*(D13), 8492, doi:10.1029/2002JD002335, **2003**.

9. Bertschi, I. T., **R. J. Yokelson**, J. G. Goode, D. E. Ward, R. E. Babbitt, R. A. Susott, and W. M. Hao, Trace gas and particle emissions from fires in large-diameter and belowground biomass fuels, *J. Geophys. Res.*, *108*, 8472, doi:10.1029/2002JD002100, **2003**.

10. Bertschi, I. T., **R. J. Yokelson**, D. E. Ward, T. J. Christian, and W. M. Hao, Trace gas emissions from the production and use of domestic biofuels in Zambia measured by

open-path Fourier transform infrared spectroscopy, *J. Geophys. Res.*, *108*, 8469, doi:10.1029/2002JD002158, **2003**.

11. **Yokelson, R. J.**, I. T. Bertschi, T. J. Christian, P. V. Hobbs, D. E. Ward, and W. M. Hao, Trace gas measurements in nascent, aged, and cloud-processed smoke from African savanna fires by airborne Fourier transform infrared spectroscopy (AFTIR), *J. Geophys. Res.*, *108*, 8478, doi:10.1029/2002JD002322, **2003**.

12. Swap, R.J., H.J. Annegarn, J.T. Suttles, J. Haywood, M.C. Helmlinger, C. Hely, P.V. Hobbs, B. N. Holben, J. Ji, M.D. King, T. Landmann, W. Maenhaut, L. Otter, B. Pak, S. J. Piketh, S. Platnick, J. Privette, D. Roy, A.M. Thompson, D. Ward, and **R. Yokelson**, The Southern African Regional Science Initiative (SAFARI 2000): Overview of the dry season field campaign, *South African J. Sci.*, *98*, 125-130, **2002**.

13. **R. J. Yokelson** and I. T. Bertschi, Vibrational Spectroscopy in the Study of Fires, in *Handbook of Vibrational Spectroscopy*, (Eds) P.Griffiths and J. Chalmers, pp. 2879-2886, John Wiley & Sons, Chichester, UK, **2002**.

14. S. A. Mason, R. J. Field, **R. J. Yokelson**, M. A. Kochivar, M. R. Tinsley, D. E. Ward, and W. M. Hao. Complex effects arising in smoke plume simulations due to inclusion of direct emissions of oxygenated organic species from biomass combustion. *J. Geophys. Res.*, *106*, 12527-12539, **2001**.

15. J. G. Goode, **R. J. Yokelson**, D. E. Ward, R. A. Susott, R. E. Babbitt, M. A. Davies, and W. M. Hao. Measurements of excess O_3, CO_2, CO, CH_4, C_2H_4, C_2H_2, HCN, NO, NH_3, HCOOH, CH_3COOH, HCHO, and CH_3OH in 1997 Alaskan biomass burning plumes by airborne Fourier transform infrared spectroscopy (AFTIR), *J. Geophys. Res.*, *105*, 22147-22166, **2000**.

16. **R. J. Yokelson**, J. G. Goode, D. E. Ward, R. A. Susott, R. E. Babbitt, D. D. Wade, I. Bertschi, D. W. T. Griffith, and W. M. Hao. Emissions of formaldehyde, acetic acid, methanol and other trace gases from biomass fires in North Carolina measured by airborne Fourier transform infrared spectroscopy (AFTIR), *J. Geophys. Res.*, *104*, 30109-30125, **1999**.

17. J. G. Goode, **R. J. Yokelson**, R. A. Susott, and D. E. Ward. Trace gas emissions from laboratory biomass fires measured by open-path Fourier transform infrared spectroscopy: Fires in grass and surface fuels, *J. Geophys. Res.*, *104*, 21237-21245, **1999**.

18. **R. J. Yokelson**, R. A. Susott, R. E. Babbitt, D. E. Ward, and W. M. Hao. Trace gas emissions from specific biomass fire-types. in *START Synthesis Workshop on Greenhouse Gas Emission, Aerosols and Land Use and Cover Change in Southeast Asia,* edited by T. Moya, pp. 60-68, SARCS, IGAC, LUCC, IGBP China-Taipei, Taipei, **1999**.

3. Full Text of Selected Publications Resulting From RMRS-99508-RJVA.

Publication 1

Comprehensive laboratory measurements of biomass-burning emissions: I, The emissions from Indonesian, African, and other fuels.

T.J. Christian[1], B. Kleiss[2], R.J. Yokelson[1,3], R. Holzinger[2], P.J. Crutzen[2], W.M. Hao[4], B.H. Saharjo[5], and D.E. Ward[4,6]

[1]University of Montana, Department of Chemistry, Missoula.

[2]Max-Planck-Institute for Chemistry, Atmospheric Chemistry Department, Mainz.

[3]Corresponding author.

[4]USDA Forest Service, Fire Sciences Laboratory, Missoula.

[5]Bogor Agricultural University, Faculty of Forestry, Bogor.

[6]Now at Enviropyronics, LLC, PO Box 968, White Salmon, WA.

Submitted for publication to Journal of Geophysical Research-Atmospheres (with companion papers): April, 2003.

Revised:

Accepted:

Abstract. The trace gas and particle emissions were measured from 47 laboratory fires burning 16 regionally-globally significant fuel types. Instrumentation included: open-path Fourier transform infrared spectroscopy; proton transfer reaction mass spectrometry; filter sampling with subsequent analysis of PM2.5, organic and elemental carbon, and other elements; and canister sampling with subsequent analysis by GC/FID, GC/ECD, and GC/MS. The emissions of 27 compounds are reported by fuel type. The results include the first detailed measurements of the emissions from Indonesian fuels. Carbon dioxide, CO, CH_4, NH_3, HCN, methanol, and acetic acid were the seven most abundant emissions (in order) from burning Indonesian peat. Hydroxyacetone was a major, previously unobserved emission from burning rice straw (21-34 g/kg). The emission factors for our simulated African fires are consistent with field data for African fires for compounds measured in both the lab and field. However, the higher concentrations and more extensive instrumentation in this work allowed quantification of at least 11 species not previously quantified for African field fires (in order of abundance): acetaldehyde, phenol, acetol (hydroxyacetone), glycolaldehyde, methylethylketone, acetone, methylvinylether, furan, acetonitrile, propenenitrile, and propanenitrile. Most of these new compounds are oxygenated organic compounds, which further reinforces the importance of these reactive compounds as initial emissions from global biomass burning. A few high combustion-efficiency fires emitted very high levels of elemental (black) carbon suggesting that biomass burning may produce more elemental carbon than previously estimated.

1. Introduction

Most of the earths ecosystems coevolved with fire since plants emerged from the sea. Humans later introduced the use of fire to improve grazing and crop production and for waste disposal, hunting, domestic cooking, heating, and lighting. These uses continue today: on the largest scale in the tropics where population is rapidly increasing. The gas and particle emissions from biomass burning strongly influence the physical and chemical properties of the atmosphere [*Crutzen and Andreae*, 1990] through: release/redistribution of carbon [*IPCC*, 1994], changes in oxidative capacity [*Lelieveld et al.*, 1993; *Mason et al.*, 2001], changes in atmospheric radiative transfer [*Hobbs et al.*, 1997; *Kaufman and Fraser*, 1997], and human health effects [*Sharkey*, 1997]. Uncertainty and natural variation, perhaps as large as a factor of 10, still exist in the amount of biomass burned and in the relative abundance of many important initial emissions [*Goode et al.*, 2000].

Most "real" fires occur unscheduled in remote areas of the tropics where a fraction of the smoke, at low concentrations, is occasionally sampled by aircraft that employ a limited number of instruments. African fires have been studied the most [*Yokelson et al.*, 2003]; some work has been done on fires in the neotropics [*Ferek et al.*, 1998]; and very little is known about SE Asian fires. To complement the field measurements, laboratory measurements have been conducted in which all the smoke from simulated fires can be captured and characterized at high concentrations [*Lobert et al.*, 1991; *Yokelson et al.*, 1996, 1997; 1998; *Holzinger et al.*, 1999; *Goode et al.*, 1999; *Bertschi et al.*, 2002a]. These laboratory studies are in good agreement with field measurements in nascent smoke [*Yokelson et al.*, 2003] and they provide details on compounds that are below detection limits in field studies. However, before this work, none of the laboratory studies had featured a comprehensive suite of instruments.

In this work, using an extensive suite of instrumentation, we quantified the emissions from 47 fires that burned 16 major fuel types from Africa, Indonesia, and elsewhere. The work was carried out in the USDA Forest Service, Fire Sciences Laboratory (FSL) in Missoula, MT. The trace gas measurements employed two recently developed methods: PTR-MS (proton transfer reaction mass spectrometry) and FTIR (Fourier transform infrared spectrometry) coupled with canister samples analyzed by GC/MS, GC/ECD, and GC/FID. PTR-MS quantifies many volatile molecules (at ppt levels) that have a proton affinity moderately above that of water, but it provides a single peak for each molecular mass making compound identification challenging under some conditions [*Williams et al.*, 2001]. Since all molecules have a unique IR signature, FTIR is well-suited for identification and quantification of most trace gases, but only at ppb levels [*Goode et al.*, 1999]. The canister techniques provide analysis at ppt levels, but they are subject to sampling and storage artifacts so they are best suited for trace gases that are not reactive or sticky. Such problematic gases account for ~70% of the organic emissions from fires and most of the organic constituents of the remote troposphere [*Yokelson et al.*, 1996, 2003; *Singh et al.*, 2001]. Open path FTIR (OP-FTIR) is not subject to sampling artifacts and the PTR-MS technique involves no sample storage. In summary, the combination of these five techniques provides the most comprehensive trace gas analysis applied to fires to date. In addition, since the smoke was well mixed, this study provided the first informal, but rigorous, intercomparison of PTR-MS, OP-FTIR, and canister sampling. The focus of this paper is presenting the emissions from Indonesian and African fuels. A detailed discussion of the intercomparison between the FTIR, the PTR-MS, and canister sampling appears in a companion paper [*Christian et al.*, this issue].

2. Experimental

2.1. Combustion Facility

The combustion facility at FSL, (described in more detail by *Christian et al.*, [this issue]) measures 12.5 m^2 x 22 m high. A 1.6 m diameter exhaust stack with a 3.6 m, inverted funnel opening extends from ~2 m above the floor to the ceiling. The room is pressurized with outside air that has been conditioned for temperature and humidity, and is then vented through the stack, completely entraining the emissions from fires burning beneath the funnel. A sampling platform surrounds the stack at 17 m elevation where all the temperature, pressure, trace gas, and particle measurement equipment for this experiment was deployed except background CO_2 (LICOR 6262). Temperature, flow, and mixing ratios were constant across the width of the stack (at the height of the sampling platform), as determined by moving probes for point measurements to different positions within the stack. The fuel bed was a (80 x 210 cm) tray covered by an inert heat shield, a layer of sand, and continuously-weighed by two electronic balances.

2.2. Fuels: selection, sampling, characterization, and fire simulations.

2.1.1. Selection, sampling, and simulations of African fuels. Key data for all the fuels burned in this study are presented in Table 1. Sixteen of the 47 fires burned grass and/or leaf/twig litter from humid savannas in Zambia (humid savannas include both pure grassland and "open" woodland and have 700-1400 mm/yr seasonal rainfall). There are ~7.7 million km^2 of humid, woodland savannas (sometimes termed tropical dry forests) in the world, of which 5.5 million are in the central African plateau. Half of these are miombo forests (~2.8 million km^2) [*IGBP*, 1997], which is the largest contiguous dry forest/woodland savanna in the world. Miombo tree species are resistant to low-medium intensity fire so that grass and leaf litter are the primary fuels [*Shea et al.*, 1996; *Hoffa et al.*, 1999]. The miombo understory burns about every two years [*Shea et al.*, 1996; *IGBP* 1997] and this likely accounts for more biomass burning than any other single ecosystem on Earth [*IGBP* 1997]. The miombo covers most of central Africa (~ 80% of Zambia is miombo [*Hoffa et al.*, 1999]) and fires in the miombo account for the great majority of sub-Sahelian fires [*Justice et al.*, 1996; *IGBP*, 1997]. Dambos are seasonally-flooded grasslands that are the major enclaves in the miombo. Dambos usually burn annually [*Hoffa et al.*, 1999] and this accounts for a large fraction of African fires.

During SAFARI 2000, several groups [*Sinha et al.*, 2003; *Yokelson et al.,* 2003] made the most extensive field measurements to date of the main emissions from African savanna fires. One goal of the work described here was to quantify additional compounds emitted by savanna fires (in the lab) by sampling more concentrated smoke and employing more extensive instrumentation. Miombo leaf/twig litter and miombo/dambo grasses were sampled in the western province of Zambia at the end of the dry season, shipped directly to Montana, and stored at low temperature until burning. For these fires, a layer of sand covered the fuel bed, which simulated the sandy miombo soils. The grass was arranged vertically in clumps to simulate natural geometry (held in place with a wire mesh with ~10 × 10 cm grid). For the miombo simulations, we added a roughly equal mass of leaf/twig litter as a layer on the sand. The fuel loading for grass fires was 0.43-0.85 kg/m^2, which overlaps the range of values measured for grass loading in central Africa (0.18-0.57 kg/m^2) [*Shea et al.*, 1996; *Hoffa et al.*, 1999; *Pereira et al.*, 2002]. The average miombo total fuel loading was 1.0 ± 0.03 $kg/m,^2$ which is in excellent agreement with field measurements described in the above studies.

2.2.2. Selection, sampling, and simulations of Indonesian fuels. Extensive biomass burning can occur in Indonesia, especially during El-Nino years [*Siegert et al.*, 2001]. However, there have been no classical fuel consumption studies for Indonesian fires to our knowledge and the

relative importance of different fuel types is unknown. A few studies observed which ecosystems burned in specific provinces of Indonesia during the fires associated with the 1997/8 El Niño haze event over southeast Asia. *Liew et al.* [1999] used C-band SAR (synthetic aperture radar) and found that the dominant ecosystem that burned in 1997/8 in South Kalimantan was peat swamp. The island of Sumatra and the province of West Papua also contain large areas of peat land. Based on Landsat TM and some limited post-fire observations of depth of burn for peat, *Page et al.* [2002] calculated that ~1.7 Pg of C was emitted by Indonesian peat fires in 1997: ~26% of the annual global carbon emissions from fossil fuels. On the other hand, *Siegert et al.* [2001] used AMI (active microwave instrument) SAR to map area burned in East Kalimantan during 1997/8. According to that study, 75% of the 5.2 million hectares burned was lowland forest (mostly previously logged), secondary forest, plantations, and farmland. Of the remaining 25%, 6% was grassland and only 6% was peat swamp forest. Much anecdotal evidence suggests that an invasive fire-maintained grass "alang-alang" (*Imperata Cylindrica*) accounts for much of the fuel consumption in Indonesia [*Jacobs*, 1988; *Seavoy et al.*, 1975; *Pickford et al.*, 1992; *J. Goldammer*, *S. Siebert*, and *R. Yokelson* personal observations]. Smoldering piles of rice straw are ubiquitous in much of Indonesia and East Asia. We decided to measure the emissions from these Indonesian fuels: peat, secondary forest floor litter, semak (brush that colonizes clearings), alang-alang (grass noted above that colonizes clearings), and rice straw.

A block of peat (~25 cm^3) was hand-cut by Dr. Saharjo from an ongoing research plot in an *Acacia* plantation in Teluk Pulai in south Sumatra [*Saharjo*, 1998]. The intact peat sample was ignited with a torch and it smoldered for ~1 hr while the emissions were monitored. Secondary forest floor litter, alang-alang, semak, and rice straw were sampled in Curug village, Jasinga subdistrict, Bogor District, West Java. The fuel loading for alang-alang in this study (0.62 kg/m^2) was typical for grass loading worldwide, but only ~1/3 the loading of alang-alang measured by *Pickford et al.* [1992] on a single plot in Depok, West Java. The rice straw smoldered in a pile since in Indonesia - and wherever rice is harvested by hand - rice straw is heaped in piles that may smolder for days.

2.2.3. Other fuels. We burned several fuels typical of North American forests (large-diameter hardwood log, shredded hardwood, organic soil, duff, and litter mainly for comparison to previous studies or to provide slowly-changing emissions for the intercomparisons [*Yokelson et al.*, this issue; *Christian et al.*, this issue]. We also burned grass collected by J. Goldammer near an industrial site in Germany to check for re-suspension of industrial pollutants.

2.3. Fuel characterization

Carbon, hydrogen, nitrogen, chlorine, and ash content for each fuel type were measured by independent laboratories on a dry weight basis. Moisture content was determined by measuring the mass loss after holding the sample at 90°C overnight. Fuel moisture (FM) is expressed as dry weight % as follows:

$$FM = \left(\frac{wet - dry}{dry} \right) 100 \qquad (1)$$

2.4. Trace Gas and Particle Instrumentation

2.4.1. Open-path FTIR. The open path Fourier transform infrared spectrometer (OP-FTIR) was positioned on the sampling platform so that the open white cell spanned the stack directly in the rising emissions stream for continuous (.83s resolution) scanning. The OP-FTIR system [*Yokelson et al.*, 1997; *Bertschi et al.*, 2003b] includes a MIDAC model 2500 spectrometer; 1.6m

base-path, open multipass cell; and an MCT (mercury-cadmium-telluride), LN_2-cooled detector. The path length was set to 57.7 m and spectral resolution was 0.5 cm^{-1}. All spectra were stored on a notebook synchronized with the rest of the data acquisition. Before each fire, we scanned for 2-3 minutes to obtain a background spectrum, and then we made absorbance spectra for each scan during the fire at .83s resolution using the background spectrum. For fires with slowly changing temperature and emissions, we increased signal to noise through spectral averaging of as many as 72 absorbance spectra (~1 min resolution). For fires with larger or more rapid temperature fluctuations spectral averaging was limited to ~6 s resolution (7 scans).

We used classical least squares (CLS) spectral analysis [*Griffith*, 1996; *Yokelson and Bertschi*, 2002] to retrieve excess mixing ratios for methane (CH_4), methanol (CH_3OH), ethylene (C_2H_4), phenol (C_6H_5OH), acetone ($CH_3C(O)CH_3$), acetol ($CH_2(OH)C(O)CH_3$), isoprene (C_5H_8), hydrogen cyanide (HCN), acetylene (C_2H_2), furan (C_4H_4O), nitric oxide (NO), and formaldehyde (HCHO). We used spectral subtraction [*Yokelson et al.*, 1997] to retrieve excess mixing ratios for ammonia (NH_3), formic acid (HCOOH), acetic acid (CH_3COOH), glycolaldehyde (GA, $CH_2(OH)CHO$), propylene (C_3H_6), and methyl vinyl ether (MVE, CH_3OCHCH_2). While CO_2 and CO are readily measured accurately by our OP-FTIR [*Goode et al.*, 1999], due to the large volume of data we opted to use the convenient, synchronized data for these molecules from the real-time instruments (vide infra). The detection limit for most molecules was 5-20 ppb for a one-minute measurement time (72 scans) and ~10-50 ppb at the highest time resolution used (6s or 7 scans). The less favorable detection limits at high temporal resolution (compared to FTIR field measurements) was more than offset by the factor of ~15 increase in trace gas mixing ratios sampled in the lab. The advantages and disadvantages of FTIR are discussed in a companion paper [*Christian et al.*, this issue].

2.4.2. PTR-MS. The PTR-MS sampled continuously from the emissions stream through ~2 m of 6 mm i.d. Teflon tubing that opened directly above the center of the OP-FTIR optical path. The sample line was short to minimize losses and assure a fast response time (around 5 s). The PTR-MS employs chemical ionization to measure volatile organic compounds (VOC) in real time [*Hansel et al.*, 1995; *Lindinger et al.*, 1998]. Briefly, the instrument features a hollow cathode ion source that produces H_3O^+ reactant ions from water vapor in the sample. The sample air then passes through a drift tube where VOC with proton affinities > water are ionized by proton transfer reactions with the H_3O^+. The product ions are analyzed by a quadrupole mass spectrometer. Under favorable operating conditions less than 5% of the H_3O^+ ions react with VOC in the sample and the concentration of product ions in the sample can be calculated using equation (2),

$$[VOC - H^+] \cong [H_3O^+]_0 [VOC] k_{VOC} t \qquad (2)$$

where $[H_3O^+]_0$ is the density of H_3O^+ ions in the absence of neutral reactants, k_{VOC} is the respective reaction rate constant for the proton transfer from H_3O^+ to the VOC and t is the reaction time, which depends on length, pressure and voltage of the drift tube. The reaction rate of most exothermic proton transfer reactions is nearly equal to the collision rate, and when specific reaction rates are unknown they can be calculated [*Su and Chesnavich*, 1982]. An average reaction rate constant of 2 x 10^{-9} cm^3 s^{-1} is used in this study for the quantification of unidentified ions.

During these experiments, the PTR-MS operated in either of two modes. In full mass scan mode the instrument was configured to scan incrementally from 17 to 142 atomic mass units,

with a sample time of 20ms per mass. In selected mass scan mode the instrument was configured to scan a selection of 30-36 masses, with a sample time of 0.1 to 0.2s. Overall time resolution for either mode was about 4 to 8s. The PTR-MS computer was synchronized with the rest of the data acquisition and the results were splined to match the OP-FTIR points. Even for molecules with unknown rate constants, the overall accuracy should be better than ±50% with the estimate of the reaction rate constant (±30%) being the main source of error. The strengths and limitations of PTR-MS are discussed in more detail in the companion paper [*Christian et al.*, this issue].

2.4.3. Canister sampling. Up to three evacuated stainless steel canisters could be simultaneously filled in ~10s to ambient pressure via a "cross" manifold and a 4 mm i.d. stainless steel sampling tube that opened next to the PTR-MS inlet. The sample line pressure was logged on the data system so that the filling time of these "quick cans" with respect to other instruments was precisely known. "Integrated" cans were filled at a pre-selected linear rate, over a precisely known period, through another collocated inlet. Forty integrated cans and 28 quick cans taken before or during most fires were analyzed by GC-FID for C_1-C_4 hydrocarbons by the USDA Forest Service. Eight of the 18 quick cans taken during the fires for analysis by GC/MS in Mainz were analyzed for acetonitrile, acetone, isoprene, methyl vinyl ketone, methyl ethyl ketone, benzene, toluene, and p-xylene. Eight quick cans taken during the fires were analyzed at UC Irvine by GC/FID, MS, and ECD for ethylene, propylene, acetylene, isoprene, benzene, toluene, and p-xylene. More details about the canister measurements are found elsewhere [*Hao et al.*, 1996; *Williams et al.*, 2001; *Colman et al.*, 2001]. The canister data was used mostly for intercomparisons.

2.4.4. Other measurements. The co-located 19 mm inlet used for filling canisters at a linear rate also provided sample air for continuous CO_2 (LICOR 6262) and CO (TECO 48C) measurements. The TECO and both LICORs (including the background air monitor) were calibrated daily with NIST traceable standards. Stack air was drawn at 30 L min^{-1} through dielectric tubing to a cyclone to remove particles larger than 2.5 μm effective diameter, then onto Teflon or quartz filters. Teflon filters were analyzed gravimetrically by the USFS [*Trent et al.*, 2000] and then by XRF, which provided halogens, potassium and sulfur. Quartz filters were analyzed for organic and elemental ("black") carbon by independent laboratories. Only one filter collection apparatus was available so quartz and Teflon filters for the same fuel type were acquired during different fires. We continuously monitored temperature, pressure, flow, and fuel mass with 2s resolution. The mass flow meter (Kurz model 455) calibration was checked frequently by burning ethanol fires. Pure ethanol has a known % C, which is efficiently converted to CO_2, thus comparison of the CO_2 and mass-loss data allows a check on the flow.

3. Results

3.1 Particle Emissions for All Fuels

Table 2 presents particle emissions data for each fuel type. PM2.5 was determined from gravimetric analysis of Teflon filters, which were collected over the entire course of the fire for all but cottonwood, fir duff, NWT duff, pine-fir duff, and rice straw. Cottonwood and duff fires can burn for hours-days and the fires of this type in this study were truncated. The PM2.5 data collected over the limited initial period very likely reflects higher emissions than are typical of the whole fire [*Bertschi et al.*, 2003a]. The rice straw fire was shorter and not truncated, but the filters were taken during periods of heavy smoke and likely return values above the average for the whole fire. Spot measurements are listed separately in the table to indicate that no filter representative of the fire-average was collected for that fuel type. The values in Table 2 are

based on only one or two filters per fuel type. The EFPM2.5 obtained for savanna-type fuels are similar to literature average values [*Andreae and Merlet*, 2001; *Sinha et al.*, 2003].

Emission factors for elemental and organic carbon (EC and OC) are also listed in Table 2. Since emission factors can depend heavily on the relative amount of flaming and smoldering combustion, we continue our discussion using an index of this known as "modified combustion efficiency" (MCE, $\Delta CO_2/(\Delta CO+\Delta CO_2)$) [*Ward and Radke*, 1993]. Our dambo and miombo fires burned with MCEs (0.97-0.98) that are near the upper end of MCEs observed for individual fires in the field [*Ferek et al.*, 1998; *Sinha et al.*, 2003; *Yokelson et al.*, 2003] (indicating nearly pure flaming). This probably contributes to our emission factor for elemental carbon (EFEC) being substantially larger (~1.5 g/kg) than the literature average for savanna fires (0.48 g/kg, at MCE ~0.94) reported by *Andreae and Merlet* [2001] (Figure 1). Our EFEC for the other fuels, which burned at lower MCE, are close to the literature averages [*Andreae and Merlet* 2001]. Similarly, our EFOC are lower than the literature average for African fuels, but close to previously reported values for the other fuels. In fact, the EC/OC ratio, for the broad mix of fuels investigated here, is weakly dependent on MCE for MCE <~0.97 (Figure 1), but above that it is positively correlated. The study-average EC/OC for African savanna fires recently measured by *Sinha et al.* [2003] and the literature-average value derived by *Andreae and Merlet* [2001] are in good agreement with our current study data at the same MCE (Figure 1). However, Figure 1 and Table 2 suggest that some naturally occurring high-MCE savanna fires may be emitting much more elemental carbon (and less OC) than is currently thought.

Gras et al. [1999] characterized smoke particles during the 1997 fires in South Kalimantan, Indonesia that burned mainly peat. They observed a very high single scattering albedo for the smoke (ω up to 0.98) and very high hygroscopic growth (the average increase in light scattering as relative humidity was ramped from 20-80% was 1.65). Since EC is the main light-absorbing component of aerosol and organic carbon can be polar, their observations are consistent with our observation of very low EC (0.04 g/kg) and very high OC/EC (~150) for peat smoke particles. The high OC/EC ratio may enhance the particles action as cloud condensation nuclei and contribute to the dense cloud cover that was observed over the 1997 Kalimantan fires by two authors (Ward and Yokelson). In addition, *Yokelson et al.* [2003] found that cloud-processing can cause large changes in gas-phase smoke chemistry.

The emission factor for chlorine in PM2.5 was loosely correlated to the widely ranging fuel chlorine content (Table 2 and Figure 2). The high r^2 for this plot is deceiving, as shown in the inset, since the regression line does not accurately represent the many lower values. The percentage of the fuel chlorine recovered in the PM2.5 was only weakly dependent on MCE (r^2 = 0.36) suggesting that incorporation of chlorine into the fine particles may not depend strongly on the ratio of flaming to smoldering combustion. Total potassium or sulfur in PM2.5 was not dependent on MCE (r^2 = 0.071 and 0.11), but an actual dependence was probably masked by variation in fuel K and S (which we did not measure), since *Ward and Hardy*, [1989] observed a large dependence of EFK on MCE.

3.2. African Fuels

The high concentrations of nascent smoke in this study revealed at least 11 gases that were not detected by FTIR or GC/FID in a recent field study of African savanna fires [*Sinha et al.*, 2003; *Yokelson et al.*, 2003]: acetaldehyde (CH_3CHO), phenol, acetol (hydroxyacetone), glycolaldehyde (GA), methylethylketone (MEK), acetone, methylvinylether (MVE), furan, acetonitrile (CH_3CN), propenenitrile (C_3H_3N), and propanenitrile (C_3H_5N). Eight of these 11 compounds are OVOC, which have large effects on modeled smoke plume chemistry [*Mason et*

al., 2001; *Jost et al.*, 2003]. It is important to use the new lab data to estimate the initial emissions of these compounds from typical African fires. However, we opted not to use the lab-average emission factors for this purpose because the lab fires we burned had a higher average MCE than the average MCE observed in the field in Africa. For example, recent airborne measurements in Africa [*Yokelson et al.*, 2003] yielded an MCE of 0.941 for a miombo fire, 0.975 for a dambo fire, and ~0.94 as the average for 10 savanna fires. In the current study, the average MCE was 0.976 for five miombo fires and 0.980 for 10 dambo fires. Since EF decrease with increasing MCE for smoldering compounds, simple adoption of our lab-average EF would underestimate the real EF for smoldering compounds for field-average fires.

However, our lab fire emission factors do have a dependence on MCE that is very similar to that of the field-fire emission factors; for compounds measured in both experiments. Figure 3 shows the lab and field EF for acetic acid vs. MCE (as measured by FTIR). There is overlap between the data sets and similar regression equations are suggested by both data sets. Table 3 compares EF calculated (at the field-average MCE) from regression equations based on either lab or field data for 4 compounds that were common to both studies. The difference between the field and lab results is small for acetic acid and ethylene, and not overly large for methane and methanol. This good agreement supports the use of lab-based regression equations (at the field-average MCE) to calculate average African EF for compounds that were below FTIR detection limits in the field.

Figure 4 shows the EF versus MCE plots from this study for acetaldehyde, methylethylketone, acetone, acetonitrile, benzene, toluene, propanenitrile, and propenenitrile as measured by PTR-MS; and for phenol, glycolaldehyde, methylvinylether, and furan as measured by OP-FTIR. (The reasons for choosing data for a compound from a particular instrument are discussed in the companion paper.) The regression equations shown were used to calculate an estimated field average EF for these compounds.

Based on field studies, *Yokelson et al.* [2003] presented what they thought was a complete list of the top 15 savanna fire emissions in order of molar abundance. We have integrated the new EF into an extended version of this list in Table 4. In Table 4, the compounds are listed in order by their emission ratio to the main C-containing emission CO_2 so that their relative abundance is clear. When both lab and field measurements of the emission ratio to CO_2 were available for initial smoke, we used the field data; although, as discussed above, the agreement between lab and field data was good. In the right hand column, we present the emission factors for each species. While the previous list of the top 15 compounds was complete (except for acetaldehyde), this extended list is missing most of the entries below an emission ratio of ~0.08 due to the lack of positive identification for OVOC. In fact, we note that some of the major emissions detected by PTR-MS are not in Table 4. For instance, a number of (protonated) masses have study-average emission factors of ~0.4-0.7 g/kg, which would place them in the middle of Table 4 on a mass basis. Some of these are listed with tentative identifications in parentheses: mass 97 (furfural, dimethylfuran), mass 99 (C7 alkenes), mass 109 (benzyl alcohol), mass 111 (trimethylfuran), and mass 113 (C8 alkenes). We estimate that we were able to positively identify about 90% of the NMOC molecules, which accounted for ~70% of the carbon emitted as NMOC. The process of compound identification, which led to gases being included in the tables in this paper, is discussed in detail elsewhere [*Christian et al.*, this issue; *Kleiss et al.* this issue].

An important feature of the earlier version of the list was that oxygenated volatile organic compounds (OVOC) accounted for ~70% of the non-methane organic compounds (NMOC) emitted by savanna fires. With the increased sensitivity of this study, OVOC still account for

~70% of the NMOC. Unfortunately, below the level of abundance for furan in Table 4 (the ~25 most abundant compounds), we cannot positively identify OVOC even though they dominate. More work is needed to extend reliable speciation of OVOC mixtures to lower levels since even relatively less abundant gases can have important effects on atmospheric chemistry.

3.3 Indonesian Fuels

Since there are no field measurements of MCE, or emission factors, for "real" Indonesian fires, the values from our carefully simulated lab fires must suffice. A few comparisons can be made that suggest that our simulated fires may be representative. The MCE for our Indonesian peat fire (0.838) was identical to the MCE for peat from Minnesota and a little above the MCE for peat from Alaska that were burned at FSL several years ago [*Yokelson et al.*, 1997]. The Indonesian grass and forest fuels burned with lower MCE than our African fuels and with MCE that were well within the range observed for grass and forest fuels in Brazil as shown in Figures 3-9 of *Ferek et al.* [1998] and Figures 7-8 of *Ward et al.* [1992].

Emission ratios and emission factors for the Indonesian fuels are presented in Tables 5 and 6. The results are listed by fuel type for both FTIR and PTR-MS. The standard deviation (in parentheses) is an indicator of the variation among separate burns of the same fuel type. In Table 5 we have presented the emission ratio for CO and flaming compounds versus CO_2 and for smoldering compounds versus CO [*Lobert et al.* 1991]. The discussion in section 3.2 of the completeness of Table 4 also applies to Tables 5 and 6. We point out some major features of this data. Acetol (hydroxyacetone), previously unreported in smoke, was emitted in very large quantities from burning rice straw (~6.5% of CO). This is a level comparable to methane, but it represents more than twice as much carbon! The acetol emissions were large for semak and litter (~2% of CO) and substantial (~0.6% of CO) for the other Indonesian fuels (peat and grass). The acetol emissions from African fuels were much lower (~0.1-0.2%). In previous studies, acetic acid, methanol, and formaldehyde were consistently the 3 most abundant OVOC emitted by fires [*Goode et al.*, 2000; *Yokelson et al.*, 2003]. On average, for the Indonesian fuels, acetol is the second most abundant OVOC, CH_3CHO is fourth, and HCHO is displaced to fifth. Acetol has a uv cross-section similar to acetone and important atmospheric chemistry [*Orlando et al.*, 1995]. We also report small emissions of methylvinylether for the first time, mostly from peat and litter.

The NH_3 emissions from the single Indonesian peat sample were very large (16% of CO). This is consistent with very large NH_3 emissions noted for Minnesota peat (15% of CO) [*Yokelson et al.*, 1997]. The NH_3 emissions were in the range of 2-6.8% of CO for the other Indonesian fuels suggesting that Indonesian fires may produce a lot of particle ammonium nitrate. The HCN and acetonitrile emissions were large for peat (~4.1 and 1.7% of CO, respectively), but much smaller for the other Indonesian fuels (0.12-0.67% of CO), which is similar to the African fuels. The emission factors for all Indonesian fuels for NO_x (as NO) were in the range of 0.6-1.7 g/kg, which is low compared to African fuels (~3.5-4.5 g/kg) [*Andreae and Merlet*, 2001; *Yokelson et al.*, 2003]) and may limit O_3 formation in Indonesian biomass burning plumes [*Tsutsumi et al.*, 1999]. *Sawa et al.* [1999] reported low NO_x/CO ratios (~0.0002-0.0005) in smoke of unknown age over South Kalimantan in 1997 where peat was a major fuel component. This ratio is lower than our measurement of the NO/CO ratio for nascent smoke from burning Indonesian peat of ~0.0046. Our measured ratio is identical to the NO_x/CO ratio of 0.0046 assumed by *Levine* [1999] for Indonesian peat based on earlier work [*Yokelson et al.*, 1997], but more than a factor of 6 below the NO_x/CO ratio of ~0.03 assumed by *Hauglustaine et al.* [1999] suggesting that they may have greatly overestimated O_3 production from the 1997/8 fires. The estimate of total carbon emissions for peat fires by *Page et al.* [2002] can be combined with our emission ratios to

CO_2 for peat fires (derived from Table 5) to roughly estimate the emissions of other compounds from these fires. As an example, this approach suggests that 328 Tg of CO and 28 Tg of NH_3 were emitted by the 1997/8 Indonesian fires. These amounts are approximately one and 22 times the total annual emissions of these compounds from biomass burning as estimated by *Crutzen and Andreae* [1990]. The large interannual variability in biomass burning is illustrated. During 1997/8, *Rinsland et al.* [1999] observed an enhancement of ~ 1% in column HCN/CO above Mauna Loa, which they attributed to biomass burning in Southeast Asia. Our HCN/CO ER for peat fires was ~4%: the difference could be due to variable ER from burning peat [*Yokelson et al.*, 1997], contribution of other fire types in Asia, and/or transport of emissions from fossil fuel burning and fires in other areas.

As stated earlier, we don't know the relative amount of the different fuels that burn on average in Indonesia. However, we can construct a plausible, and fairly comprehensive table of the main Indonesian fire emissions (except for SO_2) by weighting the results for all the fuel types in Table 5 equally. The compounds we measured are shown in order of abundance in Table 7. (We have incorporated lab data for N_2 from *Kuhlbusch et al.*, [1991] and Brazil data for H_2 from *Ward et al.* [1992]. SO_2 data for Brazil is not "imported" because of the potential for high S content in peat.) The format and caveats for Table 4 apply for Table 7. We also remind the reader that neither Table 7 or Table 4 include the fact that very large quantities of biomass are burned as domestic fuel in Indonesia and Africa [*Yevich and Logan*, 2003]. (The emissions from African biofuel use were recently found to rival or exceed the emissions from African savanna fires [*Bertschi et al.*, 2003b].) Table 7 implies that OVOC account for >80% of the NMOC emitted by non-domestic Indonesian fires. In addition, the NH_3 emissions are comparable to the CH_4 emissions.

Conclusions

These experiments demonstrate the importance of OVOC emissions from biomass burning and that our capacity to sensitively speciate OVOC in complex mixtures limits our understanding of gas-phase atmospheric chemistry. For example, 8 of the 11 "new" compounds that we measured for African fuels in the lab, due to increased sensitivity, are OVOC. OVOC accounted for 70% of NMOC emitted by African savanna fires and >80% for Indonesian fires. Indonesian rice straw emitted high levels of acetol (hydroxyacetone), a compound that influences HO_x chemistry, since its UV cross section is similar to that of acetone. We present the most comprehensive table to date of emissions from African savanna fires. Since there are no extensive field studies of biomass burning emissions from Indonesian fuels, the emissions data from this study must suffice.

Acknowledgements. This research was supported by the National Science Foundation under grants ATM-9900494 and ATM-0228003; the Interagency Joint Fire Science Program; the Rocky Mountain Research Station, Forest Service, U.S. Department of Agriculture (RMRS-99508-RJVA and 03-JV-11222049-046); and the Max Planck Society. Betina Kleiss thanks the Foundation Gran Mariscal de Ayacucho (Fundayacucho) and the German Academic Exchange Service (DAAD) for financial support. The authors thank Mike Chandler who helped carry out the fires.

References

Andreae, M.O., and P. Merlet, Emission of trace gases and aerosols from biomass burning, *Global Biogeochem. Cy.*, *15*, 955-966, 2001.

Bertschi, I., R. J. Yokelson, D. E. Ward, R. E. Babbitt, R. A. Susott, J. G. Goode, and W. M. Hao, Trace gas and particle emissions from fires in large diameter and belowground biomass fuels, *J. Geophys. Res.*, *108*, 8472, doi:10.1029/2002JD002100, 2003a.

Bertschi, I. T., R. J. Yokelson, D. E. Ward, T. J. Christian, and W. M. Hao, Trace gas emissions from the production and use of domestic biofuels in Zambia measured by open-path Fourier transform infrared spectroscopy, *J. Geophys. Res.*, *108*, 8469, doi:10.1029/2002JD002158, 2003b.

Christian, T.J., B. Kleiss, R.J. Yokelson, R. Holzinger, P.J. Crutzen, J. Williams, W.M. Hao, and T. Shirai, Comprehensive laboratory measurements of biomass-burning emissions II: First intercomparison of open-path FTIR, PTR-MS, GC/MS and GC/FID, this issue.

Cofer, W.R. III, J.S. Levine, E.L. Winstead, D.R. Cahoon, D.I. Sebacher, J.P. Pinto, and B. J. Stocks, Source compositions of trace gases released during African savanna fires, *J. Geophys. Res.*, *101*, 23597-23602, 1996.

Colman, J.J., A.L. Swanson, S. Meinardi, B.C. Sive, D.R. Blake, and F.S. Rowland, Description of the analysis of a wide range of volatile organic compounds in whole air samples collected during PEM-tropics A and B, *Anal. Chem.*, *73*, 3723-3731, 2001.

Crutzen, P.J., and M.O. Andreae, Biomass burning in the tropics: Impact on atmospheric chemistry and biogeochemical cycles, *Science*, *250*, 1669-1678, 1990.

Ferek, R.J., J.S. Reid, P.V. Hobbs, D.R. Blake, and C. Liousse, Emission factors of hydrocarbons, halocarbons, trace gases, and particles from biomass burning in Brazil, *J. Geophys. Res.*, *103*, 32107-32118, 1998.

Goode, J.G., R.J. Yokelson, D.E. Ward, R.A. Susott, R.E. Babbitt, M.A. Davies, and W.M. Hao, Measurements of excess O_3, CO_2, CO, CH_4, C_2H_4, C_2H_2, HCN, NO, NH_3, HCOOH, CH_3OOH, HCHO, and CH_3OH, in 1997 Alaskan biomass burning plumes by airborne Fourier transform infrared spectroscopy (AFTIR), *J. Geophys. Res.*, *105*, 22147-22166, 2000.

Gras, J.L., J.B. Jensen, K. Okada, M. Ikegami, Y. Zaizen and Y. Makino, Some Optical Properties of Smoke Aerosol in Indonesia and Tropical Australia, *Geophys. Res. Let., 26,* 1393-1396, 1999.

Griffith, D.W.T., Synthetic calibration and quantitative analysis of gas phase infrared spectra, *Appl. Spectrosc.*, *50*, 59-70, 1996.

Hansel, A., A. Jordan, R. Holzinger, P. Prazeller, W. Vogel, and W. Lindinger, Proton transfer reaction mass spectrometry - Online trace gas analysis at the ppb level, *Int. J. Mass Spectrom. & Ion Proc.*, *150*, 609-619, 1995.

Hao, W.M., D.E. Ward, G. Olbu, and S.P. Baker, Emissions of CO_2, CO, and hydrocarbons from fires in diverse African savanna ecosystems, J. Geophys. Res., 101, 23577-23584, 1996.

Hauglustaine, D.A., G.P. Brasseur, and J.S. Levine, A sensitivity simulation of tropospheric ozone changes due to the 1997 Indonesian fire emissions, *Geophys. Res. Lett.*, *26*, 3305-3308, 1999.

Hobbs, P.V., J.S. Reid, R.A. Kotchenruther, R.J. Ferek, and R. Weiss, Direct radiative forcing by smoke from biomass burning, *Science*, *275*, 1776-1778, 1997.

Hoffa, E.A., D.E. Ward, W.M. Hao, R.A. Susott, and R.H. Wakimoto, Seasonality of carbon emissions from biomass burning in a Zambian savanna, *J. Geophys. Res.*, *104*, 13841-13853, 1999.

Holzinger, R., C. Warneke, A. Hansel, A. Jordan, W. Lindinger, D.H. Scharffe, G. Schade, and P.J. Crutzen, Biomass burning as a source of formaldehyde, acetaldehyde, methanol, acetone, acetonitrile, and hydrogen cyanide, *Geophys. Res. Lett.*, *26*, 1161-1164, 1999.

IGBP, IGPB (International Geosphere-Biosphere Program) Report 41, 109 pp., Global Change Newsletter, Stockholm, 1997.

Jacobs, M., *The Tropical Rain Forest: A First Encounter*, Berlin, Springer-Verlag, 1988.

Jost, C., J. Trentmann, D. Sprung, M. O. Andreae, J. B. McQuaid, and H. Barjat, Trace gas chemistry in a young biomass burning plume over Namibia: Observations and model simulations, *J. Geophys. Res.*, *108*, 8482, doi:10.1029/2002JD002431, 2003.

Kaufman, Y.J., and R.S. Fraser, Confirmation of the smoke particles effect on clouds and climate, *Science*, *277*, 1636-1639, 1997.

Kuhlbusch, T. A., J. M. Lobert, P. J. Crutzen and P. Warneck, Molecular nitrogen emissions from denitrification during biomass burning, *Nature*, *351*, 135-137, 1991.

Lelieveld, J., P. J. Crutzen, D. J. Jacob, and A. M. Thompson, Modeling of biomass burning influences on tropospheric ozone, in *Fire in Southern African Savannas: Ecological and Atmospheric Perspectives*, edited by B. W. van Wilgen et al., pp. 217-238, Witwatersrand Univ. Press, Johannesburg, South Africa, 1997.

Liew, S.C., L.K. Kwoh, K. Padmanabhan, O.K. Lim, and H. Lim, Delineating land/forest fire burnt scars with ERS interferometric synthetic aperture radar, *Geophys. Res. Lett.*, *26*, 2409-2412, 1999.

Levine, J.S., The 1997 fires in Kalimantan and Sumatra, Indonesia: Gaseous and particulate emissions, *Geophys. Res. Lett.*, *26*, 815-818, 1999.

Lindinger, W., A. Hansel, and A. Jordan, On-line monitoring of volatile organic compounds at pptv levels by means of proton transfer mass spectrometry (PTR-MS) - medical applications, food control and environmental research (Review), *Int. J. Mass Spetrom. & Ion Proc.*, *173*, 191-241, 1998.

Lobert, J. M., D. H. Scharffe, W. M. Hao, T. A. Kuhlbusch, R. Seuwen, P. Warneck, and P. J. Crutzen, Experimental evaluation of biomass burning emissions: Nitrogen and carbon containing compounds, in *Global Biomass Burning: Atmospheric, Climatic, and Biospheric Implications*, edited by J. S. Levine, pp. 289-304, MIT Press, Cambridge, Mass., 1991.

Mason, S.A., R.J. Field, R.J. Yokelson, M.A. Kochivar, M.R. Tinsley, D.E. Ward, and W.M. Hao, Complex effects arising in smoke plume simulations due to inclusion of direct emissions of oxygenated organic species from biomass combustion, *J. Geophys. Res.*, *106*, 12527-12539, 2001.

Orlando, J.J., G.S. Tyndall, J.-M. Fracheboud, E. Estupinan, S. Haberkorn, and A. Zimmer, Laboratory studies of the rate and mechanism of the oxidation of hydroxyacetone. *Atmos. Environ., 33*, 1621-1629, 1999.

Page, S.E., F. Siegert, J.O. Rieley, H.-D.V. Boehm, A. Jaya, and S. Limin, The amount of carbon released from peat and forest fires in Indonesia during 1997, *Nature*, *420*, 61-65, 2002.

Pickford, S., M. Suharti, and A. Wibowo, A note on fuelbeds and fire behavior in alang-alang (Imperata cylindrica), *Int. J. Wildland Fire*, *2*, 41-46, 1992.

Rinsland, C.P., et al., Infrared solar spectroscopic measurements of free tropospheric CO, C_2H_6, and HCN above Mauna Loa, Hawaii: Seasonal variations and evidence for enhanced emissions from the southeast Asian tropical fires of 1997-1998, *J. Geophys. Res.*, *104*, 18667-18680, 1999.

Seavoy, R., The origin of tropical grasslands in Kalimantan, Indonesia, *Journal of Tropical Geography*, *40*, 48-52, 1975.

Saharjo, B.H., The changes in soil chemical properties after fire in four-year-old Acacia mangium and Eucalyptus urophylla plantations, *Tropical Ecology*, *39*, 97-102, 1998.

Sawa, Y., H. Matsueda, Y. Tsutsumi, J.B. Jensen, H.Y. Inoue, and Y. Makino, Tropospheric carbon monoxide and hydrogen measurements over Kalimantan in Indonesia and northern Australia during October, 1997, *Geophys. Res. Lett.*, *26*, 1389-1392, 1999.

Scholes, R.J., J. Kendall, and C.O. Justice, The quantity of biomass burned in southern Africa, *J. Geophys. Res.*, *101*, 23667-23676, 1996.

Sharkey, B., ed. *Health Hazards of Smoke: Recommendations of the April 1997 Consensus Conference*, Tech. Rep. 9751-2836-MTDC, USDA Forest Service, Missoula Technology and Development Center, Missoula, MT, 84 p, 1997.

Siegert, F., G. Ruecker, A. Hinrichs, and A.A. Hoffmann, Increased damage from fires in logged forests during droughts caused by El Niño, *Nature*, *414*, 437-440, 2001.

Sinha, P., P.V. Hobbs, R.J. Yokelson, I.T. Bertschi, D.R. Blake, I.J. Simpson, S. Gao, T.W. Kirchstetter, and T. Novakov, Emissions of trace gases and particles from savanna fires in southern Africa, in press, *J. Geophys. Res.*, 2003.

Singh, H. B., M. Kanakidou, P. J. Crutzen, and D. J. Jacob, High concentrations and photochemical fate of oxygenated hydrocarbons in the global troposphere, *Nature*, *378*, 50-54, 1995.

Singh. H., Y. Chen, A. Staudt, D. Jacob, D. Blake, B. Heikes, and J. Snow, Evidence from the Pacific troposphere for large global sources of oxygenated organic compounds, *Nature*, *410*, 1078-1081, 2001.

Su, T., and W.J. Chesnavich, Parameterization of the ion-polar molecule collision rate constant by trajectory calculations, *J. Chem. Phys.*, *76*, 5183-5185, 1982.

Tsutsumi, Y., Y. Sawa, Y. Makino, J.B. Jensen, J.L. Gras, B.F. Ryan, S. Diharto, and H. Harjanto, Aircraft measurements of ozone, NO_x, CO, and aerosol concentrations in biomass burning smoke over Indonesia and Australia in October 1997: Depleted ozone layer at low altitude over Indonesia, *Geophys. Res. Lett.*, *26*, 595-598, 1999.

Ward, D.E., and C.C. Hardy, Organic and elemental profiles for smoke from prescribed fires, in Receptor Models in Air Resources Management, (ed) J.G. Watson, pp. 299-321, Air and Waste Manage. Assoc., Pittsburgh, 1989.

Ward, D.E., R.A. Susott, J.B. Kauffman, R.E. Babbitt, D.L. Cummings, B. Dias, B.N. Holben, Y.J. Kaufman, R.A. Rasmussen, and A.W. Setzer, Smoke and fire characteristics for cerrado and deforestation burns in Brazil: Base-B experiment, *J. Geophys. Res.*, *97*, 14601-14619, 1992.

Williams, J., U. Pöschl, P.J. Crutzen, A. Hansel, R. Holzinger, C. Warneke, W. Lindinger, and J. Lelieveld, An atmospheric chemistry interpretation of mass scans obtained from a proton transfer mass spectrometer flown over the tropical rainforest of Surinam, *J. Atmos. Chem.*, *38*, 133-166, 2001.

Yevich, R., and J. Logan, An assessment of biofuel use and burning of agricultural waste in the developing world, in press, *Global Biogeochem. Cy.*, 2003.

Yokelson, R.J., D.W.T. Griffith, and D.E. Ward, Open-path Fourier transform infrared studies of large-scale laboratory biomass fires, *J. Geophys Res.*, *101*, 21067-21080, 1996.

Yokelson, 1996.R.J., D.E. Ward, R.A. Susott, J. Reardon, and D.W.T. Griffith, Emissions from smoldering combustion of biomass measured by open-path Fourier transform infrared spectroscopy, *J. Geophys. Res.*, *102*, 18865-18877, 1997.

Yokelson, R.J., and I.T. Bertschi, Vibrational spectroscopy in the study of fires, in *Handbook of Vibrational Spectroscopy*, edited by J.M. Chalmers and P.R. Griffiths, pp. 8, John Wiley & Sons Ltd, Chichester, 2002.

Yokelson, R. J., I. T. Bertschi, T. J. Christian, P. V. Hobbs, D. E. Ward, and W. M. Hao, Trace gas measurements in nascent, aged, and cloud-processed smoke from African savanna fires by airborne Fourier transform infrared spectroscopy (AFTIR), *J. Geophys. Res.*, *108*, 8478, doi:10.1029/2002JD002322, 2003.

Figure Captions

Figure 1. The particle EC/OC ratio and the EC emission factors measured in this study are plotted against MCE. Open circles represent EC/OC. Also shown are global averages for savanna fires: open box - [*Sinha et al.*, 2003], open triangle - [*Andreae and Merlet*, 2001]. Black diamonds represent our EC values. (Two letter fuel type abbreviations are shown at the top of the plot.) Field fires that burn at high MCE may be contributing more EC than previously thought.

Figure 2. Regression of particle chlorine content against fuel chlorine content suggesting that ~one-third of the fuel chlorine is transferred to the particles. However, the inset shows that the regression does not fit the many low values well.

Figure 3. The emission factor (EF) for acetic acid vs. MCE for field data (filled circles) and lab data (open squares). The data sets overlap, but the lab data was obtained at higher MCE on average. Independent regressions of EF vs MCE for the individual data sets predict similar EF at the field study average MCE. (The lab fire at MCE ~ 0.94 was from miombo litter only, which is not a complete fuel complex. This data point was omitted from the lab regressions, which improved the r^2 values.)

Figure 4. EF vs. MCE for 12 fire emissions that were below FTIR detection limits in an African field study, but successfully quantified in this work. The regression equations were used as described in the text to derive values for Table 4.

Table 1. Fires and Fuel Types Sorted by Country of Origin. (Two-letter fuel type abbreviation in parentheses.)

Fire Name	# Fires	Fuel Description	Origin	%C	%H	%N	%ash	FM[a]	Avg Fuel loading[b]
Dambo (db)	10	Dry land dambo grass	Zambia	46.3	5.90	0.23	3.35	5.8-17.3	0.59
Miombo (mb)	5	Miombo vegetation type (~50:50 mixture of dambo grass and miombo litter)	Zambia	48.9	5.93	0.71	3.65	8.7-10.5	1.00
MiomboLit (ml)	1	Miombo litter (mainly leaves and twigs)	Zambia	51.6	5.96	1.20	3.95	12.6	0.21
Alang-alang (al)	5	Initial, invasive, fire-maintained grass after deforestation	Indonesia	42.1	5.25	0.78	10.3	8.7-41.9	0.62
Indopeat (ip)	1	Peat	Indonesia	54.7	4.90	2.12	6.55	30.5	12.8
IndoSFLit (il)	4	Secondary forest floor litter	Indonesia	47.0	5.50	1.22	7.15	12.8-17.9	3.79
Rice Straw (rs)	3	Rice stalks after grain is removed	Indonesia	35.4	4.73	0.68	22.3	18.8-32.3	2.31
Semak (sk)	4	Successional shrub/brush after deforestation	Indonesia	46.8	5.37	1.33	6.80	12.1-26.9	5.07
German grass (gg)	3	Grass from heavily industrialized region	Germany	45.1	5.73	1.06	5.40	9.2-21.6	1.14
NWTDuff (nw)	1	Soil, litter, duff - Northwest Territories	Canada	56.8	5.09	1.62	2.80	10.7	
Cottonwood (cw)	1	Hardwood log	U.S.	48.0	5.84	0.04	1.30	14.6	[c]
Excelsior (ex)	2	Shredded hardwood (Quaking Aspen)	U.S.	47.7	5.92	0.055	0.00	6.4	2.45
FirDuff (fd)	3	Douglas Fir forest floor soil, duff, litter	U.S.	42.4	4.65	1.06	20.9	12.3-19.3	
PPine (pp)	3	Ponderosa Pine needles	U.S.	51.4	6.26	0.58	3.35	15.0-15.9	2.98
PPineFirDuff (pf)	1	Ponderosa Pine/Douglas Fir forest floor soil, duff, litter	U.S.	43.0	4.81	0.99	18.8	15.8	47.3

[a] FM (fuel moisture) expressed as dry weight %, see text. Ranges are min-max

[b] kg/m^2

[c] Cottonwood log, radius=18cm, length=47cm, mass=18.5kg

Table 2. Emission factors for total PM2.5, and EC, OC, chlorine, potassium, and sulfur in PM2.5 (g/kg fuel). Fuel chlorine content (g/kg) is also given. T indicates Teflon filter, Q indicates quartz filter obtained on a different fire.

Fuel Type	PM2.5	EC	OC	Cl in fuel	Cl in PM2.5	K in PM2.5	S in PM2.5
Fire averaged [a]							
Alang - T	6.6			4.710	1.82	1.29	0.11
Alang - Q		1.69[b]					
Dambo - T	2.9			0.248	0.013	0.044	0.006
Dambo - Q		1.39	0.99				
Excelsior - Q		0.53	3.20	0.032			
German grass - T	3.2			0.218	0.027	0.031	0.012
German grass - Q		0.38	2.74				
Indopeat - Q		0.04	6.02	0.962			
IndoSFLit - T	61.6			0.119	0.042	0.022	0.064
IndoSFLit - Q		0.54	15.7				
Miombo - T	3.6			0.246	0.028	0.065	0.009
Miombo - Q		1.52	2.58				
MiomboLit - T	9.8			0.235	0.044	0.076	0.024
PPine - T	36.0			0.141	0.032	0.040	0.031
PPine - Q		0.53	3.37				
Semak - T	39.2			4.350	1.06	0.58	0.14
Spot measurement [c] (probably not representative of fire-average)							
Cottonwood - T	20.9			0.052	0.005	0.049	0.008
Cottonwood - Q		0.68	23.8				
Fir duff - T	40.8			0.134	0.019	0.007	0.052
Fir duff - Q		4.99	122.4				
NWT duff - T	84.3			0.727	0.560	0	0.097
Pine-Fir duff - T	51.3			0.073	0.016	0	0.025
Rice straw - T	4.2			3.310			
Semak - Q		0.63	32.8	4.350			

[a] Filter duration ≈ fire duration.

[b] Total carbon.

[c] Filter duration << fire duration.

Table 3. Comparison of emission factors (for four compounds) calculated from EF versus MCE based on either field data only or lab data only. (The field data are from *Yokelson et al.* [in press]). MCE for all calculations is 0.938, the field study average.

	Field				Lab				*% difference*
	slope	intercept	r^2	EF	slope	intercept	r^2	EF	
CH_4	-48.52	47.80	0.87	2.29	-32.40	31.92	0.86	1.53	*-33.2*
CH_3OH	-21.28	21.17	0.80	1.21	-32.98	32.45	0.68	1.51	*24.8*
CH_3COOH	-45.33	45.03	0.93	2.51	-47.33	46.88	0.72	2.48	*-1.2*
C_2H_4	-15.91	16.11	0.76	1.19	-22.30	22.02	0.84	1.10	*-7.6*

Table 4. Emission ratios relative to CO_2 (ppbv/ppmv), in order of abundance, for the top trace gas emissions (excluding H_2O) reported in the initial smoke from fires in African savanna fuels. Field measurements are given precedence over lab measurements when both are available, but the field and lab measurements agree well. Below an emission ratio of ~0.08 the list is mostly incomplete due to a lack of OVOC measurements.

Compound	Emission Ratio (ppbv/ppmv CO_2)	Emission Factor[a] (g/kg)	Reference
Carbon dioxide (CO_2)	1000	1689	Yokelson et al. [2003]
Carbon monoxide (CO)	66.4	71.4	Yokelson et al. [2003]
Hydrogen (H_2)	12.6	0.97	Cofer et al. [1996]
Methane (CH_4)	3.53	2.17	Yokelson et al. [2003]
Nitrogen oxides (NO_x as NO)	3.04	3.50	Yokelson et al. [2003]
Nitrogen (N_2)	2.87	3.08	Kuhlbusch et al. [1991]
Ethylene (C_2H_4)	1.14	1.23	Yokelson et al. [2003]
Acetic acid (CH_3COOH)	1.06	2.44	Yokelson et al. [2003]
Formaldehyde (HCHO)	0.97	1.12	Yokelson et al. [2003]
Methanol (CH_3OH)	0.96	1.18	Yokelson et al. [2003]
Sulfur dioxide (SO_2)	0.85	3.13	Sinha et al. [2003]
Hydrogen cyanide (HCN)	0.57	0.59	Yokelson et al. [2003]
Ammonia (NH_3)	0.46	0.30	Yokelson et al. [2003]
Acetaldehyde (CH_3CHO)	0.45	0.76	this work (PTR-MS)
Formic acid (HCOOH)	0.39	0.69	Yokelson et al. [2003]
Acetylene (C_2H_2)	0.29	0.29	Yokelson et al. [2003]
Phenol (C_6H_5OH)	0.23	0.83	this work (OP-FTIR)
Acetol ($C_3H_6O_2$)	0.22	0.62	this work (PTR-MS)
Glycolaldehyde ($C_2H_4O_2$)	0.21	0.48	this work (OP-FTIR)
Propylene (C_3H_6)	0.20	0.32	Sinha et al. [2003]
Methylethylketone (C_4H_8O)	0.19	0.53	this work (PTR-MS)
Ethane (C_2H_6)	0.19	0.22	Sinha et al. [2003]
Acetone (C_3H_6O)	0.16	0.36	this work (PTR-MS)[b]
Methylvinylether (C_3H_6O)	0.11	0.24	this work (OP-FTIR)
Furan (C_4H_4O)	0.085	0.21	this work (OP-FTIR)
Acetonitrile (CH_3CN)	0.082	0.13	this work (PTR-MS)
Benzene (C_6H_6)	0.069	0.21	Sinha et al. [2003][c]
Toluene ($C_6H_5CH_3$)	0.052	0.18	Sinha et al. [2003][d]
Chloromethane(CH_3Cl)	0.037	0.07	Sinha et al. [2003]
Propane (C_3H_8)	0.035	0.06	Sinha et al. [2003]
1,3 Butadiene (C_4H_6)	0.035	0.07	Sinha et al. [2003]
1-butene (C_4H_8)	0.030	0.06	Sinha et al. [2003]
Propenenitrile (C_3H_3N)	0.030	0.06	this work (PTR-MS)
Propanenitrile (C_3H_5N)	0.020	0.04	this work (PTR-MS)

[a]Calculated from this set of emission ratios assuming fuel is 50% carbon ash-free.

[b]Calculated as PTR-MS mass 59 minus FTIR methylvinylether (FTIR acetone below det. limit).

[c]This work PTR-MS benzene = 0.07.

[d]This work PTR-MS toluene = 0.03.

Table 5. Average MCE and excess emission ratios (ppbv/ppmv)[a] for Indonesian fuels.

	Alang-alang (4)[b]				IndoPeat (1)		IndoSFLit (4)				Rice Straw (3)				Semak (4)			
	OP-FTIR		PTR-MS		OP-FTIR	PTR-MS	OP-FTIR		PTR-MS		OP-FTIR		PTR-MS		OP-FTIR		PTR-MS	
MCE	0.953	(0.008)			0.838		0.901	(0.030)			0.811	(0.046)			0.891	(0.012)		
$\Delta CO/\Delta CO_2$	49.9	(8.8)			194.0		110.7	(36.7)			236.1	(69.0)			122.6	(15.0)		
$\Delta CH_4/\Delta CO$	29.0	(12.5)			178.0		81.7	(14.9)			94.5	(14.9)			92.3	(11.0)		
$\Delta C_2H_4/\Delta CO$	8.59	(3.6)			12.6		11.8	(3.4)			15.9	(3.3)			19.0	(3.7)		
$\Delta C_2H_2/\Delta CO$	2.71	(0.48)			0.31		2.15	(0.44)			2.79	(0.21)			4.30	(2.1)		
$\Delta C_3H_6/\Delta CO$	2.83	(2.3)	3.13	(1.1)	10.0	12.8	4.89	(2.3)	15.1	(4.1)	5.89	(3.5)	23.5	(3.2)	8.82	(0.44)	22.9	(5.2)
ΔBenzene/ΔCO			0.70	(0.21)		5.91			1.51	(0.60)			2.12	(0.58)			2.20	(0.21)
ΔToluene/ΔCO			0.26	(0.12)		2.44			1.51	(0.59)			2.22	(0.81)			2.20	(1.3)
$\Delta HFo/\Delta CO$[c]	1.77	(0.79)	0.51	(0.17)	2.36	0.93	3.40	(0.73)	2.24	(1.1)	7.33	(1.1)	3.21	(0.37)	4.51	(1.3)	2.04	(0.70)
$\Delta HAc/\Delta CO$[d]	6.38	(2.0)			20.5		40.4	(17.2)			27.8	(2.5)			42.2	(21.5)		
$\Delta GA/\Delta CO$[e]	2.71	(1.2)			3.62		4.30	(0.87)			14.2	(3.7)			7.40	(1.6)		
mass 61[f]			8.61	(2.8)		26.6			54.9	(16.8)			83.9	(22.5)			57.5	(48.0)
$\Delta HCHO/\Delta CO$	9.88	(3.6)			6.40		13.1	(3.3)			16.6	(3.4)			18.9	(4.6)		
$\Delta CH_3CHO/\Delta CO$			4.46	(2.2)		10.7			11.3	(2.9)			29.8	(5.7)			15.6	(2.8)
$\Delta MeOH/\Delta CO$	6.30	(3.8)	5.61	(3.1)	37.2	37.2	21.4	(10.4)	22.8	(9.4)	30.3	(4.7)	34.6	(6.1)	25.7	(8.8)	25.7	(10.9)
ΔPhenol/ΔCO	1.19	(0.94)	0.79	(0.31)	5.27	5.17	6.50	(2.5)	2.76	(1.1)	4.94	(1.1)	8.82	(3.2)	4.88	(2.6)	4.60	(3.4)
ΔAcetol/ΔCO	8.09	(3.0)	1.97	(1.0)	7.91	4.31	19.5	(6.7)	8.12	(4.8)	73.6	(12.0)	55.6	(20.8)	27.0	(9.7)	14.4	(14.4)
$\Delta MEK/\Delta CO$[g]			1.82	(0.66)		4.52			6.30	(1.1)			13.6	(3.9)			6.30	(4.0)
ΔAcetone/ΔCO[h]			1.79	(1.3)	2.96	6.80	3.80	(1.8)	6.05	(1.3)	6.86	(0.49)	21.0	(5.2)	3.83	(0.59)	9.25	(5.5)
$\Delta MVE/\Delta CO$[i]	0.78	(0.17)			2.01		2.50	(0.22)			1.17	(0.19)			2.32	(0.44)		
ΔFuran/ΔCO	1.13	(0.20)			3.85		2.17	(0.68)			1.40	(0.34)			2.44	(0.82)		
ΔIsoprene/ΔCO	0.43	(0.39)			0.80		1.68	(0.84)			4.91	(1.5)			4.29	(1.7)		
mass 69[j]			0.88	(0.39)		2.23			4.11	(0.59)			10.2	(3.6)			6.33	(4.6)
$\Delta NH_3/\Delta CO$	20.4	(18.2)			160.5		42.8	(1.7)			37.0	(4.0)			68.3	(32.3)		
$\Delta HCN/\Delta CO$	3.18	(0.44)			41.1		5.41	(1.2)			5.12	(1.0)			6.68	(0.75)		
$\Delta NO/\Delta CO_2$	1.02	(0.17)			0.89		1.55	(0.13)			0.74	(0.47)			1.51	(0.40)		
$\Delta CH_3CN/\Delta CO$			1.21	(0.62)		17.3			3.57	(0.43)			5.36	(1.2)			5.23	(2.1)
$\Delta C_3H_5N/\Delta CO$			0.17	(0.06)					0.71	(0.12)			1.25	(0.28)			1.16	(0.72)
$\Delta C_3H_3N/\Delta CO$			0.36	(0.11)					0.61	(0.12)			0.70	(0.14)			1.12	(0.35)

[a] Standard deviation in parentheses.

[b] Number in parantheses following fuel type denotes number of fires sampled.

[c] HFo - Formic acid.

[d] HAc - Acetic acid.

[e] GA - Glycolaldehyde.

[f] PTR-MS mass 61 can be compared to FTIR (ΔHAc + ΔGA)/ΔCO.

[g] MEK - Methylethylketone.

[h] PTR-MS acetone values are PTR mass 59 minus FTIR MVE.

[i] MVE - Methylvinylether

[j] PTR-MS mass 69 can be compared to FTIR (ΔFuran + ΔIsoprene)/ΔCO.

Table 6. Average Emission Factors for Indonesian Fuels.[a]

	Alang-alang (4)[b]		IndoPeat (1)		IndoSFLit (4)		Rice Straw (3)		Semak (4)	
	OP-FTIR	PTR-MS	OP-FTIR	PTR-MS	OP-FTIR	PTR-MS	OP-FTIR	PTR-MS	OP-FTIR	PTR-MS
CO_2	1629 (19)		1703		1618 (83)		1216 (97)		1567 (35)	
CO	51.6 (8.6)		210.3		112.5 (31.6)		179.9 (39.8)		122.0 (12.8)	
CH_4	0.90 (0.50)		20.80		5.26 (1.95)		9.59 (2.01)		6.41 (0.86)	
C_2H_4	0.47 (0.26)		2.57		1.31 (0.55)		2.84 (0.86)		2.33 (0.59)	
C_2H_2	0.13 (0.05)		0.06		0.22 (0.08)		0.47 (0.13)		0.50 (0.26)	
C_3H_6	0.24 (0.22)	0.25 (0.12)	3.05	3.71	0.89 (0.61)	2.58 (1.32)	1.52 (0.86)	5.35 (1.21)	1.61 (0.18)	3.92 (0.66)
Benzene		0.10 (0.03)		3.19		0.43 (0.07)		0.87 (0.20)		0.71 (0.09)
Toluene		0.04 (0.02)		1.55		0.51 (0.12)		1.08 (0.35)		0.80 (0.37)
HCOOH	0.15 (0.07)	0.04 (0.01)	0.79	0.30	0.65 (0.30)	0.44 (0.29)	2.12 (0.26)	0.80 (0.20)	0.92 (0.34)	0.39 (0.14)
CH_3COOH	0.73 (0.32)		8.97		10.56 (6.96)		10.61 (1.91)		10.87 (5.45)	
Glycolaldehyde	0.27 (0.15)		1.59		1.06 (0.48)		5.31 (1.01)		1.95 (0.55)	
mass 61 [c]		0.99 (0.46)		11.04		13.66 (7.43)		26.39 (2.75)		13.51 (10.96)
HCHO	0.54 (0.26)		1.40		1.64 (0.84)		3.17 (0.88)		2.49 (0.72)	
CH_3CHO		0.38 (0.24)		3.27		2.03 (1.04)		7.05 (1.59)		2.79 (0.32)
Methanol	0.40 (0.28)	0.35 (0.24)	8.69	8.23	3.02 (2.13)	3.10 (1.98)	6.32 (2.19)	6.07 (1.77)	3.55 (1.17)	3.30 (1.19)
Phenol	0.22 (0.20)	0.14 (0.07)	3.62	3.37	2.65 (1.60)	0.95 (0.25)	2.94 (0.78)	4.34 (1.27)	1.97 (1.00)	1.68 (1.16)
Acetol	0.92-1.59	0.28 (0.18)	4.28	2.21	6.12 (3.63)	2.32 (1.69)	34.48 (6.74)	21.34 (5.15)	8.69 (3.35)	4.15 (4.15)
MEK[d]		0.25 (0.11)		2.25		1.82 (0.73)		5.12 (0.84)		1.79 (1.06)
Acetone[e]		0.21 (0.19)	1.25	2.69	0.95 (0.70)	1.32 (0.74)	2.53 (0.40)	6.39 (1.15)	0.95 (0.19)	2.11 (1.14)
MVE[f]	0.08 (0.01)		0.85		0.64 (0.16)		0.43 (0.07)		0.58 (0.13)	
Furan	0.14 (0.04)		1.91		0.63 (0.33)		0.62 (0.24)		0.71 (0.21)	
Isoprene	0.06 (0.06)		1.38		0.49 (0.36)		2.14 (0.88)		1.23 (0.37)	
mass 69[g]		0.11 (0.06)		1.05		1.09 (0.34)		3.63 (1.08)		1.67 (1.07)
NH_3	0.70 (0.68)		19.92		2.91 (0.78)		4.10 (1.24)		4.95 (2.19)	
HCN	0.16 (0.04)		8.11		0.60 (0.27)		0.87 (0.19)		0.78 (0.10)	
NO	1.13 (0.20)		1.00		1.71 (0.18)		0.62 (0.40)		1.62 (0.44)	
CH_3CN		0.09 (0.06)		4.91		0.58 (0.22)		1.19 (0.35)		0.86 (0.27)
C_3H_5N		0.02 (0.01)				0.15 (0.05)		0.35 (0.01)		0.25 (0.12)
C_3H_3N		0.04 (0.02)				0.12 (0.02)		0.19 (0.01)		0.24 (0.07)

[a] g/kg dry fuel (ash free), CO and CO_2 by TECO and LICOR, standard deviation in parentheses.

[b] Number in parentheses following fuel type denotes maximum number of fires sampled.

[c] PTR-MS mass 61 can be compared to FTIR CH_3COOH + Glycolaldehyde.

[d]MEK, Methylethylketone.

[e]PTR-MS acetone values are PTR-MS mass59 minus FTIR MVE.

[f]MVE, Methylvinylether.

[g]PTR-MS mass 69 can be compared to FTIR Furan + Isoprene.

Table 7. Emission ratios relative to CO_2 (ppbv/ppmv) for the top trace gas emissions (excluding H_2O and SO_2) from fires in Indonesian fuels, in order of abundance.

Compound	Emission Ratio (ppbv/ppmv CO_2)	Emision Factor[a] (g/kg)
Carbon dioxide (CO_2)	1000	1509
Carbon monoxide (CO)	142.7	137
Hydrogen (H_2)[b]	49.7	3.41
Methane (CH_4)	13.6	7.46
Ammonia (NH_3)	9.39	5.47
Acetic acid (CH_3COOH)	3.91	8.05
Methanol (CH_3OH)	3.45	3.79
Acetol ($C_3H_6O_2$)[c]	3.15	7.99
Nitrogen (N_2)[d]	2.87	2.76
Acetaldehyde (CH_3CHO)	2.05	3.09
Ethylene (C_2H_4)	1.90	1.82
Formaldehyde (HCHO)	1.85	1.90
Hydrogen cyanide (HCN)	1.75	1.62
Nitric oxide (NO)	1.14	1.17
Acetone (C_3H_6O)[e]	1.03	2.05
Acetonitrile (CH_3CN)	0.93	1.31
Methylethylketone (C_4H_8O)	0.93	2.30
Propylene (C_3H_6)	0.92	1.33
Glycolaldehyde ($C_2H_4O_2$)	0.92	1.89
Phenol (C_6H_5OH)	0.65	2.10
Formic acid (HCOOH)	0.55	0.87
Benzene (C_6H_6)	0.35	0.94
Acetylene (C_2H_2)	0.35	0.31
Isoprene (C_5H_8)	0.35	0.82
Furan (C_4H_4O)	0.31	0.72
Methylvinylether (C_3H_6O)	0.25	0.50
Toluene ($C_6H_5CH_3$)	0.25	0.79
Propanenitrile (C_3H_5N)	0.12	0.23
Propenenitrile (C_3H_3N)	0.10	0.18

[a]Calculated from this set of emission ratios at the average, ash-free fuel carbon content of 50%.

[b]Estimated from data for Brazil [*Ward et al.*, 1992].

[c]Average of PTR-MS and FTIR result.

[d]Estimated from data of [*Kuhlbusch et al.*, 1991].

[e]PTR-MS mass 59 minus FTIR methylvinylether. FTIR acetone = 0.62.

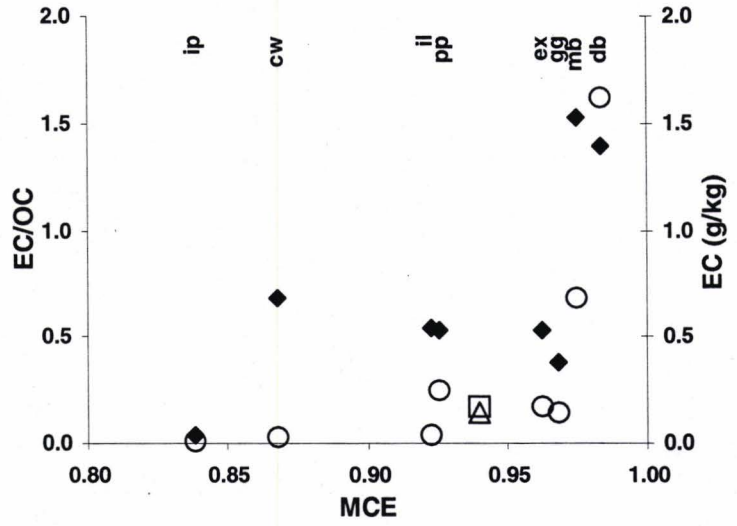

Figure 1. The particle EC/OC ratio and the EC emission factors measured in this study are plotted against MCE. Open circles represent EC/OC. Also shown are global averages for savanna fires: open box - [*Sinha et al.*, 2003], open triangle - [*Andreae and Merlet*, 2001]. Black diamonds represent our EC values. (Two letter fuel type abbreviations are shown at the top of the plot.) Field fires that burn at high MCE may be contributing more EC than previously thought.

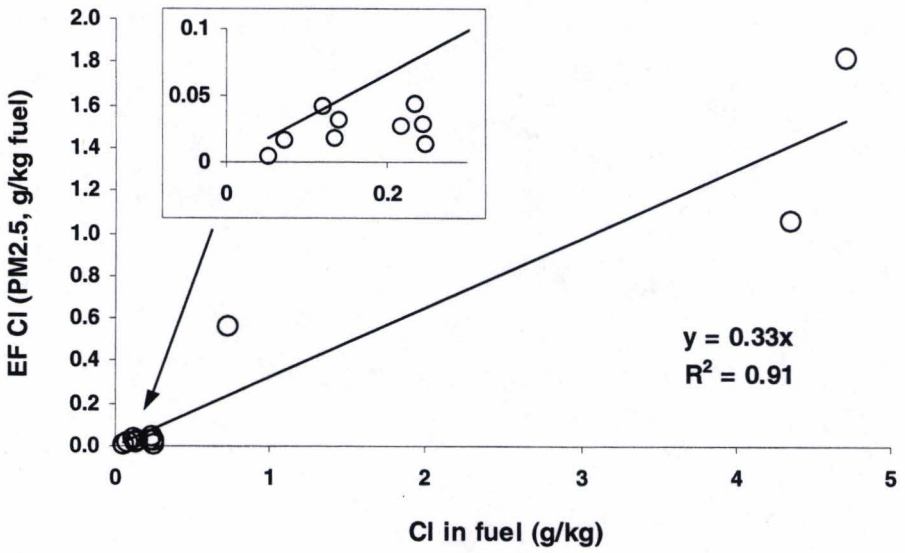

Figure 2. Regression of particle chlorine content against fuel chlorine content suggesting that ~one-third of the fuel chlorine is transferred to the particles. However, the inset shows that the regression does not fit the many low values well.

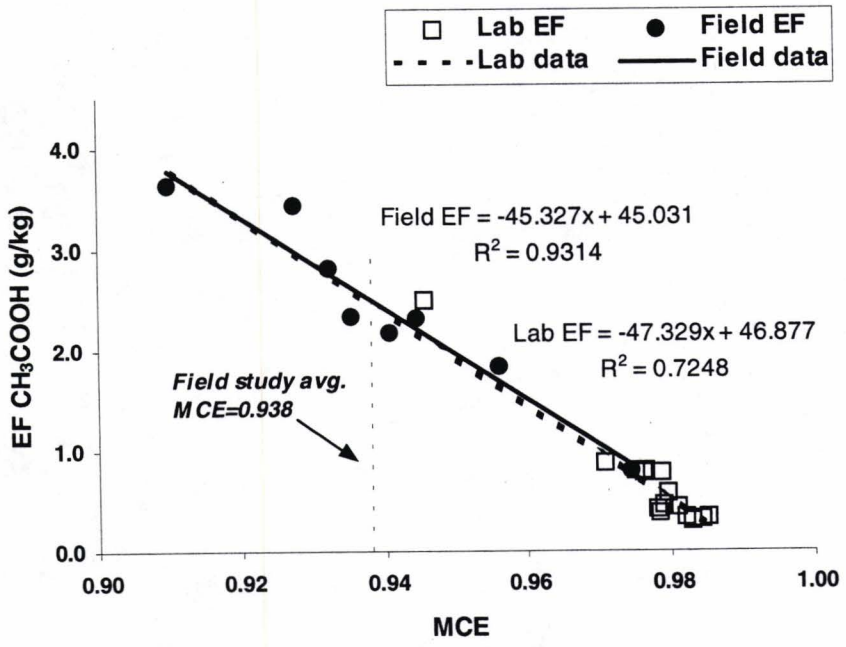

Figure 3. The emission factor (EF) for acetic acid vs. MCE for field data (filled circles) and lab data (open squares). The data sets overlap, but the lab data was obtained at higher MCE on average. Independent regressions of EF vs MCE for the individual data sets predict similar EF at the field study average MCE. (The lab fire at MCE ~ 0.94 was from miombo litter only, which is not a complete fuel complex. This data point was omitted from the lab regressions, which improved the r^2 values.)

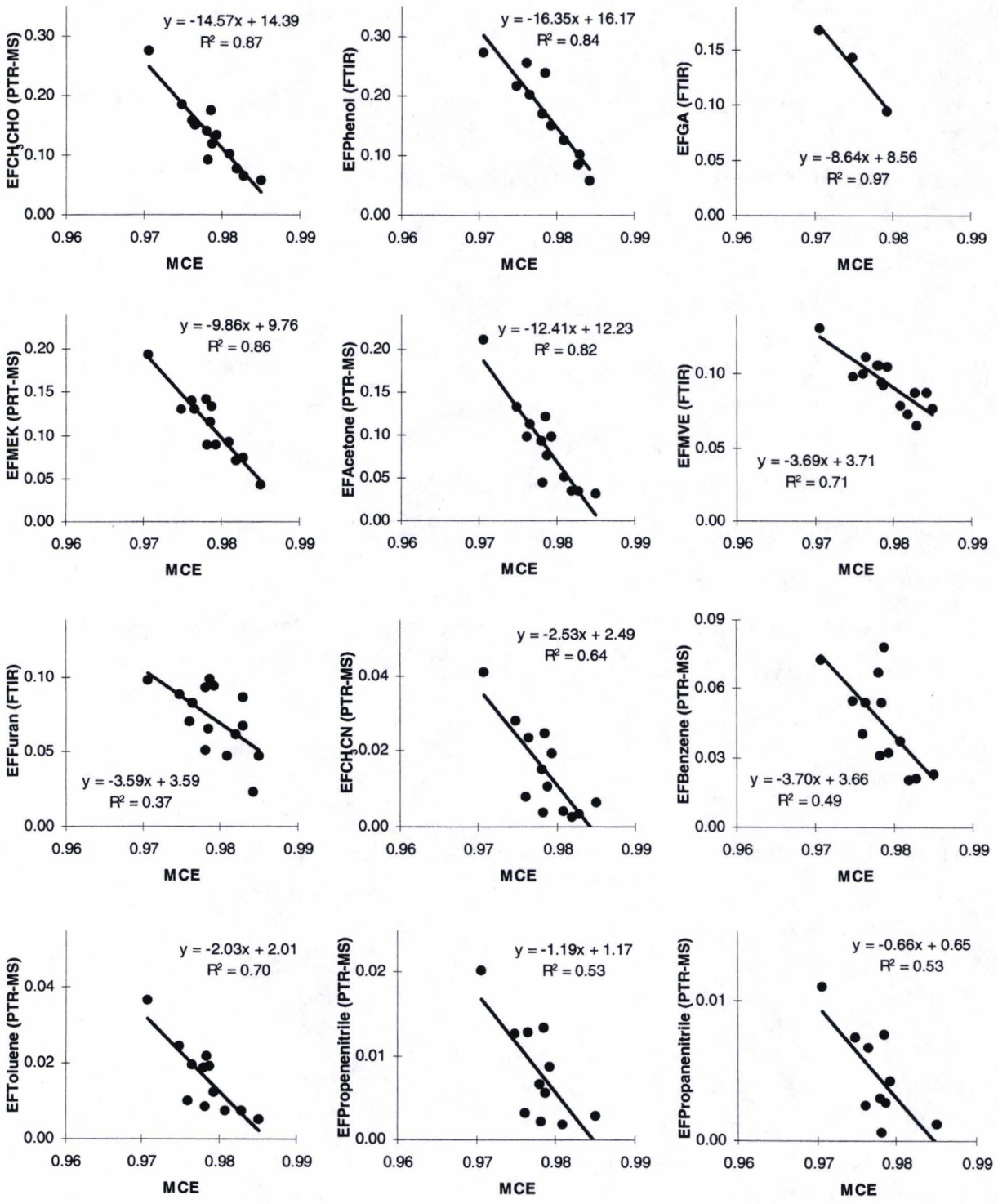

Figure 4. EF vs. MCE for 12 fire emissions that were below FTIR detection limits in an African field study, but successfully quantified in this work. The regression equations were used as described in the text to derive values for Table 4.

Publication 2

Comprehensive laboratory measurements of biomass-burning emissions: II, First intercomparison of open-path FTIR, PTR-MS, GC-MS/FID/ECD.

T.J. Christian[1], B. Kleiss[2], R.J. Yokelson[1,3], R. Holzinger[2], P.J. Crutzen[2,4], J. Williams[2], W.M. Hao[5], T. Shirai[6], and D.R. Blake[6]

[1]University of Montana, Department of Chemistry, Missoula.

[2]Max-Planck-Institute for Chemistry, Atmospheric Chemistry Department, Mainz.

[3]Corresponding author.

[4]Also at Scripps Institution of Oceanography, University of California, San Diego La Jolla.

[5]USDA Forest Service, Fire Sciences Laboratory, Missoula.

[6]University of California, Department of Chemistry, Irvine.

Submitted for publication to Journal of Geophysical Research-Atmospheres (with companion papers): April 2003.

Revised:

Accepted:

Abstract. Oxygenated volatile organic compounds (OVOC) dominate atmospheric organic chemistry, but they are difficult to measure reliably at low levels in complex mixtures. Several techniques that have been used to speciate non-methane organic compounds (NMOC) including OVOC were codeployed/intercompared in well mixed smoke generated by 47 fires in the USDA Forest Service Fire Sciences Combustion Facility. The agreement between proton transfer reaction mass spectrometry (PTR-MS) and open-path Fourier transform infrared spectroscopy (OP-FTIR) was excellent for methanol (PT/FT 1.04 ± 0.118) and good on average for phenol (0.843 ± 0.845) and acetol (~0.81). The sum of OP-FTIR mixing ratios for acetic acid and glycolaldehyde agreed (within experimental uncertainty) with the PTR-MS mixing ratios for protonated mass 61 (PT/FT 1.2 ± 0.37) and the sum of OP-FTIR mixing ratios for furan and isoprene agreed with the PTR-MS mixing ratios for protonated mass 69 (PT/FT 0.793 ± 0.463). The sum of OP-FTIR mixing ratios for acetone and methyl vinyl ether did not account for all the PTR-MS protonated mass 59 signal (PT/FT 1.79 ± 1.14) suggesting that one of these compounds was underestimated by OP-FTIR or that it failed to detect some other compounds that could contribute at mass 59. Canister grab sampling followed by gas chromatography (GC) analysis by two different groups agreed well with OP-FTIR for ethylene, acetylene, and propylene. However, these propylene levels were below those observed by PTR-MS (PT/FT 2.4 ± 0.85). The agreement between PTR-MS and GC-MS was good for methylethylketone (GC/PT ~0.85) and fair for methylvinylketone (GC/PT ~1.5). However ~2-3 times more benzene, toluene, and p-xylene were observed using GC-MS alone than by PTR-MS suggesting that these compounds formed during storage in the canisters. For a separate group of canisters analyzed by multiple detectors good average agreement with PTR-MS was obtained for benzene and toluene. At mixing ratios above a few parts per billion, the OP-FTIR has advantages for measuring sticky compounds (e.g. ammonia, formic acid) or compounds with low proton affinity (e.g. hydrogen cyanide, formaldehyde). Even at these levels, only the PTR-MS reliably measured acetonitrile and acetaldehyde (weak IR cross-sections). Below a few ppbv, only the PTR-MS has good signal to noise in real time for a variety of OVOC, but the possibility of fragmentation, interference, and sampling losses must be considered.

1. Introduction

It is widely accepted that detailed models are needed to quantify the complex chemistry of the atmosphere. It is also true that the output of these models is sensitive to trace gas species present at very low levels. A dramatic example of this is O^1D, a key species in atmospheric photochemical models that is present at levels so low that it will never be measured [*Albritton et al.*, 1990]. OH and HO_2 (collectively known as HO_x) are two other species of prime importance (largely derived from O^1D) that have been measured reliably only recently [*Mount and Williams*, 1997; *Brune et al.*, 1998].

The organic chemistry of the atmosphere is of great interest for many reasons including its major influence on O_3 (and thus O^1D), HO_x, and the oxidizing efficiency (power) of the atmosphere [*Mason et al.*, 2001]. Until recently, it was widely assumed that the organic chemistry of the atmosphere was well understood, mainly because hydrocarbons (which were thought to be the main organic constituents of the atmosphere) are routinely speciated at ppt levels by a variety of GC based techniques [e.g. *Blake et al.*, 1996]. The hydrocarbon/O_3 observations were reasonably consistent with atmospheric models, especially for smog chambers [*Carter et al.*, 1979] or urban airsheds [*McRae and Seinfeld*, 1983]. However, in the 1990s, it has become clear that oxygenated volatile organic compounds (OVOC) account for most of non-methane organic compounds (NMOC) from biomass burning [*Griffith et al.*, 1991; *Yokelson et al.*, 1996, 1997, 1999, 2003; *Worden et al.*, 1997; *Holzinger et al.*, 1999] and that they are major emissions from plants [*Konig et al.*, 1995; *Kirstine et al.*, 1998]. Together these sources are thought to be as large as the main global trace gas source: fossil fuel burning. In addition, the non-methane hydrocarbons (NMHC) emitted by fossil-fuel burning quickly become OVOC in the atmosphere, mainly by reaction with OH. Thus, it is not surprising that the recent TRACE-P campaign to characterize the background troposphere concluded that OVOC are about five times more abundant than NMHC [*Singh et al.*, 2001], more reactive than NMHC [*Singh et al.*, 1995], and consequently more important. Further, current photochemical models (at various local-global scales) are unable to rationalize the simultaneous observations of PAN, acetaldehyde etc. [*Flocke et al.*, 2002; *Chatfield et al.*, 2002; *Staudt et al.*, 2003]. This is a crucial weakness since OVOC photochemistry is a major HO_x source, especially in drier parts of the troposphere. Finally, the few initial field observations of OVOC multiphase chemistry are not explained by available chemical mechanisms [*Yokelson et al.*, 2003]. Thus, it is clear that the organic chemistry of the atmosphere is not well understood and that a great need exists for instrumentation that can reliably identify and quantify the OVOC in both field and laboratory studies. This paper describes the first informal, but rigorous, codeployment/intercomparison of the major, currently available techniques that have potential to provide broad characterization of NMOC, including OVOC. The measurements probed well-mixed smoke generated by 47 fires burned in the USDA Forest Service, Fire Sciences Laboratory (FSL) in Missoula, MT. The trace gas measurement techniques employed included canister sampling followed by GC-MS, GC-FID, and GC-ECD analysis performed by three groups along with PTR-MS (proton transfer reaction mass spectrometry) and FTIR (Fourier transform infrared spectrometry). The canister techniques have been widely used for many years and provide analysis (with preconcentration) at ppt levels [*Montzka et al.*, 1993]. However, they are subject to sampling and storage artifacts for trace gases that are reactive or sticky, which happen to comprise the majority of gases of interest to atmospheric chemistry. Open path FTIR (OP-FTIR) is artifact-free. Since all molecules have a unique IR signature, FTIR is well suited for identification and quantification of most trace gases, but not below ppb levels [*Goode et al.*, 1999], which are needed to probe the clean troposphere.

PTR-MS involves no sample storage and can quantify down to ppt levels virtually any volatile gas with a proton affinity moderately above that of water. However, PTR-MS provides only one peak for a mass/charge ratio that could represent several species, which makes compound identification challenging under some conditions [*Williams et al.*, 2001]. In summary, each technique has its strengths and weaknesses. The focus of this paper is to learn by employing these methods simultaneously. A detailed discussion of the emissions from African and Indonesian fuels appears in a companion paper [*Christian et al.*, this issue].

2. Experimental

2.1. Combustion Facility

The combustion facility at FSL is in a room that measures 12.5 m^2 x 22 m high (Figure 1). A 1.6 m diameter, inverted funnel, exhaust stack with a 3.6 m diameter opening extends from ~2 m above the floor through the ceiling. The room is pressurized with outside air that has been conditioned for temperature and humidity, and is then vented through the stack, completely entraining emissions from fires burning beneath the funnel. The fires are burned on a continuously weighed fuel bed (80 x 210 cm) covered by an inert heat shield and a layer of sand. A sampling platform surrounds the stack at 17 m elevation where all the temperature, pressure, trace gas, and particle measurement equipment for this experiment was deployed except background CO_2 (LICOR 6262). An orifice near the base of the stack promotes mixing of the emissions. Three separate tests have shown that the emissions are very well mixed in the stack at the height of the sampling platform: (1) The temperature profile across the stack at this height is "flat," even as the temperature rises and falls due to fires burning below. (2) The average mixing ratios for an optical path that spanned the stack were the same as those measured by point sampling at the stack center (for CO_2, CO and hydrocarbons) [*Goode et al.*, 1999]. (3) The mixing ratios for reactive or sticky species were constant across the width of the stack, as determined by quickly moving the inlet for the PTR-MS to different positions within the stack (Figure 2). The fuel selection criteria for African, Indonesian, and other fuels; fuel sampling and fuel characterization methodology; and fire simulations are described in detail in a companion paper [*Christian et al.*, this issue].

2.2. Trace Gas and Particle Instrumentation

2.2.1. Open-path FTIR. The open path Fourier transform infrared spectrometer (OP-FTIR) was positioned on the sampling platform so that the open white cell spanned the stack directly in the rising emissions stream for continuous (0.83 s resolution) scanning. The OP-FTIR system [*Yokelson et al.*, 1997] includes a MIDAC model 2500 spectrometer; the 1.6 m base path, open White cell; and an MCT (mercury-cadmium-telluride), LN_2-cooled detector. The path length was set to 57.7 m and spectral resolution was 0.5 cm^{-1}. All spectra were saved in real time on a laptop computer synchronized with the rest of the data acquisition. Before each fire, we scanned for 2-3 minutes to obtain a background spectrum, and then we made absorbance spectra for each scan during the fire at 0.83 s resolution using the appropriate background spectrum. For long-duration fires (~1 hr) with slowly changing temperature and emissions, we increased the signal to noise ratio (S/N) through spectral averaging of up to 72 scans (~1 min resolution). For shorter fires with larger or more rapid temperature fluctuations, spectral averaging was limited to ~6 s resolution (7 scans).

We used classical least squares spectral analysis [*Griffith*, 1996; *Yokelson and Bertschi*, 2002; *Yokelson et al.*, 1996] to retrieve excess mixing ratios for water (H_2O), methane (CH_4), methanol (CH_3OH), ethylene (C_2H_4), phenol (C_6H_5OH), acetone ($CH_3C(O)CH_3$), acetol ($CH_2(OH)C(O)CH_3$), isoprene (C_5H_8), hydrogen cyanide (HCN), acetylene (C_2H_2), furan

(C_4H_4O), nitric oxide (NO), and formaldehyde (HCHO). We used spectral subtraction [*Yokelson et al.*, 1997] to retrieve excess mixing ratios for water (H_2O), ammonia (NH_3), formic acid (HCOOH), acetic acid (CH_3COOH), glycolaldehyde ($CH_2(OH)CHO$), propylene (C_3H_6), and methylvinylether (MVE, CH_3OCHCH_2). While CO_2 and CO are accurately measured by OP-FTIR [*Goode et al.*, 1999], due to the large volume of data, we opted to use the convenient, synchronized data for these molecules from the real-time instruments (vide infra). The molecules discussed above account for all the major features observed in all the IR spectra. The detection limit for most gases was 5-20 ppb for a one-minute measurement time (72 scans) and ~10-50 ppb at the highest time resolution used (6 s or 7 scans).

The advantages of OP-FTIR trace gas measurements include: (1) There is no sampling and thus, no possibility of sampling or storage artifacts. (2) Since most molecules have multiple, unique features there is very high resistance to interference and excellent compound identification. (3) A large number of reactive and stable molecules can be simultaneously quantified with high (~1 s) temporal resolution at ppb-percent levels and unanticipated compounds can be quantified. (4) The optical path can be adjusted to integrate over the whole phenomenon being investigated, which reduces the uncertainty associated with point sampling. The main disadvantages of FTIR are: (1) a nonlinear response for some species, which requires a time-consuming analysis [*Yokelson and Bertschi*, 2002]. (2) Homonuclear diatomic molecules (e.g. H_2, N_2), some sulfur molecules (e.g. H_2S), and a few other molecules have only weak IR features. (3) Some compounds (e.g. CH_3Cl, glyoxal, acetonitrile) have strong IR features, but they are overlapped by very strong water lines. (4) FTIR is limited by source stability to ppb detection limits without preconcentration, which is inadequate for most molecules in clean air. FTIR detection limits can be in the ppt range with preconcentration [*Hanst*, 1975], but then the advantages for quantifying reactive and sticky compounds are lost.

2.2.2. PTR-MS. The PTR-MS sampled continuously from the emissions stream through ~2 m of 6 mm i.d. Teflon tubing that opened directly above the center of the OP-FTIR optical path. It was established at the outset that moving the inlet did not effect the results (Figure 2), nor did placement of a Teflon filter over the inlet entrance. The sample line was short to minimize losses and assure a fast response time (around 5 s). The PTR-MS employs chemical ionization to measure volatile organic compounds (VOC) in real time [*Hansel et al.*, 1995; *Lindinger et al.*, 1998]. Briefly, the instrument features a hollow cathode ion source that produces H_3O^+ reactant ions from water vapor in the sample. The sample air then passes through a drift tube where VOC with proton affinities > water are ionized by proton transfer reactions with the H_3O^+. The product ions are analyzed by a quadrupole mass spectrometer. Under favorable operating conditions less than 5% of the H_3O^+ ions react with VOC in the sample and the concentration of product ions in the sample can be calculated using equation (1),

$$[VOC - H^+] \cong [H_3O^+]_0 [VOC] k_{VOC} t \qquad (1)$$

where $[H_3O^+]_0$ is the density of H_3O^+ ions in the absence of neutral reactants, k_{VOC} is the respective reaction rate constant for the proton transfer from H_3O^+ to the VOC and t is the reaction time, which depends on length, pressure and voltage of the drift tube. The reaction rate of most exothermic proton transfer reactions is nearly equal to the collision rate, and when specific reaction rates are unknown they can be calculated [*Su and Chesnavich*, 1982]. An average reaction rate constant of 2×10^{-9} cm^3 s^{-1} was used for the quantification of unidentified ions.

During these experiments, the PTR-MS operated in either of two modes. In full mass scan mode the instrument was configured to scan incrementally from 17 to 142 atomic mass units, with a sample time of 20 ms per mass. In selected mass scan mode the instrument was configured to scan a selection of 30-36 masses, with a sample time of 0.1-0.2 s. Overall time resolution for either mode was about 4 to 8 s. The PTR-MS computer was synchronized with the rest of the data acquisition and the results were splined to match the OP-FTIR points. Even for molecules with unknown rate constants, the overall accuracy should be better than ±50% with the estimate of the reaction rate constant (±30%) being the main source of error.

The strengths of PTR-MS [*Lindinger et al.*, 1998] include: (1) The response is linear up to ppm levels and the detection limits are in the ppt range without preconcentration, which is adequate sensitivity for many species in clean air. (2) A wide variety of NMOC, including most OVOC, can be detected. (3) The measurement time for an individual mass is very fast (on the order of milliseconds) allowing rapid online monitoring of a single mass or sequential measurements of numerous masses repeated with high frequency. (4) The mixing ratios are available quickly without complex analysis of spectra or chromatograms even for unidentified species. Disadvantages of PTR-MS include: (1) Only molecules with a proton affinity ~10 kcal/mole or more above that of water can be routinely measured. Molecules with proton affinity closer to water (e.g. HCHO, HCN) can be measured if the water concentration is known and a correction is made, but this may be impractical in many situations. (2) Losses can occur on the sample line or within the instrument. (3) Compound identification can be complicated by the presence of isomers and quantification can be compromised by isomers and fragmentation. Fragmentation ratios can be measured for individual compounds, but, in practice, fragmentation of large, unidentified compounds could add unwanted signal to lower masses.

2.2.3. Canister sampling. Up to three evacuated stainless steel canisters could be simultaneously filled in ~10 s to ambient pressure via a "cross" manifold and a 4 mm i.d. stainless steel sampling tube that opened next to the PTR-MS inlet. The sample line pressure was logged on the data system so that the filling time of these "quick cans" with respect to other instruments was precisely known. "Integrated" cans were filled at a pre-selected linear rate, over a precisely known period, through another collocated inlet. Forty integrated cans and 28 quick cans, taken before or during most fires, were analyzed by GC-FID for C_1-C_4 hydrocarbons by the USDA Forest Service. Eight of the 18 quick cans filled during the fires for analysis by GC-MS in Mainz were analyzed for acetonitrile, acetone, isoprene, methyl vinyl ketone, methyl ethyl ketone, benzene, toluene, and p-xylene. Eight quick cans taken during the fires were analyzed at UC Irvine by collective consideration of five chromatograms (2 GC-FID, 1 GC-MS, and 2 GC-ECD) to obtain mixing ratios for ethylene, propylene, acetylene, isoprene, benzene, toluene, and p-xylene. All the cans were analyzed 2-3 months after collection. More details about the canister analysis protocols are found elsewhere [*Hao et al.*, 1996; *Williams et al.*, 2001; *Colman et al.*, 2001]. The chief advantage of canister sampling/GC analysis is reliable, linear measurements of very stable, non-sticky species down to ppt levels if preconcentration is used. The chief disadvantages include: the measurements are intermittent (high time resolution is impractical), results are not immediately available, and it is impossible to measure reactive or sticky molecules and very difficult to know which gases are being measured accurately [*Kelly and Holdren*, 1995].

2.2.4. Other measurements. The 19 mm inlet used for filling canisters at a linear rate also provided sample air for continuous CO_2 (LICOR 6262) and CO (TECO 48C) measurements. The TECO and both LICORs (including the background air monitor) were calibrated daily with NIST

traceable standards. Stack air was drawn at 30 L min^{-1} through dielectric tubing to a cyclone to remove particles larger than 2.5 μm effective diameter, then onto Teflon or quartz filters. Teflon filters were analyzed gravimetrically by the USFS [*Trent et al.*, 2000] and then by XRF, which provided halogens, potassium, and sulfur. Quartz filters were analyzed for organic and elemental ("black") carbon by independent laboratories. We continuously monitored temperature, pressure, flow (Kurz model 455), and fuel mass with 2 s resolution.

3. Results and Discussion

3.1 Detailed results organized in order of ascending mass

We present the detailed results in ascending order of the relevant PTR-MS mass channel. The PTR-MS is designed to avoid ionizing trace gases with proton affinity (PA) ≤ water. This conveniently excludes some abundant gases such as CO_2, CO, H_2, O_2, etc. that would scavenge too many reactant ions and can be measured by other means. The FTIR measured 7 trace gases with PA ≤ water - CO_2, CO, H_2O, CH_4, C_2H_2, C_2H_4, and NO. Next, we present a quantitative discussion of the agreement between PTR-MS, OP-FTIR, and canister sampling for gases with PA > H_2O. (Details of the emissions by compound and fuel type are given in the companion paper by *Christian et al.*, [this issue].)

Mass 18 – ammonia. Ammonia has a high proton affinity relative to water, but it readily sticks to surfaces [*Yokelson et al.*, this issue]. Thus, the PTR-MS response time is on the order of hours. The OP-FTIR is immune to sampling artifacts, the NH_3 S/N was high for all fires, and the IR spectral analysis by two different methods agreed well. As part of this work, *Yokelson et al.* [this issue] compared the NH_3 rise time in a closed-cell FTIR system to that of non-sticky gases. Due to passivation of the Pyrex cell the NH_3 rise was delayed by 10-30 s, depending on flow rate.

Mass 28 - HCN, mass 31 - HCHO. HCN and HCHO were initially reported by both instruments. However, these compounds have a PA close enough to that of H_2O to allow deprotonation to be important in the PTR-MS drift tube and their observed concentrations are highly dependent on humidity. It requires detailed calibration over a range of relative humidities to accurately measure HCN and HCHO by PTR-MS. Those calibrations were not done in this experiment. *Hansel et al.*, [1997] described a rough method to correct HCN and HCHO mixing ratios without calibration. Their method, applied to our experiment, suggests multiplying the mixing ratios for HCN and HCHO by 4 and 8, respectively. The rough correction results in PTR-MS/OP-FTIR ratios for HCN and HCHO of 0.35 and 1.38. Therefore, we used the OP-FTIR results for these two trace gases in the companion paper by *Christian et al.* [this issue].

Mass 33 - methanol (PT/FT = 1.04 ± 0.118, n = 38). Figure 3a shows the temporal profiles for methanol measured by PTR-MS and OP-FTIR for the third ponderosa pine fire. We integrated the methanol mixing ratios from the PTR-MS over the whole fire and divided that number by the integrated mixing ratios from the OP-FTIR (PTR-MS/OP-FTIR = 1.01). This method of comparison was generalized to all fires for all the jointly measured compounds with PA > H_2O to provide a standard way to quantify the overall agreement observed between PTR-MS and OP-FTIR. In the parentheses in each heading, we show the study-average for the integrated PTR-MS excess emission ratios divided by the integrated OP-FTIR excess emission ratios (abbreviated PT/FT). (The average and the standard deviations were computed after discarding the highest and lowest ratio for each compound and n indicates the number of fires used in the computation.) There was excellent agreement between PTR-MS and OP-FTIR for methanol for all the fires except the single miombo litter fire. The ratio for this fire (1.60) was not used in the calculation of the PT/FT ratio shown above.

Mass 42 - acetonitrile. The PTR-MS detected mass 42 in all fires. This mass is attributed to acetonitrile [*Williams et al.*, 2001], as there are no other plausible, non-radical, non-ionic candidates and there are no known fragmentation ions at this mass. The IR cross-section for acetonitrile is small and we did not detect it in any FTIR spectra. The canisters collected for Mainz GC-MS analysis were analyzed for acetonitrile. The average PTR-MS mixing ratio during the time a can was collected was usually only about one-half the canister mixing ratio (see Table 1). Since acetonitrile does not fragment, we speculate that the difference may be due to formation of acetonitrile in the canisters.

Mass 43 - propylene (PT/FT = 2.38 ± 0.849, n = 19; GC/FT = 0.79 ± 0.39, n = 10). The PTR-MS normally measured higher mixing ratios for mass 43 than the propylene mixing ratios measured by OP-FTIR. The OP-FTIR data for propylene from several fuel types, including African savanna fuels, was excluded from this comparison because of very low S/N. No other compounds with protonated mass 43 were detected by OP-FTIR (e.g. cyclopropane). Separate experiments showed that 30% of acetic acid (protonated mass 61) fragments to mass 43 in the PTR-MS. That is, some protonated acetic acid loses H_2O and forms CH_3CO^+. Other gases with protonated mass 61 may also contribute to mass 43 via similar mechanisms (e.g. glycolaldehyde to yield CH_3CO^+ or propanol to yield $C_3H_7^+$ [*Williams et al.*, 2001], but their fragmentation was not measured. A 30% correction was made to the PTR-MS mass 43 data to account for fragmentation of mass 61 (which was primarily acetic acid with smaller amounts of glycolaldehyde). Specifically the raw ppb mass 61 was adjusted upwards by 30% and then the raw ppb mass 43 was decreased by 30% of the adjusted ppb mass 61. Table 1 compares propylene mixing ratios from the UCI and USFS quick cans to the average OP-FTIR propylene mixing ratio during the time that the cans were collected. Propylene by GC averaged about 80% of the OP-FTIR propylene. Since 3 groups obtained propylene values substantially lower than the mass 43 signal, it seems likely that a larger, as yet unidentified, species contributes to this mass channel via fragmentation.

Mass 45 - acetaldehyde. Acetaldehyde has not been detected by FTIR in biomass burning emissions. However, the PTR-MS mass 45 signal for these fires was relatively high. CO_2 and N_2O have the same mass as acetaldehyde, but they have low proton affinities and they are not detected by PTR-MS. We could not attribute any IR absorption lines to other mass 45 candidates (with PA > H_2O) such as ethylene oxide. The isolated acetaldehyde features in the IR spectrum are too weak, even at the mixing ratios obtained in this study by PTR-MS to be readily detectable by FTIR. Acetaldehyde may be difficult to measure by techniques other than PTR-MS. For instance, the acetaldehyde mixing ratios measured by GC-RGD (reduction gas detector) during TRACE-P were about one-half those measured simultaneously by fast GC-MS [*Apel et al.*, 2002].

Mass 47 - formic acid (PT/FT = 0.426 ± 0.175, n = 38). The PTR-MS mass 47 signal accounted for only about half the formic acid measured by the OP-FTIR. Losses in the PTR-MS inlet are a likely problem for this sticky compound. Because a fast response was observed at this mass, the signal was probably due to some other, less sticky, mass 47 candidate(s) such as ethanol or dimethylether.

Mass 54 – propenenitrile and Mass 56 – propanenitrile. Propenenitrile seemed to be the only logical candidate for mass 54. Mass 56 was identified as propanenitrile, and included as such in the tables in the companion paper by *Christian et al.*, [this issue], mostly because its emission ratio to CO (0.023%) was similar to the propanenitrile/CO ratio reported by *Lobert et al.*, [1991] (0.02%) when the comparison is restricted to fires in similar fuels (mostly grass and

pine needles). Since fuel nitrogen is variable this identification is admittedly weaker than the others in this work. No search for either of these compounds was made in the IR spectra due to the low levels observed.

Mass 59 - acetone, methylvinylether (PT/FT = 1.79 ± 1.14, n = 29). The best IR peak for acetone is fairly broad and is overlapped by complex structure due to other compounds in smoke. As a result, the presence of acetone was obvious only in the IR spectra for the rice straw fires. The raw OP-FTIR mixing ratios for acetone were adjusted upwards by 20% after we carefully remeasured the IR cross-section and found it to be 20% lower than reported in the commercial reference spectrum. Most of the fires emitted small, but detectable (by FTIR), amounts of methylvinylether, which is also a mass 59 candidate (Figure 3b). The FTIR ratio of acetone to methylvinylether was ~6 for the fires with the highest S/N. The study-average ratio, which included fires with lower S/N, was 1.8 ± 1.9. These two gases are combined in the denominator of the PT/FT ratio shown above. For all dambo fires PT/FT was <1, but for all other fires this ratio was > 1.5. We did not reliably detect any other mass 59 candidates in any fire by FTIR, despite a concerted effort to identify the following compounds with reasonably strong and isolated IR peaks: propanal, trimethylene oxide, and propylene oxide. One other plausible mass 59 candidate is glyoxal, which has been identified as a major product of the fast pyrolysis of biomass [*Thamburaj*, 2000]. However, the glyoxal IR peaks that do not suffer from severe water interference are weak [*T. Dransfield*, personal communication]. No glyoxal features were seen in the IR spectra from the fire with the highest mass 59 signal. Thus, glyoxal accounted for <20% of the mass 59 signal from this fire. We conclude that the signal at mass 59 in these fires is mostly acetone with smaller contributions by MVE and possibly glyoxal. The GC-MS data for acetone is unfortunately inconclusive with the GC/PT ratio ranging from 0.12 to 68 in 8 trials. However, eliminating GC/PT ratios that are more than a factor of 5 different leaves 4 trials with an average value of 0.81. The cans were not analyzed for other mass 59 candidates due to low S/N.

Mass 61 - acetic acid, glycolaldehyde (PT/FT = 1.20 ± 0.367, n = 39). Normally, within experimental uncertainty, all the PTR mass 61 signal is accounted for by acetic acid and its structural isomer glycolaldehyde, as determined by OP-FTIR (Figure 3c). The FTIR signal for acetic acid was strong for all fires and its average ratio to glycolaldehyde was 5.7 ± 3.4. The FTIR glycolaldehyde measurements contribute the most scatter. As detailed in the section on mass 43, the mass 61 signal was corrected to account for fragmentation in the drift tube. In earlier PTR-MS smoke measurements acetic acid was lost on the inlet, but that was evidently overcome in this work by using a shorter wider inlet.

Mass 69 - furan, isoprene (PT/FT = 0.793 ± 0.463, n = 39). The IR spectral analysis for furan is complicated by CO_2 lines at high CO_2 and extra care was needed to correctly retrieve furan. Isoprene was unaffected by high CO_2. The sum of the furan and isoprene (by FTIR) is consistent with the PTR-MS mass 69 signal within experimental uncertainty (Figure 3d). The study-average furan to isoprene ratio was 1.9 ± 1.6. The Mainz GC-MS isoprene values were generally about one-third to one half of the PTR-MS mass 69 values, which is in good general agreement with the FTIR. However, the Mainz cans were analyzed 2-3 months after collection. Some storage tests found that isoprene was stable in cans, but both production and losses of isoprene have also been observed in similar canisters during similar storage periods [*Gong and Demerjian*, 1995; *Sin et al.*, 2001; *Habram*, 1998]. The UCI cans had <3% of the isoprene simultaneously measured by PTR-MS suggesting that storage losses may have occurred for this compound.

Mass 71 – methylvinylketone (GC-MS/PT ~1.5) and Mass 73 - methylethylketone (GC-MS /PT ~0.85). For both of these ketones the agreement between GC-MS and PTR-MS was acceptable and well within experimental uncertainty for methylethylketone. Neither compound was readily apparent in the IR spectra.

Mass 75 - acetol (PT/FT = 0.43 ± 0.30, n = 36; PT/FT = 0. 81 ± 0.018, alternate method). The rice straw fires emitted large amounts of acetol (hydroxyacetone), which is previously unreported in biomass burning emissions. The FTIR retrievals for acetol are based on our own careful measurement of the IR cross-section at five different concentrations. Acetol fragments in the PTR-MS to yield ~80% on mass 75, ~20% on mass 57, and < 2% on mass 43. This fragmentation is accounted for in the PTR-MS retrieval. In theory, a low PT/FT ratio for a compound could arise due to low proton affinity, fragmentation, or inlet losses. However, acetol is not sticky, it has high PA, and the fragmentation has been accounted for. In this case, a remaining explanation for the low ratio could be low signal to noise in some of the data, most likely from the FTIR. In other words, the comparison procedure adopted above weights the ratio from all fires equally. This procedure is justified when good signal to noise is the norm, but could fail if ratios from fires with very poor S/N, and thus high error, are given too much weight in deriving the study average. As an alternative, we can regress the PTR-MS fire-integrated mixing ratios against the simultaneously-measured OP-FTIR fire-integrated mixing ratios for all the fires. The slope of the linear regression line in such a plot gives an estimate of the study-average ratio that heavily weights the larger values, which correspond to higher S/N. While this procedure biases the study-average agreement towards the agreement obtained on fires that happened to have high signal levels, it is a valuable tool when other contributions to "low" ratios can be eliminated. We show such a plot for acetol in Figure 4a. The slope (0.81 ± 0.018), and lack of outliers, implies good agreement between OP-FTIR and PTR-MS whenever there were high signal levels. Similar plots were made to check the implications for other compounds, but, with one exception, they did not suggest a significantly different level of agreement. For acetone, such a plot implies significantly worse agreement, which may rule out low FTIR S/N as the sole cause of the disagreement on this compound.

Mass 79 – benzene (GC-MS/PT ~2.9; GC-UCI/PT ~1.2), Mass 93 - toluene (GC-MS/PT ~3.3; GC-UCI/PT ~1.3), Mass 107 – p-xylene (GC-MS/PT ~2.3; GC-UCI/PT ~0.4). The Mainz canister GC-MS/PTR-MS ratios for these compounds are shown first in the parentheses. There is large scatter in the ratios, and even after removing the ratios that differ from 1 by more than a factor of five we obtain the ratios shown, which are significantly above 1 for all three compounds (Table 1). These compounds are unlikely to fragment in the PTR-MS and additional signal from fragments or other candidates with the same mass (e.g. other xylenes) would decrease (rather than increase) the ratio. Thus, it is possible that formation occurred in the cans. Stability, production, and losses of these compounds have all been observed in canister storage tests in the past [*Schmidbauer and Oehme*, 1988; *Sin et al.*, 2001; *Habram*, 1998; *Kelly and Holdren*, 1995; *Ochiai et al.*, 2002]. These compounds are known, along with ethyl benzene, as "BTEX" compounds and they are of special interest in urban pollution studies. This study suggests that PTR-MS may have advantages over the GC-MS method mandated by the USEPA for measuring these important species. In the UCI cans good agreement was obtained with PTR-MS for benzene and toluene, which strongly supports the single compound identification for these masses in this work. There may have been storage losses of xylene in these cans.

Mass 95 - phenol (PT/FT = 0.843 ± 0.845, n = 28): On average, within the combined uncertainty for the two instruments, all the PTR-MS mass 95 signal is accounted for by the OP-

FTIR phenol, but the scatter is very high. The large scatter was mostly due to fires with lower FTIR S/N for phenol, but there was also evidence (at high S/N) of occasional contributions to the mass 95 signal from a long list of candidates with molecular mass of 94 that includes six with molecular formula C_6H_6O, 10 with formula $C_5H_6N_2$, 52 with formula C_7H_{10}, and candidates containing chlorine or sulfur. Vinyl furan could interfere with phenol at mass 95 and it has several strong, isolated IR peaks. However, no sign of vinyl furan was detected by FTIR even though it has been reported in canister analysis of smoke samples. No other mass 95 candidates were observed by OP-FTIR or in the canisters. In general, as molecular mass approaches 100, the number of candidates for PTR-MS interference grows and broader features characterize the IR spectrum. The larger compounds are harder to measure and also more likely to partially partition into the condensed phase. Finally, to investigate the contribution of low S/N to the scatter we also made a plot using the procedure described above for mass 75. The plot, in Figure 4b, shows numerous low values near the intercept, 5 points at high levels that define a line with slope 1.02 ±0.036, and two high concentration points that lie above the line and increase the slope to 1.13 ± 0.077. This suggests that the agreement was usually excellent at high signal levels, but that something else may have contributed to mass 95 on 2 of the 7 fires with high S/N.

Note on ethylene, propylene, and acetylene. The overall average ratio for light hydrocarbons for the UCI/USFS cans divided by the OP-FTIR is 1.01 ± 0.39, n = 30 (Table 1). This is similar to the agreement for cans and OP-FTIR observed previously by *Goode et al.*, [1999]. This suggests that differences up to ~0.4 can be expected from normal instrumental uncertainties, timing uncertainty, leaks, etc. Thus, other sources of error probably contributed the bulk of the much larger differences observed for some compounds in can/PTR-MS comparisons.

3.2. Summary of results by proton affinity

As stated earlier, we found excellent agreement between FTIR and PTR-MS for methanol for all fires in this study and good overall agreement between cans and OP-FTIR. This suggests that differences that occurred for some other compounds were not due to incomplete mixing, sampling artifacts for "non-sticky" molecules, instrument drift, or other factors. Proton affinity is a key variable affecting detectability by PTR-MS. In Figure 5, for selected individual compounds, we show the study-average value of the integrated PTR-MS mixing ratios divided by the integrated FTIR mixing ratios. Error bars represent one standard deviation. The x-axis is the difference in proton affinity between the compound of interest and water (ΔPA, kcal/mol). When two compounds were detected at the same PTR-MS mass, the average ΔPA is used. Where proton affinity is unknown, we estimated the value. In summary, at low ΔPA the ratio was much less than one due to rapid deprotonation (HCHO and HCN). A simple correction described by *Hansel et al.* [1997] improved the agreement as shown. Sample line or internal losses (NH_3 and HCOOH) and uncorrected fragmentation of the ion being monitored could lead to ratios below 1 even with ΔPA > 10 kcal/mole. Ratios larger than one could result from fragmentation of larger molecules creating spurious signal for the ion being monitored. This may cause the ratio to be larger than one for mass 43 (propylene) since mass 43 is known to be a common fragment mass. The addition of signal from several isomers appearing on the same mass channel could also cause ratios larger than one. In fact, the sum of two compounds detected by FTIR at mass 61 (acetic acid and glycolaldehyde) and mass 69 (furan and isoprene) agrees very well with the total PTR-MS signal. However, at mass 59, the sum of FTIR compounds does not account for all the PTR-MS signal. This could be due to unusually complex interference causing systematically low FTIR retrievals for acetone or the failure of FTIR to detect mass 59 isomers. Smaller deviations from one (positive or negative) could occur from inaccuracy in the

calibration of either instrument. The large spread or standard deviation in the ratio, which is observed in some cases, is likely due to a combination of low FTIR S/N for several gases and changing concentrations of interfering species for PTR-MS.

3.3 Summary of results by the observed agreement and instrument notes

3.3.1. FTIR and PTR-MS similar. For methanol only, we obtained agreement that was excellent for all fires. The PTR-MS would have an advantage measuring methanol in clean air due to its better detection limits. The average agreement is good for PTR-MS mass 95 and FTIR phenol, but with high scatter. At high signal levels, the agreement was usually excellent, but occasionally appears to reflect contributions from other mass 95 candidates. For acetol the agreement was always good at high signal levels.

3.3.2 Sum of FTIR signals similar to PTR-MS. This category includes PTR-MS masses 61 and 69. The FTIR detected two compounds with molecular mass of 60 - acetic acid and glycolaldehyde. Except for the rice straw fires, the PTR-MS mass 61 signal is explained by these two gases. (The PTR-MS signals for masses 61 and 43 were adjusted assuming that 30% of mass 61 fragments to yield a mass 43 ion.) Isoprene and furan are the only two candidates detected by FTIR for PTR-MS mass 69. On average, the agreement is good, but there is high scatter. The FTIR data are likely preferred for monitoring individual compounds at > ppb levels, but the PTR-MS data for the sum of the compounds may be more accurate. It is also the only choice for < ppb levels.

3.3.3. PTR-MS preferred. Compounds in this category have good signal to noise by PTR-MS, unlikely interference from other gases with the same molecular mass, known fragmentation patterns (or known not to fragment), and no sampling losses. In addition, FTIR signal to noise for these compounds is poor. This category includes acetonitrile (mass 42), acetaldehyde (mass 45), propenenitrile (mass 54), methylethylketone (MEK, mass 73), benzene (mass 79), and toluene (mass 93). There were no detectable peaks in the FTIR spectra for these compounds, which are reliably detected by PTR-MS [*Holzinger et al.*, 1999; *Williams et al.*, 2001].

3.3.4. FTIR preferred. A few factors may cause gases to fall into this category: (1) Compounds with proton affinity ≤ H_2O are not detected by PTR-MS. This includes water, methane, ethylene, acetylene, CO_2, CO, and NO. Proton affinities for HCHO and HCN are only slighter greater than that of water, so the equilibrium between protonation and deprotonation must be included to quantify these gases with PTR-MS. (2) At mixing ratios above the ppm level the PTR-MS can suffer from depletion of the reagent ion while FTIR (or cans/GC) can analyze gases up to any level. (3) Ammonia and formic acid exhibit slow response in the PTR-MS because of reactivity and/or sticking to surfaces. (Similar problems could occur for acetic acid without appropriate caution.) Ammonia is notoriously difficult to sample/handle as discussed in more detail in a paper describing simultaneous tests of a closed cell FTIR system [*Yokelson et al.*, this issue].

3.3.5. Remaining problematic compounds. Acetic acid and possibly glycolaldehyde and propanol may contribute to the propylene signal at mass 43 via fragmentation. No evidence of propanol appeared in the FTIR spectra and the fragmentation of acetic acid has been included. The agreement for propylene between FTIR and PTR-MS for various fuel types ranged from 0.74 to 3.12. The possibility exists that larger, unidentified molecules that fragment to mass 43 were sometimes present. The PTR-MS normally identified higher levels of mass 59 than the FTIR acetone. We searched our spectra unsuccessfully for propanal, glyoxal, trimethylene oxide, and propylene oxide, all of which would be detected by PTR-MS at mass 59. We discovered

some signal due to methyl vinyl ether (MVE), but the combined FTIR signal for MVE and acetone did not fully account for the PTR-MS mass 59 signal on average.

Conclusions

These experiments further demonstrate the importance of OVOC emissions from biomass burning, which is consistent with the domination of global atmospheric organic chemistry by OVOC. However, the experiments also demonstrate that only a few OVOC can be reliably measured at the desired levels with current technology. The best agreement between FTIR and PTR-MS is obtained for alcohols. Unfortunately, OVOC were not extensively speciated in the canisters collected in this experiment although a wide variety of OVOC measurements based on canister analysis have been reported [*Greenberg et al.*, 1984; *Kirstine et al.*, 1998; *Friedli et al.*, 2001]. It is interesting that we obtained better agreement between PTR-MS and GC-MS for 4-carbon ketones (which are OVOC) than for the BTEX compounds (hydrocarbons). Taken together, the large scatter in can comparison ratios obtained in this work and the different outcomes of previously reported storage tests suggest that canister-based results for a gas may be sensitive to storage time, canister type, and the other species co-sampled with the primary analyte. It is likely that the scatter in some can comparisons would have been reduced if the canisters had been analyzed more promptly. Future improvement in atmospheric field measurements may require developing a more stable source for FTIR (to lower detection limits) or finding a method to make the PTR-MS more selective. Perhaps the latter is more likely by increasing the specificity of the ionization or ion detection process or by increased use of isotope information. However, schemes to increase the selectivity of PTR-MS should ideally not decrease the ability to measure sticky or reactive species. Meanwhile, with a combination of instruments, we can measure the top 25 or so initial emissions from biomass burning and PTR-MS can provide highly sensitive measurements of acetonitrile, which is a good indicator of biomass burning. The PTR-MS measurement of acetonitrile is likely more accurate than the PTR-MS measurement of HCN, which has also been proposed as an indicator of biomass burning [*Li et al.*, 2000]. Because of variable fuel nitrogen, neither of these compounds is likely to serve as a true tracer for fires. We made an unsuccessful attempt to determine which molecule(s) contribute to the characteristic odors of biomass burning. Acetone is an important HO_x source that is subject to several potential interference problems, but substantial interference was not observed in this work.

Acknowledgements. This research was supported by the National Science Foundation under grants ATM-9900494 and ATM-0228003; the Interagency Joint Fire Science Program; the Rocky Mountain Research Station, Forest Service, U.S. Department of Agriculture (RMRS-99508-RJVA and 03-JV-11222049-046); and the Max Planck Society. Betina Kleiss thanks the Foundation Gran Mariscal de Ayacucho (Fundayacucho) and the German Academic Exchange Service (DAAD) for financial support. We thank Tim Dransfield for sharing a prepublication copy of their glyoxal spectrum.

References

Albritton, D.L., F.C. Fehsenfeld, and A.F. Tuck, Instrumental requirements for global atmospheric chemistry, *Science*, *250*, 75-81, 1990.

Apel, E.C., D.D. Riemer, A. Hills, R. Lueb, A. Fried, G. Sachse, J. Crawford, H. Singh, and D. Blake, Measurements of alcohols, ketones, and aldehydes during TRACE-P, *Eos Trans. AGU*, *83*(47), Fall Meet. Suppl., Abstract A62A-0138, 2002.

Blake, N.J., D.R. Blake, B.C. Sive, T.Y. Chen, F.S. Rowland, J.E. Collins, G.W. Sachse, and B.E. Anderson, Biomass burning emissions and vertical distribution of atmospheric methyl halides and other reduced carbon gases in the South Atlantic region, *J. Geophys. Res.*, *101*, 24151-24164, 1996.

Brune, W.H., I.C. Faloona, D. Tan, A.J. Weinheimer, T. Campos, B.A. Ridley, S.A. Vay, J.E. Collins, G.W. Sachse, L. Jaegle, and D.J. Jacob, Airborne in-situ OH and HO_2 observations in the cloud-free troposphere and lower stratosphere during SUCCESS, *Geophys. Res. Lett.*, *25*, 1701-1704, 1998.

Carter, W.P.L., A.C. Lloyd, J.L. Sprung, and J.N. Pitts, Jr., Computer modeling of smog chamber data: Progress in validation of a detailed mechanism for the photooxidation of propene and n-butane in photochemical smog, *Int. J. Chem. Kinet.*, *11*, 45-**xx**, 1979.

Chatfield, R.B, H.B. Singh, A. Fried, M.J. Evans, D.J. Jacob, D. Blake, B. Heikes, R.W. Talbot, and G.W. Sachse, Oxygenated organic chemicals in the Pacific troposphere: Sources and chemical consequences, *Eos Trans. AGU*, *83*(47), Fall Meet. Suppl., Abstract A52D-06, 2002.

Christian, T.J., B. Kleiss, R.J. Yokelson, R. Holzinger, P.J. Crutzen, J. Williams, W.M. Hao, T. Shirai, B.H. Saharjo, and D.E. Ward, Comprehensive laboratory measurements of biomass-burning emissions: I, The emissions from Indonesian, African, and other fuels, this issue.

Colman, J.J., A.L. Swanson, S. Meinardi, B.C. Sive, D.R. Blake, and F.S. Rowland, Description of the analysis of a wide range of volatile organic compounds in whole air samples collected during PEM-tropics A and B, *Anal. Chem.*, *73*, 3723-3731, 2001.

Flocke, F., A. Weinheimer, Y. Kondo, M. Koike, F. Eisele, M. Zondlo, D. Blake, S. Vay, M. Avery, G. Sachse, H. Singh, D. Westberg, H. Fuelberg, and J. Crawford, Observations of PANs on Board the NASA P-3 During TRACE-P, *Eos. Trans. AGU*, *83(47)*, Fall Meet. Suppl., Abstract A62A-0133, 2002.

Friedli, H.R., E. Atlas, V.R. Stroud, L. Giovanni, T. Campos, and L.F. Radke, Volatile organic trace gases emitted from North American wildfires, *Global Biogeochem. Cycles*, **pp.** 2001.

Greenberg, J.P., P.R. Zimmerman, L. Heidt, and W. Pollock, Hydrocarbon and carbon monoxide emissions from biomass burning in Brazil, *J. Geophys. Res.*, *89*, 1350-1354, 1984.

Griffith, D.W.T., W.G. Mankin, M.T. Coffey, D.E. Ward, and A. Riebau, FTIR remote sensing of biomass burning emissions of CO_2, CO, CH_4, CH_2O, NO, NO_2, NH_3 and N_2O, *Global Biomass Burning: Atmospheric, Climatic, and Biospheric Implications*, edited by J.S. Levine, pp. 230-239, MIT Press, Cambridge, Mass., 1991.

Griffith, D.W.T., Synthetic calibration and quantitative analysis of gas phase infrared spectra, *Appl. Spectrosc.*, *50*, 59-70, 1996.

Gong, Q., and K.L. Demerjian, Hydrocarbon Losses on a Regenerated Nafion(R) Dryer, *J. Air & Waste Manage.*, 45, 490-493, 1995.

Goode, J.G., R.J. Yokelson, R.A. Susott, and D.E. Ward, Trace gas emissions from laboratory biomass fires measured by Fourier transform infrared spectroscopy: Fires in grass and surface fuels, *J. Geophys. Res.*, *104*, 21237-21245, 1999.

Habram, Maurice, "Entwicklung einer gaschromatographischen Methode für die Bestimmung atmospärischer C2-C9 Kohlenwasserstoffe", Band 53-98, Fraunhofer Institut Atmosphärische Umweltvorschung, Garmisch-Partenkirchen, March 1998.

Hansel, A., A. Jordan, R. Holzinger, P. Prazeller, W. Vogel, and W. Lindinger, Proton transfer reaction mass spectrometry - Online trace gas analysis at the ppb level, *Int. J. Mass Spetrom. & Ion Proc.*, 150, 609-619, 1995.

Hansel, A., W. Singer, A. Wisthaler, M. Schwarzmann, and W. Lindinger, Energy dependencies of the proton transfer reactions $H_3O^+ + CH_2O \leftrightarrow CH_2OH^+ + H_2O$, *Int. J. Mass Spectrom. Ion Processes*, *167/168*, 697-703, 1997.

Hanst, P.L., L.L. Spiller, D.M. Watts, J.W. Spence, and M.F. Miller, Infrared measurement of fluorocarbons, carbon tetrachloride, carbonyl sulfide, and other atmospheric trace gases, *JAPCA*, *25*, 1220-1226, 1975.

Hao, W.M., D.E. Ward, G. Olbu, and S.P. Baker, Emissions of CO_2, CO, and hydrocarbons from fires in diverse African savanna ecosystems, *J. Geophys. Res.*, *101*, 23577-23584, 1996.

Holzinger, R., C. Warneke, A. Hansel, A. Jordan, W. Lindinger, D.H. Scharffe, G. Schade, and P.J. Crutzen, Biomass burning as a source of formaldehyde, acetaldehyde, methanol, acetone, acetonitrile, and hydrogen cyanide, *Geophys. Res. Lett.*, *26*, 1161-1164, 1999.

Kelly, T.J. and M.W. Holdren, Applicability of canisters for sample storage in the determination of hazardous air pollutants, *Atmospheric Environment*, *29*, 2595-2608, 1995.

Kirstine, W., I. Galbally, Y. Ye and M. Hooper, Emissions of volatile organic compounds (primarily oxygenated species) from pasture, *J. Geophys. Res.*, *103*, 10,605-10,619, 1998.

Konig, G., M. Brunda, H. Puxbaum, C.N. Hewitt, S.C. Duckham and J. Rudolph, Relative contribution of oxygenated hydrocarbons to the total biogenic VOC emissions of selected mid-European agricultural and natural plant species, *Atmos. Environ.*, *29*, 861-874, 1995.

Li, Q.B., D.J. Jacob, I. Bey, R.M. Yantosca, Y.J. Zhao, Y. Kondo, and J. Notholt, Atmospheric hydrogen cyanide (HCN): Biomass burning source, ocean sink? *Geophys. Res. Lett. 27*, 357-360, 2000.

Lindinger, W., A. Hansel, and A. Jordan, On-line monitoring of volatile organic compounds at pptv levels by means of proton transfer mass spectrometry (PTR-MS) - medical applications, food control and environmental research (Review), *Int. J. Mass Spetrom. & Ion Proc.*, *173*, 191-241, 1998.

Mason, S.A., R.J. Field, R.J. Yokelson, M.A. Kochivar, M.R. Tinsley, D.E. Ward, and W.M. Hao, Complex effects arising in smoke plume simulations due to inclusion of direct emissions of oxygenated organic species from biomass combustion, *J. Geophys. Res.*, *106*, 12527-12539, 2001.

McRae, G.J., and J.H. Seinfeld, Development of a second generation mathematical model for urban air pollution. II. Evaluation of model performance, *Atmos. Environ.*, *17*, 501-**xxx**, 1983.

Montzka, S.A., R.C. Myers, J.H. Butler, J.W. Elkins and S.O. Cummings, Global tropospheric distribution and calibration scale of HCFC-22, *Geophys. Res. Lett.*, *20*, 703-706, 1993.

Mount, G.H. and E.J. Williams, An overview of the tropospheric OH photochemistry experiment, Fritz Peak/Idaho Hill, Colorado, fall 1993, *J. Geophys. Res.*, *102*, 6171-6186, 1997.

Ochiai, N., A. Tsuji, N. Nakamura, S. Daishima, and D.B. Cardin, Stabilities of 58 organic compounds in fused-silica-lined and SUMMA polished canisters under various humidified conditions, *J. Environ. Monit.*, *4*, 879-889, 2002.

Schmidbauer, N., and M. Oehme, Comparison of solid adsorbent and stainless-steel canister sampling for very low ppt-concentrations of aromatic-compounds (greater-than-or-equal-to-C-6) in ambient air from remote areas, *Fresenius Zeitschrift Fur Analytische Chemie*, *331*, 14-19, 1988.

Sin, D.W., Y.C. Wong, W.C. Sham, and D. Wang, Development of an analytical technique and stability evaluation of 143 C3-C12 volatile organic compounds in Summa canisters by gas chromatography-mass spectrometry, *The Analyst*, *126*, 310-321, 2001.

Singh, H.B., M. Kanakidou, P.J. Crutzen, and D.J. Jacob, High concentrations and photochemical fate of oxygenated hydrocarbons in the global troposphere, *Nature*, *378*, 50-54, 1995.

Singh. H., Y. Chen, A. Staudt, D. Jacob, D. Blake, B. Heikes, and J. Snow, Evidence from the Pacific troposphere for large global sources of oxygenated organic compounds, *Nature*, *410*, 1078-1081, 2001.

Staudt, A.C., D.J. Jacob, F. Ravetta, J.A. Logan, D. Bachiochi, T.N. Krishnamurti, S. Sandholm, B. Ridley, H.B. Singh, and B. Talbot, Sources and chemistry of nitrogen oxides over the tropical Pacific, *J. Geophys. Res.*, *108*, 8239, doi:10.1029/2002JD002139, 2003.

Su, T., and W.J. Chesnavich, Parameterization of the ion-polar molecule collision rate constant by trajectory calculations, *J. Chem. Phys.*, *76*, 5183-5185, 1982.

Thamburaj, R., *Fast Pyrolysis of Biomass for Green Power Generation*, presented at 1st World Conference on Biomass for Energy and Industry, Seville, Spain, 2000.

Trent, A., M.A. Davies, R. Fisher, H. Thistle, and R. Babbitt, Evaluation of optical instruments for real-time, continuous monitoring of smoke particulates, *Tech. Rep. 0025-2860-MTDC*, USDA Forest Service, Missoula Technology and Development Center, Missoula, MT., 38 pp., 2000.

Williams, J., U. Pöschl, P.J. Crutzen, A. Hansel, R. Holzinger, C. Warneke, W. Lindinger, and J. Lelieveld, An atmospheric chemistry interpretation of mass scans obtained from a proton transfer mass spectrometer flown over the tropical rainforest of Surinam, *J. Atmos. Chem.*, *38*, 133-166, 2001.

Worden, H., R. Beer, and C.P. Rinsland, Airborne infrared spectroscopy of 1994 western wildfires, *J. Geophys. Res.*, *102*, 1287-1299, 1997.

Yokelson, R.J., D.W.T. Griffith, and D.E. Ward, Open-path Fourier transform infrared studies of large-scale laboratory biomass fires, *J. Geophys Res.*, *101*, 21067-21080, 1996.

Yokelson, R.J., D.E. Ward, R.A. Susott, J. Reardon, and D.W.T. Griffith, Emissions from smoldering combustion of biomass measured by open-path Fourier transform infrared spectroscopy, *J. Geophys. Res.*, *102*, 18865-18877, 1997.

Yokelson, R.J., J.G. Goode, I. Bertschi, R.A. Susott, R.E. Babbitt, D.E. Ward, W.M. Hao, D.D. Wade, and D.W.T. Griffith, Emissions of formaldehyde, acetic acid, methanol, and other trace gases from biomass fires in North Carolina measured by airborne Fourier transform infrared spectroscopy (AFTIR), *J. Geophys. Res.*, *104*, 30,109-30,125, 1999.

Yokelson, R.J., and I.T. Bertschi, Vibrational spectroscopy in the study of fires, in *Handbook of Vibrational Spectroscopy*, edited by J.M. Chalmers and P.R. Griffiths, pp. 8, John Wiley & Sons Ltd, Chichester, 2002.

Yokelson, R.J., I.T. Bertschi, T.J. Christian, P.V. Hobbs, D.E. Ward, and W.M. Hao, Trace gas measurements in nascent, aged, and cloud-processed smoke from African savanna fires by airborne Fourier transform infrared spectroscopy (AFTIR), *J. Geophys. Res.*, *108*(D13), 8478, doi:10.1029/2002JD002322, 2003.

Yokelson, R.J., T.J. Christian, I.T. Bertschi, and R.A. Susott, Extractive sampling of ammonia, acetic acid, methanol, and other atmospheric trace gases, submitted to this issue, *J. Geophys. Res.* 2003JD003549.

Figure Captions

Figure 1. A schematic diagram of the USDA Forest Service, Fire Sciences Laboratory combustion facility. All measurements except background CO_2 were made in well-mixed smoke from the sampling platform.

Figure 2. a) The ratio of PTR-MS methanol (point-source) to OP-FTIR methanol (path integrated) as the PTR inlet is repeatedly moved from the center of the stack (80 cm) to within 4 cm of the stack wall. The ratio is independent of position, which indicates that the smoke is well mixed. b) No position dependence was observed for acetic acid, which is a stickier compound. Rapid switching between two PTR-MS inlets, one of which was filtered with a Teflon filter, also had no measurable effect, indicating that particles did not interfere with the trace gas measurements.

Figure 3. Typical agreement between the PTR-MS and OP-FTIR is illustrated by co-plotting the real time mixing ratios from the two instruments. The above data were measured during the third fire in ponderosa pine needles. a) mass 33 (methanol); b) mass 59 (acetone and methyl vinyl ether); c) mass 61 (acetic acid and glycolaldehyde); d) mass 69 (furan and isoprene).

Figure 4. Regression of the PTR-MS fire-integrated mixing ratios against the OP-FTIR fire-integrated mixing ratios for all the fires. This is an alternative method to determine the study-average agreement between the instruments that is biased towards the agreement obtained for the fires with higher mixing ratios (see text). a) For acetol and mass 75 good agreement is always obtained at high mixing ratios. b) For phenol and mass 95 excellent agreement is observed on 5 of the 7 occasions with high mixing ratios. Another mass 95 candidate may contribute to the outliers.

Figure 5. The x-axis is the proton affinity (PA) of the compound minus the PA of water (ΔPA). The black symbols show the average value and one standard deviation for the fire-integrated PTR-MS mixing ratios divided by the fire-integrated OP-FTIR mixing ratios. The gray symbols show the agreement obtained after corrections for HCHO and HCN discussed in the text or from the alternate analysis for acetol shown in Figure 4a. GA, glycolaldehyde; MVE, methylvinylether.

Table 1. The canister mixing ratios divided by the simultaneously-measured PTR-MS or OP-FTIR mixing ratios.

Mainz GC-MS "Can" Compounds	Fire Name								Average all	Average selected[2]	Average steady fires[3]
	Excelsior2	*IndoLitter1*[1]	*Firduff3*	Cottonwood1	Dambo13	Miombo5	GermanGrass1	*Miombo3*			
Acetonitrile/PT[4]	8.36	2.55	0.30	4.51	0.09	8.01	0.70	1.46	3.25	1.90	2.46
Acetone/PT	0.34	67.96	2.36	0.13	0.12	18.38	0.33	0.21	11.23	0.81	23.48
Isoprene/PT	0.28	0.07	0.34	0.18	0.00	1.11	0.78	0.00	0.35	0.63	0.20
Methylvinylketone/PT	0.96	3.44	1.05	0.15	1.06	2.40	1.27	1.07	1.42	1.61	1.55
Methylethylketone/PT	1.52	1.48	0.28	0.66	0.22	1.20	0.89	0.55	0.85	0.85	0.81
Benzene/PT	4.79	12.68	0.35	2.28	2.92	14.03	4.33	5.62	5.87	2.93	5.10
Toluene/PT	8.39	16.60	11.62	2.34	4.18	21.84	5.24	6.45	9.58	3.26	10.19
p-Xylene/PT	3.27	8.94	5.98	1.07	0.86	8.40	3.36	2.79	4.34	2.27	5.33

UCI GC/MS-FID-ECD "Can" Compounds	Fire Name							Average all	Average selected	Average steady fires
	Alangalang4	*IndoLitter1*	*Firduff3*	Dambo3	Miombo2	GermanGrass3	*Miombo3*			
Ethylene/FT	0.914	1.449	0.671	0.954	0.748	1.137	1.008	0.983		1.060
Propylene/FT	0.741	0.988	0.730	nFT[5]	0.225	0.649	1.473	0.801		0.859
Acetylene/FT	0.969	1.787	0.870	1.192	1.180	1.665	1.431	1.299		1.328
Isoprene/PT	0.003	0.082	0.062	0.018	0.021	0.004	0.003	0.028		0.072
Benzene/PT	1.581	1.489	0.100	1.360	1.045	0.996	1.603	1.168	1.345	0.794
Toluene/PT	1.860	1.506	0.817	1.517	1.149	0.808	1.595	1.322		1.162
p-Xylene/PT	0.102	0.683	0.378	nPT	0.299	0.169	0.740	0.395	0.525	0.531

USFS GC-FID "Can" Compounds	Fire Name							Average all	Average selected	Average steady fires
	Alangalang4	*IndoLitter1*	*Firduff3*	Dambo3	Miombo2	GermanGrass3	*Miombo3*			
Ethylene/FT	1.26	1.61	nC	0.72	0.96	1.28	nC	1.17		
Propylene/FT	0.92	1.28	nC	nC	0.29	0.60	nC	0.77		
Acetylene/FT	0.51	nC	nC	nC	nC	nC	nC	0.51		

[1]Cans collected simultaneously from the same fire by all groups are in the same column and the fire name is italicized . Otherwise the cans are listed in the same column as the Mainz can of closest fuel type.

[2]The average of the ratios that differ from one by less than a factor of five.

[3]The average of the ratios from the fires with slowly-changing emissions.

[4]PT indicates the ratio of canister analysis to the PTR-MS analysis, FT indicates the ratio is to the OP-FTIR analysis.

[5]nFT, no FTIR data; nPT, no PTR-MS data; nC, no can data.

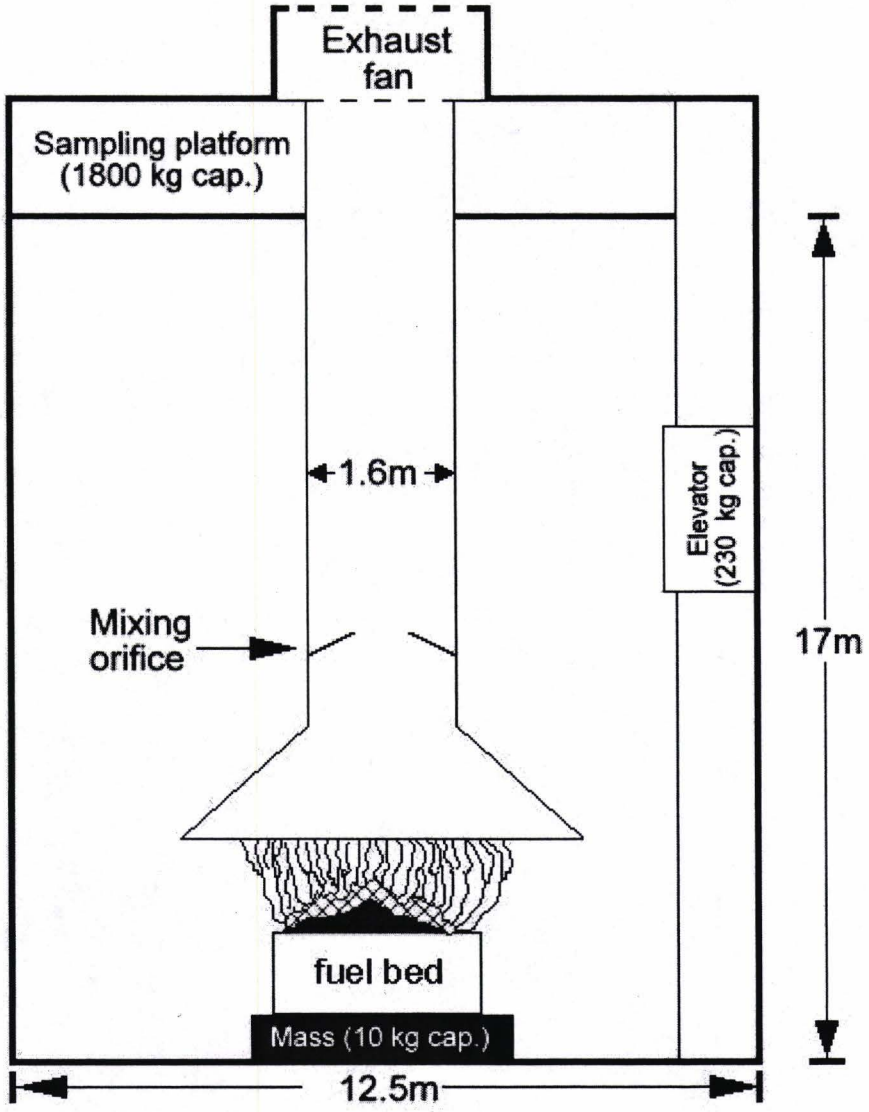

Figure 1. A schematic diagram of the USDA Forest Service, Fire Sciences Laboratory combustion facility. All measurements except background CO_2 were made in well-mixed smoke from the sampling platform.

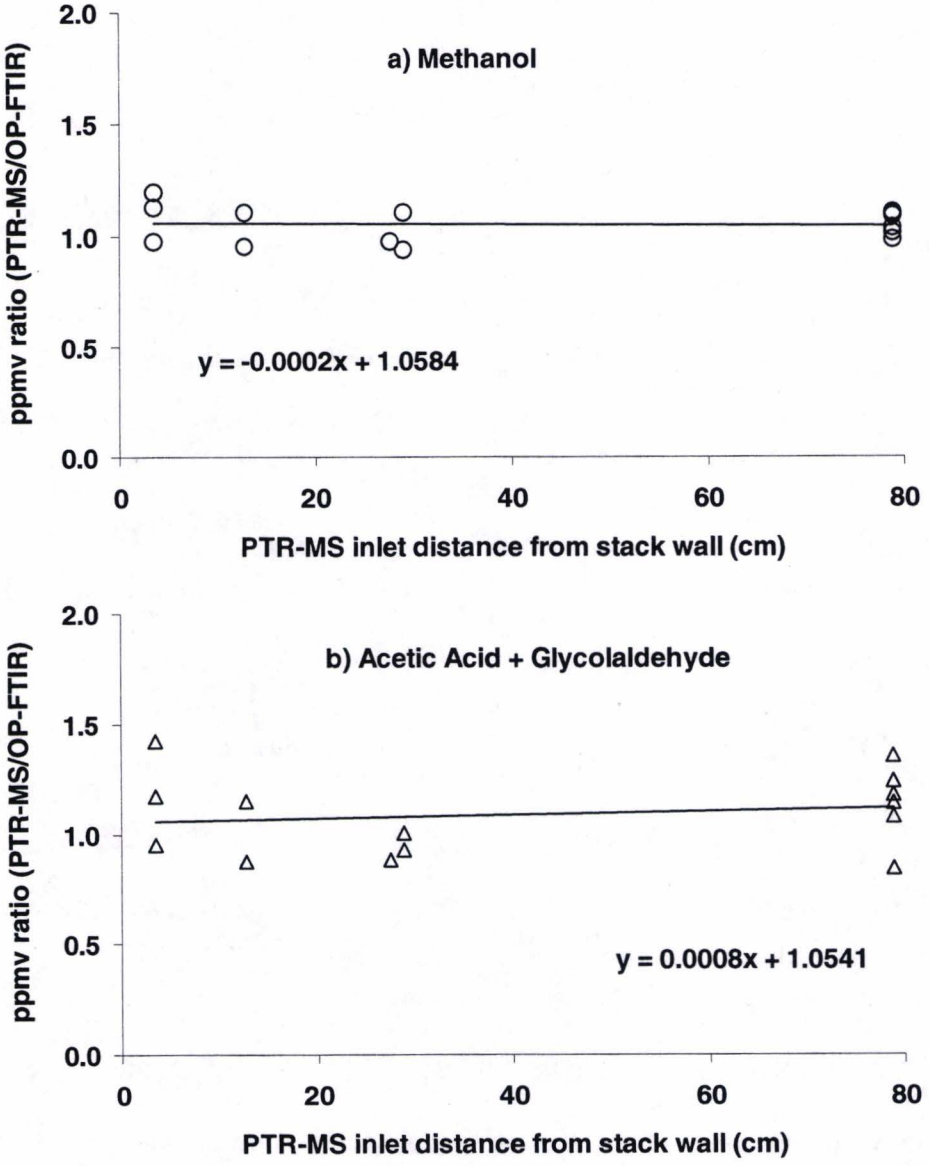

Figure 2. a) The ratio of PTR-MS methanol (point-source) to OP-FTIR methanol (path integrated) as the PTR inlet is repeatedly moved from the center of the stack (80 cm) to within 4 cm of the stack wall. The ratio is independent of position, which indicates that the smoke is well mixed. b) No position dependence was observed for acetic acid, which is a stickier compound. Rapid switching between two PTR-MS inlets, one of which was filtered with a Teflon filter, also had no measurable effect, indicating that particles did not interfere with the trace gas measurements.

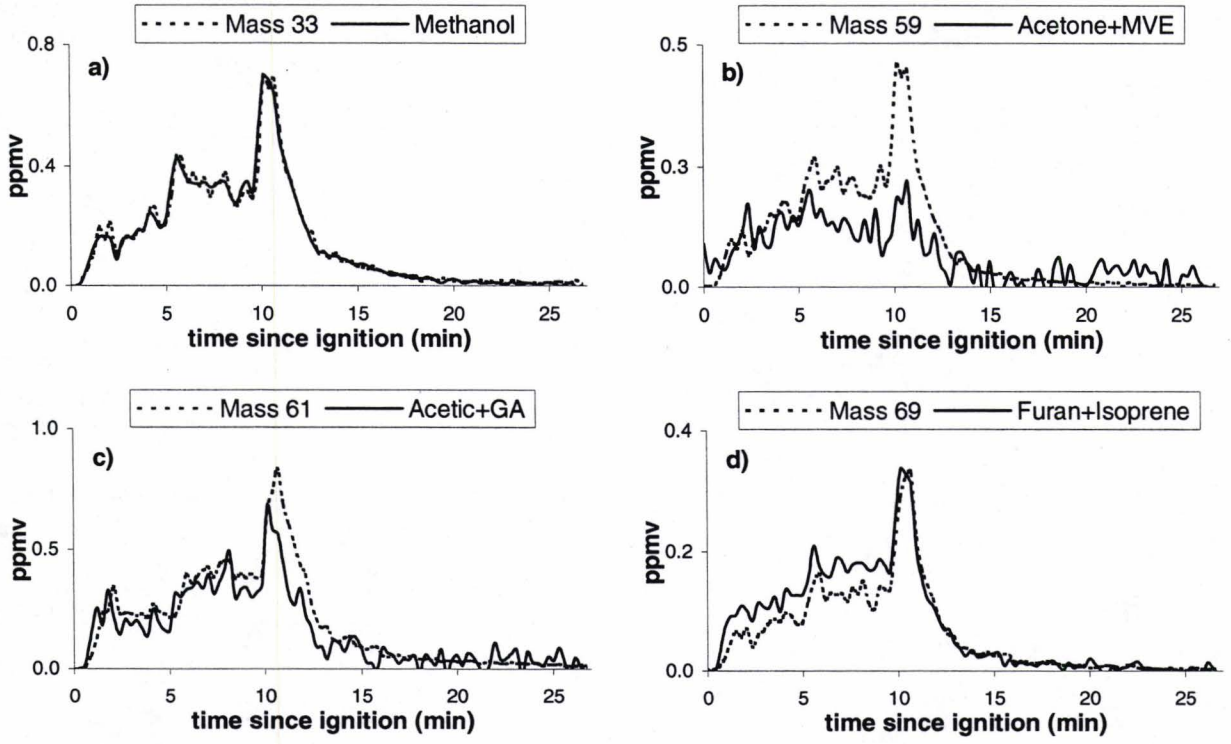

Figure 3. Typical agreement between the PTR-MS and OP-FTIR is illustrated by co-plotting the real time mixing ratios from the two instruments. The above data were measured during the third fire in ponderosa pine needles. a) mass 33 (methanol); b) mass 59 (acetone and methyl vinyl ether); c) mass 61 (acetic acid and glycolaldehyde); d) mass 69 (furan and isoprene).

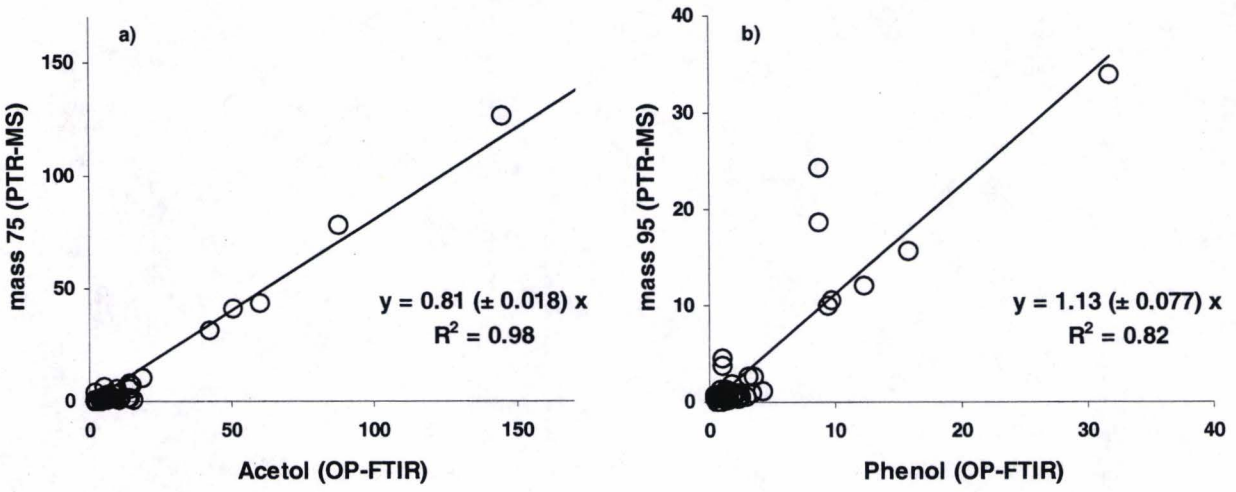

Figure 4. Regression of the PTR-MS fire-integrated mixing ratios against the OP-FTIR fire-integrated mixing ratios for all the fires. This is an alternative method to determine the study-average agreement between the instruments that is biased towards the agreement obtained for the fires with higher mixing ratios (see text). a) For acetol and mass 75 good agreement is always obtained at high mixing ratios. b) For phenol and mass 95 excellent agreement is observed on 5 of the 7 occasions with high mixing ratios. Another mass 95 candidate may contribute to the outliers.

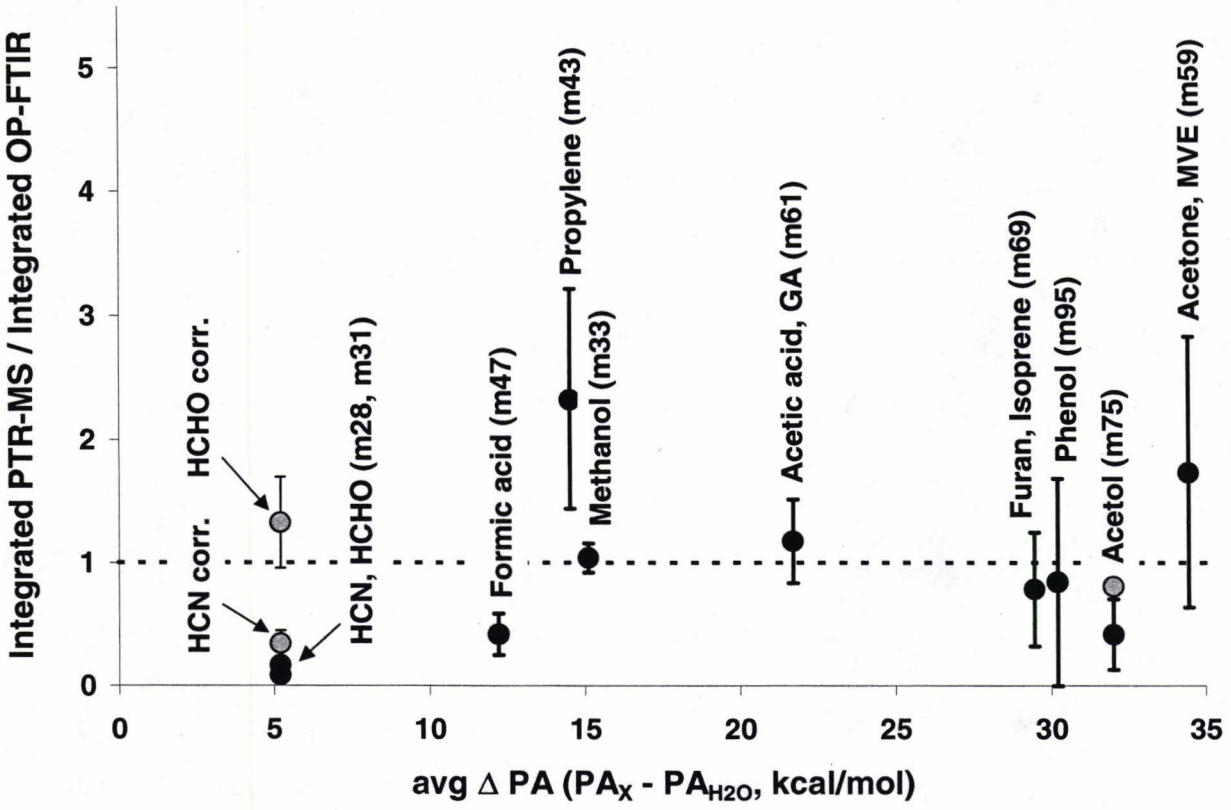

Figure 5. The x-axis is the proton affinity (PA) of the compound minus the PA of water (ΔPA). The black symbols show the average value and one standard deviation for the fire-integrated PTR-MS mixing ratios divided by the fire-integrated OP-FTIR mixing ratios. The gray symbols show the agreement obtained after corrections for HCHO and HCN discussed in the text or from the alternate analysis for acetol shown in Figure 4a. GA, glycolaldehyde; MVE, methylvinylether.

Publication 4

Extractive sampling of ammonia, acetic acid, methanol, and other atmospheric trace gases

R. J. Yokelson,[1,2] T. J. Christian,[1] I. T. Bertschi,[1,3] and W.M. Hao[4]

[1]University of Montana, Department of Chemistry, Missoula, Montana.

[2]Corresponding author.

[3]Now at Interdisciplinary Arts and Sciences, University of Washington-Bothell, Bothell, Washington.

[4]USDA Forest Service, Fire Sciences Laboratory, Missoula, Montana

Submitted for publication to *Journal of Geophysical Research-Atmospheres*: February 28, 2003.

Revised:

Accepted:

Abstract. The performance of an FTIR-based instrument that employs a Pyrex gas cell was tested for measurements of carbon dioxide (CO_2), carbon monoxide (CO), methane (CH_4), nitric oxide (NO), nitrogen dioxide (NO_2), methanol (CH_3OH), acetic acid (CH_3COOH), and ammonia (NH_3). When flowing, mixed standards were delivered to the instrument, temporarily reduced passing efficiency was observed for CH_3OH and NH_3 if stainless steel was employed as the system inlet. However, a halocarbon wax coating on the stainless steel gave it excellent passing efficiency (similar to that of Teflon) for both methanol and NH_3, even at temperatures as low as 5°C. Thus, the wax is valuable for coating sampling system components that cannot be fashioned from Teflon. An additional passivation lag (of 10-40 s) occurs in the instrument for NH_3 only, which is attributed to the Pyrex walls of the multipass cell. To determine the sampling artifacts that could arise from the complex sample matrix presented by smoke, the closed-cell FTIR system was intercompared with an open-path FTIR system (which is immune to sampling artifacts) in well-mixed smoke. NH_3 was the only problematic compound in this test, but no new effects were observed due to the smoke matrix. Overall, the results suggest that; for our fast-flow, closed-cell system, a sampling time of ~10 s is sufficient to detect >80% of a delivered NH_3/CO ratio. Longer sampling times or consecutive samples return better results.

Keywords: ammonia, acetic acid, methanol, halocarbon wax, surface passivation, trace gas sampling.

1. Introduction

Understanding the Earth's atmospheric chemistry and climate requires widespread, accurate measurements of stable, reactive, and "sticky" trace gases [*Albritton et al.*, 1990; *Singh et al.*, 1995; *Roscoe*, 1997; *Mason et al.*, 2001]. Accuracy is compromised if trace gases react or stick to surfaces in sample inlets, storage containers, or instruments. Open-path spectroscopic measurements do not suffer from these types of artifacts and thus, open-path Fourier transform infrared (OP-FTIR) spectroscopy has been used to measure the emissions from biomass burning [*Yokelson et al.*, 1996], which is the second largest global trace gas source [*Crutzen and Andreae*, 1990]. OP-FTIR showed that 50-80% of the VOCs and many other emissions from fires are reactive or sticky or present other potential problems for conventional, contained sampling/measurement systems [*Yokelson et al.*, 1996, 1997; *Worden et al.*, 1997; Goode et al., 1999 *Bertschi et al.*, 2003a, b; *Christian et al.*, 2003a, b].

To enable sampling of the plumes from large-scale fires, in-situ measurements of downwind plume chemistry, and to generally access a larger portion of the atmosphere we developed a lightweight airborne FTIR (AFTIR) system that can fit on a small, dedicated aircraft. For reasons discussed in detail by *Yokelson et al*, [1999] we designed our system to acquire IR spectra of the contents of a gas cell inside an aircraft. The flow of air through the system is driven by ram pressure so that it requires no pumps or flow meters, thus eliminating the associated weight, power, electronics, and maintenance. Such an approach is easily mimicked for extractive, ground-based sampling with closed cells by coupling an inexpensive, oil-free blower to the outlet of the system. In addition, a pair of pneumatic valves on the inlet and outlet of the cell allows us to make continuous, real time measurements (valves open), or capture a "grab" sample by closing the valves and then scanning the sample repeatedly to improve the signal to noise ratio (SNR).

To minimize sampling losses, AFTIR employs fast flow, a Teflon sample line, a Pyrex cell and halocarbon wax coating on all metal parts [*Webster et al.*, 1994]: namely the external inlet and cell-inlet valve. If sample transformations occur in the cell after acquiring a "grab sample," our continuous, fast monitoring of the cell contents allows us to correct for them [*Yokelson et al.*, 1999, 2003]. However, losses that could occur on the sample inlet, or due to passivation of the cell during sample exchange, require independent characterization. Prior to this work, the halocarbon wax coating (Halocarbon Products Corp., River Edge, NJ) had been shown to have good passing efficiency for HCl [*Webster et al.*, 1994] and OH [*Bertram et al.*, 2001] and glass was known to be associated with passivation losses for HNO_3 [*Schiff et al.*, 1990; *Neuman et al.*, 1999; *Langmuir*, 1918]. This paper characterizes the passing efficiency of our inlet coating and the passivation of our Pyrex cell for additional compounds (ammonia, acetic acid, and others). The tests were run for sample matrices of varying complexity and at both room and reduced temperature (~5°C). Thus, these results have general significance for analytical chemists. In addition, the characteristics of a system designed to exchange gases at ambient pressure rather than employing pump/purge/fill cycles should be of general interest.

2. Experimental Details

2.1 Overview of the Design and Use of the AFTIR System.

A brief overview of the design and in-flight use of the AFTIR system provides a context for the tests described in this paper. The AFTIR system obtains FTIR spectra of

air flowing through, or detained within, a multipass cell inside an aircraft [*Yokelson et al.*, 1999, 2003; *Goode et al.*, 2000]. Outside air is forced by ram pressure into a 25 mm i.d., forward-facing inlet with an opening 22 cm from the outer skin of the aircraft cabin roof. The air then flows through 10 m of 25 mm i.d. flexible, Teflon bellows; a 14 liter, Pyrex, multipass cell; and ~5 m of 25 mm i.d. tubing to a rear-facing outlet. Fast-acting valves (19 mm i.d.) on the inlet and outlet of the cell are used to temporarily trap the cell contents for signal averaging at desired times. In addition, closing the inlet and outlet valves reduces the noise in the 900-1100 cm^{-1} region of the AFTIR spectrum providing lower detection limits for many species [*Yokelson et al.*, 1999]. At typical aircraft research speeds (80 m/s) the flow rate through the system is ~ 100 l/min based on a $1/e$ exchange time of 4-5 s for a compound when flushing the cell contents. The residence time in the exterior inlet tubing is ~ 2.5 ms.

Infrared spectra of the cell contents are acquired continuously (every 0.83 s) throughout most of each flight and the flow-control valves are normally open, which flushes the cell with ambient air. To temporarily trap smoke plume "grab" samples we fly into a smoke plume and then close the valves 10-60 s later when the cell is well flushed with smoke. The valves remain closed for 1-3 minutes while several hundred spectra of the detained smoke sample are acquired. The valves are then opened to flush the cell for several minutes before background grab samples are trapped at the same altitude just outside the plume and processed in the same way.

The IR optical system used to quantify the cell contents is described elsewhere [*Yokelson et al.*, 1999]. Briefly, it features a MIDAC model 2500 FTIR with 0.5 cm^{-1} spectral resolution. The spectrometer IR beam is directed through a tripled White cell [*White*, 1942] enclosed in a 14 cm i.d. × 90 cm sealed glass tube and onto an LN_2-cooled MCT (mercury-cadmium-telluride) detector. Mixing ratios for trace gases present above 5-20 ppb are retrieved from the IR spectra with custom software [*Yokelson et al.*, 1996, 1997; *Yokelson and Bertschi*, 2002].

2.2 Overview of the Test Configurations.

2.2.1. General Experimental Considerations. In phase 1 of the testing, AFTIR (coupled to various inlet materials) was challenged with standards mixed in a carrier gas flow at both room and reduced temperature (~5°C). In phase 2, the full range of possible effects due to the other components of smoke (water, particles, etc…) was investigated by codeploying AFTIR with our open-path FTIR in well-mixed smoke. An important experimental constraint is that passivation of surfaces is faster at higher analyte concentrations [*Neuman et al.*, 1999]. The tests described are designed to determine if passivation of the inlet or cell affects our results at the levels of trace gases we actually encounter in the field in smoke plumes (20-500 ppb). Thus, rather than run the tests at high mixing ratios where SNR is optimized, we used levels < 300 ppb where we obtained slower passivation, bigger fractional losses (of a less abundant standard), and more relevant results. The AFTIR detection limit for most compounds is 5-20 ppb for ~100 scans and ~10 times higher for single scans. Thus, the accuracy of much of the data is limited to ~ ±10-20% (based on SNR).

2.2.2. Configuration of tests with standard mixtures. This phase of the testing followed the work of *Neuman et al.*, [1999] in which an HNO_3 standard was delivered through tubing made from a variety of materials used in instrument construction to a fast HNO_3 detector and delays (or failure) in reaching the delivered concentration were

attributed to passivation losses on the test material. *Neuman et al.*, [1999] found that Teflon was the best material, but HNO_3 did stick to it reversibly below ~10°C. Our procedure was slightly different. Since our 14 liter AFTIR cell requires >30 s to completely exchange, we compared the temporal profile for reaching a delivered amount of a test gas to the temporal profile for reaching a delivered amount of a simultaneously introduced "non-sticky" tracer (CO). We also emphasized faster flow rates, which are similar to our actual field sampling conditions.

Figure 1 is a simplified representation of the plumbing for the phase 1 tests. The primary carrier gas flow to AFTIR was controlled with a 100-slpm (standard liter per minute) mass flow controller (MKS 1500) accurate to ±1.0% of full scale. Carrier gas (CG) flow for these experiments ranged from 25 to 100 slpm. The upper end of this range coincides with typical flow rates in airborne deployments of the AFTIR system. The ultra high purity (UHP) nitrogen that we purchased for use as a CG contained 670 ppbv CO as determined by three separate analyses using GC/FID, GC/RDA (reduction gas analyzer), and FTIR. The helium we obtained was essentially "CO-free." Since CO was used as a stable tracer in the experiments and because of the spectral noise (at some frequencies) that accompanies a fast flow of N_2 through AFTIR, the majority of tests were run using He CG to allow continuous monitoring at all frequencies. Some stopped-flow experiments or higher-noise runs with N_2 CG were done to spot check for effects of the CG.

Flow from a 100 ppmv CO standard in N_2 (EPA protocol, ±1%) was routed through a 1.0 slpm mass flow meter and a needle valve to a Teflon valve that allowed introduction at desired times into the CG stream. The mixing ratio of additional, "non-CG" CO delivered to AFTIR (typically 200-500 ppbv) was simply: (CO-line flow/total flow)*(mixing ratio of standard). CO_2, CH_4, CH_3OH, NO, and NO_2 standards in cylinders (20,000, 9.65 (NIST), 106, 104, and 99 ppmv, all $\pm \leq 2\%$) were also routed through a flow meter and needle valve and then premixed with the CO standard before introduction to the CG stream. Delivery mixing ratios (~100-300 ppbv) were calculated using the method above. Permeation tubes (20.0 cm length; VICI Metronics, Inc.) that emitted ammonia (7730 ±2% ng/min at 35°C) or methanol (22,560 ±2% ng/min at 80°C) were held at constant temperature in a calibrated oven (Dynacalibrator model 190) and the output was entrained into a small, measured flow of UHP nitrogen. The oven output was also premixed with the CO standard before introduction to the CG stream. The mixing ratios delivered to AFTIR (for oven output) were calculated from the constant mass-loss rate for the tube and the total flow. They ranged from 101-202 ppbv for NH_3 and 199-273 ppbv for CH_3OH.

The entire system for gas delivery to AFTIR was assembled using Teflon tubing, valves, and fittings, except for the flow controller, needle valves, and flow meters, which had stainless steel, nickel, or Viton® parts. These devices were, however, only employed upstream of the introduction of any problematic gases. A 90 cm section of the 2 m Teflon tubing connecting the standards with AFTIR was removable, allowing tests of two separate sections of 1.6 x 90 cm, 316 stainless steel tubing. Both tubes were cleaned with a mild laboratory soap and then thoroughly rinsed and dried. One section was used uncoated and the other was coated with the same halocarbon wax (and application technique) used in AFTIR. These metal tubes were ~ 40% longer and 30% narrower than the combination of the AFTIR external metal inlet and inlet valve. Thus, any effects

observed would reflect about twice the surface exposure as occurs in actual use of the AFTIR system (for a given flow rate). The temperature of the stainless steel inlet sections was controlled by winding them with 0.635 cm o.d. copper tubing connected to a refrigerated, re-circulating bath (Forma Scientific model 2095) and then insulating the assembly with 1.27 cm-thick foam. The inlet sections were tested at 4.8°C, 9°C, and at room temperature (22-25°C). Gas exiting a cooled inlet returned to room temperature before it entered the AFTIR cell, as measured with temperature probes at each end of the cell.

Reynolds number calculations indicate laminar flow ($R_e < 2000$) within the AFTIR cell for all flow rates and carrier gases used. The nature of the flow within the inlet depended on the CG. When He was the CG, R_e never exceeded 1800, indicating laminar flow. However, for N_2, R_e exceeded 2800 in all cases.

2.2.3. Configuration for 2-FTIR Tests in Well-Mixed Smoke. The above tests determine the effect of various surfaces and temperatures on individual compounds in a low-humidity carrier gas flow. Under field conditions, artifacts could arise due to the presence of many other components in the sample matrix. For instance, one can speculate that the high levels of water and CO_2 in combustion emissions could lead to the formation of carbonic acid on inlet/instrument surfaces and change their properties. To individually investigate all the effects possible due to the interactions between surfaces and all the components of smoke is beyond the scope of any experiment. We adopted a novel approach to check for AFTIR sampling artifacts in "real" smoke that entailed comparing AFTIR to our open-path FTIR in well-mixed smoke. The OP-FTIR system was deployed so that it's 1.6 m basepath, open White cell spanned the smoke plume rising through a stack above a gently smoldering fire in the USDA Forest Service, Fire Sciences Laboratory combustion facility [*Yokelson et al.*, 1997; *Christian et al.*, 2003a, b]. The OP-FTIR continuously quantified the slowly changing trace gases. The OP-FTIR system has an identical spectrometer, but no inlet tubing or enclosed sample cell and it is therefore not subject to sampling- or storage-related artifacts [*Yokelson et al.*, 1997; *Goode et al.*, 1999; *Bertschi et al.*, 2003a, b; *Christian et al.*, 2003a, b]. This provides a benchmark against which any sampling artifacts in AFTIR can be quantified. A blower on the outlet of the AFTIR generated a system flow of 98 slpm. For this test, we used the AFTIR Teflon sample line as an inlet, which was periodically inserted just above the center of the OP-FTIR path. Using the AFTIR cell inlet/outlet valves we sampled the emissions at 17 known times with respect to the OP-FTIR data using different "cell exchange" or "sample-acquisition times" ranging from 4.1 to 64.2 s. AFTIR was flushed with clean air between smoke samples.

The requirement that the smoke sampled by the open-path and point-sampling techniques is well mixed is critical to the interpretation of these results. Three separate tests confirmed this for the smoke at the sampling platform of the combustion facility. 1) The temperature profile across the stack is "flat" even as the temperature changes during a burn. 2) The OP-FTIR results for 5 hydrocarbons were similar to those measured by point-sampling into canisters [*Goode et al.*, 1999]. 3) The ratio between the OP-FTIR and a point sampling PTR-MS was independent of the distance of the point-sampling location from the stack wall: even for sticky compounds such as acetic acid [*Christian et al.*, 2003a].

3. Results and Discussion

3.1. Results of the Tests in Standard Mixtures.

First, we verified the flow rate through the AFTIR system actually obtained during flight. We had previously estimated this flow rate by measuring the decay time for CO when the smoke-filled cell was opened instantaneously to flush with clean air and assuming plug flow within the cell. In this work, using the apparatus shown in Figure 1, we measured the CO 1/*e* exchange time as a function of a precisely measured flow rate. In Figure 2, the reciprocal of flow rates from 25 to 100 slpm is plotted linearly against exchange time (which was independent of carrier gas). In AFTIR deployments on a Forest Service King Air B-90 [*Yokelson et al.*, 1999; *Goode et al.*, 2000] and the University of Washington Convair 580 [*Yokelson et al.*, 2003] the 1/*e* exchange time for CO was ~4-5 s, which, according to the regression in Figure 2, corresponds to flow rates of 96-108 slpm. This result is in good agreement with the plug flow assumption and verifies that our tests were conducted at relevant flow rates.

3.1.1. Tests with Teflon Inlet. Tests were conducted with all-Teflon plumbing so that the effects of uncoated/coated steel as an inlet could be isolated by comparison. In these tests, a stable, controlled flow of carrier gas was established through the cell while a mixture of the CO-standard tracer and the test gas flowed stably to a dump. At a selected time, valves were switched so that the premixed flow of CO and test gas instantaneously joined the carrier gas flow into the cell. Any lag in the test gas rise in the cell in comparison to the rise of CO was taken as evidence of passivation losses.

The rise profile for CO_2, CH_4, NO, NO_2, CH_3OH (cylinder or oven), and NH_3 standards were compared (in turn) to that of the premixed, co-delivered CO standard with a variety of carrier gases and flow rates. For all the gases except NH_3, the test gas rise profile was always identical to that of CO (and independent of carrier gas) indicating that no passivation losses were occurring in the system for CO_2, CH_4, NO, NO_2, and CH_3OH (Figure 3a, b). In contrast, at 58 slpm using the Teflon inlet, the NH_3 1/*e* rise time is approximately 3.1 s slower than that for CO and the total time for NH_3 to reach the delivered concentration at this flow rate is ~40 s (Figure 3c). In addition, there was a "symmetrical delay" in the decay of NH_3 once the standard mixture was shut off (Figure 3d). When consecutive samples were obtained within ~100 s the passivation lag was noticeably smaller for the second sample (Figure 3d). When the Teflon inlet was shortened from 200 to <30 cm, there was no change in NH_3 1/*e* rise time relative to CO, suggesting that the passivation losses occur mainly on the walls of the AFTIR Pyrex cell. These effects were highly reproducible: even for runs that were done before and after a field campaign in Africa. The effects are also consistent with the fact that NH_3 was the only compound found to exhibit fast losses when detained in the Pyrex cell [*Yokelson et al.*, 1999, 2003]. For example, in a separate experiment, the NH_3 mixing ratio was brought to ~100 ppbv and the cell inlet and outlet valves were closed: subsequently the mixing ratio dropped by 10% in 40 s. These storage losses are already routinely corrected for.

Fast system flow rates have the advantage of reducing the percentage of analyte molecules (including those not tested here) that contact the external inlet. In addition, for a given mixing ratio, system passivation could be faster at high flow since the cell-exchange time is reduced and the mass flow rate is increased. We could not directly test this hypothesis in this work because our gas system delivered a single, constant NH_3

mass-flow rate. Thus, increasing the flow simultaneously reduced the delivered mixing ratio (which would tend to slow passivation). However, indirect evidence suggests that faster flow would speed passivation at a fixed mixing ratio. For instance, in Figure 4a-b the measured/actual NH_3/CO is shown for back-to-back runs at 58 and 101 slpm. The data are noisy (especially at low concentration), but the measured/actual ratio appears to reach unity faster at the higher flow rate despite the lower concentration. A more detailed analysis that incorporates 3 runs at 58 slpm, 1 run at 79.5 slpm, and 2 runs at 101 slpm suggests that all the passivation rates are statistically similar despite the fact that high flow was associated with reduced concentrations, which would have tended to slow passivation (Figure 4c). The indirect implication is that the slowing effects of reduced concentration were compensated by a tendency for faster flow to hasten passivation. We conclude that, for a fixed concentration, higher flow would speed passivation.

Despite the passivation losses, the NH_3 rise time was not measurably dependent on CG, which would affect diffusion rates (Figure 5a). The higher noise when using N_2 as the carrier gas is responsible for the higher noise in the NH_3/N_2 trace. To verify the lag time independence of CG for NH_3 we performed four "stopped flow" experiments in N_2 (Figure 5b). With a CG flow of 50 slpm N_2, we waited 2 minutes once and 10 s 3 times before closing the AFTIR valves to enable a high SNR NH_3 analysis in N_2. When waiting 2 minutes to close the valves the measured NH_3/CO was the delivered ratio. When waiting 10 s, the measured NH_3/CO was 75.7 ± 2.1% of the delivered NH_3/CO. The measured ratio at 10 s is not significantly different from the measured ratio obtained at 10 s in He at 58 slpm (Figure 5c). We note that the NH_3 passivation losses described above were mostly observed at flow rates below our field flow rates of ~100 slpm and the losses should be smaller in the field, since passivation time evidently decreases with increased flow. In summary, these tests show that: 1) AFTIR performed well for many compounds. 2) Even with no significant inlet losses, the Pyrex cell leads to small, temporary passivation losses for NH_3. 3) Longer sample acquisition times or consecutive samples (as long as the interval between samples is sufficient to avoid cross-contamination) return more quantitative results. 4) Teflon coating the Pyrex cell may decrease the cell passivation time.

3.1.2. Tests with coated or uncoated stainless steel inlets. When 90 cm of the Teflon inlet was replaced by room temperature stainless steel, the lag in the NH_3 $1/e$ risetime (at 58 slpm) with respect to CO increased from 3.1 s to ~6 s (Figure 6a and b). The total time to reach the delivered concentration was also longer. However, when the stainless steel inlet section is coated with halocarbon wax, the NH_3 lag time (in comparison to CO) is the same as what is observed with the Teflon inlet (Figure 6a and c), even at reduced temperature (~5°C) where the lag on uncoated steel was more pronounced than at room temperature. We also observed a small increase in passivation lag time for methanol on cold uncoated steel, but the increased lag was not observed on cold, coated steel. Our methanol results are analogous to HCHO results reported by *Wert et al.* [2002]. They observed HCHO passivation delays on uncoated steel inlets that were longer at low temperature, but good performance on silica-coated steel inlets even at low temperature. In summary, 1) even with an uncoated steel inlet AFTIR worked well for many compounds. 2) Uncoated steel always caused additional losses for NH_3 and cold, uncoated steel caused losses for CH_3OH. 3) Using the halocarbon wax to coat the steel

gave it performance similar to Teflon down to 5°C: thus, the coating is recommended for sampling these compounds.

3.2. Results of 2-FTIR Tests in Well-Mixed Smoke.

For this test, the AFTIR and OP-FTIR system were co-deployed in slowly changing, well-mixed smoke in the combustion facility stack as described earlier. Because the background levels of CO_2, CO, and CH_4 were substantial and somewhat variable, we used another major smoke component, ethene (C_2H_4), as the non-sticky tracer in these tests [*Goode et al.*, 1999]. For each of the 17 AFTIR samples, the ratios of NH_3, CH_3COOH, and CH_3OH to C_2H_4 were determined and directly compared to the analogous ratio measured at the same time by OP-FTIR. An AFTIR ratio substantially below that of OP-FTIR indicates sample losses associated with the AFTIR cell. The results of this test are shown in Figure 7a. As expected, when using very short sample acquisition times, the AFTIR underestimated the NH_3/C_2H_4 ratio. However, even at the shortest sample acquisition time, the AFTIR ratios for CH_3OH/C_2H_4 and CH_3COOH/C_2H_4 were not significantly lower than the OP-FTIR ratios. At sample acquisition times of 10 ± 2 s the AFTIR NH_3/C_2H_4 ratios range from 77-97% of the "delivered value;" slightly above the 10 s average in the simple mixture tests (Figure 5b and c), but the difference is not statistically significant.

Since the passivation rate should depend on the mixing ratio, we also plot the AFTIR/OP-FTIR ratios as a function of the product of sample acquisition time and "actual" ppm NH_3 (SAT*NH_3) in Figure 7b. (The representation of these results in Figure 7b may have some application to sampling NH_3 at lower levels.) Again, the agreement with the simple mixture tests shown in Figure 5 is remarkable. For the data in Figure 5b, the product SAT*NH_3 was 2.0 s ppmv and the average ratio of measured to delivered NH_3/CO was 75.7 ± 2%. In Figure 7b, the five runs with an SAT*NH_3 of 2 ± 1 s ppmv have a remarkably similar average value of 76.8 ± 6%. This result (although from 2 different flow rates) indicates that shortfalls in real smoke, which were detected only for NH_3, are mainly due to the interaction between Pyrex and NH_3. No new sampling artifacts could be assigned to the more complex sample matrix.

3.3 Overall Implications of Test Results.

Under conditions relevant to many kinds of atmospheric sampling, halocarbon wax gave steel surfaces excellent passing efficiency (similar to Teflon) for both NH_3 and CH_3OH despite temperatures as low as 5°C or complex sample matrices. Uncoated steel induced a passivation delay for these compounds. Brief passivation delays (10-40 s) occurred for NH_3 only, due to the Pyrex cell. Under situations where ambient air is slowly changing (i.e. a few percent per minute) AFTIR (representing a generic closed cell system) requires ~60 s to ensure that absolute ambient levels are reached in the cell. This time is also likely sufficient to passivate the cell (at least at the levels tested). In rapidly changing air, or when sampling plumes of limited extent from a rapidly moving platform, there are additional considerations. In these cases, the cell mixing ratios may not be identical to the rapidly-changing absolute ambient values. However, in plume sampling the absolute levels strongly reflect the instantaneous amount of plume dilution and the more important measurement is usually the ratio between compounds as explained in *Yokelson et al.*, [1999]. With plume sample acquisition times of ~10 s the proper ratios between compounds should be returned for most compounds and the error for NH_3 was ~15% (Figure 7a). Longer sample times or sufficiently-spaced, consecutive samples are

better. A Teflon-coated Pyrex cell may eliminate passivation lags; a hypothesis we plan to test soon.

In previous airborne campaigns we used AFTIR with long sample acquisition times and, when possible, obtained consecutive samples [*Yokelson et al.*, 1999, 2003; *Goode et al.*, 2000]. Thus the error in the NH_3 mixing ratios in these studies was probably small, but difficult to quantify; especially since instrument performance could change over the years. (Our priority is to test a Teflon-coated cell.) It is worth noting that an all-Pyrex sampling/storage system is used in a new NH_3 instrument [*Owens et al.*, 1999] and that the EPA requires the use of glass for sampling NH_3 [*EPA*, 1982]. Our results indicate that sampling NH_3 with glass requires great caution. In addition, the good performance of Teflon or coated steel for NH_3 may be specifically for fresh surfaces since *Lee et al.*, [1991] detected H_2O_2 losses on degraded Teflon. Finally, the intercomparison between our OP-FTIR and other instruments in well-mixed smoke is a generally useful approach for testing all point-sampling instruments. We recently intercompared our OP-FTIR with a proton transfer mass spectrometer [*Holzinger et al.*, 1999] and stainless steel canisters [*Christian et al.*, 2003a].

4. Conclusions

Halocarbon wax imparts excellent passing efficiency to steel surfaces for both basic (NH_3) and acidic (HCl) compounds. For the AFTIR system, the only sampling artifact was a brief (10-40 s) passivation delay for NH_3, which was attributed to the Pyrex cell. Passivation rates were independent of carrier gas, but should be hastened by higher concentrations or flow rates. All detected effects in the tests were due to interactions between NH_3 and Pyrex or uncoated steel; or interaction between CH_3OH and cold, uncoated steel. No additional effects due to the many other components of smoke were observed.

Acknowledgements. This research was supported by funds provided by the National Science Foundation under grant ATM-9900494, the Interagency Joint Fire Science Program, and the Rocky Mountain Research Station, Forest Service, U.S. Department of Agriculture (INT-97082-RJVA and RMRS-99508-RJVA). We thank Carl Howard and Greg Huey for guidance and comments throughout this work.

References

Albritton, D.L., F.C. Fehsenfeld, and A.F. Tuck, Instrumental requirements for global atmospheric chemistry, *Science*, *250*, 75-81, 1990.

Bertram, A.K., A.V. Ivanov, M. Hunter, L.T. Molina, and M.J. Molina, The reaction probability of OH on organic surfaces of tropospheric interest, *J. Phys. Chem. A*, *105*, 9415-9421, 2001.

Bertschi, I., R.J. Yokelson, D.E. Ward, R.E. Babbitt, R.A. Susott, J.G. Goode, and W.M. Hao, Trace gas and particle emissions from fires in large diameter and belowground biomass fuels, *J. Geophys. Res.*, *108*(D13), 8472, doi:10.1029/2002JD002100, 2003a.

Bertschi, I.T., R.J. Yokelson, D.E. Ward, T.J. Christian, and W.M. Hao, Trace gas emissions from the production and use of domestic biofuels in Zambia measured by open-path Fourier transform infrared spectroscopy, *J. Geophys. Res.*, *108*(D13), 8469, doi:10.1029/2002JD002158, 2003b.

Christian, T.J., B. Kleiss, R.J. Yokelson, R. Holzinger, P.J. Crutzen, J. Williams, W.M. Hao, and T. Shirai, Comprehensive laboratory measurements of biomass-burning emissions: II, First intercomparison of open-path FTIR, PTR-MS, GC-MS/FID/ECD, submitted to *J. Geophys. Res.*, 2003a.

Christian, T.J., B. Kleiss, R.J. Yokelson, R. Holzinger, P.J. Crutzen, D.E. Ward, B.H. Saharjo, and W.M. Hao, Comprehensive laboratory measurements of biomass-burning emissions: I, The emissions from Indonesian, African, and other fuels, submitted to *J. Geophys. Res.*, 2003b.

Crutzen, P.J., and M.O. Andreae, Biomass burning in the tropics: Impact on atmospheric chemistry and biogeochemical cycles, *Science*, *250*, 1669-1678, 1990.

EPA Quality Assurance Handbook for Air Pollution Measurement Systems, Volume III - Stationary Source Specific Methods, Section 3.11, January, 1982 (EPA-600/4-77- 027b). Figure 17-3 of 40 CFR 60, Appendix A.

Goode, J.G., R.J. Yokelson, R.A. Susott, and D.E. Ward, Trace gas emissions from laboratory biomass fires measured by Fourier transform infrared spectroscopy: Fires in grass and surface fuels, *J. Geophys. Res.*, *104*, 21,237-21,245, 1999.

Goode, J.G., R.J. Yokelson, D.E. Ward, R.A. Susott, R.E. Babbitt, M.A. Davies, and W.M. Hao, Measurements of excess O_3, CO_2, CO, CH_4, C_2H_4, C_2H_2, HCN, NO, NH_3, HCOOH, CH_3OOH, HCHO, and CH_3OH, in 1997 Alaskan biomass burning plumes by airborne Fourier transform infrared spectroscopy (AFTIR), *J. Geophys. Res.*, *105*, 22,147-22,166, 2000.

Holzinger, R., C. Warneke, A. Hansel, A. Jordan, W. Lindinger, D.H. Scharffe, G. Schade, and P.J. Crutzen, Biomass burning as a source of formaldehyde, acetaldehyde, methanol, acetone, acetonitrile, and hydrogen cyanide, *Geophys. Res. Lett.*, *26*, 1161-1164, 1999.

Langmuir, I., The adsorption of gases on plane surfaces of glass, mica, and platinum, *J. Am. Chem. Soc.*, 40, 1361-1375, 1918.

Lee, J.H., Y. Chen, and I.N. Tang, Heterogeneous loss of gaseous H_2O_2 in an atmospheric air sampling system, *Environ. Sci. Technol.*, *25*, 339-342, 1991.

Mason, S.A., R.J. Field, R.J. Yokelson, M.A. Kochivar, M.R. Tinsley, D.E. Ward, and W.M. Hao, Complex effects arising in smoke plume simulations due to inclusion of direct emissions of oxygenated organic species from biomass combustion, *J. Geophys. Res.*, *106*, 12,527-12,539, 2001.

Neuman, J.A., L.G. Huey, T.B. Ryerson, and D.W. Fahey, Study of inlet materials for sampling atmospheric nitric acid, *Environ. Sci. Technol.*, *33*, 1133-1136, 1999.

Owens, M.A., C.C. Davis, and R.R. Dickerson, A photothermal interferometer for gas-phase ammonia detection, *Anal. Chem.*, *71*, 1391-1399, 1999.

Roscoe, H.K., and K.C. Clemitshaw, Measurement techniques in gas-phase tropospheric chemistry: A selective view of the past, present, and future, *Science*, *276*, 1065-1072, 1997.

Schiff, H.I., D.R. Karecki, G.W. Harris, D.R. Hastie, and G.I. Mackay, A tunable diode laser system for aircraft measurements of trace gases, *J. Geophys. Res.*, *95*, 10147-10153, 1990.

Singh, H. B., M. Kanakidou, P. J. Crutzen, and D. J. Jacob, High concentrations and photochemical fate of oxygenated hydrocarbons in the global troposphere, *Nature*, *378*, 50-54, 1995.

Webster, C.R., R.D. May, C.A. Trimble, R.G. Chave, and J. Kendall, Aircraft (ER-2) laser infrared absorption spectrometer (ALIAS) for in situ stratospheric measurements of HCl, N_2O, CH_4, NO_2, and HNO_3, *Appl. Opt.*, *33*, 454-472, 1994.

Wert, B.P., A. Fried, B. Henry, S. Cartier, Evaluation of inlets used for airborne measurement of formaldehyde, *J. Geophys. Res.*, *107*(D13), doi:10.1029/2001JD001072, 2002.

White, J.U., Long optical paths of large aperture, *J. Opt. Soc. Am.*, *32*, 285-288, 1942.

Worden, H., R. Beer, and C.P. Rinsland, Airborne infrared spectroscopy of 1994 western wildfires, *J. Geophys. Res.*, *102*, 1287-1299, 1997.

Yokelson, R.J., D.W.T. Griffith, and D.E. Ward, Open-path Fourier transform infrared studies of large-scale laboratory biomass fires, *J. Geophys Res.*, *101*, 21,067-21,080, 1996.

Yokelson, R.J., R. Susott, D.E. Ward, J. Reardon, and D.W.T. Griffith, Emissions from smoldering combustion of biomass measured by open-path Fourier transform infrared spectroscopy, *J. Geophys. Res.*, *102*, 18,865-18,877, 1997.

Yokelson, R.J., J.G. Goode, D.E. Ward, R.A. Susott, R.E. Babbitt, D.D. Wade, I.T. Bertschi, D.W.T. Griffith, and W.M. Hao, Emissions of formaldehyde, acetic acid, methanol, and other trace gases from biomass fires in North Carolina measured by airborne Fourier transform infrared spectroscopy, *J. Geophys. Res.*, 104, 30,109-30,125, 1999.

Yokelson, R.J. and I.T. Bertschi, Vibrational spectroscopy in the study of fires, in *Handbook of Vibrational Spectroscopy*, edited by J.M. Chalmers and P.R. Griffiths, Vol. 4, pp. 2879 – 2886, John Wiley & Sons, Ltd, 2002.

Yokelson, R.J., I.T. Bertschi, T.J. Christian, P.V. Hobbs, D.E. Ward, and W.M. Hao, Trace gas measurements in nascent, aged, and cloud-processed smoke from African savanna fires by airborne Fourier transform infrared spectroscopy (AFTIR), *J. Geophys. Res.*, *108*(D13), 8478, doi:10.1029/2002JD002322, 2003.

Figure Captions.

Figure 1. A simplified schematic of the system built to deliver standards to AFTIR. CG, carrier gas; FC, flow controller (mass flow range in standard liters per minute); CV, control valve; PV, pneumatic valve (halocarbon-wax coated); TV, Teflon valve; FM, flow meter; NV, needle valve; STD, standard. The regulator and shutoff on each gas tank is not shown.

Figure 2. The reciprocal of the flow rate delivered to AFTIR versus the CO $1/e$ exchange time for the AFTIR cell.

Figure 3. NH_3 passivation losses compared to gases that track CO (see text).

Figure 4. Effect of flow rate on rate of system passivation (see text).

Figure 5. The NH_3 passivation rate for the AFTIR cell is independent of carrier gas (see text).

Figure 6. The passivation lag for NH_3 is longer with an uncoated steel inlet (b) than with a Teflon inlet (a). However, the passivation lag for NH_3 with a halocarbon-wax, coated steel inlet (c) is the same as with a Teflon inlet even at low temperature.

Figure 7. The ratio of three different trace gases to C_2H_4 (as measured by AFTIR) compared to the actual ratio determined by OP-FTIR (which is immune to sampling artifacts) in well-mixed smoke. In a) the independent axis is the length of time that each smoke sample was drawn into the AFTIR Pyrex cell. Four samples at longer sample acquisition times are not shown to highlight details at the shorter times. In b) the independent axis is the sample acquisition time multiplied by the sample-specific, absolute NH_3 mixing ratio measured by OP-FTIR. These values ranged from 148 to 802 ppb.

Figure 1.

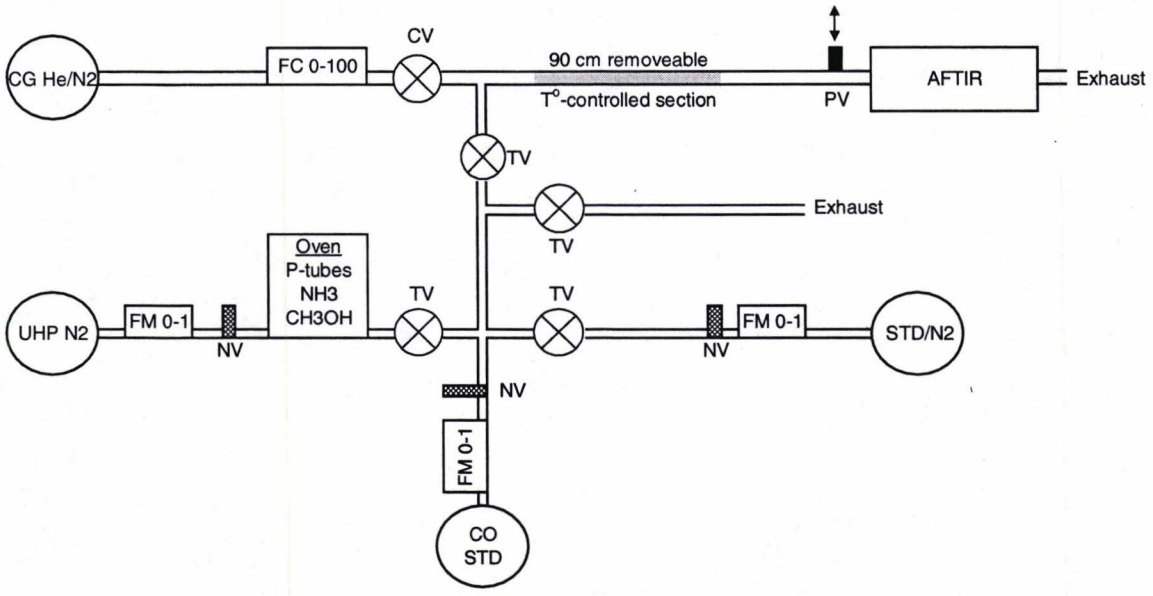
CG He/N2
FC 0-100
CV
90 cm removeable
T°-controlled section
PV
AFTIR
Exhaust
TV
Exhaust
TV
Oven
P-tubes
NH3
CH3OH
UHP N2
FM 0-1
NV
TV
TV
FM 0-1
NV
STD/N2
NV
FM 0-1
CO
STD

Figure 2.

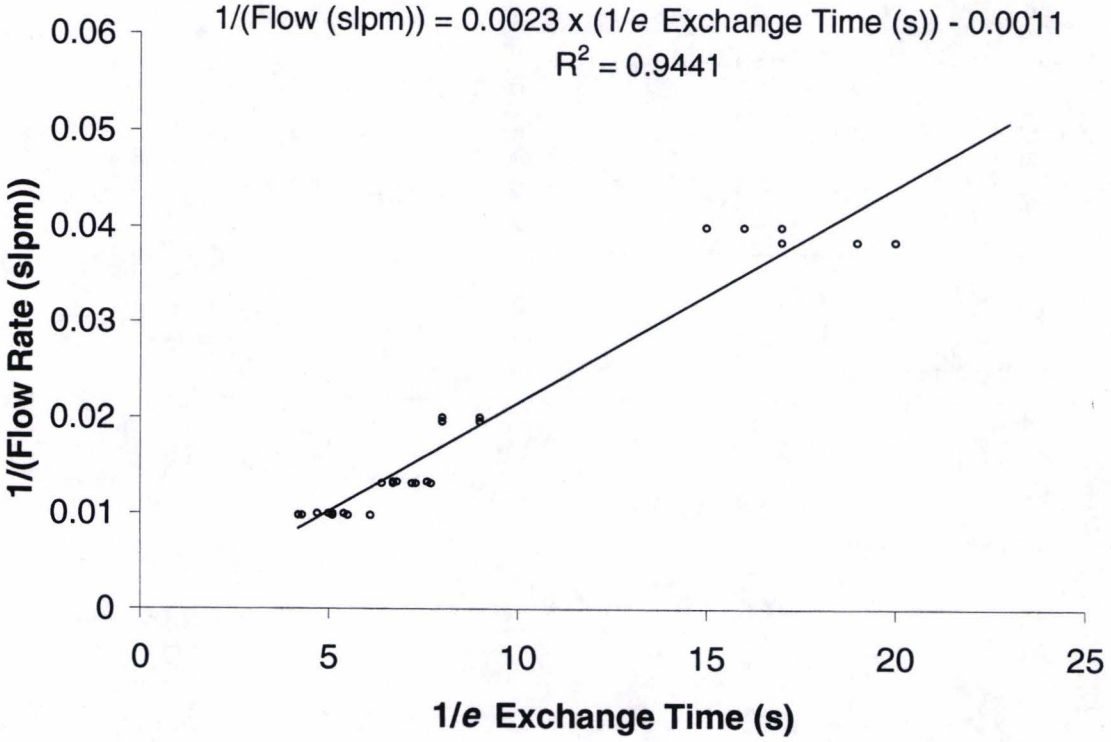
1/(Flow (slpm)) = 0.0023 x (1/e Exchange Time (s)) - 0.0011
R2 = 0.9441
1/(Flow Rate (slpm))
0.06
0.05
0.04
0.03
0.02
0.01
0
0
5
10
15
20
25
1/e Exchange Time (s)

Figure 3.

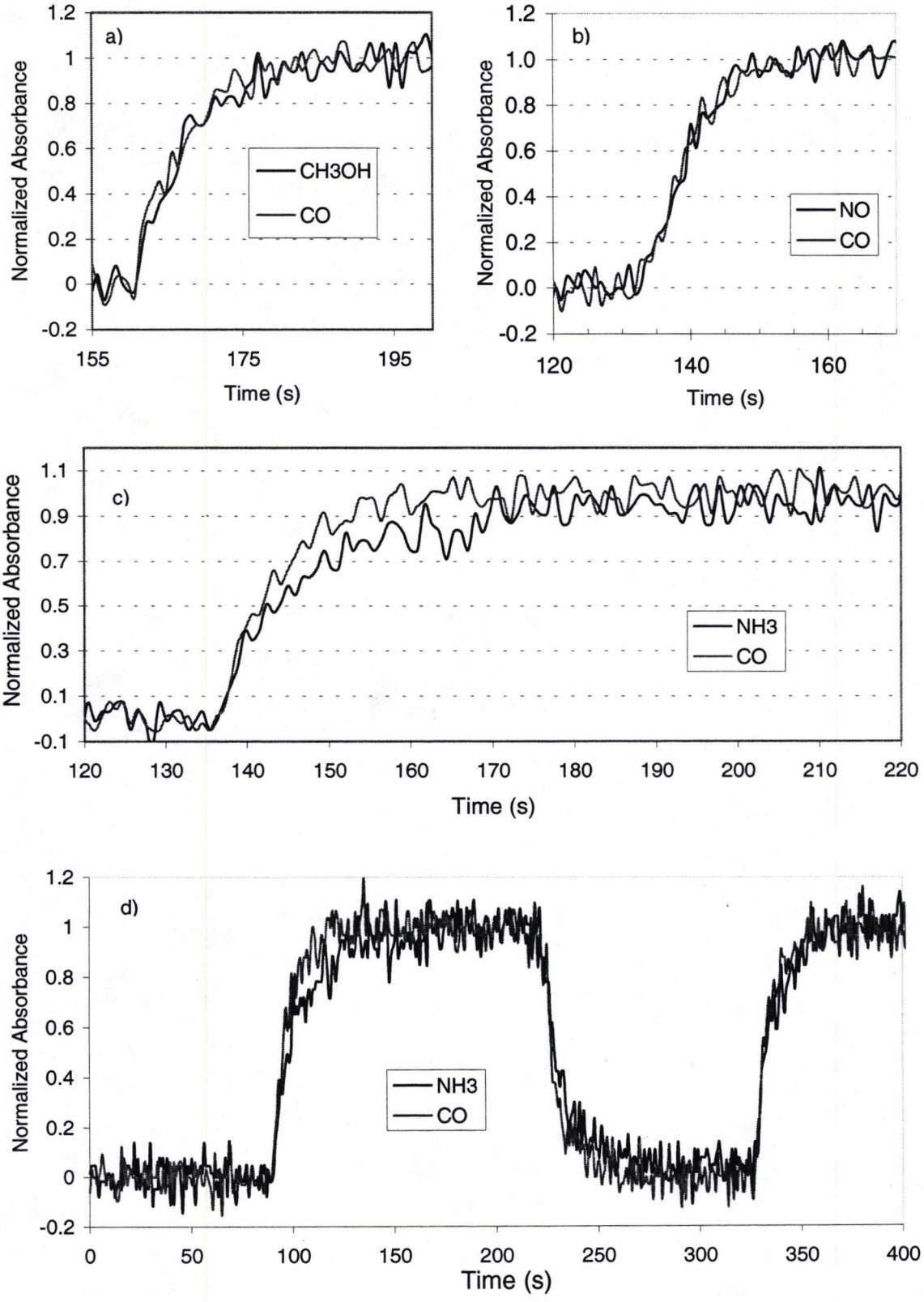
a)
Normalized Absorbance
Time (s)
CH3OH
CO
b)
Normalized Absorbance
Time (s)
NO
CO
c)
Normalized Absorbance
Time (s)
NH3
CO
d)
Normalized Absorbance
Time (s)
NH3
CO

Figure 4.

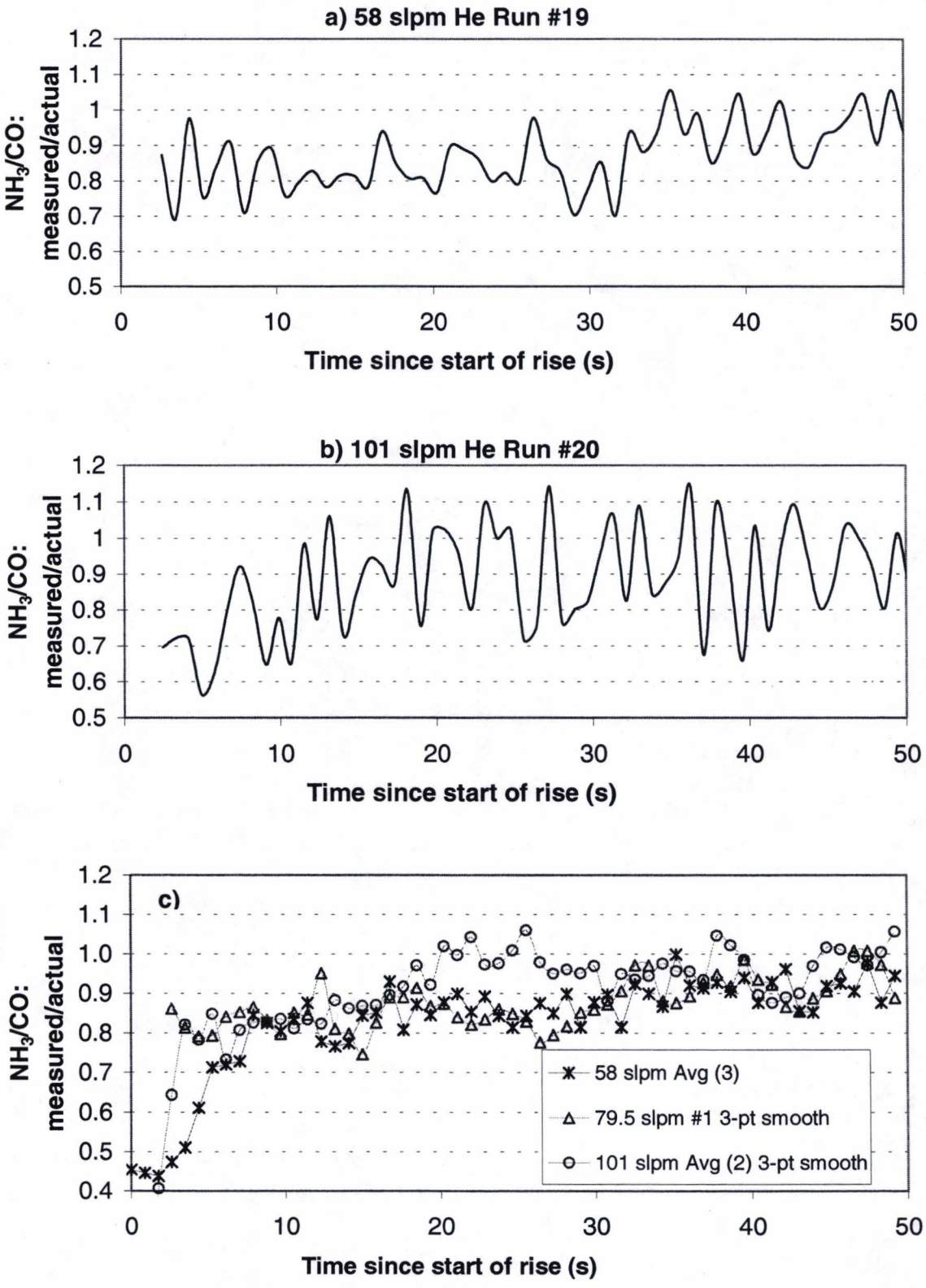
a) 58 slpm He Run #19
NH3/CO: measured/actual
Time since start of rise (s)
b) 101 slpm He Run #20
NH3/CO: measured/actual
Time since start of rise (s)
c)
NH3/CO: measured/actual
58 slpm Avg (3)
79.5 slpm #1 3-pt smooth
101 slpm Avg (2) 3-pt smooth
Time since start of rise (s)

Figure 5.

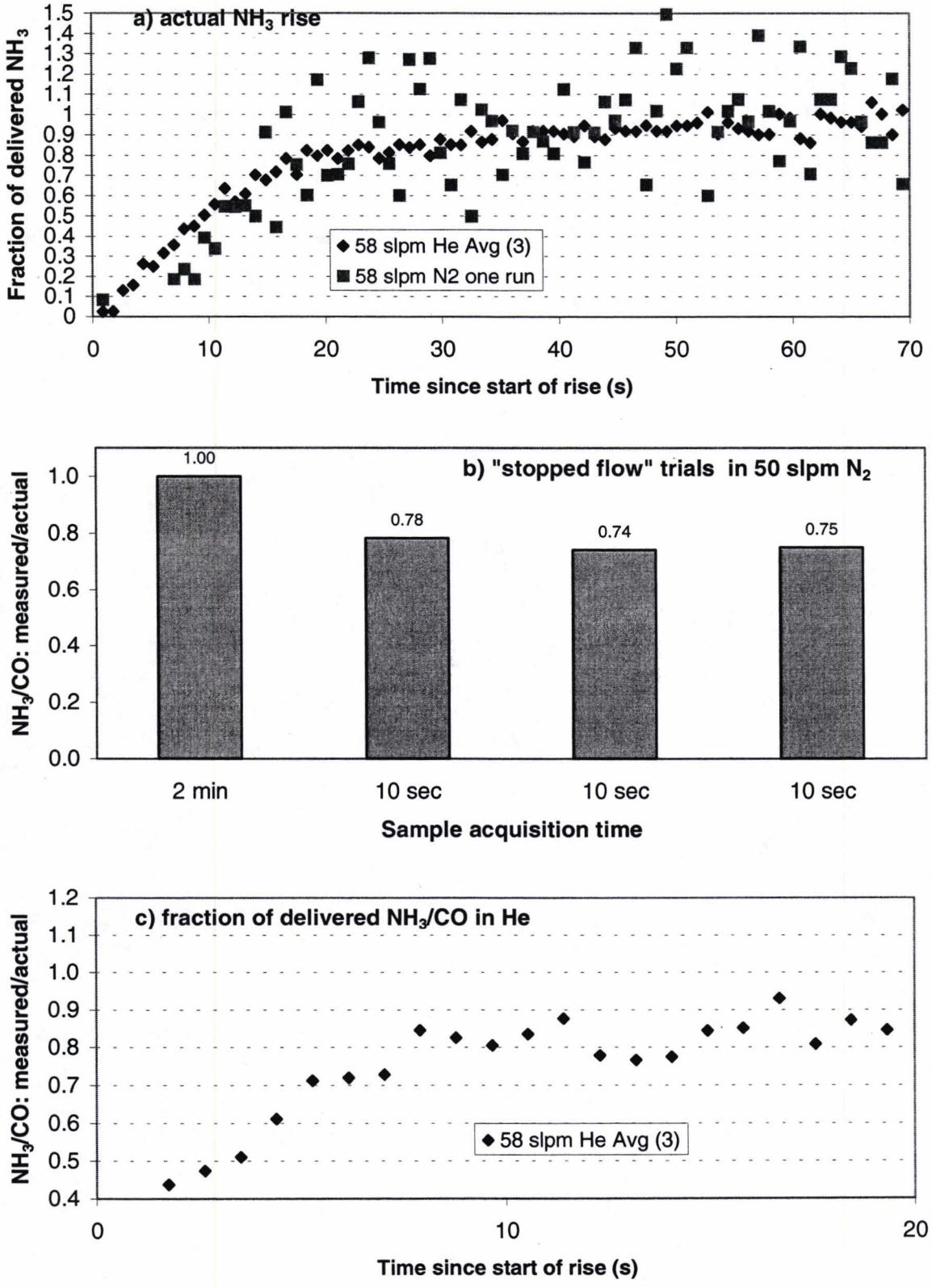
a) actual NH3 rise
Fraction of delivered NH3
Time since start of rise (s)
58 slpm He Avg (3)
58 slpm N2 one run
b) "stopped flow" trials in 50 slpm N2
NH3/CO: measured/actual
1.00
0.78
0.74
0.75
2 min
10 sec
10 sec
10 sec
Sample acquisition time
c) fraction of delivered NH3/CO in He
NH3/CO: measured/actual
58 slpm He Avg (3)
Time since start of rise (s)

Figure 6.

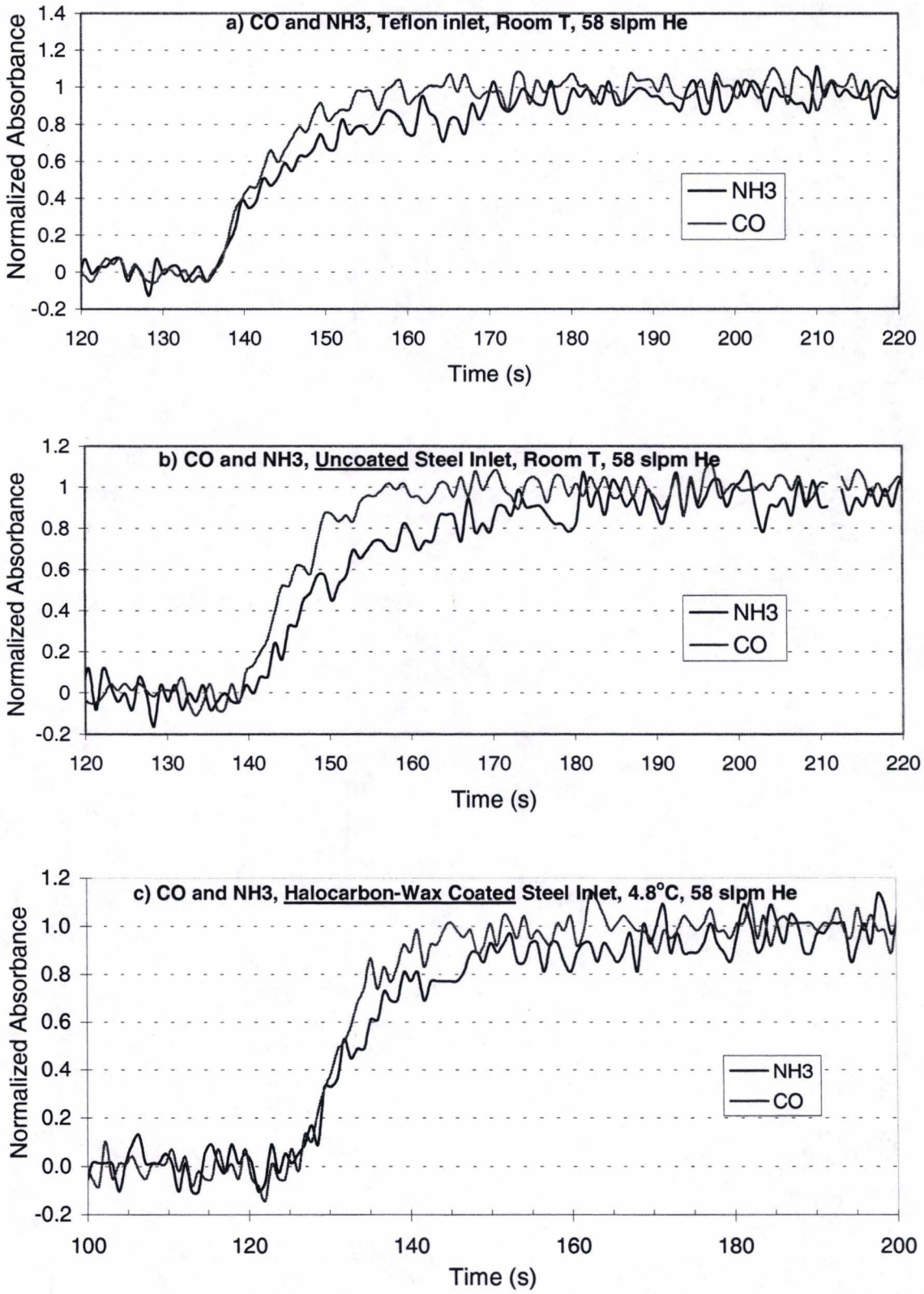
a) CO and NH3, Teflon inlet, Room T, 58 slpm He
Normalized Absorbance
Time (s)
NH3
CO
b) CO and NH3, Uncoated Steel Inlet, Room T, 58 slpm He
Normalized Absorbance
Time (s)
NH3
CO
c) CO and NH3, Halocarbon-Wax Coated Steel Inlet, 4.8°C, 58 slpm He
Normalized Absorbance
Time (s)
NH3
CO

Figure 7.

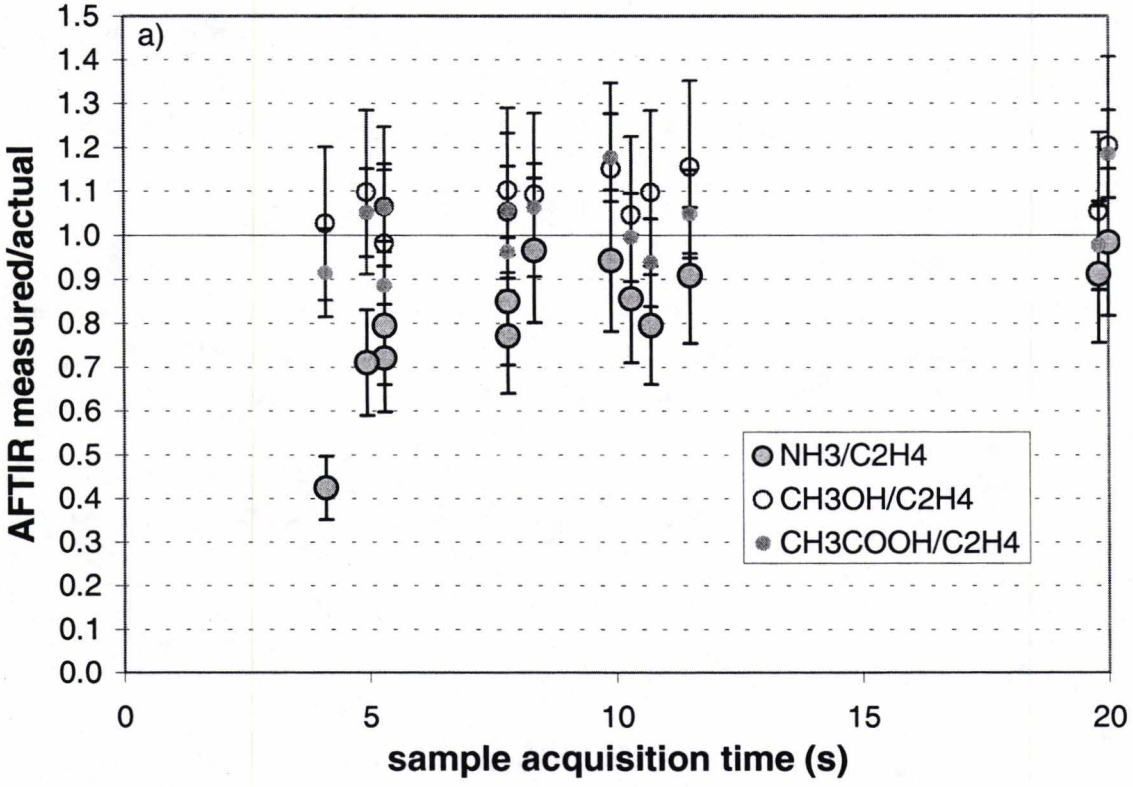
a)
AFTIR measured/actual
sample acquisition time (s)
NH3/C2H4
CH3OH/C2H4
CH3COOH/C2H4

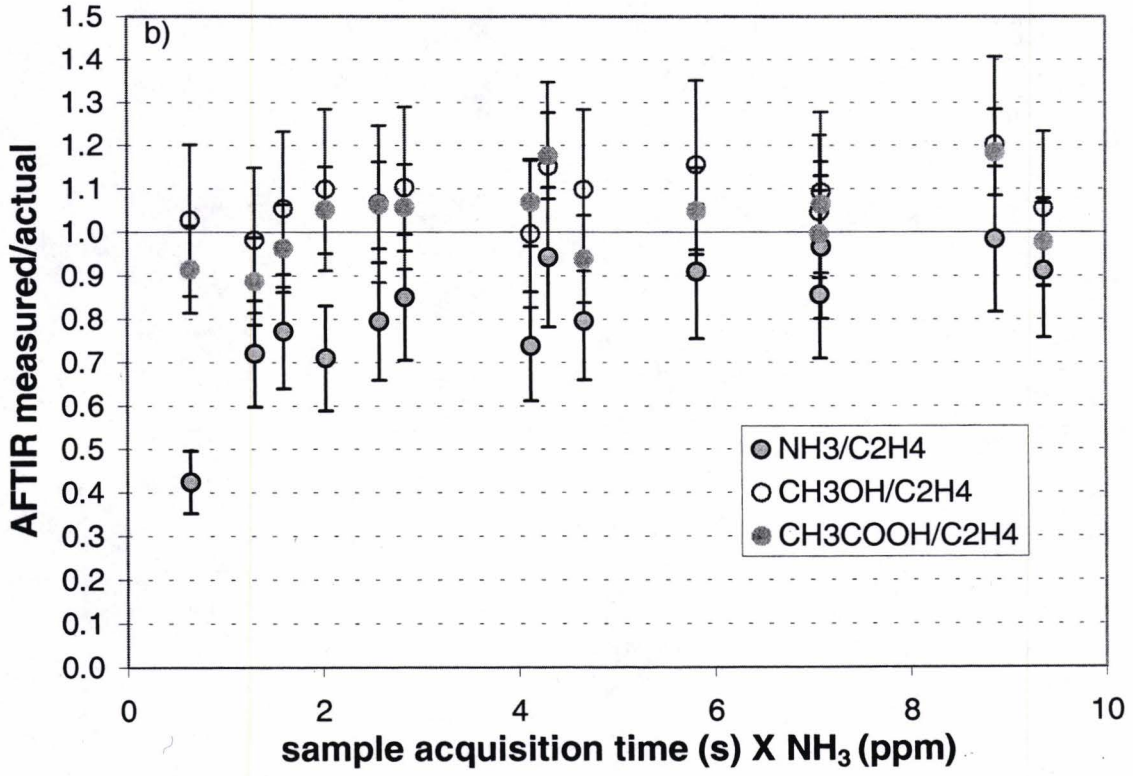
b)
AFTIR measured/actual
sample acquisition time (s) X NH3 (ppm)
NH3/C2H4
CH3OH/C2H4
CH3COOH/C2H4

JOURNAL OF GEOPHYSICAL RESEARCH, VOL. 108, NO. D13, 8472, doi:10.1029/2002JD002100, 2003

Trace gas and particle emissions from fires in large diameter and belowground biomass fuels

Isaac Bertschi,[1,2] Robert J. Yokelson,[1] Darold E. Ward,[3,4] Ron E. Babbitt,[3] Ronald A. Susott,[3] Jon G. Goode,[1,5] and Wei Min Hao[3]

Received 15 January 2002; revised 30 July 2002; accepted 6 August 2002; published 15 February 2003.

[1] We adopt a working definition of residual smoldering combustion (RSC) as biomass combustion that produces emissions that are not lofted by strong fire-induced convection. RSC emissions can be produced for up to several weeks after the passage of a flame front and they are mostly unaffected by flames. Fuels prone to RSC include downed logs, duff, and organic soils. Limited observations in the tropics and the boreal forest suggest that RSC is a globally significant source of emissions to the troposphere. This source was previously uncharacterized. We measured the first emission factors (EF) for RSC in a series of laboratory fires and in a wooded savanna in Zambia, Africa. We report EF_{RSC} for both particles with diameter <2.5 μm (PM2.5) and the major trace gases as measured by open-path Fourier transform infrared (OP-FTIR) spectroscopy. The major trace gases include carbon dioxide, carbon monoxide, methane, ethane, ethene, acetylene, propene, formaldehyde, methanol, acetic acid, formic acid, glycolaldehyde, phenol, furan, ammonia, and hydrogen cyanide. We show that a model used to predict trace gas EF for fires in a wide variety of aboveground fine fuels fails to predict EF for RSC. For many compounds, our EF for RSC-prone fuels from the boreal forest and wooded savanna are very different from the EF for the same compounds measured in fire convection columns above these ecosystems. We couple our newly measured EF_{RSC} with estimates of fuel consumption by RSC to refine emission estimates for fires in the boreal forest and wooded savanna. We find some large changes in estimates of biomass fire emissions with the inclusion of RSC. For instance, the wooded savanna methane EF increases by a factor of 2.5 even when RSC accounts for only 10% of fuel consumption. This shows that many more measurements of fuel consumption and EF for RSC are needed to improve estimates of biomass burning emissions. *INDEX TERMS:* 0345 Atmospheric Composition and Structure: Pollution—urban and regional (0305); 0368 Atmospheric Composition and Structure: Troposphere—constituent transport and chemistry; 0394 Atmospheric Composition and Structure: Instruments and techniques; 0365 Atmospheric Composition and Structure: Troposphere—composition and chemistry; *KEYWORDS:* biomass burning, smoldering combustion, oxygenated organic compounds, ammonia, methanol, smoke

Citation: Bertschi, I., R. J. Yokelson, D. E. Ward, R. E. Babbitt, R. A. Susott, J. G. Goode, and W. M. Hao, Trace gas and particle emissions from fires in large diameter and belowground biomass fuels, *J. Geophys. Res.*, *108*(D13), 8472, doi:10.1029/2002JD002100, 2003.

1. Introduction

[2] The Earth's atmosphere is a complex mixture of gases and particles from many natural and anthropogenic sources. Since the emergence of plant life from the oceans, fires have strongly influenced the atmosphere [*Wallace and Hobbs*, 1977]. The past several decades have seen rapidly expanding research into how biomass fire emissions affect the physics and chemistry of the atmosphere. It is now well known that biomass fires emit globally significant amounts of carbon dioxide (CO_2), carbon monoxide (CO), nitrogen oxides (NO_x), methane (CH_4), nonmethane hydrocarbons (NMHC), oxygenated volatile organic compounds (OVOC), and reduced nitrogen-containing species such as ammonia (NH_3) and hydrogen cyanide (HCN) [*Crutzen and Andreae*, 1990; *Yokelson et al.*, 1996, 1999; *Holzinger et al.*, 1999]. Several of these gases contribute to the greenhouse effect. Additionally, biomass fire emissions influence the amount of tropospheric ozone (O_3), which is a greenhouse gas and a reactive oxidant involved in many photochemical processes [*Stith et al.*, 1981; *Delany et al.*, 1985; *Finlayson-Pitts and Pitts*, 1986; *Fishman et al.*, 1991; *Mason et al.*, 2001]. Biomass burning also produces large amounts of particles that influence the radiative properties of the atmosphere and,

[1]Department of Chemistry, University of Montana, Missoula, Montana, USA.
[2]Now at Interdisciplinary Arts and Sciences, University of Washington-Bothell, Bothell, Washington, USA.
[3]Fire Sciences Laboratory, U.S. Department of Agriculture (USDA) Forest Service, Missoula, Montana, USA.
[4]Now at Enviropyronics, LLC, White Salmon, Washington, USA.
[5]Now at Bruker Optics, Inc., Billerica, Massachusetts, USA.

Copyright 2003 by the American Geophysical Union.
0148-0227/03/2002JD002100$09.00

thus, the global climate [*Kaufman and Nakajima*, 1993; *Charlson et al.*, 1992].

[3] Nearly all previous field and laboratory studies of biomass burning quantified the emissions and/or fuel consumption for fires burning mostly in surface and aboveground, fine fuels (i.e., grasses, litter, shrubs, and foliage). In these fires, more than 80% of the fuels are normally consumed by flaming combustion and most of the emissions are entrained in a convection column associated with large flaming fronts. This study focuses on a different type of biomass combustion. Specifically, stumps, logs, downed branches, and "belowground biomass" (duff, roots, and organic soils) can smolder long after flaming and strong convection from a burned area has ceased. The phenomenon of smoldering combustion that consumes biomass (and produces smoke) at any location that is no longer influenced by the strong convection associated with a flame front has been defined as residual smoldering combustion (RSC) [*Wade and Lunsford*, 1989]. RSC has also been defined as "independent smoldering combustion not requiring a flame" [*Sandberg*, 1983]. We adopt the former definition of RSC for this atmospheric study because it is more closely related to the weak convection that normally characterizes the dispersion of the smoke that is produced. RSC can occur when a fire is producing a convection column that is unable to draw in all the fire emissions or after all strong convection from the fire has ceased.

[4] Several studies have already shown that RSC can be responsible for much of the fuel consumption in fires that have considerable atmospheric significance. For instance, *Kauffman et al.* [1998] reported that pasture maintenance burns on the site of former tropical woodlands are the most prevalent use of fire in the Brazilian Amazon and that RSC of large diameter woody fuels accounted for up to 38–44% of the biomass consumed by these fires. Typically, the original forests on these sites are slashed at the beginning of the dry season and burned after 2–3 months of drying [*Kauffman et al.*, 1995]. Large woody fuels remain and they are gradually consumed in pasture maintenance fires in subsequent years. Eventually the site is degraded and abandoned and a new pasture is established. The smoldering combustion of dead woody fuels is a significant part of each fire in the cycle and it often lasts for days or weeks after flaming combustion has subsided [*Ward et al.*, 1992; *Kauffman et al.*, 1994; *Barbosa and Fearnside*, 1996; *Guild et al.*, 1998; *Carvalho et al.*, 1998]. *Levine* [1999] estimated that 89% of the smoke in the extensive 1997 haze event in southeast Asia was produced by peat fires, which would probably involve RSC. Therefore, it seems likely that both global deforestation and pasture maintenance in former woodlands produce large amounts of RSC emissions. RSC has also been reported to consume over 50% of the biomass in temperate and boreal fires [*Sandberg*, 1983; *Fransden*, 1991; *Reinhardt et al.*, 1991; *Kasischke et al.*, 1999] (Sandberg, personal communication, 2001). Many smoke management problems associated with prescribed fires in the United States (e.g., smoke impacting highways or towns) involve RSC [*Hardy et al.*, 2002].

[5] To our knowledge, despite the importance of RSC, comprehensive measurements of RSC emissions were not available when this work began. Several factors contributed to this lack of data. Many previous measurements of biomass burning emissions relied on airborne sampling, which can only sample the emissions lofted by convection. However, RSC emissions (according to our definition) are not influenced by strong, fire-induced convection and, at least initially, stay near the ground. Quantifying site average RSC emissions in a ground-based field experiment would have required characterizing many point sources distributed over a large, remote area for many days with variable winds. As a result of the lack of data, atmospheric chemistry and smoke production models were (implicitly or explicitly) based on very uncertain assumptions about RSC emissions.

[6] Because of the general need to better understand biomass burning, and also increased public concern about the impacts of smoke on air quality, we recently carried out laboratory and field studies dedicated explicitly to RSC. We report preliminary observations regarding a few key environmental variables that influence the extent of RSC in fires and the first comprehensive measurements of the emissions from the RSC of RSC-prone fuels. Specifically, we used filter sampling and spectroscopic techniques to measure PM2.5 (particles with diameter < 2.5 μm), CO_2, CO, CH_4, NMHC, OVOC, NH_3, and HCN emitted by RSC of large diameter logs, wood debris, duff, and organic soils in a controlled laboratory setting where we could capture and analyze all the emitted smoke. We also report field measurements of RSC at an African woodland site made during September 2000 as part of SAFARI 2000. Our RSC emission factors (EF) for many species are quite different than the EF measured during the "non-RSC" portion of similar fires. The large impact this can have on biomass burning emissions estimates is demonstrated with a few examples.

2. Experimental

2.1. Fuel Characteristics

[7] We selected fuels for the laboratory fires that represent the types of biomass most commonly consumed by RSC (Table 1). We burned three duff samples from a pine/fir forest in Montana and two organic soil samples from a jack pine forest floor near Fort Providence, Northwest Territories, Canada. We burned a stump (35 cm diameter, 40 cm height) along with the surrounding duff that was extracted from a Montana pine forest. Our other wood fuels were large diameter, dead hardwood logs collected from a riparian zone outside Missoula, MT and smaller diameter softwood debris (partially decayed) sampled from a pine/larch forest in rural western Montana. We measured the moisture, carbon, hydrogen, and nitrogen content of many of the fuels with the exception of the miombo logs.

[8] In addition to our fire-integrated laboratory measurements, we made spot measurements of the RSC emissions, in situ, from a group of smoldering large diameter (>30 cm) logs in a wooded savanna (miombo) in Zambia, Africa approximately 3 days after a flaming front had passed through the area igniting the logs. Similar dead and downed logs likely account for nearly all the RSC that occurs in Zambia's tropical woodlands.

2.2. Laboratory Sampling Platforms

[9] As noted above, most of the fires were burned at the USDA Forest Service Fire Science Laboratory (FSL). The

Table 1. Fuels Prone to RSC That Were Burned in This Study[a]

Fire Name	Fuel Type	Sample Location	Overstory/Understory	Fuel Properties %C	%N	$\%H_2O$	Combustion Factor (%)[b]
Lolo 1	Duff/Organic Soil	Lolo National Forest, Lolo Pass, Montana	Lodgepole Pine/Subalpine fir (*Pinus contorta/Abies lasiocarpa*)	47.6[c]	1.22[d]	8.5	45.8
Lolo 2				48.3[c]	1.22[d]	8.2	47.5
Lolo 3				48.8[c]	1.22[d]	11.4	65.4
NWT 1	Duff/Organic Soil	Fort Providence, Northwest Territories, Canada	Jack Pine/Black Spruce (*Pinus banksiana/Picea mariana*)	45.3[c]	1.67[d]	18.8	76.4
NWT 2				48.8[c]	1.67[d]	9.1	10.2
Stump	Mixture of Softwood/ Duff/Organic Soil	Blue Mountain, Missoula, MT	Douglas fir/Pinegrass (*Pseudotsuga menziesii/ Calamagrotis rubesceus*)	50[e]		70.6[f] 25.3[g]	79.8
Cottonwood Log 2	Large Diameter (>30 cm) Hardwood Logs	USDA FSL, Missoula, Montana	Black Cottonwood (*Populus balsamifera*)	50[e]	0.04[d]		94.2
Zambia Log	Large Diameter (>30 cm) Hardwood Logs	Wooded Savanna, West Central Zambia, Africa	*Julbernardia globiflora*, *Brachystegia* sp.	50[e]			
PC 1	Softwood Debris	Plum Creek, Inc. Timberland, Seeley Lake, MT	Larch, Ponderosa Pine, Douglas fir (*Larix occidentalis*, *Pinus* sp., *Pseudotsuga menziesii*)	50[e]			90.6
PC 2				50[e]			94.2

[a]Blank indicates not measured.
[b]The combustion factor is defined here as the percentage of the fuel actually exposed to fire that was volatilized. For the duff, organic soils, and stump fire, the fuel includes all the material above the mineral soil and there was a large residual mass that included ash and char.
[c]Based on analysis of the sample that was burned.
[d]Based on analysis of a sample similar to the sample that was burned.
[e]Based on the study of *Susott et al.* [1996].
[f]Fuel moisture of wood fuel (stump).
[g]Fuel moisture of duff/organic soil.

FSL combustion facility has a floor area of 12.3 × 12.3 m and a ceiling height of 18.0 m. Outside air is drawn into the room and then exhausted through a stack attached to the ceiling. The stack has an inner diameter of approximately 1.6 m with an "inverted funnel" base opening to 3.6 m. The base of the stack was positioned 3 m above a continuously weighed fuel bed situated slightly above floor level. A sampling platform surrounds the stack 15.5 m above the floor where several ports can be used to sample pressure, temperature, and particle and trace gas emissions.

[10] The FSL combustion facility is ideal for measuring the prolonged emissions from RSC of biomass since all of the emissions are entrained into the combustion chamber stack where they become well mixed [*Goode et al.*, 1999] and their composition can be measured for the duration of the fire. However, especially near the end of these very slow burning fires (e.g., consumption rates as low as a few grams per hour), the entrained emissions are so dilute that many species could only be measured with low signal to noise from the sampling platform. Therefore, we employed the following sampling strategy. For each laboratory fire, real-time instruments for CO_2 and CO were deployed on the sampling platform to continuously measure the carbon production profile. The open-path Fourier transform infrared (OP-FTIR) spectrometer was deployed with its optical path spanning the smoke column about one meter above the fires for frequent spot measurements of CO_2, CO and most other stable and reactive gases present above several ppbv. This arrangement optimized the FTIR signal to noise and allowed us to scale the FTIR measurements to the total emissions produced over time.

[11] Our OP-FTIR system consists of an FTIR spectrometer and an open, adjustable path White cell comounted on Super-Invar, Teflon-coated girders. The system was described in detail by *Yokelson et al.* [1997] and only a brief description is given here. The FTIR spectrometer (MIDAC 2500) was used with a spectral resolution of 0.5 cm^{-1} and the open-path White cell had a path length of 51 m for all the laboratory measurements reported here. The entire OP-FTIR system was supported at each end by two mobile carts allowing spectra to be collected alternately for the smoke and chamber "background" air. Separate spectra could have been collected every 1.7 s, but that would have generated an enormous volume of data over the period of the RSC fires. Instead, we averaged 100–500 spectral scans for each, alternating, spot measurement of the smoke or background. We acquired many averaged spectra of the emissions during the entire period of RSC of each fire to provide temporal profiles of the trace gases produced. A handheld, chromel-alumel thermocouple positioned close to the White cell path measured the path temperature and pressure was measured with a pressure transducer (Baratron, MKS).

[12] The total CO_2 and CO emitted from the fires was captured, mixed, and exhausted up the stack where it was measured throughout the course of each fire. We measured the carbon production profile with nondispersive infrared (NDIR) CO_2 and CO analyzers (LI-COR, Inc., model 6262; Thermo Environmental Instruments, Inc., model 48C, respectively). A second NDIR CO_2 analyzer was used to measure CO_2 fluctuations in the ambient background air. The temperature, pressure, and the stack flow were measured at the sampling platform using calibrated chromel-alumel thermocouples, pressure transducers (Baratron, MKS), and two mass flowmeters (Kurz, model 455), respectively. A digital scale (Mettler, PM 35) measured the mass loss during the fires. All of these data were logged every 2 s. Teflon filters of the smoke and background air were collected for 10–30 min each at the sampling platform using a cyclone that rejected particles with an effective aerodynamic diameter >2.5 μm at the flow controller set point of 30 L min^{-1}. The flow reading was logged every second so that clogged filters could be identified and rejected. Both the exposed filters and unexposed control filters were weighed before and after the fire in a dedicated room maintained at 50 ± 2% RH and 20°C. Our instrumen-

tation and method for quantifying PM2.5 has been compared to the Federal Reference Method for PM2.5 and has good accuracy [*Trent et al.*, 2000].

2.3. Field Measurements of RSC Emissions in Zambia

[13] We used the OP-FTIR system described above with minor modifications to measure RSC emissions from smoldering logs in a miombo woodland in rural Zambia. Two automotive batteries powered the laptop computer controlling the FTIR data acquisition and the MIDAC spectrometer. We used two shipping crates ($\sim$1 $\times$ 0.5 $\times$ 0.5 m) to elevate the instrument above the smoldering wood debris and optimize the concentration of smoke passing through the FTIR path. Background spectra were collected by deploying the OP-FTIR in a smoke-free area upwind of the emission source. We used a chromel-alumel thermocouple and a portable, digital barometer (Cole-Parmer) to measure temperature and pressure in the FTIR optical path. Individual IR spectra were collected every 0.8 s and subsequently signal averaged as appropriate to improve the signal-to-noise and accuracy of the spectral analysis.

2.4. Retrieval of Excess Mixing Ratios From Spectra

[14] We acquired hundreds of spot measurements of smoke and background air by FTIR (each averaged over 3–15 min) during our laboratory and field measurements of RSC emissions. Mixing ratios for CO_2, CO, and CH_4 were obtained by fitting regions of the transmission spectra with synthetic calibration, classical least squares (CLS) methods described in detail elsewhere [*Griffith*, 1996; *Yokelson et al.*, 1996, 1997; *Yokelson and Bertschi*, 2002]. We take the excess mixing ratios in smoke, for these compounds, to be the smoke mixing ratio minus the background mixing ratio. We also generated absorbance spectra of the smoke (using background spectra obtained between the smoke spectra) and analyzed them by synthetic calibration CLS for formaldehyde (CH_2O), ethane (C_2H_6), acetylene (C_2H_2), hydrogen cyanide (HCN), and ammonia (NH_3) to directly yield excess mixing ratios. In addition, the absorbance spectra were analyzed by spectral subtraction [*Yokelson et al.*, 1997] to directly yield excess mixing ratios for water (H_2O), ethene (C_2H_4), propene (C_3H_6), acetic acid ($CH_3C(O)OH$), methanol (CH_3OH), formic acid (HC(O)OH), phenol (C_6H_5OH), furan (C_4H_4O), glycolaldehyde ($HOCH_2C(O)H$), and ammonia (NH_3). This suite of compounds accounts for all of the significant features found in our IR smoke spectra, with the exception of a large peak at 2848 cm^{-1} that is yet to be identified. The detection limit for each species varied depending on the amount of signal averaging, fluctuations in the spectrometer performance, and the analysis method. For most compounds the detection limit was in the range 5–20 ppbv and the uncertainty is approximately $\pm$5% (1σ) or the detection limit, whichever is greater.

3. Results and Discussion

[15] We used the excess mixing ratios from each smoke spectrum (or spot measurement) obtained during the fires to calculate spot measurement specific values for emission ratios (ER) between coemitted trace gases; modified combustion efficiency (MCE defined as $\Delta CO_2/(\Delta CO_2 + \Delta CO)$ where Δ indicates an excess value in smoke above background), and EF (g compound per kg fuel (dry weight)). The EF were calculated using the carbon mass balance method [*Ward and Radke*, 1993], which assumes that all the "burned" carbon is volatilized and detected and that the fuel carbon percentage (by mass) is the measured value (Table 1) or 50%. We refer to these spot measurement specific values as "instantaneous" values and abbreviate them as IER, IMCE, and instantaneous EF (IEF). The IEF calculated in this manner for CO_2 and CO were in good agreement with IEF calculated from the NDIR and mass loss data. The instantaneous values changed slowly, but significantly over the course of most fires as discussed in section 3.1 (see Figures 1–4).

[16] We also calculate ER, MCE, and EF that are representative of all the fuel consumed by RSC for each entire fire. To do this we used weighted averaging as follows. Each spectrum was assumed valid for the time it was collected and for one half of any unmeasured time interval before and after the spectrum. The sum of the CO_2 and CO production measured by the real time instruments over this time period was assumed to be proportional to fuel consumption during that period and was used as the weighting factor. (For the field measurements of the smoldering miombo logs, we assumed the weighting factors were equal as justified in section 3.1.) The weighted average ER was then used to calculate weighted average MCE and EF. Table 2 lists these RSC average ER, MCE, and EF for each fire. We denote these quantities as ER_{RSC}, MCE_{RSC}, and EF_{RSC}, respectively. We will use the instantaneous values to show important trends in the emissions during a fire and the RSC average values to compare with integrated values from other types of fires and (in combination with estimates of fuel consumption by RSC) to estimate the effect of RSC on total emissions.

[17] Previous work usually reported fire-integrated ER, MCE, and EF, which were representative of entire fires in aboveground fine fuels that did not feature RSC. Under those conditions, the fire-integrated MCE values are useful as an indicator of the relative amount of flaming and smoldering over the course of the fire. Further, *Yokelson et al.* [1996, 1997, 1999] and *Goode et al.* [2000] reported a high correlation between the fire-integrated MCE and the fire-integrated EF for various compounds. In contrast, in this work, the RSC average quantities should represent the entire RSC process and the MCE are simply typical values for "pure" smoldering combustion.

3.1. Chemistry and Physics of RSC

3.1.1. Initiation and Duration of RSC

[18] In nature, RSC is usually initiated by flaming combustion of fine, surface fuels. To mimic this, we started each lab RSC fire by igniting 200 g of dry fine fuels on top of the RSC-prone fuel. (Emissions measurements began after the starter fuel was consumed and combustion of the RSC-prone fuel had commenced.) We burned additional experimental fires to explore the effects of a few, key physical variables. We found that low fuel moisture in organic soils [*Fransden*, 1987, 1997] and decomposition of woody fuels promoted easier ignition of the target fuels. In contrast, postignition fuel consumption was heavily dependent on whether fuel geometry promoted efficient heat transfer. For instance, dry, sound wooden blocks were only slightly

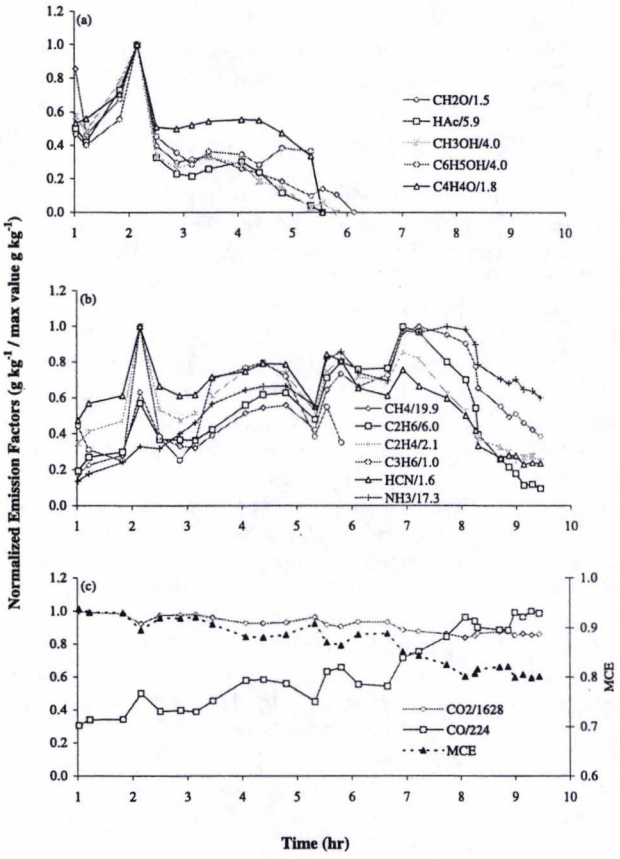

Figure 1. The trace gases detected by OP-FTIR in the smoke from the Northwest Territories Organic Soil 1 fire are shown as normalized IEF versus hours since ignition. (Specifically, each IEF is divided by the maximum IEF, which is shown in the legend.) The emissions are grouped according to their formation process: (a) the products of low-temperature pyrolysis of fresh biomass, which creates "low-temperature char," (b) the products of high-temperature pyrolysis of low-temperature char, and (c) the products of gasification. Part (c) also shows the MCE.

charred when they were placed 7 cm apart directly above small "starter fires." More than 50% of identical blocks were consumed by RSC if they were placed only 1 cm apart directly above identical starter fires. These observations are mentioned because, ultimately, fuel moisture, fuel geometry classifications, and other key environmental variables found to affect RSC might be mapped over large regions by remote sensing. In view of the large effect RSC can have on emissions estimates, such an effort could be warranted.

3.1.2. Combustion Processes and Emissions During RSC

[19] In this section, we describe and interpret the degree of variability in the IEF observed during the lab fires. The combustion of biomass involves many different chemical and physical processes that release many different particles and trace gases. To aid in assigning the emissions to specific processes, we describe the progression of emissions from an individual element of biomass as its temperature is rapidly raised (as would occur during a fire). *Yokelson et al.* [1996, 1997] described this previously and we offer a summary here. Distillation occurs when the biomass temperature is raised enough to exceed the boiling point of bound liquids. For instance, the fuel moisture will begin to "boil off" when the temperature reaches 100°C. At 100–200°C, the biomass begins to undergo pyrolysis, which is the thermal cleavage of molecular bonds in the cellulosic and lignin macromolecules that make up the solid biomass. Low-temperature pyrolysis (primarily occurring at 200–300°C) releases a white smoke, which is a complex, flammable mixture including reflective aerosol, low molecular weight oxygenated organic compounds, and water. The composition of these pyrolysis products is influenced by the temperature (or rate of change in temperature) and the chemical composition of the biomass [*Overend et al.*, 1995]. The release of oxygenated compounds and water by low-temperature pyrolysis produces a carbon-enriched, solid intermediate called "low-temperature char" that has high aliphatic content. When temperatures reach 400–600°C, the "low-temperature char" is subjected to "high-temperature pyrolysis," which produces gas-phase products such as alkanes and a solid intermediate called "high-temperature char" that is high in aromatic content. Once char is formed, "gasification" can begin to accompany pyrolysis. This is because the exothermic chemisorption of O_2 on char provides energy for gasification reactions in which solid char is converted to gas-phase products such as H_2, CO_2, CO, and H_2O. "Glowing combustion" is simply a popular term

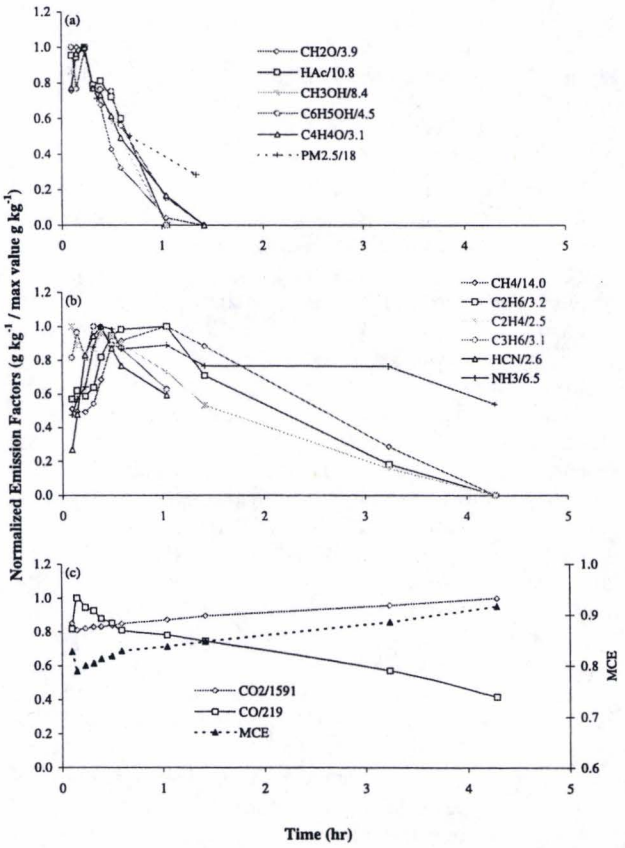

Figure 2. As in Figure 1, but for the Lolo Duff 1 fire.

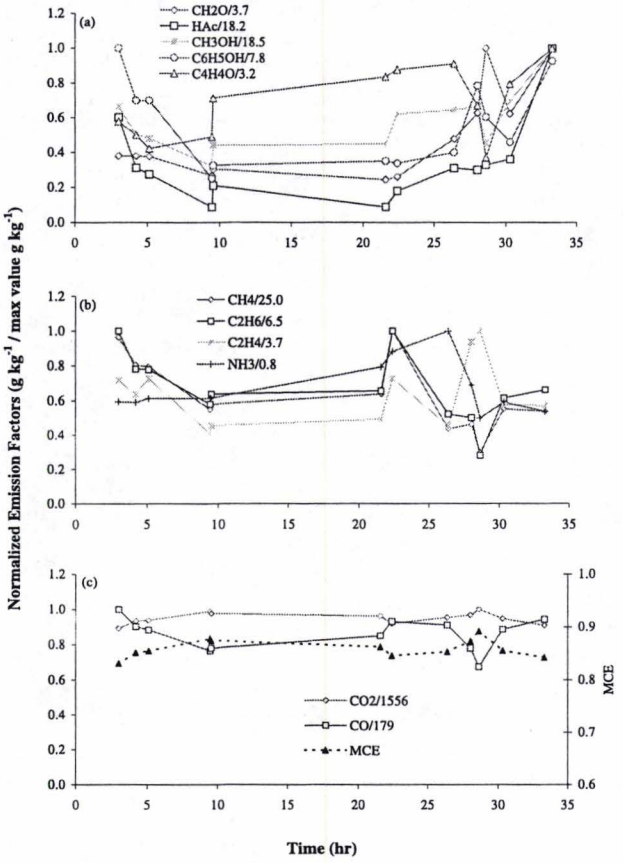

Figure 3. As in Figure 1, but for the Cottonwood Log 2 fire.

indicating gasification of sufficient intensity to emit visible light. The combination of gasification and high-temperature pyrolysis produces a faint bluish white smoke.

[20] In biomass fires, low- and high-temperature pyrolysis and gasification all produce flammable gases from biomass. Often, these gases are entrained in turbulent, diffusion flames and oxidized to CO_2, H_2O, and NO. Under these circumstances, both the flames and gasification supply the heat that drives pyrolysis. The combination of all these processes is commonly called "flaming combustion." In the absence of flames, the products of pyrolysis and gasification directly enter the atmosphere; a situation commonly termed "smoldering combustion." Many of the important differences between biomass fires and industrial combustion are due to significant amounts of smoldering combustion and high oxygen content (~45% dry mass) in biomass. In many of our RSC lab fires, the IEF varied significantly over the course of the fire. Flames were usually absent and we propose that the variation in the IEF could be due to the various smoldering combustion processes coming into dominance at different times.

[21] Figures 1 – 4 illustrate some typical emission profiles for different types of RSC-prone fuels. The data for each of these figures are based on the series of IEF calculated for each species from OP-FTIR spot measurements over the duration of the smoldering fire. Because the IEF may vary by 2 orders of magnitude for the array of compounds measured, the IEF were normalized by plotting each IEF value for a given species i as a fraction of the maximum IEF value for species i measured during a fire (i.e., during measurement interval n, the normalized IEF equals $IEF_{n,i}/IEF_{max,i}$).

[22] Figure 1 shows the IEF versus hours since ignition for the RSC during the first laboratory fire in organic soil from the Northwest Territories. These profiles are typical for RSC of the duff and organic soil samples. After the starter fuel was quickly consumed, a glowing front burned slowly downward from the surface pyrolyzing fresh biomass and generating white smoke ahead of the front. After 6 hours, white smoke production had ceased and the oxygenated compounds were below our detection limits (Figure 1a). We speculate that this coincides with the arrival of the glowing front at the mineral soil. The oxygenates from low-temperature pyrolysis may "disappear" at this point because the fresh biomass may be encapsulated by a char layer and also the emissions are filtered by overlying ash. About 7 hours after ignition the IEF for hydrocarbons begin a steep decline (Figure 1b). This could be because low-temperature char on the surface of the fuel elements is being converted to high-temperature char. Nine hours after ignition, gasification emissions dominate the fire (Figure 1c). This could signal that the surface of all the organic matter has progressed to the high-temperature char stage. Figure 1 shows clearly that an IEF measured at any one point during an organic soil/duff fire could easily be very different from the RSC average EF.

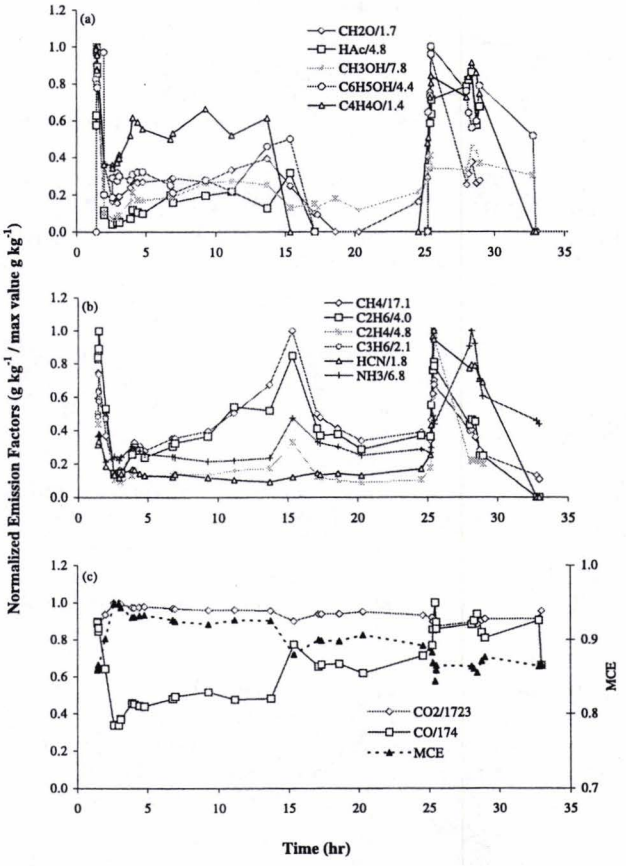

Figure 4. As in Figure 1, but for the Stump fire.

Table 2. Weighted Average ER and EF for RSC of Wood Debris and Duff/Organic Soils[a]

		ER (%)														
		% of CO_2	% of CO													
Fire Name	MCE	CO	CH_4	C_2H_4	C_2H_2	C_3H_6	C_2H_6	CH_2O	GA[b]	HFo[c]	HAc[d]	CH_3OH	C_6H_6O	C_4H_4O	NH_3	HCN
Lolo 1	0.879	13.8	14.1	1.61		1.06	4.60	1.20	0.07	0.08	2.07	2.72	0.57	0.48	6.47	0.96
Lolo 2	0.858	16.5	9.3	1.11		0.45	1.18	0.91	0.07	0.75	1.53	1.98	0.89	0.37	6.74	1.12
Lolo 3	0.857	16.7	4.5	0.63		0.58	0.46	1.09	0.18	0.84	2.29	2.99	0.67	0.40	2.07	1.01
NWT 1	0.891	12.2	14.1	1.01		0.23	2.27	0.41	0.02	0.19	0.60	0.84	0.30	0.24	12.80	0.85
NWT 2	0.848	17.9	6.7	0.80		0.44	1.37	2.58	0.36	1.34	1.95	2.61	0.77	0.36	7.89	1.33
Stump	0.904	10.6	11.9	1.40	0.23	0.33	1.68	0.64	0.02	0.22	0.69	2.18	0.55	0.31	3.30	0.45
Cwd 2	0.854	16.6	18.2	1.52	0.06	1.01	2.66	1.16	0.13	0.46	2.03	6.10	0.92	0.53	0.56	
Zambia Log[e]	0.854	17.1	25.6	1.33		0.86	2.59	2.05		0.44	2.48	4.46	0.42	0.53	1.99	
PC 1	0.861	16.2	2.6	0.19				0.05							0.44	
PC 2	0.861	16.1	6.7	0.21			0.32	0.12	0.06	0.08	0.09	0.37		0.04	0.28	

		EF (g kg^{-1})															
Fire Name	MCE	PM2.5	CO_2	CO	CH_4	C_2H_4	C_2H_2	C_3H_6	C_2H_6	CH_2O	GA[b]	HFo[c]	HAc[d]	CH_3OH	C_6H_6O	C_4H_4O	NH_3	HCN
Lolo 1	0.879	11.3	1454	128	10.4	2.06		2.03	6.32	1.64	0.19	0.17	5.67	3.97	2.44	1.48	5.04	1.19
Lolo 2	0.858	6.6	1460	153	8.2	1.71		1.03	1.94	1.49	0.21	1.89	5.05	3.47	4.59	1.37	6.29	1.66
Lolo 3	0.857		1478	157	4.0	0.99		1.37	0.78	1.84	0.60	2.16	7.72	5.38	3.54	1.53	1.98	1.53
NWT 1	0.891		1436	112	9.0	1.13		0.39	2.71	0.49	0.05	0.34	1.43	1.07	1.14	0.65	8.69	0.92
NWT 2	0.848	15.1	1448	165	6.3	1.32		1.08	2.43	4.56	1.29	3.63	6.90	4.91	4.29	1.44	7.91	2.12
Stump	0.904	15.8	1612	109	7.4	1.53	0.23	0.53	1.96	0.74	0.06	0.39	1.60	2.70	2.02	0.83	2.18	0.47
Cwd 2	0.856		1469	155	16.2	2.36	0.08	2.36	4.42	1.92	0.43	1.16	6.73	10.80	4.78	2.01	0.53	
Zambia Log[e]	0.854		1454	158	23.2	2.11		2.04	4.39	3.48		1.15	8.43	8.09	2.26	2.04	1.92	
PC 1	0.861		1570	162	2.4	0.30				0.09							0.43	
PC 2	0.861		1558	160	6.2	0.33			0.54	0.20	0.21	0.21	0.30	0.68		0.15	0.27	

[a]Blank indicates value below detection limit or not measured.
[b]Glycolaldehyde (other names include hydroxyacetaldehyde and hydroxyethanal).
[c]Formic acid.
[d]Acetic acid.
[e]Reported values are from equally weighted spot field measurements.

[23] Figure 2 shows that the progression of normalized IEF for the Lolo 1 duff fire is similar to that in the (larger) NWT 1 fire. In addition, during the Lolo 1 fire we collected a nearly continuous series of filters. As seen in Figure 2a, the PM2.5 emissions tracked the oxygenated organics (and the presence of visible white smoke) remarkably well. During RSC, the IEFPM2.5 started at a maximum of 17.5 and dropped to 5.0 g kg^{-1}. The RSC average EFPM2.5 for the Lolo duff samples were 6.6 and 11.3 g kg^{-1} (Table 2). The average of these first EF_{RSC} for PM2.5 from duff (~9 g kg^{-1}) is <70% of the recommended average EFPM2.5 for fires consuming mostly aboveground biomass in extratropical forests (14 g kg^{-1} [*Ward et al.*, 1993] and 13 g kg^{-1} [*Andreae and Merlet*, 2001]). In addition, complete combustion of the duff samples left large amounts of ash and, on average, only volatilized 53% of the total mass of the duff (Table 1). These observations suggest that a significant overestimate of PM2.5 emissions for RSC of duff could result if one used the mass of the duff available and previously reported EFPM2.5 for aboveground biomass. This should be considered when projecting the air quality impacts of boreal forest fires or prescribed fires that involve RSC of duff.

[24] In contrast to the RSC of duff and organic soils, the RSC of the large cottonwood log produced significant emissions of low-temperature pyrolysis products until the end of the fire (Figure 3a). During this fire, the heat from a slowly advancing, glowing front pyrolyzed adjacent areas of fresh biomass and the log was gradually consumed over ~34 hours with a relatively constant proportion of pyrolysis and glowing combustion. Because of the persistence of pyrolysis, the RSC average EF (EF_{RSC}) for the pyrolysis products are generally higher than those reported for the duff fires (Table 2). The EFPM2.5 was not measured, but is probably higher also based on the tracking of PM2.5 with oxygenates noted above. Because of the fairly stable mixture of combustion processes, most of the IEF measured during RSC of the log were within ±20% of the EF_{RSC}. Our field measurements of the smoldering logs in Zambia lasted ~1 hour and produced average EF that were close to the EF_{RSC} for the cottonwood log (Table 2) and, we estimate, within ±20% of the "real" RSC average EF. Finally, we note that the large diameter woody fuels have lower EF for nitrogen-containing compounds. This is probably due to the lower nitrogen content of the woody fuels (~ 0.05% N) relative to the soil samples (1.0–1.7% N).

[25] Figure 4 shows the temporal profiles of the emissions from the fire that burned a stump and the surrounding duff. The top of the stump was ignited with a propane torch. During the first hour, the fire included pyrolysis, gasification, and small flames and produced large amounts of white, brown and yellowish smoke. The PM2.5 peaked with an IEF of 109 g kg^{-1} during this period. From 1 to 1.5 hours after ignition, the combustion intensity decreased, flaming ceased, and the active front began to include the duff. During this transition, the MCE increased and the IEF for PM2.5 and smoldering products dropped significantly. For the next 14 hours, the emissions followed a modified duff-like profile with an increase in high-temperature pyrolysis products, but the decrease in oxygenates was slowed by the availability of fresh wood in the stump. Twenty hours after ignition, most of the stump had been consumed. The only

visible sign of combustion was faint, bluish white smoke from a depression in the soil where the stump had been. Twenty-five hours after ignition, the combustion rate suddenly increased with small flames and intense pyrolysis and gasification consuming a freshly exposed section of the roots. This was accompanied by a "spike" in the IEF for smoldering products. The rest of the fire involved slow consumption of the remaining duff. The EF_{RSC} values for smoldering compounds from the "stump/duff" fire are closer to the duff fire values than the log values, suggesting that the fire consumed more organic soil than wood.

[26] Finally, we briefly discuss the emissions from the fires in decayed softwood debris (not shown in figures). We collected these samples as part of a project to measure typical fuel moistures for RSC-prone fuels. The decayed softwood debris had relatively high fuel moistures compared to other fuels on the day we sampled. However, these samples were burned several months after having been oven dried for the moisture determination. Consequently, mostly glowing combustion consumed these fuels and these fires had the lowest EF for pyrolysis compounds (Table 2). The results are probably not relevant except for fires in extremely dry field conditions.

3.2. Comparison of RSC Emission Measurements to Other Biomass Burning Emission Measurements

[27] The main goal of this work was to determine if the emissions from RSC (which had not been previously measured) were different from the emissions observed in the many previous studies of biomass burning that did not include RSC. We address this in two steps. First, using selected OVOC we show that the RSC average EF can indeed be quite different from previously reported fire-integrated EF. Next, we explore the impact that including RSC has on estimates of total fire emissions using a general mathematical approach that shows that RSC can have a widespread and large impact on emissions estimates.

3.2.1. RSC Emissions Compared to Previous Emission Production Models

[28] Previous work showed that for fires in a wide variety of aboveground fine fuels from many temperate and boreal ecosystems, the OVOC EF were tightly correlated with MCE [*Yokelson et al.*, 1996, 1997, 1999, 2003; *Goode et al.*, 1999, 2000] and a single linear regression line was useful for predicting the EF from a wide range of fires. This was particularly true for EF versus MCE for methanol, acetic acid, and formaldehyde (the principal OVOC emitted by fires). Since RSC is a significant component of some fires, it is interesting to determine if EF_{RSC} for OVOC fit the previous models. Figure 5 shows the EF and linear fit from the previous laboratory and airborne FTIR measurements of various aboveground fuels not prone to RSC along with the EF_{RSC} from this study. It is apparent that the EF_{RSC} are not tightly correlated with the previous linear fit and are highly fuel dependent. In general, during RSC, the large diameter woody fuels tend to be consumed by a higher proportion of pyrolysis and have higher OVOC EF than the duff and organic soil fuel types. In summary, the agreement between lab and field measurements is good for both aboveground fine fuels and for RSC-prone fuels, but the simple emissions model for "all" aboveground fine fuels does not work for all RSC-prone fuels because they produce more fuel-dependent values.

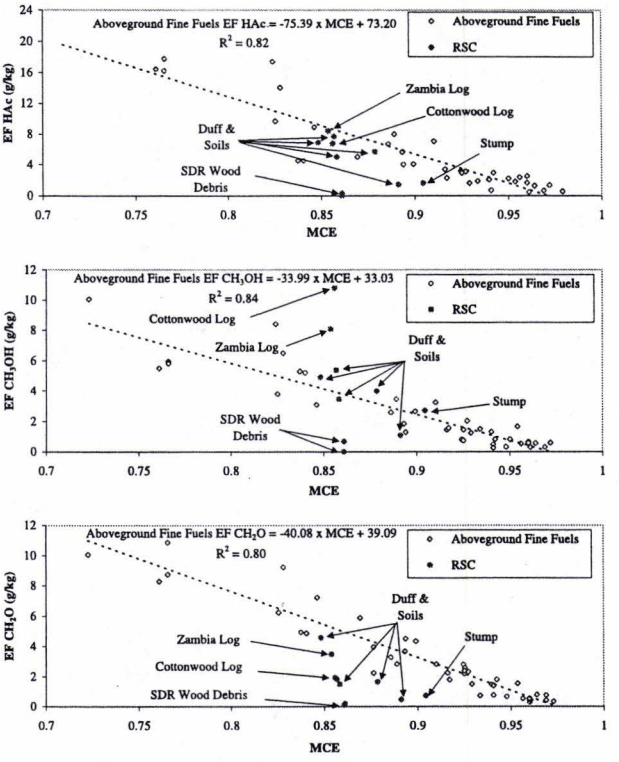

Figure 5. A comparison of the RSC average EF for selected gases to the fire-integrated EF for the same gases measured previously for fires in a wide variety of aboveground fine fuels. The previous data [*Yokelson et al.*, 1996, 1997, 1999; *Goode et al.*, 1999, 2000] are highly correlated with MCE and are fit with a regression line that serves as a simple model for predicting emissions from many different fuel types. The EF for the RSC-prone fuels do not group about the regression line and are highly fuel dependent. ("SDR wood debris" indicates small, dry, and rotted wood debris. These RSC-prone fuels were extremely dry in this study and they burned with a significant amount of flaming and glowing.)

3.2.2. General Significance of RSC Emissions

[29] As noted above, previous studies of the impact of biomass burning on local to global atmospheres relied on available measurements that did not include the emissions from RSC. There were no measurements of the RSC EF and very little data regarding the proportion of biomass consumed by RSC in tropical, boreal, and temperate forest fires. However, if the RSC EF and the proportion of fuel consumed by RSC are known for a fire, then a "true" (or corrected) fire-integrated EF for a given compound i, ($EF_{i,tot}$) can be estimated by coupling this data with data from studies of similar fires that did not include RSC using (1).

$$EF_{i,tot} = (f) \times EF_{i,RSC} + (1 - f) \times EF_{i,conv} \quad (1)$$

$EF_{i,conv}$ and $EF_{i,RSC}$ are the EF measured for compound i in the lofted emissions and during RSC, respectively, and f is

Table 3. Calculated Effect of RSC on Fire-Integrated EF for Boreal Forest and Tropical Wooded Savanna

	CO_2 (g kg^{-1})	CO (g kg^{-1})	NO_x (g kg^{-1})	CH_4 (g kg^{-1})	C_2H_6 (g kg^{-1})	C_2H_4 (g kg^{-1})	C_2H_2 (g kg^{-1})	C_3H_6 (g kg^{-1})	CH_2O (g kg^{-1})	HC(O)OH (g kg^{-1})	$CH_3C(O)OH$ (g kg^{-1})	CH_3OH (g kg^{-1})	NH_3 (g kg^{-1})	HCN (g kg^{-1})
							Boreal Forest[a]							
EF_{conv}[b]	1660	89	1.5	2.8	0.66	1.80	0.24	0.51	1.85	0.99	3.61	1.66	0.86	0.69
EF_{RSC}[c]	1436	112	0.00	9.0	2.71	1.13	0.00	0.39	0.49	0.34	1.43	1.07	8.69	0.92
EF_{tot}	1548	100	0.8	5.9	1.69	1.47	0.12	0.45	1.17	0.67	2.52	1.37	4.78	0.81
EF_{tot}/EF_{conv}	0.93	1.13	0.50	2.11	2.55	0.81	0.50	0.88	0.63	0.67	0.70	0.82	5.55	1.17
							African Miombo[d]							
EF_{conv}[e]	1711	69	3.5	1.4		0.82	0.24		0.75	0.57	2.18	1.03	0.40	0.37
EF_{RSC}[f]	1454	158	0.0	23.2	4.39	2.11	0.00	2.04	3.48	1.15	8.43	8.09	1.92	0.00
EF_{tot}	1685	78	3.2	3.6	0.44	0.95	0.22	0.20	1.02	0.63	2.81	1.74	0.55	0.33
EF_{tot}/EF_{conv}	0.98	1.13	0.90	2.52		1.16	0.90		1.36	1.10	1.29	1.69	1.38	0.90

[a]Assuming RSC of organic soils represents 50% of the total fuel consumption.
[b]The EF for boreal forest fires reported in airborne study of *Goode et al.* [2000].
[c]EF for RSC of boreal forest organic soils from this work.
[d]Assuming RSC of logs represents 10% of the total fuel consumption.
[e]Airborne FTIR measurements of miombo fire EF from the study of *Yokelson et al.* [2003].
[f]EF for smoldering miombo logs from this work.

the fraction of the fuel consumed by RSC. Table 3 illustrates the significance RSC emissions can have by implementing (1) for two "realistic biomass burning scenarios": a boreal forest and an African tropical woodland (miombo).

[30] To develop a realistic estimate of the fraction of total fuel consumption due to RSC for a reasonably common example of a boreal forest fire we note that *Dyrness and Norum* [1983] reported that duff in boreal regions could sustain a spreading fire featuring glowing combustion for many days. In addition, it was recently estimated that 84% of fuel consumption was by RSC during an Alaskan forest fire (Sandberg, personal communication, 2001). Therefore, we make the prognostic assumption that RSC of duff can consume 50% of the fuel in some boreal forest fires. To estimate EF_{RSC}, we use our laboratory measurements for the Northwest Territories 1 fire since it was the boreal forest duff sample that burned in the most representative fashion. (We exclude the NWT 2 fire because an anomalously low percentage of the sample was consumed and without much glowing combustion.) To estimate EF_{conv} we use the Alaskan boreal forest fire, airborne FTIR measurements of *Goode et al.* [2000]. RSC was not thought to be extensive for the early season fires probed by Goode et al., but in any case, they could not probe RSC emissions directly. (The possibility exists that RSC emissions accumulated overnight and were lofted by convective activity the next day). Next, we use (1) to calculate the EF_{tot} (see Table 3). Comparison of EF_{tot} to EF_{conv} suggests that, for a fire of this type, the real fire-integrated emissions of NO_x and OVOC are about one half of what is suggested by airborne sampling alone. On the other hand, the "true" EF for CO, CH_4, C_2H_6, and NH_3 are raised by factors of 1.1, 2.1, 2.6, and 5.6, respectively. *Nance et al.* [1993] reported an airborne measurement of EFPM2.5 of 21 ± 4.8 g kg^{-1} for an Alaskan fire. Since this is higher than any EFPM2.5 obtained in this study, consideration of RSC would probably lower EFPM2.5 for boreal forest fires.

[31] For the wooded savanna example, we use airborne FTIR measurements of miombo fire emissions collected by *Yokelson et al.* [2003] in Zambia during September 2000 for EF_{conv} and our ground-based OP-FTIR spot measurements of smoldering miombo logs for EF_{RSC}. Detailed, fuel consumption measurements made in conjunction with the airborne measurements of *Yokelson et al.* [2003] suggested that perhaps 10% of the fuel consumption on that fire occurred after convection from the site ceased (J. M. C. Pereira et al., Biomass burning parameters of four experimental fires in the Western Province, Zambia, submitted to *International Journal of Wildland Fire*, 2002). Therefore, we implement (1) assuming that RSC of logs represents 10% of the fuel consumed in a miombo fire (see Table 3). The comparison of EF_{tot} to EF_{conv} shows no large decreases in EF. However, there are significant increases for a number of compounds, with CH_4, CH_3OH, and NH_3 increasing by factors of 2.5, 1.7, and 1.4, respectively.

[32] In a previous study, *Hoffa et al.* [1999] reported that grass fire MCE tended to be lower early in the dry season, which could mean that smoldering compounds have higher EF. If lower fuel moistures promote RSC of larger fuels then this could cause higher EF for smoldering compounds later in the dry season.

[33] In summary, "correcting" emissions estimates by including RSC caused large effects in both scenarios; even when RSC consumed only 10% of the fuel. Thus, more measurements of fuel consumption and EF for RSC are needed to improve local to global estimates of biomass fire emissions. In addition, there will be atmospheric effects because the RSC portion of the total fire emissions has different dispersion (e.g., release closer to ground, possible canopy processing, and relatively more release at night).

3.3. Additional Details on the Emissions of Selected Trace Gases

3.3.1. Verification of Significant Phenol Emissions From RSC

[34] In a previous study, *Yokelson et al.* [1997] reported spot measurements of smoldering combustion in many different fuels using OP-FTIR. They observed high concentrations of phenol (C_6H_5OH) emitted from smoldering grass and hardwood fuels and a "study average" ER to CO of 0.69%. This ratio was an order of magnitude higher than the phenol ER reported by *McKenzie et al.* [1995]. In this study, we observe phenol ER to CO (0.3–0.9) (Table 2) from most RSC-prone fuels that are in good agreement with the study average of *Yokelson et al.* [1997]. This confirms that phenol is frequently an important fire emission although it is

emitted at variable levels. *Mason et al.* [2001] used a detailed atmospheric chemistry model to investigate smoke plume photochemistry. They reported that phenol reacts with NO_x within a few hours after emission to form significant amounts of nitrophenol compounds. The fate of the nitrophenols is unknown, but they will probably not rerelease NO_x and, thus, reduce the production of ozone in aged smoke.

3.3.2. FTIR Measurements of Furan in Smoke

[35] Furan (C_4H_4O), an oxygenated heterocyclic organic compound, also appears to be a ubiquitous, but variable, emission from the combustion of RSC-prone fuels. Furan has not been previously detected spectroscopically in biomass burning emissions, but *Greenberg et al.* [1984] reported significant concentrations of furan in field measurements of tropical woodland and grassland fire emissions using electropolished stainless steel canisters for collecting smoke with subsequent trace gas analysis using gas chromatography/flame ionization detection (GC/FID). Our spot measurements of furan ER relative to CO range from 0% to 1.5% and the RSC weighted average values in Table 2 range from 0.24% to 0.53%. These values are close to the average furan ER to CO (0.49%) reported by *Greenberg et al.* [1984] for fires in Brazilian woodlands. *Shepson et al.* [1984] reported that a major source of furan found in forest fire smoke is from the OH-initiated photooxidation of toluene and *ortho*-xylene. However, our measurements in smoke less than 1 s old indicate that a significant amount of furan is produced by low-temperature pyrolysis of biomass (see Figures 1–4).

[36] Furan is a reactive molecule under tropospheric daytime conditions. The major sink of furan is reaction with OH radicals ($k \sim 4 \times 10^{-11}$ cm^3 mol^{-1} s^{-1}) [*Atkinson et al.*, 1983; *Wine and Thompson*, 1984; *Bierbach et al.*, 1992]. This gives an atmospheric lifetime for furan of approximately 7 hours if a 12 hour average OH radical concentration of 1.0×10^6 mol cm^{-3} is assumed. The actual lifetime may be much shorter since OH concentrations are reportedly elevated in fresh smoke plumes [*Mason et al.*, 2001; *Hobbs et al.*, 2003]. *Bierbach et al.* [1995] found that the major products from the OH-initiated photooxidized furan reaction are *cis*- and *trans*-butenedial and maleic anhydride. Since OVOC have a large effect on modeled smoke plume photochemistry [*Mason et al.*, 2001], we will include our furan measurements in future simulations to explore the role furan plays in the chemistry of aged smoke plumes.

3.3.3. Emissions of Nitrogenous Gases From RSC

[37] The major nitrogen-containing gases emitted from biomass burning are N_2, NO_x, and NH_3, and they account for most of the fuel nitrogen volatilized [*Goode et al.*, 1999]. Ammonia and hydrogen cyanide (HCN) were the only nitrogenous species we detected from our fires in RSC-prone fuels. On a molar basis, NH_3 emissions were 5–10 times higher than HCN emissions for our duff and organic soil fires and NH_3 was the only nitrogen-containing species we detected from the smoldering combustion of the woody fuels. These findings confirm previous reports that NH_3 is the major nitrogenous gas produced from smoldering combustion [*Yokelson et al.*, 1996, 1997; *Goode et al.*, 1999, 2000]. Overall, the NH_3 temporal profiles most closely resembled CH_4 profiles during RSC (Figures 1–4), suggesting that NH_3 may be a high-temperature pyrolysis product. We also note that our boreal, organic soil fires emitted significantly more NH_3 than our temperate forest, duff fires; most likely due to the higher nitrogen content in the boreal soils (Tables 1 and 2). Finally, boreal forest fires exert a major influence on the summertime photochemistry of much of the Northern Hemisphere [*Wotawa and Trainer*, 2000; *McKeen et al.*, 2002; *Forster et al.*, 2001] and we suggest that future studies of the regional impact of boreal fires should consider the effect that RSC has on emissions estimates for these fires. This is particularly true for nitrogenous compounds since we estimated that RSC decreased EFNO by a factor of 2 and increased $EFNH_3$ by a factor of ~6 (see section 3.2.2 and Table 3).

4. Conclusions

[38] We adopt a qualitative, working definition of RSC as biomass combustion that produces smoke emissions that are not strongly lofted by fire-induced convection. RSC-prone biomass fuels include duff, organic soils, logs, stumps, and dead woody debris. We cite several previous studies that suggest that RSC probably accounts for a globally important amount of biomass burning.

[39] We used NDIR, filter sampling, and OP-FTIR to make the first measurements explicitly of the trace gas and particle emissions from residual smoldering of the major RSC-prone fuels in our laboratory and in a wooded savanna in Zambia. An important finding was that the distribution of emissions from RSC can sometimes change dramatically over the course of a fire. Taking this into account, we calculated RSC average EF (EF_{RSC}) for the main RSC-prone fuels for PM2.5 and the most abundant trace gas emissions (as determined by FTIR): carbon dioxide, carbon monoxide, methane, ethane, ethene, acetylene, propene, formaldehyde, methanol, acetic acid, formic acid, glycolaldehyde, phenol, furan, ammonia, and hydrogen cyanide.

[40] A significant feature of these results is that the emissions from RSC can be markedly different from previously reported fire EF, which were mainly for fires in aboveground fine fuels. Specifically, the EF_{RSC} for PM2.5 and some trace gases were sometimes much larger or smaller than the EF measured in convection columns above fires in environments similar to those where the RSC-prone fuels were collected. This has important implications for emissions estimates. For example, our newly measured EFPM2.5 for smoldering duff and organic soils is lower than EFPM2.5 for most aboveground biomass fuels. (In addition, the combustion factor (the percentage of fuel exposed to fire that was volatilized) was also lower for duff and organic soils (50–75% by mass) than for aboveground fine fuels.) These observations suggest that using previously measured EFPM2.5 coupled with the mass of the available duff would significantly overestimate the PM2.5 emissions from these types of fires.

[41] Finally, we demonstrate a general method for refining emissions estimates using our EF_{RSC} and estimates of fuel consumption by RSC. Application of this method in two examples shows that consideration of RSC can have a large impact on estimates of biomass burning emissions. For instance, assuming that RSC accounts for 50% of fuel

consumption in a boreal forest fire reduces the NO_x EF by one half and increases $EFNH_3$ by almost a factor of 6. Assuming that only 10% of the fuel is consumed by RSC in an African wooded savanna increases the CH_4 EF by a factor of 2.5. These examples clearly demonstrate that additional measurements of the EF and fuel consumption due to RSC should be stressed in future biomass burning research.

[42] **Acknowledgments.** This research was supported by funds provided by the National Science Foundation under grants ATM-9631219 and ATM-9900494, the Rocky Mountain Research Station, Forest Service, U.S. Department of Agriculture (INT-97082-RJVA and RMRS-99508-RJVA), and the interagency Joint Fire Science Program. The authors thank SAFARI 2000 and Geoff Richards for informative discussions on the chemistry of smoldering combustion, Jim Reardon for the duff and organic soil samples, and Michael Chandler for helping extract the stump/duff sample burned in this work.

References

Andreae, M. O., and P. Merlet, Emission of trace gases and aerosols from biomass burning, *Global Biogeochem. Cycles*, *15*, 955–966, 2001.

Atkinson, R., S. M. Aschmann, and W. P. L. Carter, Kinetics of the reaction of O_3 and OH radicals with furan and thiophene at 298 ± 2 K, *Int. J. Chem. Kinet.*, *15*, 51–61, 1983.

Barbosa, R. I., and P. M. Fearnside, Pasture burning in Amazonia: Dynamics of residual biomass and the storage and release of aboveground carbon, *J. Geophys. Res.*, *101*, 25,847–25,857, 1996.

Bierbach, A., I. Barnes, and K. H. Becker, Rate coefficients for the gas-phase reactions of hydroxyl radicals with furan, 2-methylfuran, 2-ethylfuran and 2, 5-dimethylfuran at 300 ± 2 K, *Atmos. Environ.*, *26A*, 813–817, 1992.

Bierbach, A., I. Barnes, and K. H. Becker, Product and kinetic study of the OH-initiated gas-phase oxidation of furan, 2-methylfuran and furanaldehydes at ≈300 K, *Atmos. Environ.*, *29*, 2651–2660, 1995.

Carvalho, J. A., N. Higuchi, T. M. Araújo, and J. C. Santos, Combustion completeness in a rainforest clearing experiment in Manaus, Brazil, *J. Geophys. Res.*, *103*, 13,195–13,199, 1998.

Charlson, R. J., S. E. Schwartz, J. M. Hales, R. D. Cess, J. A. Coakley Jr., J. E. Hansen, and D. J. Hofmann, Climate forcing by anthropogenic aerosols, *Science*, *255*, 423–430, 1992.

Crutzen, P. J., and M. O. Andreae, Biomass burning in the tropics: Impact on atmospheric chemistry and geochemical cycles, *Science*, *250*, 1669–1678, 1990.

Delany, A. C., P. Haagensen, S. Walters, A. F. Wartburg, and P. J. Crutzen, Photochemically produced ozone in the emission from large-scale tropical vegetation fires, *J. Geophys. Res.*, *91*, 2425–2429, 1985.

Dyrness, C. T., and R. A. Norum, The effects of fires on black spruce forest floors in interior Alaska, *Can. J. For. Res.*, *13*, 879–893, 1983.

Finlayson-Pitts, B. J., and J. N. Pitts Jr., *Atmospheric Chemistry: Fundamentals and Experimental Techniques*, pp. 142–150, John Wiley, New York, 1986.

Fishman, J., K. Fakhruzzaman, B. Cros, and D. Nganga, Identification of widespread pollution in the Southern Hemisphere deduced from satellite analysis, *Science*, *252*, 1693–1696, 1991.

Forster, C., et al., Transport of boreal forest fire emissions from Canada to Europe, *J. Geophys. Res.*, *106*, 22,887–22,906, 2001.

Fransden, W. H., The influence of moisture and mineral soil on the combustion limits of smoldering forest duff, *Can. J. For. Res.*, *17*, 1540–1544, 1987.

Fransden, W. H., Burning rate of smoldering peat, *Northwest. Sci.*, *65*, 166–172, 1991.

Fransden, W. H., Ignition probability of organic soils, *Can. J. For. Res.*, *27*, 1471–1477, 1997.

Goode, J. G., R. J. Yokelson, R. A. Susott, and D. E. Ward, Trace gas emissions from laboratory biomass fires measured by Fourier transform infrared spectroscopy: Fires in grass and surface fuels, *J. Geophys. Res.*, *104*, 21,237–21,245, 1999.

Goode, J. G., R. J. Yokelson, D. E. Ward, R. A. Susott, R. E. Babbitt, M. A. Davies, and W. M. Hao, Measurements of excess O_3, CO_2, CO, CH_4, C_2H_4, C_2H_2, HCN, NO, NH_3, HCOOH, CH_3OOH, HCHO, and CH_3OH, in 1997 Alaskan biomass burning plumes by airborne Fourier transform infrared spectroscopy (AFTIR), *J. Geophys. Res.*, *105*, 22,147–22,166, 2000.

Greenberg, J. P., P. R. Zimmerman, L. Heidt, and W. Pollock, Hydrocarbon and carbon monoxide emissions from biomass burning in Brazil, *J. Geophys. Res.*, *89*, 1350–1354, 1984.

Griffith, D. W. T., Synthetic calibration and quantitative analysis of gas-phase FTIR spectra, *Appl. Spectrosc.*, *50*, 59–70, 1996.

Guild, L. S., J. B. Kauffman, L. J. Ellingson, D. L. Cummings, E. A. Castro, R. E. Babbitt, and D. E. Ward, Dynamics associated with total aboveground biomass, C, nutrient pools, and biomass burning of primary forest and pasture in Rondonia, Brazil during SCAR-B, *J. Geophys. Res.*, *103*, 32,091–32,100, 1998.

Hardy, C. C., R. D. Ottmar, J. L. Peterson, J. C. Core, and P. Seamon, (eds), *Smoke Management Guide for Prescribed and Wildland Fire: 2001 Edition, PMS 420-2*, 226 pp., Natl. Wildfire Coord. Group, Natl. Interagency Fire Cent., Boise, Idaho, 2002.

Hobbs, P. V., P. Sinha, R. J. Yakelson, T. J. Christian, D. R. Blake, S. Gao, T. W. Kirchstetter, T. Novakov, and P. Pilewskie, Evolution of gases and particles from a savanna fire in South Africa, *J. Geophys. Res.*, *108*, doi:10.1029/2002JD002352, in press, 2003.

Hoffa, E. A., D. E. Ward, W. M. Hao, R. A. Susott, and R. H. Wakimoto, Seasonality of carbon emissions from biomass burning in a Zambian savanna, *J. Geophys. Res.*, *104*, 13,841–13,853, 1999.

Holzinger, R., C. Warneke, A. Hansel, A. Jordan, W. Lindinger, D. H. Scharffe, G. Schade, and P. J. Crutzen, Biomass burning as a source of formaldehyde, acetaldehyde, methanol, acetone, acetonitrile, and hydrogen cyanide, *Geophys. Res. Lett.*, *26*, 1161–1164, 1999.

Kasischke, E. S., K. Bergen, R. Fennimore, F. Sotelo, G. Stephens, A. Janetos, and H. H. Shugart, Satellite imagery gives clear picture of Russia's boreal forest fires, *Eos Trans. AGU*, *80*, 141, 1999.

Kaufman, Y. J., and T. Nakajima, Effect of Amazon smoke on cloud microphysics and albedo-analyses from satellite imagery, *J. Appl. Meteorol.*, *32*, 729–744, 1993.

Kauffman, J. B., D. L. Cummings, and D. E. Ward, Relationship of fire, biomass and nutrient dynamics along a vegetation gradient in the Brazilian cerrado, *J. Ecol.*, *82*, 519–531, 1994.

Kauffman, J. B., D. L. Cummings, D. E. Ward, and R. Babbitt, Fire in the Brazilian Amazon: Biomass, nutrient pools, and losses in slashed primary forests, *Oecologia*, *104*, 397–408, 1995.

Kauffman, J. B., D. L. Cummings, and D. E. Ward, Fire in the Brazilian Amazon, 2, Biomass, nutrient pools and losses in cattle pastures, *Oecologia*, *113*, 415–427, 1998.

Levine, J. S., The 1997 fires in Kalimantan and Sumatra, Indonesia: Gaseous and particulate emissions, *Geophys. Res. Lett.*, *26*, 815–818, 1999.

Mason, S. A., R. J. Field, R. J. Yokelson, M. A. Kochivar, M. R. Tinsley, D. E. Ward, and W. M. Hao, Complex effects arising in smoke plume simulations due to inclusion of direct emissions of oxygenated organic species from biomass combustion, *J. Geophys. Res.*, *106*, 12,527–12,539, 2001.

McKeen, S. A., G. Wotawa, D. D. Parrish, J. S. Holloway, M. P. Buhr, G. Hubler, F. C. Fehsenfeld, and J. F. Meagher, Ozone production from Canadian wildfires during June and July of 1995, *J. Geophys. Res.*, *107*(D14), 4192, doi:10.1029/2001JD000607, 2002.

McKenzie, L. M., W. M. Hao, G. N. Richards, and D. E. Ward, Measurement and modeling of air toxins from smoldering combustion of biomass, *Environ. Sci. Technol.*, *29*, 2047–2054, 1995.

Nance, J. D., P. V. Hobbs, L. F. Radke, and D. E. Ward, Airborne measurements of gases and particles from an Alaskan wildfire, *J. Geophys. Res.*, *98*, 14,873–14,882, 1993.

Overend, R. P., T. A. Milne, and L. K. Mudge, *Fundamentals of Thermochemical Biomass Conversion*, Elsevier Sci., New York, 1995.

Reinhardt, E. D., J. K. Brown, W. C. Fischer, and R. T. Graham, Woody fuel and duff consumption by prescribed fire in northern Idaho mixed conifer logging slash, Res. Pap. INT-443, USDA For. Serv., Int. Res. Stn., Ogden, Utah, 1991.

Sandberg, D. V., Research leads to less smoke from prescribed fires, in *Proceedings, 1983 Northwest Fire Council Annual Meeting 1983 November 21–22, Olympia, Wash.*, 27 pp., Western For. and Conserv. Assoc., Portland, Oreg., 1983.

Shepson, P. B., E. O. Edney, and E. W. Corse, Ring fragmentation reactions on the photo-oxidations of toluene and *o*-xylene, *J. Phys. Chem.*, *88*, 4122–4126, 1984.

Stith, J. L., L. F. Radke, and P. V. Hobbs, Particle emissions and the production of ozone and nitrogen oxides from the burning of forest slash, *Atmos. Environ.*, *15*, 73–82, 1981.

Susott, R. A., G. J. Olbu, S. P. Baker, D. E. Ward, J. B. Kauffman, and R. Shea, Carbon, hydrogen, nitrogen, and thermogravimetric analysis of tropical ecosystem biomass, in *Biomass Burning and Global Change*, edited by J. S. Levine, pp. 350–360, MIT Press, Cambridge, Mass., 1996.

Trent, A., M. A. Davies, R. Fisher, H. Thistle, and R. Babbitt, Evaluation of optical instruments for real-time, continuous monitoring of smoke particulates, Tech. Rep. 0025-2860-MTDC, 38 pp., USDA For. Serv., Missoula Technol. and Dev. Cent., Missoula, Mont., 2000.

Wade, D. D., and J. D. Lunsford, A guide for prescribed fire in southern forests, R8-TP-11, USDA For. Serv. Tech. Publ., Washington, D. C., 1989.

Wallace, J. M., and P. V. Hobbs, *Atmospheric Science: An Introductory Survey*, Academic, San Diego, Calif., 1977.

Ward, D. E., and L. F. Radke, Emissions measurements from vegetation fires: A comparative evaluation of methods and results, in *Fire in the Environment: The Ecological, Atmospheric and Climatic Importance of Vegetation Fires*, edited by P. J. Crutzen and J. G. Goldammer, pp. 53–76, John Wiley, New York, 1993.

Ward, D. E., R. A. Susott, J. B. Kauffman, R. E. Babbitt, D. L. Cummings, B. Dias, B. N. Holben, Y. J. Kaufman, R. A. Rasmussen, and A. W. Setzer, Smoke and fire characteristics for cerrado and deforestation burns in Brazil: Base-B experiment, *J. Geophys. Res.*, *97*, 14,601–14,619, 1992.

Ward, D. E., J. Peterson, and W. M. Hao, An inventory of particulate matter and air toxic emissions from prescribed fires in the USA for 1989, in *Proceedings of the Air and Waste Management Association, Denver, Colo.*, June 14–18, Air and Waste Manage. Assoc., Pittsburgh, Pa., 1993.

Wine, P. H., and R. J. Thompson, Kinetics of OH reactions with furan, thiophene, and tetrahydrothiophene, *Int. J. Chem. Kinet.*, *16*, 867–878, 1984.

Wotawa, G., and M. Trainer, The influence of Canadian forest fires on pollutant concentrations in the United States, *Science*, *288*, 324–328, 2000.

Yokelson, R. J., and I. Bertschi, Vibrational spectroscopy in the study of fires, in *Handbook of Vibrational Spectroscopy*, vol. 4, edited by P. Griffiths and J. Chalmers, pp. 2879–2886, John Wiley, New York, 2002.

Yokelson, R. J., D. W. T. Griffith, and D. E. Ward, Open-path Fourier transform infrared studies of large-scale laboratory biomass fires, *J. Geophys Res.*, *101*, 21,067–21,080, 1996.

Yokelson, R. J., R. Susott, D. E. Ward, J. Reardon, and D. W. T. Griffith, Emissions from smoldering combustion of biomass measured by open-path Fourier transform infrared spectroscopy, *J. Geophys. Res.*, *102*, 18,865–18,877, 1997.

Yokelson, R. J., J. G. Goode, D. E. Ward, R. A. Susott, R. E. Babbitt, D. D. Wade, I. Bertschi, D. W. T. Griffith, and W. M. Hao, Emissions of formaldehyde, acetic acid, methanol, and other trace gases from biomass fires in North Carolina measured by airborne Fourier transform infrared spectroscopy, *J. Geophys. Res.*, *104*, 30,109–30,125, 1999.

Yokelson, R. J., I. Bertschi, T. C. Christian, P. V. Hobbs, D. E. Ward, and W. M. Hao, Trace gas measurements in nascent, aged, and cloud-processed smoke from African savanna fires by airborne Fourier transform infrared spectroscopy (AFTIR), *J. Geophys. Res.*, *108*, doi:10.1029/2002JD002322, in press, 2003.

R. E. Babbitt, W. M. Hao, and R. A. Susott, Fire Sciences Laboratory, U.S. Department of Agriculture (USDA) Forest Service, Missoula, MT, USA.

I. Bertschi, Interdisciplinary Arts and Sciences, University of Washington-Bothell, Bothell, WA, USA.

J. G. Goode, Bruker Optics, Inc., Billerica, MA, USA.

D. E. Ward, Enviropyronics, LLC, White Salmon, WA, USA.

R. J. Yokelson, Department of Chemistry, University of Montana, Missoula, MT, USA. (byok@selway.umt.edu)

JOURNAL OF GEOPHYSICAL RESEARCH, VOL. 108, NO. D13, 8469, doi:10.1029/2002JD002158, 2003

Trace gas emissions from the production and use of domestic biofuels in Zambia measured by open-path Fourier transform infrared spectroscopy

Isaac T. Bertschi,[1,2] Robert J. Yokelson,[1,5] Darold E. Ward,[3,4] Ted J. Christian,[1] and Wei Min Hao[3]

Received 1 February 2002; revised 10 June 2002; accepted 10 June 2002; published 13 February 2003.

[1] Domestic biomass fuels (biofuels) were recently estimated to be the second largest source of carbon emissions from global biomass burning. Wood and charcoal provide approximately 90% and 10% of domestic energy in tropical Africa. In September 2000, we used open-path Fourier transform infrared (OP-FTIR) spectroscopy to quantify 18 of the most abundant trace gases emitted by wood and charcoal cooking fires and an earthen charcoal-making kiln in Zambia. These are the first in situ measurements of an extensive suite of trace gases emitted by tropical biofuel burning. We report emission ratios (ER) and emission factors (EF) for (in order of abundance) carbon dioxide (CO_2), carbon monoxide (CO), methane (CH_4), acetic acid (CH_3COOH), methanol (CH_3OH), formaldehyde (HCHO), ethene (C_2H_4), ammonia (NH_3), acetylene (C_2H_2), nitric oxide (NO), ethane (C_2H_6), phenol (C_6H_5OH), propene (C_3H_6), formic acid (HCOOH), nitrogen dioxide (NO_2), hydroxyacetaldehyde ($HOCH_2CHO$), and furan (C_4H_4O). Compared to previous work, our emissions of organic acids and NH_3 are 3–6.5 times larger. Another significant finding is that reactive oxygenated organic compounds account for 70–80% of the total nonmethane organic compounds (NMOC). For most compounds, the combined emissions from charcoal production and charcoal burning are larger than the emissions from wood fires by factors of 3–10 per unit mass of fuel burned and ~2 per unit energy released. We estimate that Zambian savanna fires produce more annual CO_2, HCOOH, and NO_x than Zambian biofuel use by factors of 2.5, 1.7, and 5, respectively. However, biofuels contribute larger annual emissions of CH_4, CH_3OH, C_2H_2, CH_3COOH, HCHO, and NH_3 by factors of 5.1, 3.9, 2.7, 2.4, 2.2, and 2.0, respectively. Annual CO and C_2H_4 emissions are approximately equal from both sources. Coupling our data with recent estimates of global biofuel consumption implies that global biomass burning emissions for several compounds are significantly larger than previously reported. Biofuel emissions are produced year-round, disperse differently than savanna fire emissions, and could strongly impact the tropical troposphere. *INDEX TERMS:* 0345 Atmospheric Composition and Structure: Pollution—urban and regional (0305); 0365 Atmospheric Composition and Structure: Troposphere—composition and chemistry; 0368 Atmospheric Composition and Structure: Troposphere—constituent transport and chemistry; 0394 Atmospheric Composition and Structure: Instruments and techniques; *KEYWORDS:* oxygenated organic compounds, biomass burning, biofuel, fuelwood, charcoal, biomass energy

Citation: Bertschi, I. T., R. J. Yokelson, D. E. Ward, T. J. Christian, and W. M. Hao, Trace gas emissions from the production and use of domestic biofuels in Zambia measured by open-path Fourier transform infrared spectroscopy, *J. Geophys. Res.*, *108*(D13), 8469, doi:10.1029/2002JD002158, 2003.

1. Introduction

[2] Biomass burning is a globally important source of gases and particles in the atmosphere [*Crutzen and Andreae*, 1990]. Approximately 80% of biomass burning occurs in the tropics [*Crutzen and Andreae*, 1990]. Savanna fires and domestic biofuel use are the two main types of biomass burning consuming about 3160 and 2701 Tg dry mass (dm) yr^{-1}, respectively [*Andreae and Merlet*, 2001]. Biofuels are the main source of energy in almost all African countries providing 90–98% of residential energy and ~75% of the total primary energy in all of sub-Saharan Africa (excluding

[1]Department of Chemistry, University of Montana, Missoula, Montana, USA.
[2]Now at Interdisciplinary Arts and Sciences, University of Washington-Bothell, Bothell, Washington, USA.
[3]Fire Science Laboratory, U.S. Department of Agriculture (USDA) Forest Service, Missoula, Montana, USA.
[4]Now at Enviropyronics, LLC, White Salmon, Washington, USA.
[5]Corresponding author.

Copyright 2003 by the American Geophysical Union.
0148-0227/03/2002JD002158$09.00

the Republic of South Africa) [*FAO*, 1999]. Zambia has the 12th largest annual biofuel consumption rate out of 55 countries in Africa. Wood and charcoal are the major biofuels in tropical Africa and they accounted for ~90% and 10%, respectively, of the Zambian annual biofuel use from 1980 to 1994 [*FAO*, 1999]. Wood is the major fuel in rural areas and charcoal is used mostly in urban areas [*Chidumayo*, 1994].

[3] Despite the fact that biofuel fires are the second largest type of global biomass burning, there were very few emissions data for biofuel use [*Andreae and Merlet*, 2001]. Therefore, as part of SAFARI 2000, we used open-path Fourier transform infrared (OP-FTIR) spectroscopy to measure the trace gases emitted from several wood and charcoal fires and an earthen charcoal-making kiln in Zambia during the second week of September 2000. We quantified 18 of the most abundant emissions. These are the first in situ measurements of an extensive suite of trace gases emitted from the production and use of biofuels in the tropics.

2. Experimental Details

2.1. Description of the OP-FTIR System

[4] The OP-FTIR system was described previously by *Yokelson et al.* [1997] so only a brief description emphasizing updates is given here. The key elements are an FTIR spectrometer (MIDAC 2500) and unenclosed, multipass optics (1.6 m basepath) comounted on Super-Invar, Teflon-coated girders (see Figure 1). The IR beam from the spectrometer is directed into the open-path White cell (Infrared Analysis, Inc.) by in-house transfer optics. The White cell path length was either 38.4 or 51.2 m in the work reported here. The White cell exit beam is focused onto an LN_2-cooled, mercury-cadmium-telluride (MCT) detector (Graseby, FTIR-M16). The system can measure the mid-infrared spectrum (400–4000 cm^{-1}) of the optical path every 0.83 s with a spectral resolution of 0.5 cm^{-1}. The spectra are stored on a laptop computer and later analyzed to yield the mixing ratios for stable and reactive gases as described in section 2.3.

2.2. Sources of Biofuel Emissions and Measurement Configurations

[5] Kaoma, Zambia served as a central base for all the measurements described in this paper. Kaoma is a small city located about 400 km west of Lusaka in the Western Province of Zambia. Subsistence agriculture is practiced by a majority of the inhabitants of the large rural region surrounding Kaoma. Detailed photographs that complement the experimental descriptions below can be viewed at http://www.umt.edu/chemistry/faculty/yokelson/galleries/s2k/index.htm.

2.2.1. Wood Cooking Fires

[6] In rural areas of Zambia, open wood fires are the main source of heat for cooking. We measured the emissions from three open wood cooking fires that were built and tended by local residents in both Kaoma (1 fire) and the remote village of Milumbwa (2 fires; location ~50 km west of Kaoma on a one-lane dirt road). The cooking fire in Kaoma was in a sheltered area of the backyard of our rented house and the Milumbwa cooking fires were conducted inside traditional huts (~2 × 2 m floor area). The fires in both locations were built with the regions most commonly used firewood (the Miombo tree species *Julbernardia* sp. and *Brachystegia* sp.). The fuel was typically 3–5 pieces of small diameter (2.5–7.0 cm) wood branches or logs with their long axes arranged radially. The fires were ignited at the center of the group where they burned gently (to minimize wasted heat or wood). The wood was pushed toward the center as the fire burned and quickly extinguished after cooking. At both locations, the OP-FTIR was supported by shipping crates ~1 m above the fires and weak convection from the fires directed the emissions through the optical path of the open White cell. Spectra were acquired continuously over the course of each fire with each individual spectrum lasting 3–11 s. Background spectra were collected in clean air upwind of the fires before and after each fire. We used a hand-held, chromel-alumel thermocouple and a portable, digital barometer (Cole-Parmer) to measure the temperature and pressure in the OP-FTIR optical path. AC power was available for the FTIR and computer in Kaoma, but they were powered by automotive batteries in Milumbwa and other rural locations.

2.2.2. Charcoal Cooking Fires

[7] Charcoal is used mostly in urban areas and it is normally burned in a rudimentary stove or metal container. We measured the emissions from one charcoal cooking fire in Kaoma. The charcoal was produced locally from the same tree species used for firewood above and it was burned in a simple stove consisting of an open, perforated metal cylinder supported by three legs and underlain by a "floor" to catch ashes. The OP-FTIR deployment was the same as for the wood cooking fires (described above).

2.2.3. Earthen Charcoal-Making Kiln

[8] Charcoal is produced in rural areas for use mainly in urban areas. Our kiln study site was in a remote clearing in the Miombo woodland ~20 km SE of Kaoma (14.86°S, 24.82°E). Local residents experienced in charcoal making constructed the kiln and tended it throughout the experiment. The wood used for making the charcoal (*Julbernardia* sp. and *Brachystegia* sp.) was felled nearby and cut into logs 1–2 m in length. After drying, the logs were stacked ~1.5 m high. Soil clumps (~40 × 40 × 20 cm) that were held together by dry grass roots were excavated next to the wood stack and used to encase the wood in an earthen layer 20–40 cm thick. This was a small kiln designed to produce five bags of charcoal weighing ~40 kg each. The wood was ignited through a small opening at one end of the kiln on the morning of 10 September. A few minutes after ignition, the opening was sealed with more soil clumps to reduce airflow into the kiln and promote carbonization of the wood charge. On the morning of 14 September, the kiln was broken to retrieve the charcoal.

[9] The kiln emissions emanated from numerous small holes in the walls and they were conveniently directed horizontally by a strong easterly wind through the optical path of the OP-FTIR system, which was operated as described above. Background spectra were collected in a smoke-free area upwind of the kiln before and after each smoke measurement. Because of the need to sample both cooking fires and kiln emissions within 1 week and at different locations, we could not measure the kiln emissions continuously. Instead, we collected three extended measurements of the emissions lasting ~1–2 hours each on 10, 11,

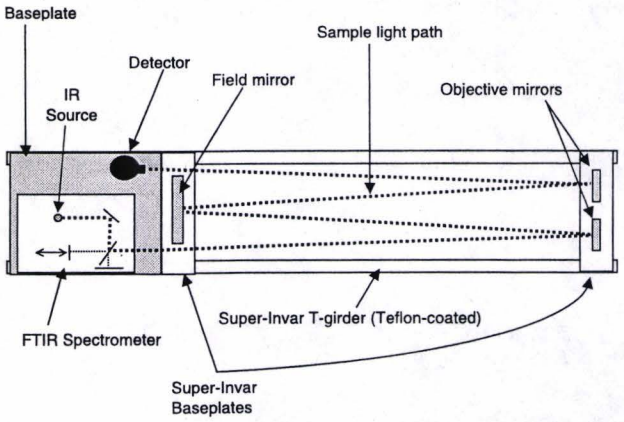

Figure 1. A simplified, top view schematic (not to scale) of the OP-FTIR we deployed in Zambia to measure the trace gas emissions from the production and use of biofuels.

and 13 September, which spanned the 4-day lifetime of the kiln. We estimate the charcoal yield (charcoal produced dry mass (dm)/wood used dm) and the charcoal carbon content based on previous work [*Chidumayo*, 1994; *Lacaux et al.*, 1994; *Ishengoma et al.*, 1997; *Smith et al.*, 1999; *Pennise et al.*, 2001].

2.3. Analysis of the OP-FTIR Spectra

[10] We obtained absolute mixing ratios for H_2O, nitrous oxide (N_2O), carbon dioxide (CO_2), carbon monoxide (CO), and methane (CH_4) by fitting regions of the transmission, or "single-beam," spectra with synthetic calibration classical least squares (CLS) methods described in detail elsewhere [*Griffith*, 1996; *Yokelson et al.*, 1996, 1997; *Yokelson and Bertschi*, 2002]. The excess mixing ratios in the smoke (ΔX for a species "X") are the absolute mixing ratios in the smoke spectra minus the absolute mixing ratios in the appropriate background spectra. We also generated absorbance spectra of the smoke using background spectra obtained between the smoke measurements. We analyzed these absorbance spectra by synthetic calibration CLS to directly yield excess mixing ratios in smoke for formaldehyde (HCHO), ethane (C_2H_6), acetylene (C_2H_2), nitric oxide (NO), nitrogen dioxide (NO_2), and ammonia (NH_3). Analysis of these absorbance spectra by spectral subtraction [*Yokelson et al.*, 1997] directly yielded excess mixing ratios in the smoke for H_2O, ethene (C_2H_4), propene (C_3H_6), acetic acid (CH_3COOH), methanol (CH_3OH), formic acid (HCOOH), phenol (C_6H_5OH), furan (C_4H_4O), hydroxyacetaldehyde ($HOCH_2CHO$), and NH_3. The above compounds accounted for all of the significant features in the spectra collected during this study. The detection limit for each species depended on the amount of signal averaging and the analysis method, but was usually in the range 5–20 ppbv. For most of the spectra, the excess mixing ratios retrieved for all of the reported species were 20–1000 times higher than the detection limit and the uncertainty for a typical excess mixing ratio was $\sim\pm5\%$ (1σ). However, the excess mixing ratios for N_2O were near our detection limit so we do not present results for this compound. We did not find features in the spectra from this study (or in the spectra from a separate study of smoldering logs in Zambia [*Bertschi et al.*, 2003]) that were due to a number of compounds sometimes reported in smoke such as acetonitrile, OCS, and HCN. HCN was a major emission from savanna fires [*Yokelson et al.*, 2003].

3. Results and Discussion

[11] As noted above, we were able to quantify 18 of the 19 trace gases identified as emissions during the combustion of biofuels. Since IR spectroscopy can measure most gases present above 5–20 ppb [*Goode et al.*, 1999] and these species accounted for all of the major features in our smoke spectra, they are then 18 of the most abundant emissions. The main trace gases that were probably emitted, but not detected here are H_2 [*Cofer et al.*, 1996] and N_2 [*Kuhlbusch et al.*, 1991], which are weak absorbers of IR.

3.1. Calculation of Emission Ratios (ER)

[12] The excess mixing ratios (ΔX, the mixing ratio of species "X" in the smoke minus the mixing ratio of "X" in the background air) that are observed in biomass burning studies reflect the degree of dilution of the smoke at the point of measurement. Thus, a more widely used, derived quantity is the normalized excess mixing ratio where ΔX is compared to a simultaneously measured smoke tracer such as ΔCO or ΔCO_2. A measurement of $\Delta X/\Delta CO$ or $\Delta X/\Delta CO_2$ made in nascent smoke ($< \sim 5$ min old) is an ER. We used the fire-integrated excess mixing ratios to calculate fire-average ERs. The fire-average ER for each wood cooking fire and the study-average ER for all the wood cooking fires are shown in Table 1. The fire-average ER for the charcoal cooking fire is shown in Table 2. For the charcoal kiln, we calculated an ER for each day and averaged them together to obtain the kiln-average ER. These ER are reported in Table 3. We include in Tables 1, 2, and 3 the previously measured ER for biofuel use to facilitate comparisons (next).

3.2. Comparison of ERs With Previous Work

3.2.1. Wood Cooking

[13] Four previous studies measured some of the emissions from open wood cooking fires. *Kituyi et al.* [2001] measured trace gas emissions from wood burned in both open fires and different types of stoves. They found that the use of various stoves strongly influenced the mix of trace gases emitted. Therefore, we limit this discussion to open wood cooking fires, which are what we sampled and the most common type of cooking fire in Africa.

[14] The ER $\Delta CO/\Delta CO_2$ and the modified combustion efficiency (MCE) ($\Delta CO_2/(\Delta CO_2 + \Delta CO)$) indicate both the relative amount of the two main emissions and the relative amount of flaming and smoldering combustion during a fire. Higher $\Delta CO/\Delta CO_2$ or lower MCE indicates more smoldering [*Ward and Radke*, 1993]. *Kituyi et al.* [2001, Table 1] reported an average ER $\Delta CO/\Delta CO_2$ of 0.072 ± 0.03 for 20 open wood cooking fires in Kenya. *Brocard et al.* [1996] sampled 43 open wood cooking fires in the Ivory Coast. They described these fires as having four "phases" and estimated that ~80% of the wood was consumed in the "cooking phase," which had an ER $\Delta CO/\Delta CO_2$ of 0.057 ± 0.011. The other phases consumed less fuel and had ER $\Delta CO/\Delta CO_2$ from 0.15 to 0.26. They

Table 1. ERs and EFs for Open Wood Cooking Fires

	ERs													Average EFs (g kg^{-1} dm)			
	This Work					*Brocard et al.* [1996]		*Smith et al.* [2000]		*Kituyi et al.* [2001]		*Ludwig et al.* [2003]					
	Fire 1	Fire 2	Fire 3	Average	SD	Average	SD	Average	SD	Average	SD	Average	SD	Trace Gas	This Work[a]	*Brocard et al.* [1996]	*Smith et al.* [2000]
MCE	0.933	0.906	0.892	0.910	0.021	0.927		0.966		0.933		0.913		CO_2	1525	1467	1455
$\Delta CO/\Delta CO_2$	0.0716	0.1035	0.1217	0.0989	0.0254	0.079	0.015	0.035	0.005	0.072	0.03	0.095	0.022	CO	96	70	62
$\Delta CH_4/\Delta CO$	0.1957	0.1491	0.2334	0.1930	0.0420	0.048	0.0014	0.369	0.282					CH_4	10.6	2.0	6.1
$\Delta C_2H_6/\Delta CO$	0.0142	0.0116	0.0178	0.0145	0.0031									C_2H_6	1.50		
$\Delta C_2H_4/\Delta CO$	0.0380	0.0141	0.0213	0.0245	0.0123									C_2H_4	2.35		
$\Delta C_2H_2/\Delta CO$	0.0267		0.0107	0.0187										C_2H_2	1.67		
$\Delta C_3H_6/\Delta CO$	0.0038	0.0082	0.0079	0.0066	0.0024									C_3H_6	0.95		
$\Delta HAc^b/\Delta CO$	0.0634	0.0202	0.0348	0.0394	0.0219	0.008	0.004							HAc	8.12	1.27	
$\Delta HFo^c/\Delta CO$	0.0090	0.0018	0.0022	0.0043	0.0040	0.001	0.0005							HFo	0.68	0.12	
$\Delta CH_2O/\Delta CO$	0.0464	0.0270	0.0291	0.0342	0.0106									CH_2O	3.52		
$\Delta GA^d/\Delta CO$			0.0027	0.0027										GA	0.66		
$\Delta CH_3OH/\Delta CO$	0.0492	0.0172	0.0390	0.0351	0.0164									CH_3OH	3.61		
$\Delta C_6H_5OH/\Delta CO$		0.0103		0.0103										C_6H_5OH	3.32		
$\Delta C_4H_4O/\Delta CO$		0.0017		0.0017										C_4H_4O	0.40		
$\Delta NMOC^e/\Delta CO$	0.2506	0.1121	0.1654	0.1760	0.0699	0.081	0.03	0.465	0.083					NMOC	26.78		
														gC(NMOC)	14.85	3.04	5.89
$\Delta NO/\Delta CO_2$	0.0021	0.0020	0.0009	0.0016	0.0007					0.0019	0.0006	0.0010	0.0004	NO	1.72		
$\Delta NO_2/\Delta CO_2$	0.0005	0.0003	0.0002	0.0003	0.0002									NO_2	0.49		
$\Delta NO_x/\Delta CO_2$	0.0026	0.0022	0.0011	0.0020	0.0008	0.0015	0.0004							NO_x as NO	2.04	1.48	
$\Delta NH_3/\Delta CO$	0.0192	0.0204	0.0266	0.0221	0.0040									NH_3	1.29		

[a]Computed from average ERs.
[b]HAc = acetic acid.
[c]HFo = formic acid.
[d]GA = glycoladehyde. Other names include hydroxyacetaldehyde and hydroxyethanal.
[e]For Brocard et al., we calculated NMOC by adding their organic acid values to their ΣNMHC.

Table 2. ERs and EFs for Charcoal Cooking Fires

	ERs									EFs (g kg^{-1} Dry Charcoal Burned)			
	This Work	*Kaoma and Kasali* [1994]		*Brocard et al.* [1996]		*Smith et al.* [2000]		*Kituyi et al.* [2001]					
	Average	Average	SD	Average	SD	Average	SD	Average	SD	Compound	This Work[a]	*Brocard et al.* [1996]	*Smith et al.* [2000]
MCE	0.919	0.914		0.867		0.847		0.927		CO_2	2402	2226	2411
$\Delta CO/\Delta CO_2$	0.0878	0.094	0.046	0.155	0.003	0.180	0.032	0.0785	0.015	CO	134	208	275
$\Delta CH_4/\Delta CO$	0.0735			0.016	0.012	0.051	0.016			CH_4	6.88	2.4	7.9
$\Delta C_2H_6/\Delta CO$	0.0043									C_2H_6	0.747		
$\Delta C_2H_4/\Delta CO$	0.0044									C_2H_4	0.720		
$\Delta C_2H_2/\Delta CO$	0.0034									C_2H_2	0.514		
$\Delta HAc^b/\Delta CO$	0.0091									HAc	3.20		
$\Delta HFo^c/\Delta CO$	0.0006									HFo	0.159		
$\Delta CH_2O/\Delta CO$	0.0042									CH_2O	0.733		
$\Delta CH_3OH/\Delta CO$	0.0066									CH_3OH	1.24		
$\Delta NMOC^d/\Delta CO$	0.0326			0.0039	0.0004	0.0597	0.0105			NMOC	7.31		
										gC(NMOC)	3.77	0.36	7.0
$\Delta NO/\Delta CO_2$	0.0007							0.0020	0.0003	NO	1.16		
$\Delta NO_2/\Delta CO_2$	0.0002									NO_2	0.384		
$\Delta NO_x/\Delta CO_2$	0.0009									NO_x as NO	1.41		
$\Delta NH_3/\Delta CO$	0.0097									NH_3	0.97		

[a]Computed from average ERs.
[b]HAc = acetic acid.
[c]HFo = formic acid.
[d]The value for Brocard et al. is their ΣNMHC.

estimated the fuel consumption weighted, average ER $\Delta CO/\Delta CO_2$ for the overall wood cooking process as 0.079. *Smith et al.* [2000] sampled six open wood cooking fires built with native wood in a laboratory in India and they reported an average ER $\Delta CO/\Delta CO_2$ of 0.035 indicating that relatively more of the fuel was consumed by flaming combustion in their fires. *Ludwig et al.* [2003] reported an average, fire-integrated ER $\Delta CO/\Delta CO_2$ of 0.095 ± 0.022 for 94 open wood cooking fires in Zimbabwe and also for 17 open wood cooking fires in Nigeria. They proposed that 0.095 should be adopted as the global average ER $\Delta CO/\Delta CO_2$ for biofuel use. For the three wood fires we measured, the fire-average ER $\Delta CO/\Delta CO_2$ ranged from 0.07 to 0.12 with a study average of 0.0989 (Table 1). Our study-average ER $\Delta CO/\Delta CO_2$ is within 4% of the value obtained in the most extensive study [*Ludwig et al.*, 2003]. Thus, our fires may have had an average flaming to smoldering ratio (F/S) that was similar to the average F/S for the fires in the largest study. This observation and some of the ER comparisons below suggest that our fires may be reasonably representative of African biofuel use.

[15] Our average ER for both $\Delta CH_4/\Delta CO$ and excess nonmethane organic compounds/ΔCO (ΔNMOC/ΔCO) are in the middle of the very different values reported by *Brocard et al.* [1996] and *Smith et al.* [2000]. We do not have an explanation for the wide range in the CH_4 results, but the large range in the results for NMOC could be due partly to the different measurement methods employed. Brocard et al. actually measured individual, "light" nonmethane hydrocarbons and reported the sum as NMHC. The sum of the individual light ΔNMHC/ΔCO we measured is very close to their total ΔNMHC/ΔCO value. To derive the ER ΔNMOC/ΔCO for Brocard et al. in Table 1, we add their organic acid ER to their ΔNMHC/ΔCO. However, our value for ΔNMOC/ΔCO includes oxygenated organic compounds not measured by Brocard et al. Therefore, it is not surprising that our ΔNMOC/ΔCO is considerably larger than their ΔNMOC/ΔCO. In contrast, Smith et al. measured total organic compounds by flame ionization and then subtracted their CH_4 value to estimate total NMOC. Their approach should be sensitive to higher molecular weight compounds not measured in the other studies and they report the highest ΔNMOC/ΔCO value. However, it is surprising that Smith et al. report both the lowest $\Delta CO/\Delta CO_2$ (which indicates flaming combustion) and the highest ER to CO for smoldering compounds.

[16] Our $\Delta NO/\Delta CO_2$ ER is 16% smaller than reported by *Kituyi et al.* [2001] and our $\Delta NO_x/\Delta CO_2$ ER is 33% larger than reported by *Brocard et al.* [1996]. These small differences probably arise from variation in the fuel nitrogen content [*Kituyi et al.*, 2001], which was not measured in most of the studies. Other differences with previous studies may be partially related to the measurement techniques used. For instance, we report study-average ERs for CH_3COOH and HCOOH to CO that are 5 and 4 times larger, respectively, than Brocard et al. measured using a mist chamber [*Cofer et al.*, 1985]. This may be partly due to differences in the emissions since our ratios vary significantly from fire to fire. However, our much larger study-average ratios might also reflect some of the advantages of open-path spectroscopic methods for measuring sticky or reactive compounds. In particular, production or loss of species on sample lines, in containers, or within instruments cannot occur and our broadband, spectroscopic technique is also very resistant to interference [*Yokelson and Bertschi*, 2002]. A direct comparison of the mist chamber and OP-FTIR on the same smoke (and standards) would help quantify the possible causes for the observed interstudy variation.

[17] This study triples the number of ER reported for tropical, open wood cooking fires from 6 to 18. Perhaps the most important new finding is that many of the most abundant compounds emitted by open wood cooking fires are oxygenated volatile organic compounds (OVOC): they account for ~70% of the NMOC. Because OVOC were previously found to be major emissions from large-scale biomass fires in boreal, temperate, and tropical ecosystems

Table 3. ERs and EFs for Earthen Charcoal-Making Kilns

ERs											Average EFs					
	This Work					*Lacaux et al.* [1994]	*Smith et al.* [1999]		*Pennise et al.* [2001]			This Work[a]		*Lacaux et al.* [1994]	*Smith et al.* [1999]	*Pennise et al.* [2001]
	Date (2000)															
	10 September	11 September	13 September	Average	SD	Average	Average	SD	Average	SD	Compound	g kg^{-1} Wood	g kg^{-1} Charcoal	g kg^{-1} Charcoal	g kg^{-1} Charcoal	g kg^{-1} Charcoal
MCE	0.820	0.792	0.737	0.783	0.042	0.806	0.768		0.831		CO_2	542	1935	1571	1140	1802
$\Delta CO/\Delta CO_2$	0.220	0.263	0.358	0.280	0.071	0.24	0.302	0.05	0.204	0.04	CO	96.8	346	250	226	223
$\Delta CH_4/\Delta CO$	0.160	0.264	0.301	0.242	0.073	0.28	0.217	0.03	0.418	0.12	CH_4	13.4	47.7	38.0	27.7	44.6
$\Delta C_2H_6/\Delta CO$	0.015	0.023	0.060	0.033	0.024						C_2H_6	3.40	12.2			
$\Delta C_2H_4/\Delta CO$	0.013	0.012	0.015	0.013	0.002						C_2H_4	1.31	4.66			
$\Delta C_3H_6/\Delta CO$	0.010	0.006	0.015	0.010	0.005						C_3H_6	1.50	5.35			
ΔHAc[b]/ΔCO	0.020	0.031	0.078	0.043	0.031	0.0067					HAc	8.92	31.9	3.43		
ΔHFo[c]/ΔCO	0.002	0.002	0.004	0.003	0.001	0.0004					HFo	0.45	1.62	0.16		
$\Delta CH_2O/\Delta CO$	0.014	0.007		0.011							CH_2O	1.06	3.80			
$\Delta CH_3OH/\Delta CO$	0.059	0.083	0.191	0.111	0.070						CH_3OH	12.3	43.8			
$\Delta C_6H_5OH/\Delta CO$	0.007	0.003	0.016	0.009	0.007						C_6H_5OH	2.75	9.83			
$\Delta C_4H_4O/\Delta CO$	0.004	0.003	0.008	0.005	0.003						C_4H_4O	1.15	4.11			
ΔNMOC[d]/ΔCO	0.144	0.170	0.387	0.234	0.133	0.061	0.740	0.700	0.692	0.190	NMOC	32.8	117			
											gC(NMOC)	16.7	59.9	8.55	81.7	62
$\Delta NO/\Delta CO_2$	0.0003			0.0003					0.000035		NO	0.12	0.45			0.057
$\Delta NO_2/\Delta CO_2$											NO_2					
$\Delta NO_x/\Delta CO_2$	0.0003			0.0003		0.0002			0.000036		NO_x as NO	0.12	0.45	0.15		0.063
$\Delta NH_3/\Delta CO$	0.0070	0.0080	0.0040	0.006	0.002	0.002					NH_3	0.37	1.32	0.30		

[a]Computed from average ERs.
[b]HAc = acetic acid.
[c]HFo = formic acid.
[d]For Lacaux et al., we calculate NMOC by adding their organic acid values to their ΣNMHC.

[*Yokelson et al.*, 1996, 1997, 1999, 2003; *Worden et al.*, 1997; *Holzinger et al.*, 1999; *Goode et al.*, 1999, 2000], *Mason et al.* [2001] explored their influence on modeled smoke plume chemistry. They found that OVOC have a large impact on HO_x, O_3, and nitrogen chemistry. Since we measure ER to CO for all the OVOC (except HCOOH) that are larger than what we obtained for African savanna fires [*Yokelson et al.*, 2003], it would be of interest to explore the influence of these reactive biofuel emissions on the tropical troposphere. In contrast to the other types of biomass burning, biofuel emissions are produced year-round and they have different dispersion characteristics. The implications of our measurements are discussed further in sections 3.5 and 3.6.

3.2.2. Charcoal Cooking

[18] At least four previous studies quantified some trace gas emissions for charcoal cooking fires. Our average ER $\Delta CO/\Delta CO_2$ (0.0878 ± 0.051) is lower than the values of *Brocard et al.* [1996] (0.155 ± 0.003) and *Smith et al.* [2000] (0.18 ± 0.03) but close to the reports of *Kituyi et al.* [2001] (0.0785 ± 0.015) and *Kaoma and Kasali* [1994] (0.094 ± 0.046). The variation in this ER could be caused partly by the different types of stoves used. Our average $\Delta CH_4/\Delta CO$ is larger than the other two reports. Our average $\Delta NMOC/\Delta CO$ lies between those of the other two reports, as was the case for wood cooking fires. All the studies that measured $\Delta NMOC/\Delta CO$ concluded that this ratio is much lower for charcoal cooking than for wood cooking. We report a much lower ER $\Delta NO/\Delta CO_2$ than the value of *Kituyi et al.* [2001], but, as discussed above, this may be due to differences in fuel nitrogen content. Again, our study greatly expands the number of compounds quantified and OVOC again account for ~70% of the NMOC.

3.2.3. Earthen Charcoal-Making Kiln

[19] ERs for earthen charcoal-making kilns were reported in three previously published studies. The $\Delta CO/\Delta CO_2$ ER for all four studies is between 0.2 and 0.3 reflecting the importance of pyrolysis in the carbonization process. Three of the four $\Delta CH_4/\Delta CO$ ER are in good agreement, but that of *Pennise et al.* [2001] is much larger than the others. Our $\Delta NMOC/\Delta CO$ is between that of *Lacaux et al.* [1994] and the other studies. We observe much lower NO_x emissions from charcoal than from wood yet we report a $\Delta NO_x/\Delta CO_2$ ER that is ~8 times larger than that of *Pennise et al.* [2001]. Again, this variation may be mainly due to differences in fuel nitrogen content.

[20] Large differences occur between our measurements of organic acids and those made by *Lacaux et al.* [1994] using a mist chamber; as reported in more detail by *Brocard et al.* [1996]. Our ER for total excess organic acids/ΔCO is about 6.5 times higher. We also observe an ER $\Delta NH_3/\Delta CO$ that is ~3 times higher than Lacaux et al. measured by chemiluminescence. Our larger values could arise from differences in the kilns and/or the measurement approach. Unlike the kiln sampled by *Lacaux et al.* [1994], our kiln had no chimney or branch bed and this may have led to different combustion characteristics. In addition, our kiln probably had higher nitrogen content in the initial wood charge since our $\Delta NO_x/\Delta CO_2$ ER is 50% larger than Lacaux et al. observed. This probably accounts for some of our higher NH_3 emissions. Our smoke measurements probed ~0.05 m^3 of the plume emitted by the kiln, whereas, Lacaux et al. used a metal tube to draw samples from a point inside the kiln. The trace gases could change between these locations or the concentrations of reactive species (e.g., CH_3COOH or NH_3) could be altered on the walls of the metal tube. In studies of other types of biomass burning, FTIR returned higher values for organic acids than had been observed using mist chambers (see section 3.2.1 or the studies of *Yokelson et al.* [1996] and *Goode et al.* [2000]). Finally, Lacaux et al. probably sampled for a greater fraction of the time that emissions were produced and both studies sampled only one kiln, which means that the kiln–kiln variation is not well known. In summary, more measurements are needed, but our study approximately doubles the amount of ER reported for earthen kilns and almost 80% of the NMOC are oxygenated organic compounds. Thus, OVOC are a major component of the emissions from both the production and use of biofuels.

3.3. Calculation of Emission Factors (EF)

3.3.1. Cooking Fires

[21] We calculated EF (g compound emitted per kg dm fuel burned) for each trace gas emitted from the wood cooking fires using the carbon mass balance method, which is described in full by *Ward and Radke* [1993]. In brief, we assume that all the burned carbon is volatilized, partitioned according to our ER, and that the fuel carbon content is known. By ignoring unmeasured gases, particles, and other condensed-phase carbon products, we are probably inflating the EFs by a few percent. To estimate the fuel carbon content for the wood cooking fires, we use previously reported values for Miombo tree species. *Chidumayo* [1994] reported a carbon content (by mass) of 47.4 ± 1.8% for 21 Miombo tree species. Similarly, *Susott et al.* [1996] reported a carbon content of 48.4 ± 1.3% in the wood of tree species found in the Zambian Miombo. We use the average of the values from these two studies, 48 ± 2% (2σ), to estimate the carbon content of the wood consumed in this study. We calculated the EF for the charcoal cooking fires in the same way as for the wood cooking fires except that the charcoal is enriched in carbon. *Chidumayo* [1994] reported an average carbon content of 72% for 103 charcoal samples collected from 65 separate earthen kilns and this is close to the values reported by *Ishengoma et al.* [1997] (70%), *Lacaux et al.* [1994] (74.5%), and *Smith et al.* [1999] (74.8%). Therefore, we assume a carbon content of 72 ± 3% (2σ) for the charcoal burned in this study. The EFs for the wood and charcoal cooking fires are reported in Tables 1 and 2, respectively.

3.3.2. Charcoal Kilns

[22] We cannot use the carbon mass balance method to calculate kiln EF in the same way that we did to calculate cooking fire EF because the carbon content changes during the kiln lifetime and a lot of the burned carbon is not volatilized. Also, kiln EFs can be expressed as g compound emitted per kg wood used or as g compound emitted per kg charcoal produced; with each form having its advantages. Attempts have been made by previous authors to estimate kiln EF and the methods seem to conflict though each method may have been accurate for the particular circumstances. We describe the various methods and justify our estimate next.

[23] The first estimate of earthen kiln EFs was by *Lacaux et al.* [1994]. These authors formulated the carbon balance for charcoal making as in (1).

$$C_w = C_s + C_l + C_g \quad (1)$$

where C_w, C_s, C_l, and C_g represent the carbon (on a dry matter basis) in the wood charge, charcoal, pyrolignous liquid (tar), and gases, respectively. In their kiln, the initial wood was 46% C (by mass) and 27.6% of the wood was converted to charcoal that was 74.5% C. Thus, they directly measured C_w and C_s and found that ~44.8% of the carbon in the wood remained in the charcoal. *Lacaux et al.* [1994] assumed that 20.6% of the carbon in the wood was converted to pyrolignous liquid based on a separate laboratory study of wood pyrolysis by *Dumont and Gelus* [1982]. They then calculated C_g as 34.6% by difference and their EF are based on partitioning C_g according to their ERs. Their assumption of a high liquid yield may not be appropriate for our kiln as discussed in more detail later.

[24] In a study of three Thai earthen kilns, *Smith et al.* [1999] reported wood and charcoal carbon contents of 44% and 74.8% and a charcoal yield (charcoal mass/wood dm) of 29.8 ± 2.5% similar to values obtained above. (Smith et al. did not measure the moisture content of the charcoal.) In contrast to the study of *Lacaux et al.* [1994], *Smith et al.* [1999] found that the sum of the carbon condensed on the inner walls of the kiln and inside a hood they placed over the kiln accounted for only 0.24% of the carbon in the wood. Even with a cooled apparatus to process the emitted gases, they could only condense a small fraction of the emissions, indicating that ~3% of the wood carbon became condensable gases. Of course, most earthen kilns are not fitted with any condensing device. In another difference with Lacaux et al., *Smith et al.* [1999] found that 15% of the initial carbon ended up in the "brands" (partially carbonized wood pieces). The data of Smith et al. suggests to us that (on average) charcoal, brands, and trace gas emissions (by difference) accounted for ~48%, 15%, and 37% of the carbon in the initial wood charge, respectively.

[25] *Pennise et al.* [2001] measured a charcoal yield of 27.5 ± 5.4% for five earthen kilns in Kenya. Based in large part on the measurements and assumptions of *Smith et al.* [1999], they estimated that 47 ± 9% of the wood carbon was converted to charcoal. In an intriguing contrast with Smith et al., they found that in four out of the five kilns, the brands accounted for less than 4% of the wood carbon. Finally, we note that one of us (Darold Ward) has completed detailed measurements of the carbon mass balance for Zambian earthen kilns. A preliminary analysis of that data does not appear to directly support a large yield of brands or liquid.

[26] We need to estimate the carbon content of the wood charge and the fraction of that carbon that is emitted as gases to use our ER to calculate EF as g compound emitted per kg dry wood used. We take the carbon content of the wood to be 48 ± 2% (2σ) as justified in section 3.3.1. To estimate the fraction of that carbon emitted as gases, we first note that *Lacaux et al.* [1994], *Pennise et al.* [2001], and *Smith et al.* [1999] found that (on average) 45%, 47%, and 48% of the wood carbon ended up in the charcoal, respectively. Thus, 50% seems like an upper limit for an average yield of gases. On the other hand, the assumption of large yields of liquid or brands is consistent with a gas yield approaching 40%. Since we are not convinced that a large yield of liquid or brands is typical, we estimate that 45% of the wood carbon is emitted as gases. Our earthen kiln EF for g compound per kg wood used are based on this assumption and are therefore, somewhat higher than previous estimates (see Table 3).

[27] We can derive EF (g per kg charcoal produced) from the EF (g per kg wood used) with an estimate of the average charcoal yield. We note that *Chidumayo* [1994] found an average charcoal yield of 23.4 ± 7.2% (i.e., 1 kg of wood (dm) produces ~234 g of charcoal) for Zambian, earthen kilns. This is lower than the charcoal yields reported by *Pennise et al.* [2001], *Lacaux et al.* [1994], and *Smith et al.* [1999] of 27.5 ± 10%, 27.6%, and 29.8 ± 2.5%, respectively. Therefore, we assume a charcoal yield of 28% (and a conversion factor of 1000/280) to calculate EF per kg charcoal produced. We note that coupling the assumptions we have made above does not account for some 10% of the wood carbon and thus these assumptions are consistent with modest yields of brands or liquid. In summary, we assume a higher gas yield than previous workers and that will contribute to higher EF.

3.4. Comparison of EFs With Previous Measurements

3.4.1. Wood and Charcoal Cooking Fires

[28] Since the calculation of EF for cooking fires is straightforward, the comparison of EF yields conclusions similar to the comparison of ERs given in sections 3.2.1 and 3.2.2 (e.g., we obtained significantly higher EF for organic acids). We note one interesting anomaly. *Smith et al.* [2000] report a considerably higher ER ΔNMOC/ΔCO than us for wood fires, but a considerably lower g C emitted as NMOC.

3.4.2. Earthen Charcoal-Making Kilns

[29] We have already made the most direct comparisons between kiln studies in section 3.2.3. As noted above, in comparison to other studies our kiln EF are increased across the board by 25–30% because of our assumption of a higher yield of gaseous emissions. Equivalently, if *Lacaux et al.* [1994] and *Smith et al.* [1999] had assumed a negligible yield of both liquid and uncarbonized wood, their reported EF would increase by approximately 60% and 50%, respectively. However, the large differences between our EF and previous reports for reactive and sticky trace gases (i.e., OVOC, NH_3, etc.) are due mostly to our much larger ERs discussed earlier. In summary, this work has expanded our knowledge of kiln emissions, but more work is needed to improve the understanding of the carbon balance and the variation in emissions for earthen (and other) kilns. When this information becomes available, our ERs could be incorporated into refined EF estimates.

3.5. Comparison of Wood and Charcoal Use: Emissions Per Unit Energy

[30] According to a recent estimate, African fuelwood use is increasing at ~1% yr^{-1} and African charcoal use is increasing at ~3% yr^{-1} [*FAO*, 1999]. The main advantage of charcoal over wood is the greater quantity of energy released per unit mass of fuel burned (~31 MJ kg^{-1} for charcoal compared to ~16 MJ kg^{-1} for wood) [*FAO*, 1985]. However, it is also important to compare these fuels based on the amount of emissions produced per unit energy released.

Table 4. EFs and "Energy-Normalized EFs" From Charcoal Production/Consumption and Wood Burning

	EFs				Energy-Normalized EFs[a]	
Species	Charcoal[b] Production (g kg^{-1} Charcoal Made)	Charcoal[c] Fires (g kg^{-1} Charcoal Used)	Total[d] Charcoal (g kg^{-1} Charcoal Made and Used)	Wood[e] Fires (g kg^{-1} Wood Used)	Wood[f] Fires (g MJ^{-1})	Total[g] Charcoal (g MJ^{-1})
CO_2	1935	2402	4337	1525	95	140
CO	346	134	480	96.0	6.0	15
CH_4	47.7	6.9	55	10.6	0.66	1.8
C_2H_6	12.2	0.75	13	1.50	0.09	0.42
C_2H_4	4.66	0.72	5.4	2.35	0.15	0.17
C_2H_2		0.51	0.51	1.67	0.10	0.02
C_3H_6	5.35		5.4	0.95	0.06	0.17
HAc[h]	31.9	3.20	35	8.12	0.51	1.13
HFo[i]	1.62	0.16	1.8	0.68	0.04	0.06
CH_2O	3.80	0.73	4.5	3.52	0.22	0.15
CH_3OH	43.8	1.24	45	3.61	0.23	1.45
C_6H_5OH	9.83		9.83	3.32	0.21	0.32
C_4H_4O	4.11		4.1	0.40	0.03	0.13
NO	0.45	1.16	1.6	1.72	0.11	0.05
NO_2		0.38	0.38	0.49	0.03	0.01
NH_3	1.32	0.97	2.3	1.29	0.08	0.07

[a]Units in g of species emitted per MJ of energy released.
[b]EFs from average EFs reported in Table 3 [this work].
[c]EFs from average EFs reported in Table 2 [this work].
[d]Sum of EFs from charcoal burning and making [this work].
[e]EFs from average EFs reported in Table 1 [this work].
[f]Based on 16 MJ kg^{-1} wood consumed.
[g]Based on 31 MJ kg^{-1} charcoal consumed.
[h]HAc = acetic acid.
[i]HFo = formic acid.

[31] The emissions per unit energy are compared for wood and charcoal in Table 4. First, we sum the charcoal production EF (g compound emitted per kg charcoal produced) and the charcoal burning EF (g per kg charcoal burned) to obtain a "total charcoal EF" (g per kg charcoal produced and burned). Then we tabulate the study-average, wood fire EF (g per kg burned) to directly compare the g of emissions per kg of fuel used (including production if applicable). On a per mass basis the total charcoal EF are 3–10 times larger than the wood fire EF for most compounds. Next, we divide the total charcoal EF by 31 MJ kg^{-1} and the wood EF by 16 MJ kg^{-1} to yield the "EFs per unit energy" (g compound emitted per MJ energy released) shown in the right-hand columns of Table 4. After normalizing for energy release, the wood fires emit more C_2H_2, HCHO, and nitrogen compounds than the combined production and use of charcoal (the higher nitrogen emissions from wood burning could have been due to higher fuel N content, which we did not measure). However, for all the other trace gases the combined production and use of charcoal releases about twice the amount of emissions as wood burning does per unit energy yielded (see Table 4 and Figure 2).

[32] Wood is generally a cleaner energy source from the standpoint of trace gas emissions because traditional charcoal making releases both trace gases and unused energy. There are other related issues such as the efficiency of heat transfer in cooking, potentially lower particle emissions from charcoal use, or emissions associated with fuel transport. Nonetheless, this preliminary analysis is relevant to energy and environmental policies wherever biofuels are a major energy source. Strategies to reduce wasted energy could involve high-yield kilns [*Antal et al.*, 2000], energy plantations near urban areas [*Shafizadeh et al.*, 1976] or other approaches.

3.6. The Contribution of Biofuel Use to Regional and Global Trace Gas Emissions

[33] The local–global impacts of biofuel emissions are poorly understood. Much of the uncertainty stems from the previous lack of emissions data [*Andreae and Merlet*, 2001] and the difficulty of estimating the amount of biofuels burned. For instance, we measure ERs for some compounds that are 5–8 times higher than previously reported and estimates of the global, biofuel consumption range from 310 to 1085 Tg C yr^{-1}, which is a factor of 3 [*Hao and Liu*, 1994; *Andreae and Merlet*, 2001]. In contrast to the large uncertainty surrounding biofuels, savanna fires are well known to have a large impact on the regional–global atmosphere [*Delany et al.*, 1985; *Crutzen and Andreae*, 1990; *Fishman et al.*, 1991; *Yokelson et al.*, 2003]. Since the above estimates suggest that global carbon consumption due to biofuel burning is ~10–85% of that due to savanna fires, it is of some interest to further explore the relative magnitude of these sources.

[34] *Brocard and Lacaux* [1998] estimated that biofuel use produced a significant fraction of the annual pyrogenic emissions for West Africa. In this section, we couple our EFs with estimates of biomass consumption to compare the amount of emissions from biofuel burning and savanna fires in Zambia (see Table 5). *Chidumayo* [1994] estimated Zambian charcoal use at 0.905 Tg for the year 2000. The Zambian charcoal use for 1996 was estimated at 0.586 Tg by the *FAO* [1999]. The average of these two recent estimates is 0.75 Tg and that is used in Table 5. If we again assume a 28% charcoal yield, then 2.7 Tg of wood were

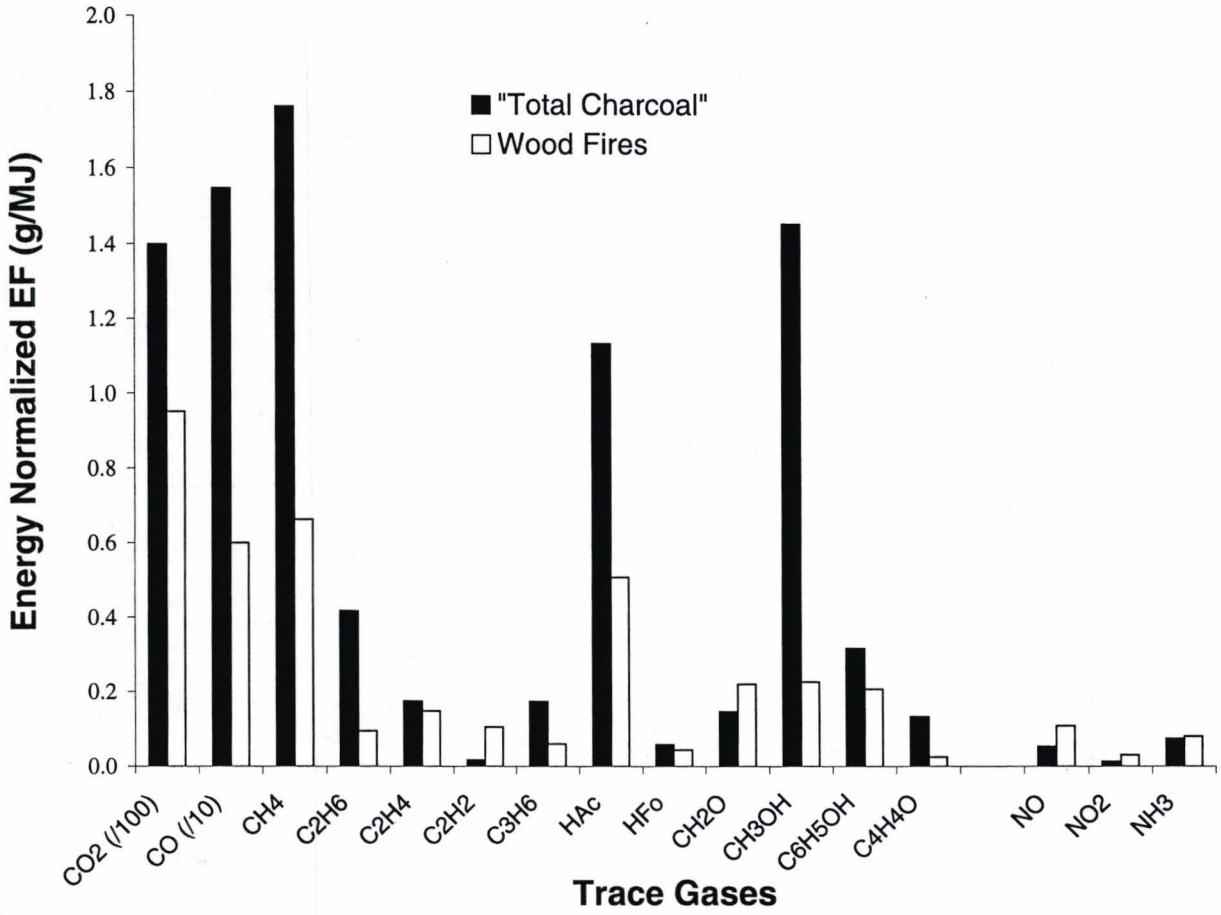

Figure 2. The energy-normalized EFs (g compound emitted per MJ energy released) are compared for wood burning and the combined production and use of charcoal. The values are computed in Table 4 as outlined in section 3.5. Note the scaling factors for CO_2 and CO.

used to make that charcoal. *Zhu et al.* [1998] estimated that 5.6 Tg of wood were consumed directly for domestic cooking during 2000 in Zambia. The Zambian fuelwood use for 1996 was estimated at 7.1 Tg by the *FAO* [1999]. The average of these two estimates is 6.4 Tg (Table 5). *Ludwig et al.* [2003] argued that FAO estimates are based on marketed wood and are therefore conservative. Their measurements supported the use of a formula quoted from the study of *Hall et al.* [1994] for biofuel use in Africa: 1000 kg cap^{-1} yr^{-1} (rural) and 500 kg cap^{-1} yr^{-1} (urban). Applying this formula to Zambia with a population of ~10 million [*The World Factbook*, 2001] that is 40% urban and 60% rural [*United Nations Statistics Division*, 2000] gives a total biofuel use of 8.0 Tg. This is 23% less than the sum of our speciated consumption terms derived above. Thus, in light of the difficulty of measuring biofuel consumption and the tendency for recent estimates to be larger, our estimates seem reasonable. *Hao and Liu* [1994] presented a figure based on satellite data from the late 1970s that suggests that ~18.6 Tg dm of biomass are consumed annually by savanna burning in Zambia.

[35] In Table 5, we multiply these biomass consumption estimates by our appropriate EFs to estimate speciated, annual, emissions for Zambia from charcoal production and use, firewood use, and savanna fires. (For savanna fire emissions, we use the savanna fire EFs recently measured in Zambia by *Yokelson et al.* [2003].) We complete the comparison by showing estimated ratios of biofuel emissions to savanna fire emissions (by species) in the right-hand columns of Table 5. We find that savanna fires account for most of the annual pyrogenic CO_2 (71%), HCOOH (63%), and NO_x (83%), while biofuel use accounts for most of the CH_4 (84%), CH_3OH (80%), C_2H_2 (73%), CH_3COOH (71%), HCHO (69%), and NH_3 (67%). The annual CO and C_2H_4 production is about equal from both sources. For West Africa, *Brocard and Lacaux* [1998] found that a similar fraction of the total pyrogenic emissions were due to biofuels (approximately one third), but they attributed a smaller fraction of the pyrogenic CO, CH_4, and NMOC to biofuel use than we did. Both estimates suggest that biofuel burning produces an annual amount of reactive compounds comparable to savanna fires; and that indicates a potential to strongly influence the tropical troposphere.

[36] Most of the biofuel emissions are too reactive to become globally mixed, but our measurements do impact

Table 5. Comparison of Estimated Annual Emissions From Biofuel Production and Use to Savanna Fires in Zambia

Species	EFs Wood Fires[a] (g kg^{-1} Wood Used)	Annual Emissions[b] Wood Fires (Tg yr^{-1})	EFs Total Charcoal[c] (g kg^{-1} Charcoal Made and Used)	Annual Emissions[d] Total Charcoal (Tg yr^{-1})	EFs Savanna Fires[e] (g kg^{-1} Biomass Burned)	Annual Emissions[f] Savanna Fires (Tg yr^{-1})	Ratio: Biofuel/Savanna This work Zambia	Ratio: Biofuel/Savanna *Brocard and Lacaux* [1998][g] West Africa
CO_2	1525	9.8	4337	3.3	1734	32.3	0.40	0.32
CO	96	0.61	480	0.36	55.7	1.0	0.9	0.42
CH_4	10.6	0.068	55	0.041	1.16	0.022	5.1	0.46
C_2H_6	1.50	0.010	13	0.010		–	–	
C_2H_4	2.35	0.015	5.4	0.004	0.77	0.014	1.3	
C_2H_2	1.67	0.011	0.51	0.0004	0.22	0.004	2.7	
C_3H_6	0.95	0.006	5.4	0.004		–	–	
HAc[h]	8.12	0.052	35	0.026	1.72	0.032	2.4	
HFo[i]	0.68	0.004	1.8	0.001	0.53	0.010	0.6	
CH_2O	3.52	0.023	4.5	0.003	0.63	0.012	2.2	
CH_3OH	3.61	0.023	45	0.034	0.79	0.015	3.9	
C_6H_5OH	3.32	0.021	9.83	0.007		–	–	
C_4H_4O	0.40	0.003	4.1	0.003		–	–	
NMOC	26.1	0.167	124.5	0.093	4.7	0.087	3.0	0.44
NO_x	2.04	0.013	2.0	0.001	3.14	0.058	0.2	
NH_3	1.29	0.008	2.3	0.002	0.27	0.005	2.0	

[a]EFs from the average "wood cooking" EFs reported in Table 1 [this work].
[b]Based on 6.4 Tg annual fuelwood use (see section 3.4).
[c]EFs from "Total Charcoal" EFs reported in Table 4 [this work].
[d]Based on 0.75 Tg annual charcoal use (see section 3.4).
[e]EFs for Zambian savanna burning reported by *Yokelson et al.* [2003].
[f]Based on 18.6 Tg biomass burned in savanna fires annual from the study of *Hao and Liu* [1994] (see section 3.4).
[g]The estimates of *Brocard et al.* [1996] for West Africa are assumed to supersede those from 1996.
[h]HAc = acetic acid.
[i]HFo = formic acid.

global budgets. For instance, *Singh et al.* [1995] estimated a global source of ~45 Tg yr^{-1} for CH_3OH based on its abundance in the remote troposphere and its reaction rate with OH. They estimated that global biomass burning produced ~6 Tg yr^{-1} of CH_3OH. If we couple our EFCH_3OH for wood cooking fires (3.61 g kg^{-1}) with the Yevich and Logan (YL) estimate of global biofuel burning (2701 Tg dm yr^{-1}) (quoted in the study of *Andreae and Merlet* [2001]), the result is 9.75 Tg yr^{-1}. Coupling our EFCH_3OH for savanna fires (1.17 g kg^{-1}) [*Yokelson et al.*, 2003] with the YL estimate of global savanna fire burning (3160 Tg dm yr^{-1}) results in 3.7 Tg yr^{-1}. Combining the YL estimate for total forest fires (1970 Tg dm yr^{-1}) with a EFCH_3OH for forest fires from the study of *Yokelson et al.* [1999] produces an estimate of 5.5 Tg yr^{-1}. Thus, biofuel use is significant compared to the other types of biomass burning on a global scale. In addition, we obtain a CH_3OH source from these three types of biomass burning (19 Tg yr^{-1}) that is 3 times larger than the estimate of Singh et al. for total biomass burning. This larger source is partially counteracted by the discovery of *Yokelson et al.* [2003] that CH_3OH is readily scavenged in smoke-impacted clouds.

[37] CH_4 is more stable than CH_3OH. Our EFCH_4 of 10.6 g kg^{-1} for fuelwood is 40% larger than the EF in an earlier study (7.6 g kg^{-1}) [*Hao and Ward*, 1993]. Coupling our EF with the YL biofuel estimate yields 28.6 Tg yr^{-1}. This is 4 times larger than the fuelwood contribution estimated by Hao and Ward, and almost as large as their estimate for CH_4 from global biomass burning (30.5 Tg yr^{-1}). Using the YL estimates for each biomass burning category with our most recent EFCH_4 [*Yokelson et al.*, 1999, 2003; *Bertschi et al.*, 2003; T. Christian, personal communication, 2003] implies a global biomass burning source for CH_4 of ~59 Tg yr^{-1}. Source estimates similar to those in the above examples can be made for each trace gas measured in this study. We also plan measurements of the trace gas emissions from biofuel use in other regions of the tropics to further probe the representativeness of our data. Finally, the impact of biofuel burning in atmospheric chemistry models should be reexamined, now that the initial emissions are better characterized.

4. Conclusions

[38] We used OP-FTIR spectroscopy to quantify 18 of the most abundant trace gases emitted by wood and charcoal cooking fires and an earthen, charcoal-making kiln in Zambia. These are the first, in situ measurements of an extensive suite of trace gases emitted by tropical biofuel burning. We report ERs and EFs for (in order of abundance) CO_2, CO, CH_4, CH_3COOH, CH_3OH, HCHO, C_2H_4, NH_3, C_2H_2, NO, C_2H_6, C_6H_5OH, C_3H_6, HCOOH, NO_2, $HOCH_2CHO$, and C_4H_4O. Compared to previous work, our emissions of organic acids and ammonia are much larger. Another significant finding is that reactive oxygenated organic compounds account for 70–80% of the total NMOCs. Our data suggest that (for most compounds) the combined emissions from charcoal production and charcoal burning are 3–10 times higher than the emissions from wood fires per unit mass of fuel burned. In addition, the combined emissions from the production and use of charcoal exceed the emissions from wood burning per unit energy released. We compare the annual emissions from biofuel use and savanna fires in Zambia. For many compounds (e.g., CH_4, C_2H_2, CH_3COOH,

CH_3OH, HCHO, and NH_3), the biofuel production significantly exceeds that due to savanna fires. In summary, biofuel emissions are an important and growing influence on the tropical troposphere that should be studied further in atmospheric models.

[39] **Acknowledgments.** This research was supported by funds provided by the National Science Foundation under grant ATM-9900494, the Interagency Joint Fire Science Program, and the Rocky Mountain Research Station, Forest Service, U.S. Department of Agriculture (INT-97082-RJVA and RMRS-99508-RJVA). The authors thank Rachel Mayers (deceased), Sidney Ilukena, Freddy Mubita, Alick Rabanda, and the chief and residents of Milumbwa who provided assistance in our measurements and useful information about traditional cooking and charcoal-making methods. We thank Mike King, Bob Swap, Harold Annegarn, Tim Suttles, NASA, and SAFARI 2000 for planning and logistical support. We thank J. Ludwig et al. for an advance copy of their manuscript.

References

Andreae, M. O., and P. Merlet, Emission of trace gases and aerosols from biomass burning, *Global Biogeochem. Cycles*, *15*, 955–966, 2001.

Antal, M. J., Jr., S. G. Allen, X. Dai, B. Shimizu, M. S. Tam, and M. Gronli, Attainment of the theoretical yield of carbon from biomass, *Ind. Eng. Chem. Res.*, *39*, 4024–4031, 2000.

Bertschi, I., R. J. Yokelson, J. G. Goode, D. E. Ward, R. A. Susott, R. E. Babbitt, and W. M. Hao, Trace gas and particle emissions from fires in large-diameter and belowground biomass fuels, *J. Geophys. Res.*, *108*, doi:10.1029/2002JD002100, in press, 2003.

Brocard, D., and J. P. Lacaux, Domestic biomass combustion and associated atmospheric emissions in West Africa, *Global Biogeochem. Cycles*, *12*, 127–139, 1998.

Brocard, D., C. Lacaux, J. P. Lacaux, G. Kouadio, and V. Yoboué, Emissions from the combustion of biofuels in western Africa, in *Biomass Burning and Global Change*, edited by J. S. Levine, pp. 350–360, MIT Press, Cambridge, Mass., 1996.

Chidumayo, E. M., Inventory of wood used in charcoal production in Zambia, Final Report to Kate Newman, 48 pp., Biodiversity Support Program, World Wildlife Fund, Washington, D. C., 1994.

Cofer, W. R., III, V. G. Collins, and R. W. Talbot, Improved aqueous scrubber for collection of soluble atmospheric trace gases, *Environ. Sci. Technol.*, *19*, 557–560, 1985.

Cofer, W. R., III, J. S. Levine, E. L. Winstead, D. R. Cahoon, D. I. Sebacher, J. P. Pinto, and B. J. Stocks, Source compositions of trace gases released during African savanna fires, *J. Geophys. Res.*, *101*, 23,597–23,602, 1996.

Crutzen, P. J., and M. O. Andreae, Biomass burning in the tropics: Impact on atmospheric chemistry and biogeochemical cycles, *Science*, *250*, 1669–1678, 1990.

Delany, A. C., P. Haagensen, S. Walters, A. F. Wartburg, and P. J. Crutzen, Photochemically produced ozone in the emission from large-scale tropical vegetation fires, *J. Geophys. Res.*, *91*, 2425–2429, 1985.

Dumont, H., and M. Gelus, *La valorization chimique du bois*, pp. 4–49, Masson, Paris, France, 1982.

Food and Agriculture Organization (FAO), Technologies for charcoal making, FAO For. Pap. 63, Food and Agric. Organ. of the U. N., For. Ind. Div., Rome, 1985.

Food and Agriculture Organization (FAO), The role of wood energy in Africa, FAO Working Pap. FOPW/99/3, Food and Agric. Organ. of the U. N., For. Dept., Rome, Italy, 1999.

Fishman, J., K. Fakhruzzaman, B. Cros, and D. Nganga, Identification of widespread pollution in the Southern Hemisphere deduced from satellite analysis, *Science*, *252*, 1693–1696, 1991.

Goode, J. G., R. J. Yokelson, R. A. Susott, and D. E. Ward, Trace gas emissions from laboratory biomass fires measured by Fourier transform infrared spectroscopy: Fires in grass and surface fuels, *J. Geophys. Res.*, *104*, 21,237–21,245, 1999.

Goode, J. G., R. J. Yokelson, D. E. Ward, R. A. Susott, R. E. Babbitt, M. A. Davies, and W. M. Hao, Measurements of excess O_3, CO_2, CO, CH_4, C_2H_4, C_2H_2, HCN, NO, NH_3, HCOOH, CH_3OOH, HCHO, and CH_3OH, in 1997 Alaskan biomass burning plumes by airborne Fourier transform infrared spectroscopy (AFTIR), *J. Geophys. Res.*, *105*, 22,147–22,166, 2000.

Griffith, D. W. T., Synthetic calibration and quantitative analysis of gas-phase FTIR spectra, *Appl. Spectrosc.*, *50*, 59–70, 1996.

Hall, D. O., F. Rosillo-Calle, and J. Woods, Biomass utilization in households and industry: Energy use and development, *Chemosphere*, *29*, 1099–1119, 1994.

Hao, W. M., and M. H. Liu, Spatial and temporal distribution of tropical biomass burning, *Global Biogeochem. Cycles*, *8*, 495–503, 1994.

Hao, W. M., and D. E. Ward, Methane production from global biomass burning, *J. Geophys. Res.*, *98*, 20,657–20,661, 1993.

Holzinger, R., C. Warneke, A. Hansel, A. Jordan, W. Lindinger, D. H. Scharffe, G. Schade, and P. J. Crutzen, Biomass burning as a source of formaldehyde, acetaldehyde, methanol, acetone, acetonitrile, and hydrogen cyanide, *Geophys. Res. Lett.*, *26*, 1161–1164, 1999.

Ishengoma, R. C., P. R. Gillah, A. S. Majaliw, and R. V. Rao, The quality of charcoal produced from *Leucanea leucocephalia* in earth kilns from Tanzania, *Indian J. For.*, *20*, 265–268, 1997.

Kaoma, J., and G. Kasali, *Efficiency and Emission Characteristics of Two Zambia Cookstoves Using Charcoal and Coal Briquettes*, 25 pp., Stockholm Environ. Inst., Stockholm, 1994.

Kituyi, E., L. Marufu, S. O. Wandiga, I. O. Jumba, M. O. Andreae, and G. Helas, Carbon monoxide and nitric oxide from biofuel fires in Kenya, *Energy Convers. Manage.*, *42*, 1517–1542, 2001.

Kuhlbusch, T. A., J. M. Lobert, P. J. Crutzen, and P. Warneck, Molecular nitrogen emissions from denitrification during biomass burning, *Nature*, *351*, 135–137, 1991.

Lacaux, J. P., D. Brocard, C. Lacaux, R. Delmas, B. Ajoua, V. Yoboué, and M. Koffi, Traditional charcoal making: An important source of atmospheric pollution in the African tropics, *Atmos. Res.*, *35*, 71–76, 1994.

Ludwig, J., L. T. Marufu, B. Huber, M. O. Andreae, and G. Helas, Domestic combustion of biomass fuels in developing countries: A major source of atmospheric pollutants, *J. Atmos. Chem.*, in press, 2003.

Mason, S. A., R. J. Field, R. J. Yokelson, M. A. Kochivar, M. R. Tinsley, D. E. Ward, and W. M. Hao, Complex effects arising in smoke plume simulations due to inclusion of direct emissions of oxygenated organic species from biomass combustion, *J. Geophys. Res.*, *106*, 12,527–12,539, 2001.

Pennise, D. M., K. R. Smith, J. P. Kithinji, M. E. Rezende, T. J. Raad, J. Zhang, and C. Fan, Emissions of greenhouse gases and other airborne pollutants from charcoal making in Kenya and Brazil, *J. Geophys. Res.*, *106*, 24,143–25,155, 2001.

Shafizadeh, F., K. V. Sarkanen, and D. A. Tillman (eds.), *Thermal Uses and Properties of Carbohydrates and Lignins*, Academic, San Diego, Calif., 1976.

Singh, H. B., M. Kanakidou, P. J. Crutzen, and D. J. Jacob, High concentrations and photochemical fate of oxygenated hydrocarbons in the global troposphere, *Nature*, *378*, 50–54, 1995.

Smith, K. R., D. M. Pennise, P. Khummongkol, V. Chaiwong, K. Ritgeen, J. Zhang, W. Panyathanya, R. A. Rasmussen, and M. A. K. Khalil, Greenhouse gases from small-scale combustion devices in developing countries: Charcoal-making kilns in Thailand, U.S. EPA Rep. EPA-600/R-99-109, Natl. Risk Manage. Res. Lab., Research Triangle Park, N. C., 1999.

Smith, K. R., R. Uma, V. V. N. Kishore, K. Lata, V. Joshi, J. Zhang, R. A. Rasmussen, and M. A. K. Khalil, Greenhouse gases from small-scale combustion devices in developing countries: Household stoves in India, U.S. EPA Rep. EPA-600/R-00-052, Natl. Risk Manage. Res. Lab., Research Triangle Park, N. C., 2000.

Susott, R. A., G. J. Olbu, S. P. Baker, D. E. Ward, J. B. Kauffman, and R. Shea, Carbon, hydrogen, nitrogen, and thermogravimetric analysis of tropical ecosystem biomass, in *Biomass Burning and Global Change*, edited by J. S. Levine, pp. 249–259, MIT Press, Cambridge, Mass., 1996.

The World Factbook, 2001. (Available at http://www.cia.gov/cia/publications/factbook/).

United Nations Statistics Division, 2000. (Available as http://www.un.org/Depts/unsd/social/hum-set.html).

Ward, D. E., and L. F. Radke, Emissions measurements from vegetation fires: A comparative evaluation of methods and results, in *Fire in the Environment: The Ecological, Atmospheric and Climatic Importance of Vegetation Fires*, edited by P. J. Crutzen and J. G. Goldammer, pp. 53–76, John Wiley, New York, 1993.

Worden, H., R. Beer, and C. P. Rinsland, Airborne infrared spectroscopy of 1994 western wildfires, *J. Geophys. Res.*, *102*, 1287–1299, 1997.

Yokelson, R. J., and I. T. Bertschi, Vibrational spectroscopy in the study of fires, in *Handbook of Vibrational Spectroscopy*, vol. 4, edited by J. M. Chalmers and P. R. Griffiths, pp. 2879–2886, John Wiley, New York, 2002.

Yokelson, R. J., D. W. T. Griffith, and D. E. Ward, Open-path Fourier transform infrared studies of large-scale laboratory biomass fires, *J. Geophys Res.*, *101*, 21,067–21,080, 1996.

Yokelson, R. J., R. Susott, D. E. Ward, J. Reardon, and D. W. T. Griffith, Emissions from smoldering combustion of biomass measured by open-path Fourier transform infrared spectroscopy, *J. Geophys. Res.*, *102*, 18,865–18,877, 1997.

Yokelson, R. J., J. G. Goode, D. E. Ward, R. A. Susott, R. E. Babbitt, D. D. Wade, I. Bertschi, D. W. T. Griffith, and W. M. Hao, Emissions of formaldehyde, acetic acid, methanol, and other trace gases from biomass fires in North Carolina measured by airborne Fourier transform infrared spectroscopy, *J. Geophys. Res.*, *104*, 30,109–30,125, 1999.

Yokelson, R. J., I. Bertschi, T. C. Christian, P. V. Hobbs, D. E. Ward, and W. M. Hao, Trace gas measurements in nascent, aged, and cloud-processed smoke from African savanna fires by airborne Fourier transform infrared spectroscopy (AFTIR), *J. Geophys. Res.*, *108*, doi:10.1029/2002JD002322, in press, 2003.

Zhu, S., D. Tomberlin, and J. Buongiorno, Global forest products consumption, production, trade and prices: Global forest products model projections to 2010, Food and Agric. Organ. (FAO) Working Pap. GFPOS/WP/01, For. Plann. and Policy Div., Rome, 1998.

I. T. Bertschi, Interdisciplinary Arts and Sciences, University of Washington-Bothell, Bothell, WA, USA.

T. J. Christian and R. J. Yokelson, Department of Chemistry, University of Montana, Missoula, MT, USA. (byok@selway.umt.edu)

W. M. Hao, Fire Science Laboratory, U.S. Department of Agriculture (USDA) Forest Service, Missoula, MT, USA.

D. E. Ward, Enviropyronics, LLC, White Salmon, WA, USA.

JOURNAL OF GEOPHYSICAL RESEARCH, VOL. 108, NO. D13, 8478, doi:10.1029/2002JD002322, 2003

Trace gas measurements in nascent, aged, and cloud-processed smoke from African savanna fires by airborne Fourier transform infrared spectroscopy (AFTIR)

Robert J. Yokelson,[1] Isaac T. Bertschi,[1,2] Ted J. Christian,[1] Peter V. Hobbs,[3] Darold E. Ward,[4,5] and Wei Min Hao[4]

Received 15 March 2002; revised 18 July 2002; accepted ~~16 December~~ 30 August 2002; published ~~16 July~~ 26 Feb 2003.

[1] We measured stable and reactive trace gases with an airborne Fourier transform infrared spectrometer (AFTIR) on the University of Washington Convair-580 research aircraft in August/September 2000 during the SAFARI 2000 dry season campaign in Southern Africa. The measurements included vertical profiles of CO_2, CO, H_2O, and CH_4 up to 5.5 km on six occasions above instrumented ground sites and below the TERRA satellite and ER-2 high-flying research aircraft. We also measured the trace gas emissions from 10 African savanna fires. Five of these fires featured extensive ground-based fuel characterization, and two were in the humid savanna ecosystem that accounts for most African biomass burning. The major constituents that we detected in nascent smoke were (in order of excess molar abundance) H_2O, CO_2, CO, CH_4, NO_2, NO, C_2H_4, CH_3COOH, HCHO, CH_3OH, HCN, NH_3, HCOOH, and C_2H_2. These are the first quantitative measurements of the initial emissions of oxygenated volatile organic compounds (OVOC), NH_3, and HCN from African savanna fires. On average, we measured 5.3 g/kg of OVOC and 3.6 g/kg of hydrocarbons (including CH_4) in the initial emissions from the fires. Thus, the OVOC will have profound, largely unexplored effects on tropical tropospheric chemistry. The HCN emission factor was only weakly dependent on fire type; the average value (0.53 g/kg) is about 20 times that of a previous recommendation. HCN may be useful as a tracer for savanna fires. $\Delta O_3/\Delta CO$ and $\Delta CH_3COOH/\Delta CO$ increased to as much as 9% in <1 h of photochemical processing downwind of fires. Direct measurements showed that cloud processing of smoke greatly reduced CH_3OH, NH_3, CH_3COOH, SO_2, and NO_2 levels, but significantly increased HCHO and NO. *INDEX TERMS:* 0320 Atmospheric Composition and Structure: Cloud physics and chemistry; 0345 Atmospheric Composition and Structure: Pollution—urban and regional (0305); 0368 Atmospheric Composition and Structure: Troposphere—constituent transport and chemistry; 0365 Atmospheric Composition and Structure: Troposphere—composition and chemistry; 0394 Atmospheric Composition and Structure: Instruments and techniques; *KEYWORDS:* biomass burning, savanna fires, oxygenated organic compounds, cloud chemistry, photochemistry, HCN

Citation: Yokelson, R. J., I. T. Bertschi, T. J. Christian, P. V. Hobbs, D. E. Ward, and W. M. Hao, Trace gas measurements in nascent, aged, and cloud-processed smoke from African savanna fires by airborne Fourier transform infrared spectroscopy (AFTIR), *J. Geophys. Res.*, *108*(D13), 8478, doi:10.1029/2002JD002322, 2003.

1. Introduction

[2] Biomass burning is a major source of trace gases for the global atmosphere [*Crutzen and Andreae*, 1990]. Savanna fires, occurring mostly in Africa, are the single largest type of biomass burning globally with domestic biofuel use second [*Andreae and Merlet*, 2001]. African savanna fires have been the focus of several major research campaigns including: FOS/DECAFE [*Lacaux et al.*, 1995], TRACE A [*Fishman et al.*, 1996], and SAFARI 92 [*Lindesay et al.*, 1996]. *Andreae* [1997] and *Andreae and Merlet* [2001] reviewed emissions measurements from these campaigns. In summary, previous work carried out mostly in southern Africa included: (1) Measurements of biomass consumption by fires in several savanna types ranging from "dry" savannas with "low" fire frequency (3–10 years) [*Trollope et al.*, 1996; *Stocks et al.*, 1996; *Shea et al.*, 1996] to "humid" savannas with high fire frequency (1–2 years) [*Shea et al.*, 1996; *Ward et al.*, 1996; *Hoffa et al.*, 1999].

[1]Department of Chemistry, University of Montana, Missoula, Montana, USA.
[2]Now at Interdisciplinary Arts and Sciences, University of Washington-Bothell, Bothell, Washington, USA.
[3]Department of Atmospheric Sciences, University of Washington, Seattle, Washington, USA.
[4]Fire Sciences Laboratory, USDA Forest Service, Missoula, Montana, USA.
[5]Now at Enviropyronics, LLC, White Salmon, Washington, USA.

Copyright 2003 by the American Geophysical Union.
0148-0227/03/2002JD002322$09.00

(Humid savannas have 700–1400 mm/yr of markedly seasonal rainfall and faster fuel buildup than dry savannas.) (2) Ground-based measurements of the initial emissions of CO_2, CO, and hydrocarbons [*Hao et al.*, 1996] and of CO_2, CO, and NO_x [*Lacaux et al.*, 1996] from fires in both humid and dry savannas. (3) Airborne measurements of the initial emissions from a "dry" savanna fire for CO_2, CO, CH_4, H_2, N_2O, and total nonmethane hydrocarbons [*Cofer et al.*, 1996] and CO_2, CO, NO_x, methyl halides, and some organic species [*Andreae et al.*, 1996]. (4) Measurements of haze layers and long range transport/photochemistry over southern Africa and the South Atlantic [*Swap et al.*, 1996; *Browell et al.*, 1996; *Talbot et al.*, 1996; *Singh et al.*, 1996] and interpretation of these measurements with models [*Jacob et al.*, 1996; *Thompson et al.*, 1996; *Chatfield et al.*, 1996; *Mauzerall et al.*, 1998]. A similar suite of savanna fires emissions was measured in West Africa in FOS/DECAFE [*Lacaux et al.*, 1995].

[3] Despite these accomplishments, many critically important gaps remained in our knowledge of African savanna fire emissions. For instance, there were no quantitative measurements, on any African fires, of the emissions of oxygenated volatile organic compounds (OVOC; alcohols, acids, aldehydes, etc.), even though OVOC were known to comprise about one-half of the organic emissions from fires in temperate and boreal ecosystems [*Yokelson et al.*, 1996, 1997, 1999; *Worden et al.*, 1997; *Holzinger et al.*, 1999; *Goode et al.*, 1999, 2000] and strongly influence smoke plume chemistry [*Mason et al.*, 2001]. There were almost no data on African fire emissions of important nitrogen-containing species such as HCN and NH_3. Earlier African measurements had focused either on "old" smoke of unknown (and probably mixed) ages in regional haze layers, or on nascent smoke (which we define as smoke $<\sim$5 min old) within a few kilometers of the flames. There was no explicit information on the transition between these two states. Also, most African fire measurements had been made in the dry savannas, forests, and plantations of South Africa rather than the humid savannas located north of 17°S where the vast majority of fires occur [*Justice et al.*, 1996]. Finally, there were very few data on emissions from the production and use of domestic biomass fuels.

[4] To help address these crucial gaps in knowledge, and as part of the Southern Africa Regional Science Initiative (SAFARI 2000: S2K), the University of Montana participated in both ground-based and airborne campaigns during the southern African dry season of 2000. The ground-based campaign focused on the trace gas emissions from the production and use of biofuels [*Bertschi et al.*, 2003a] and the unlofted emissions sometimes produced by prolonged smoldering combustion in wooded savannas [*Bertschi et al.*, 2003b]. In the airborne campaign we measured trace gases, mostly in smoke and haze from savanna fires, with an airborne Fourier transform infrared spetrometer (AFTIR) during 19 flights (>86 hours) between 14 August and 14 September aboard the University of Washington's (UW) Convair-580 research aircraft (UW Convair-580). The complete set of instruments for measuring trace gases and particles aboard the UW Convair-580 is described by *Sinha et al.* [2003a].

[5] In this paper we discuss some of the AFTIR trace gas measurements acquired on the UW Convair-580. In particular: (1) Vertical profiles of CO_2, CO, CH_4, and H_2O below 5.5 km in the regional haze layers that dominate southern Africa during the dry season due mostly to emissions from biomass burning. The profiles were measured above instrumented ground sites in association with overpasses by the NASA TERRA satellite and the ER-2. (2) The first broad characterization of the most abundant trace gases in nascent smoke from African savanna fires (i.e., including oxygen- and nitrogen-containing species). These measurements (which include fires in the humid savanna region) are used to calculate emission factors for savanna fires that can be used for regional emissions estimates. (3) Comparisons of nascent and downwind smoke samples of well-measured age reveal intriguing postemission changes in smoke composition due to photochemistry and cloud processing. This demonstrates the need to measure smoke less than a few moments in age to properly determine the "initial emissions" from fires and the value of measuring older smoke (of known age) to understand plume chemistry and characterize regional impacts. Plume chemistry links measurements in nascent smoke in the laboratory or field [e.g., *Lobert et al.*, 1991; *Hao et al.*, 1996; *Yokelson et al.*, 1996, 1999] with measurements in regional haze layers [e.g., *Talbot et al.*, 1996; *Blake et al.*, 1996].

2. Experimental Details

2.1. Measurement Strategy

[6] The AFTIR system is designed to obtain FTIR spectra of air flowing through, or detained within, a multipass cell inside an aircraft [*Yokelson et al.*, 1999; *Goode et al.*, 2000]. On the UW Convair-580, outside air samples were forced by ram pressure into a forward-facing inlet (25 mm internal diameter (i.d.)) with an opening 22 cm from the outer skin of the aircraft cabin roof. The air flowed next through 10 m of 25 mm i.d. Teflon bellows; a 16 liter, Pyrex, multipass cell; and ~5 m of 25 mm i.d. tubing to a rear-facing outlet. Fast-acting valves (19 mm i.d.) on the inlet and outlet lines of the cell were used to temporarily trap the cell contents for signal averaging at desired times. In addition, closing the inlet and outlet valves reduced the noise in the 900–1100 cm^{-1} region of the AFTIR spectrum providing lower detection limits for many species [*Yokelson et al.*, 1999]. At the aircraft research speed (80 m/s) the flow rate through the system was ~100 l/min. The $1/e$ decay time for a signal when exchanging the cell contents was 4–5 s, indicating a faster flow in the center of the cell where most of the optical path is located. The residence time in the exterior inlet tubing was only ~2.5 ms. We further guarded against sampling artifacts by coating all the metal surfaces in the system with a nonreactive halocarbon wax [*Webster et al.*, 1994]. Recent tests in our laboratory showed that this wax imparts Teflon-like properties to metal surfaces [*Yokelson and Bertschi*, 2002].

[7] Infrared spectra of the cell contents were acquired continuously (every 0.83 s) throughout most of each flight and the flow-control valves were normally open, which flushed the cell with ambient air. To temporarily trap smoke plume "grab" samples we flew into the smoke plume and then closed the valves when the cell was well flushed with smoke. The valves remained closed for 1–3 min while several hundred spectra of the detained smoke sample were

acquired. The valves were then opened, which flushed the cell. Background grab samples were trapped at the same altitude just outside the plume and processed in the same way. We usually flushed the cell for one to many minutes before closing the valves for a smoke or background air sample. The low-noise spectra, acquired with the valves closed, were later averaged together (by sample) to further improve the signal-to-noise ratio.

[8] To measure initial emissions from a fire, we sampled smoke less than several minutes old by penetrating the rapidly rising column of smoke just above the flame front. "Aged" smoke samples were acquired within the plumes up to 30 km downwind. The age of downwind samples was computed from GPS and wind speed measurements. Vertical profiles of trace gases in regional haze layers, and in the free troposphere, were obtained by continuous sampling during rapid ascent/descent, or from a series of detained samples obtained during the horizontal legs of a "ladder" type flight profile.

2.2. Instrumental Details

[9] A detailed description of AFTIR and a schematic were given by *Yokelson et al.* [1999]. A brief, updated description follows. The system consisted of an infrared spectrometer (MIDAC, Inc.; resolution 0.5 cm^{-1}), a White cell (IR Analysis, Inc.), and optical components comounted on an aluminum, optical table (Newport, Inc.; 28 × 175 × 11 cm) that was shock mounted (Aeroflex, Inc) to the floor of the aircraft. The infrared beam exiting the spectrometer was directed by transfer optics to the "tripled" White cell. The beam made 120 passes of the 0.81 m basepath cell for a total path length of 97.5 m. After exiting the cell, the infrared beam was directed through a 25 mm focal length ZnSe lens onto a LN_2-cooled, MCT detector (Graseby, Inc., model FTIR M-16). Thermocouples were mounted inside each end of the cell and cell pressure was measured by a capacitive transducer (Type 626 MKS, Inc.). Pressure and temperature were stored at 1 Hz on the notebook computer that controlled and logged the AFTIR spectra. The total system weight was 133 kg.

2.3. Mixing Ratio Retrievals: Precision and Accuracy

[10] During S2K we recorded spectra of 264 "grab samples." Fifty-six samples were of biomass burning plumes, 5 of ship plumes [*Sinha et al.*, 2003b], and 203 of background air adjacent to plumes or in vertical profiles. We quantified the compounds responsible for all the major peaks in these spectra, which accounts for most of the trace gases present above 5–20 ppbv [*Goode et al.*, 1999]. Mixing ratios for H_2O, CO_2, and CH_4 were obtained by fitting sections of the transmission spectra of these samples with synthetic calibration classical least squares (CLS) methods [*Griffith*, 1996; *Yokelson et al.*, 1996, 1997; *Yokelson and Bertschi*, 2002]. The CO mixing ratios were obtained from a deployment-specific, mathematical interpolation based on a large set of pre- and postexperiment calibration spectra that spanned the relevant temperatures, pressures, and mixing ratios. Excess mixing ratios in smoke (ΔX) were assumed to be the mixing ratio of a species "X" in smoke minus the mixing ratio of X in the closest sample of background air. Absorbance spectra of smoke were generated using background-sample spectra collected nearby at the same altitude. Excess mixing ratios in smoke were obtained directly from the smoke-absorbance spectra using synthetic-calibration CLS methods for NO, NO_2, and formaldehyde (HCHO). Excess mixing ratios for H_2O, formic acid (HCOOH), acetic acid (CH_3COOH), ethylene (C_2H_4), acetylene (C_2H_2), hydrogen cyanide (HCN), methanol (CH_3OH), and ozone (O_3) were retrieved from the absorbance spectra by spectral subtraction [*Yokelson et al.*, 1997].

[11] One sample of background air was retained and remeasured 23 and 27 min later to test the precision of the AFTIR mixing ratios. The standard deviation/average was CO_2 (0.11%, 0.46 ppm), CO (0.63%, 0.9 ppb), and CH_4 (0.77%, 14 ppb). The detection limits varied by spectrum depending mostly on the amount of signal averaging or H_2O concentration. For most compounds the detection limit was usually 5–10 ppbv, but for NO_x, formaldehyde, acetic acid, and ozone it was usually closer to 15–20 ppbv. The typical absolute uncertainty in the excess mixing ratios is estimated to be ±5% (1σ), or the detection limit, whichever is larger. The accuracy, as determined by testing with calibration standards, for several molecules was: CO_2, CO and CH_4 (1–2%); NO, NO_2, and CH_3OH (1–5%); and NH_3 (variable as discussed below). The CO values obtained by AFTIR were not significantly different from those obtained on a nearby aircraft using a CMDL flask-sampling system [*McMillan et al.*, 2003].

[12] NH_3 was the only compound affected by brief storage in the cell. The spectra acquired during storage were analyzed at 0.83 s resolution and the NH_3 mixing ratios at the beginning of the storage periods were obtained from the NH_3 decay profiles. Laboratory tests with a wide variety of gases (acetic acid, methanol, NO_x, etc), carried out just before the S2K flights (Yokelson et al., in preparation), showed that AFTIR could have additional, variable losses (0–50%) for NH_3 only, which result from passivation of the Pyrex cell during sample acquisition. The NH_3 losses were negligible when the cell was exposed to the sample for longer times before closing the valves (30 s) or when several smoke samples were taken consecutively. Larger losses occurred when very short "cell exposure times" were used (3–4 s). During S2K we minimized passivation losses by using long cell exposure times and sometimes acquiring consecutive smoke samples. We estimate that the NH_3 values reported here are 5–20% low on the average.

3. Results and Discussion

3.1. Typical Trace Gas Profiles for the Southern African Dry Season Troposphere

[13] To provide a context for this study, we describe a few typical trace gas profiles up to 5.5 km during S2K. (The location of many vertical profiles is given by *Sinha et al.* [2003a] and one profile is discussed by *McMillan et al.* [2003].) Most of southern Africa was dominated during the dry season of 2000 by a well-mixed haze layer that extended to 3–6 km in altitude and contained aged emissions from savanna fires, cooking fires, vegetation and industry. This layer was characterized by low visibility and high levels of O_3 (30–100 ppbv), CO (200–650 ppbv), and water (<10,000 ppm). At the top of the haze layer there was usually a transition (~0.2 km thick) to the free tropo-

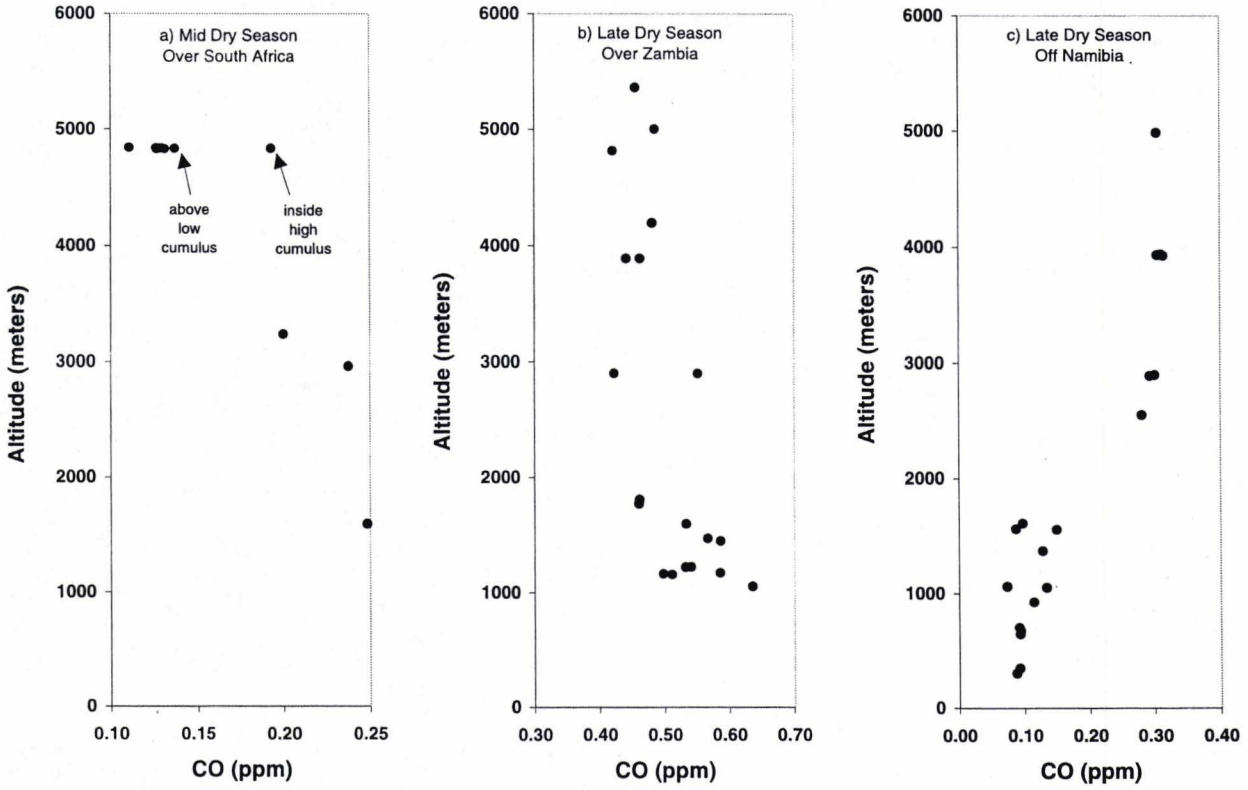

Figure 1. Examples of CO mixing ratios measured with AFTIR well away from distinct smoke plumes. a) 23 August 2000 (mid dry season) over Pietersburg, South Africa, well south of most fire activity. A well-mixed haze layer extended to ~3.5 km with much cleaner, drier air above. The data points obtained above or within nonprecipitating cumulus show mixing of the layers by cloud-related convection. b) Above the airport in Mongu, Zambia on 6 September 2000 (late dry season) in the humid savanna region where most fires occur. The CO values are much greater and show that the haze layer extended to above 5.5 km. c) Over the South Atlantic Ocean off Namibia on 13 September 2000 (late dry season) showing the continental outflow above 2.4 km. The profile is inverted when compared to the situation in a) and the O_3 was 40 ppbv higher in the outflow layer than in the clean, maritime layer. Multiple values at the same altitude are from samples at different times and/or locations.

sphere, which had much lower levels of CO (<120 ppb) and H_2O (<500 ppm). Especially in the humid savanna region it was common to observe many small fires burning within a 10–20 km radius. Very few savanna fire plumes penetrated the top of the well-mixed haze layer. Thus, as the nascent smoke from fires aged it was diluted by the background haze and it faded into the haze layer within 10–30 km downwind of the fire. The vertical profiles away from distinct plumes can be classified into the three categories illustrated in Figure 1.

[14] Figure 1a shows a few AFTIR, CO mixing ratios obtained on 23 August (UW Flight 1821) over Pietersburg, South Africa that reflect a typical vertical profile over South Africa (which is well south of most of the fire activity) during the mid dry season. In these profiles, the well-mixed layer extended to ~3.5–3.7 km and it was topped by much cleaner, drier air. In some cases, a shallow clean layer was found near this altitude sandwiched between layers of dirty air [*Hobbs*, 2003]. The sparse data from flight 1821 are shown here, because they also demonstrate some interesting effects of cumulus convection. During a level flight leg in the clean, dry free troposphere at ~4.8 km we encountered strongly elevated water vapor and modestly elevated CO above nonprecipitating cumulus clouds (as indicated). Other effects measured above these clouds, by UW instruments, were increased upwelling uv and decreased O_3. As also shown in Figure 1a, when we penetrated the interior of a taller cumulus cloud at 4.8 km, both CO and $H_2O_{(g)}$ increased to values measured in the haze layer ~2 km below. These observations show that convection in non-precipitating cumulus can enhance mixing between atmospheric layers. Clouds such as these were common during the 2000 dry season and did not produce rain that could have diminished biomass burning. Thus, convection could be an important regional mechanism for the long-range transport of smoke that would otherwise be confined to the well-mixed layer [*Hobbs*, 2003]. However, as discussed in section 3.3.2, even a brief residence time in clouds can cause large changes in the chemical composition of smoke. Thus, it is important to know the amount of African smoke that is both elevated and modified by passage through a "cloud gateway." Cloud effects on smoke may be even more important in Brazil and Southeast Asia where dry season clouds are more common [*Reid et al.*, 1998].

[15] A second type of vertical profile is illustrated by the AFTIR CO mixing ratios obtained over Mongu, Zambia on 6 September (UW Flight 1832, Figure 1b). This type of profile was commonly observed in the final third of the 2000 dry season over or near the humid savanna, which featured much more intense biomass burning. As a result the CO mixing ratios were much higher and the mixed haze layer extended to a much greater altitude. On this particular day, the Cloud Physics Lidar onboard the ER-2 indicated that the haze layer extended to ~6 km [*Schmid et al.*, 2003]. This deeper, more concentrated haze covered vast regions of southern Africa north of 20°S. Satellite images of the distribution of African fires suggest that such haze might have extended as far north as the equator [*Cahoon et al.*, 1992].

[16] Finally, in Figure 1c, we show the AFTIR CO profile obtained off the Namibia coast on 13 September (UW Flight 1837). Clean marine air with low CO was found near the surface and high CO was observed above ~2.4 km. Backward trajectories indicate that the lower, clean air was transported from much further south over the Atlantic, and that the upper-level haze was continental outflow that had passed through the active burning region 2–4 days previously (HYSPLIT4 (Hybrid Single-Particle Lagrangian Integrated Trajectory) Model, 1997. Web address: http://www.arl.noaa.gov/ready/hysplit4.html, NOAA Air Resources Laboratory, Silver Spring, MD). There was a sharp increase of 40 ppbv in the AFTIR ozone on entering the continental outflow from below, probably due to photochemical processing of fire emissions. Photochemistry in this aged haze layer may be enhanced because it is often located above a layer of reflective, low elevation marine clouds. The continental outflow (studied in SAFARI 92 and TRACE A) is another avenue for transport/processing of biomass burning emissions in addition to clouds.

3.2. Major Trace Gases Emitted by African Savanna Fires

3.2.1. Fire Descriptions

[17] We describe key features of the 10 savanna fires sampled in this study. We sampled three fires of opportunity in grassland, with some brush and small trees, in southern Kruger National Park near Skukuza, South Africa during UW Flights 1815 and 1822. We sampled two other fires of opportunity on UW Flight 1825. One was in a coastal lowland, open forest with a grass/brush understory, located ~100 km south of Beira, Mozambique. We also obtained a single, high elevation sample of a 3.4 km tall, vertical smoke column above the Lebombo Mountains of Mozambique. This smoke may have been processed by a capping cumulus cloud that dissipated before our arrival. We do not know the fuel type for this fire. The other five fires were planned burns and the airborne sampling was carried out in close coordination with ground-based teams. Two large prescribed fires were sampled in the Madikwe Game Reserve in the Limpopo River valley (UW Flights 1816 and 1819). These fires burned in nearly pure grassland with only a few scattered small bushes. The first of these fires produced a 3.4 km tall, vertical smoke column with a large capping cumulus cloud that allowed sampling of cloud-processed smoke. We sampled a large (1000 ha) prescribed fire in the Timbavati Game Reserve (adjacent to Kruger National Park) on 7 September (UW flight 1834). During this fire we carried out extensive downwind sampling [*Hobbs et al.*, 2003]. The fuel consumption and fire behavior for the prescribed burns at Madikwe and Timbavati were measured by T. Landmann personal communication, 2002).

[18] We also sampled two planned fires in the humid savannas of Zambia. Both fires were burned in the traditional manner by local crews. The fuel consumption and fire behavior were measured by J. Pereira (personal communication, 2002). The first of these fires was in miombo woodland (1 September, UW Flight 1826). Miombo woodland can be classified as humid (wooded) savanna or tropical dry forest. Central Africa has 2.8 million km^2 of miombo, which comprises the largest contiguous ecosystem of this type on Earth [*Desanker et al.*, 1997]. The miombo understory (mostly grass and leaf litter) burns about every two years [*Shea et al.*, 1996; *Desanker et al.*, 1997] and this likely accounts for more biomass burning than any other single ecosystem on Earth [*Desanker et al.*, 1997]. The miombo covers much of central Africa (~80% of Zambia is miombo [*Hoffa et al.*, 1999]) and fires in the miombo account for the great majority of sub-Sahelian fires [*Justice et al.*, 1996; *Desanker et al.*, 1997]. Therefore, this planned fire likely represents the most common type of African savanna fire. The other planned fire in Zambia (5 September, UW Flight 1831) was in a dambo. Dambos are seasonally flooded grasslands that are the major enclaves in the miombo. Most dambos burn annually [*Hoffa et al.*, 1999], which accounts for a large fraction of African fires.

3.2.2. Excess Mixing Ratios Measured in Biomass Burning Plumes

[19] Most gases (exceptions include N_2, H_2, and some sulfur compounds [*Goode et al.*, 1999]) can be detected by FTIR when they are present at mixing ratios >5–20 ppbv. In the AFTIR smoke spectra acquired in this study all the major features were due to H_2O, O_3, CO_2, CO, CH_4, C_2H_4, C_2H_2, HCHO, CH_3OH, HCOOH, CH_3COOH, NO, NO_2, NH_3, and HCN. Thus, these compounds are 15 of the most abundant compounds in smoke. In Table 1 we show the excess mixing ratios obtained in samples of distinct biomass-burning plumes along with fire name, UW flight number, date, and the UTC time (local time = UTC + 2 hr), longitude, latitude, and altitude of the sample. Each sample has a brief descriptive comment, which indicates when samples were obtained downwind from the source or had undergone cloud processing. In some of the more dilute samples the excess mixing ratios of some compounds were "reasonable," but below our estimated detection limit of 5 ppbv so they were omitted from Table 1. Note also the much higher levels of CO encountered in nascent plumes (up to ~11 ppm) than in the background haze (Figure 1).

3.2.3. Estimation of Fire-Average, Initial Emission Ratios

[20] We estimated fire-average, initial emission ratios (ER) between compounds from the slope of the least squares line, with the intercept forced to zero, in a plot of one set of excess mixing ratios versus another [*Yokelson et al.* 1999]. We omitted any samples that were affected by photochemistry or cloud processing from our emission ratio plots to determine initial emission ratios. Two examples of these plots are shown in Figure 2. Omitting the excess mixing ratios below 5 ppb reduced the correlation coeffi-

Table 1. Sample Type, Location, Time, and Excess Mixing Ratios (>0.005 ppm) for AFTIR Measurements in African Biomass Burning Plumes During SAFARI 2000

Sample Description	Altitude, masl	Latitude, °	Longitude, °	Time, UTC	CO_2, Δppmv	CO, Δppmv	CH_4, Δppmv	O_3, Δppmv	C_2H_4, Δppmv	C_2H_2, Δppmv	HCHO, Δppmv	CH_3OH, Δppmv	HAc,[a] Δppmv	HCO_2H, Δppmv	NH_3, Δppmv	NO, Δppmv	NO_2, Δppmv	HCN, Δppmv
Excess Mixing Ratios for the Compounds Detected in Smoke Directly Above Two Fires Near Skukuza (SA) (17 August 2000; UW Flight 1815)																		
Smoldering fire no. 1	1255	−25.463	31.604	0944:27	0.6	0.031			0.006					0.016				
Repeat	865	−25.454	31.567	0953:57	11.1	0.569	0.049		0.014		0.013	0.010	0.006				0.020	0.007
Repeat	884	−25.454	31.576	1002:11	8.9	0.612	0.058		0.015		0.014	0.012	0.019	0.006	0.031		0.022	
"Dark brown" haze	2036	−25.279	31.394	1040:02	11.1	0.100	0.023											
Repeat	2057	−25.298	31.380	1046:47	7.6	0.089												
Flaming fire no. 2	1124	−24.466	31.830	1104:48	60.3	8.892	0.527	−0.023	0.159	0.021	0.131	0.137	0.192	0.020	0.048	0.032	0.124	0.070
Repeat	1160	−24.468	31.839	1109:10	163.1	11.510	0.688	−0.034	0.228	0.044	0.200	0.159	0.204	0.024	0.104	0.158	0.248	0.118
Repeat	1084	−24.457	31.837	1126:13	67.8	4.940	0.279	−0.030	0.099	0.018	0.053	0.066	0.096	0.010	0.031	0.055	0.133	0.048
Excess Mixing Ratios for the Compounds Detected in Smoke Directly Above the Fire and in Cloud-Processed Smoke at Madikwe (SA) (18 August 2000; UW Flight 1816)																		
Nascent smoke	1084	−24.695	26.445	0915:00	34.4	5.917	0.417		0.084	0.015	0.054	0.101	0.094	0.042	0.053	0.024	0.097	0.040
Repeat	1129	−24.659	26.431	0920:26	80.0	3.364	0.196	−0.037	0.062	0.015	0.048	0.053	0.042	0.038		0.120	0.138	0.041
Repeat	1163	−24.652	26.447	0932:58	16.8	1.059	0.123	−0.022	0.009			0.016	0.012	0.012		0.037	0.033	
Weak sample	1692	−24.838	26.327	0955:52	6.2	0.029	0.016											
Nascent smoke below cumulus	1945	−24.620	26.300	1222:46	92.5	5.043	0.136	−0.073	0.071	0.027	0.102	0.068	0.102	0.018	0.054	0.185	0.191	0.064
Cloud-processed smoke	3866	−24.669	26.301	1234:07	41.4	2.663	0.071		0.047	0.005	0.059	0.015	0.050	0.014		0.122	0.086	0.046
More intense cloud processing	4166	−24.597	26.359	1239:12	35.1	2.215	0.095		0.036		0.076		0.022	0.011		0.121	0.058	0.039
Excess Mixing Ratios for the Compounds Detected in Smoke Directly Above the Fire at Madikwe (SA) (20 August 2000; UW Flight 1819)																		
Near plume base	1373	−24.788	26.264	1302:17	61.8	2.394	0.130		0.036	0.019	0.043	0.037	0.036	0.021		0.040	0.078	0.034
Repeat	1363	−24.785	26.270	1302:29	22.0	1.060	0.080	−0.020	0.016		0.042	0.021		0.008		0.037	0.053	0.015
Repeat	1390	−24.713	26.192	1310:41	54.1	2.964	0.115	−0.063	0.063	0.014	0.071	0.042	0.057	0.024		0.054	0.160	0.044
Repeat	1616	−24.675	26.322	1327:10	104.6	4.557	0.202	−0.061	0.097	0.023	0.103	0.066	0.070	0.044		0.113	0.228	0.058
Repeat	1340	−24.737	26.295	1352:01	34.8	2.374	0.101		0.046	0.012	0.050	0.038	0.049	0.015	0.029	0.021	0.108	0.025
Excess Mixing Ratios for the Compounds Detected in Smoke Directly Above the Fire Near Skukuza (SA) (29 August 2000; UW Flight 1824)																		
Nascent smoke	712	−25.133	31.401	1412:55	27.4	2.032	0.143		0.033	0.010	0.014	0.039	0.042	0.006		0.028	0.070	0.006
Repeat	761	−25.145	31.401	1420:47	69.7	5.042	0.355		0.078	0.021	0.055	0.103	0.082	0.029	0.016	0.080	0.128	0.032
Excess Mixing Ratios for the Compounds Detected in Smoke Directly Above and Downwind From a Fire 100 km South of Beira, Mozambique (31 August 2000; UW Flight 1825)																		
Smoke at source	263	−20.972	34.697	1120:03	53.8	4.852	0.296		0.089	0.020	0.069	0.064	0.068	0.028			0.137	0.030
Repeat	217	−20.973	34.699	1126:07	60.2	6.734	0.415	−0.016	0.098	0.022	0.076	0.099	0.104	0.021			0.192	0.034
Repeat	213	−20.976	34.701	1134:20	38.6	3.233	0.177		0.043	0.016	0.047	0.034	0.084	0.026			0.138	0.018
19.5 km downwind	176	−21.147	34.668	1144:14	2.1	0.290	0.029	0.021					0.007	0.009			0.036	
19.9 km downwind	200	−21.149	34.646	1200:15	3.9	0.314	0.021	0.017					0.018	0.006				
19.2 km downwind	347	−21.143	34.652	1220:48	2.5	0.348	0.015						0.032	0.011				
26.4 km downwind	332	−21.205	34.628	1223:55	1.3	0.334	0.017	0.028					0.013	0.007				
Excess Mixing Ratios for the Single Sample of a Plume Penetrating the Haze Layer Over the Northern Lebombo Mountains, Mozambique (31 August 2000; UW Flight 1825)																		
Smoke above haze layer	3874	−23.394	31.846	1328:49	38.9	3.286	0.046		0.057		0.081	0.023	0.043	0.036		0.076	0.059	
Excess Mixing Ratios for the Compounds Detected in Smoke Above and Near the Miombo Fire Near Kaoma, Zambia (1 September 2000; UW Flight 1826)																		
Ignition 0856 UTC; first source sample	1340	−14.798	24.487	0857:17	28.5	1.971	0.083	−0.037	0.032	0.007	0.029	0.027	0.045		0.035	0.020	0.070	0.016
Repeat; UW bag 1; Terra overpass	1332	−14.822	24.478	0901:46	43.0	4.929	0.217	−0.062	0.051	0.014	0.052	0.074	0.084	0.018	0.080	0.060	0.097	0.026

Table 1. (continued)

Sample Description	Altitude, masl	Latitude, °	Longitude, °	Time, UTC	CO_2, Δppmv	CO, Δppmv	CH_4, Δppmv	O_3, Δppmv	C_2H_4, Δppmv	C_2H_2, Δppmv	HCHO, Δppmv	CH_3OH, Δppmv	HAc,[a] Δppmv	HCO_2H, Δppmv	NH_3, Δppmv	NO, Δppmv	NO_2, Δppmv	HCN, Δppmv
3rd source sample	1248	−14.814	24.477	0909:04	95.4	5.109	0.164	−0.079	0.062	0.022	0.052	0.062	0.071	0.027	0.028	0.099	0.167	0.033
Repeat; UW bag 2	1330	−14.829	24.482	0919:18	59.6	3.698	0.113	−0.061	0.045	0.015	0.029	0.043	0.031	0.025	0.017	0.056	0.131	0.015
5th source sample; top of plume	1905	−14.817	24.461	0926:36	30.1	1.506	0.044	−0.038	0.026		0.018	0.021	0.036	0.007	0.004		0.060	
8 km downwind, smoke from two fires	1976	−14.822	24.364	0938:49	2.9	0.276	0.015						0.018		0.012			
Excess Mixing Ratios for the Compounds Detected in Smoke Directly Above the Dambo Fire Near Kaoma, Zambia (5 September 2000; UW Flight 1831)																		
Ignition 1149 UTC, sample no. 1	1308	−14.824	24.453	1155:18	50.9	4.222	0.111	−0.021	0.071	0.018	0.026	0.044	0.077	0.031		0.027	0.120	0.021
Sample no. 2	1342	−14.813	24.455	1157:29	81.9	3.593	0.100	−0.048	0.070	0.022	0.068	0.036	0.065	0.037		0.028	0.147	0.021
Sample no. 3	1353	−14.804	24.459	1202:18	194.0	4.489	0.198	−0.100	0.117	0.039	0.028	0.041	0.049	0.038		0.135	0.216	0.061
Sample no. 4	1368	−14.823	24.448	1204:36	308.2	7.673	0.314	−0.100	0.191	0.060	0.112	0.067	0.077	0.068		0.318	0.307	0.097
Sample no. 5, fire almost over	1351	−14.808	24.450	1232:50	18.2	0.741	0.013	−0.028	0.011			0.013		0.010		0.017	0.038	
Excess Mixing Ratios for the Compounds Detected in Smoke Above and Downwind From the Prescribed Fire at Timbavati, South Africa (7 September 2000; UW Flight 1834)																		
Ignition 0801 UTC, TERRA 0828 UTC, ER2 0829 UTC, Source sample no. 1, UW bag no. 1	601	−24.373	31.257	0842:47	79.2	5.738	0.345	−0.052	0.091	0.019	0.109	0.086	0.075	0.033	0.005	0.057	0.137	0.037
Source sample no. 2	837	−24.371	31.240	0846:11	68.6	4.024	0.214	−0.052	0.058	0.014	0.074	0.055	0.058	0.033	0.013	0.052	0.123	0.029
9 km downwind	643	−24.290	31.269	0855:10	19.1	1.776	0.109	0.022	0.021	0.006	0.016	0.028	0.014	0.017			0.051	0.018
Source sample no. 3, UW bag no. 3	1005	−24.358	31.229	0921:26	6.9	0.911	0.080	−0.012	0.012		0.020	0.020	0.023					0.009
16 km downwind	1615	−24.235	31.280	0932:58	13.9	1.042	0.055	0.060	0.031		0.031	0.010	0.030	0.011		0.033		0.008
18 km downwind	1547	−24.215	31.207	0934:22	21.3	1.625	0.117	0.098	0.044		0.037		0.071					0.018
20 km downwind, UW bag no. 4	1570	−24.194	31.213	0939:51	10.1	0.954	0.060	0.086	0.029		0.031	0.007	0.036	0.005				0.011
Source sample no. 4	659	−24.356	31.248	0945:53	15.6	1.592	0.067		0.020		0.025	0.019	0.053	0.006			0.051	
5 km downwind	656	−24.340	31.224	0950:53	3.3	0.459	0.026											
17 km downwind	587	−24.232	31.150	0953:39	8.9	0.629	0.039											
27 km downwind	585	−24.142	31.122	0956:50	6.6	0.485												
24 km downwind	632	−24.177	31.088	1014:42	6.1	0.549	0.033	0.031			0.010		0.027				0.006	
25 km downwind, UW bag no. 5	523	−24.165	31.094	1020:31	6.3	0.644	0.028	0.054			0.010	0.009	0.035					
28 km downwind	605	−24.145	31.077	1036:21	7.1	0.426	0.021	0.019			0.020	0.005	0.032					

masl, meters above sea level.

[a]HAc is an abbreviation for acetic acid.

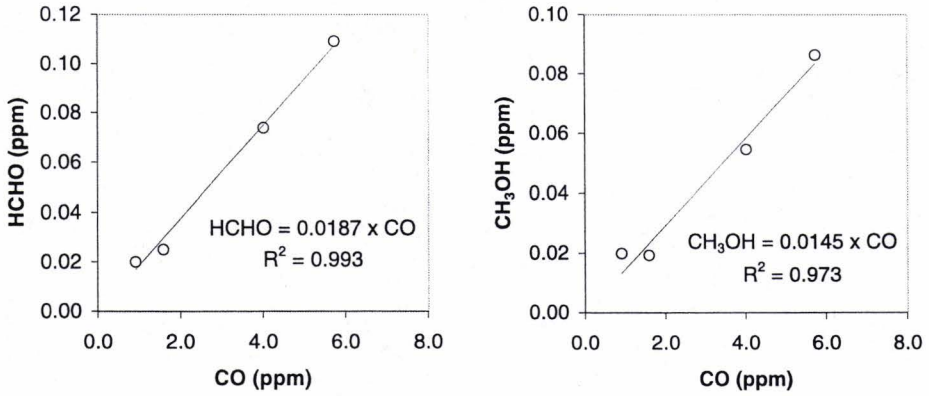

Figure 2. Fire-average, initial emission ratios for each compound are estimated for each fire from the slope of the regression line in a plot of the compound's excess mixing ratios versus the simultaneously measured excess mixing ratios of CO or CO_2. The two examples here (out of >100) show how ΔHCHO/ΔCO and $\Delta CH_3OH/\Delta CO$ were derived for all AFTIR samples obtained in smoke from the Timbavati Fire (UW Flight 1834) that was less than a few minutes old.

cient (R^2) for a few plots, but never affected the slope. We list the emission ratios (as determined from the slopes) for each fire and compound in Table 2. We sampled two fires in similar fuels near Skukuza on flight 1815, which we treated as one fire in the emission ratio plots and in Table 2.

3.2.4. Estimation of Fire-Average, Initial Emission Factors

[21] We estimated fire-average, initial emission factors (EF) for each observed trace gas from our fire-average, initial emission ratios using the carbon mass balance method [*Ward and Radke*, 1993] as described by *Yokelson et al.* [1999]. In brief, we assume that all the volatilized carbon is detected and that the fuel carbon content is known. By ignoring particulate and unmeasured gases we are probably inflating the emission factors by 1–2% [*Andreae and Merlet*, 2001]. We acquired two samples each of dambo grass and miombo litter, which are the major fuel components for humid savanna fires [*Shea et al.*, 1996]. We measured average carbon contents for these fuel types of 47.9 and 53.7%, respectively. Thus we assumed in our EF calculations that all the fires burned in fuels containing 50% carbon by mass. This is in good agreement with previous studies of tropical biomass [*Susott et al.*, 1996], but the actual fuel carbon percentage may vary by ±10% (2σ). We also calculated the fire-average modified combustion efficiency (MCE, $\Delta CO_2/(\Delta CO_2 + \Delta CO)$) for each fire using the fire-average $\Delta CO/\Delta CO_2$ emission ratio and the equation $MCE = 1/((\Delta CO/\Delta CO_2) + 1)$ [*Ward and Radke*, 1993]. MCE is useful as an index of the relative amount of flaming and smoldering combustion throughout a fire. The fire-average, initial emission factors for each compound and fire, along with the fire average MCE, are listed in Table 2. Because NO is mostly converted to NO_2 within minutes of emission (largely due to reaction with O_3 in the entrained background air), we report a single EF for "NO_x as NO." Our EF (and ER) values are also shown by *Sinha et al.* [2003a] to facilitate integration/comparison with EF (and ER) measured by other instruments on the Convair-580 using independent sampling strategies. In Figure 3 we plot the emission factors for each smoldering compound we detected (except CO) versus MCE [*Yokelson et al.*, 1996]. This gives some idea of the natural gradient in emission factors that results from savanna fires burning under a range of vegetative/environmental conditions and, therefore, with different mixtures of flaming and smoldering combustion.

3.2.5. How Well Do Our ER and EF Values Represent African Savanna Fires?

[22] A number of factors suggest that the values shown in Table 2 are representative of African savanna fires in general. For example, the measurements include the humid savanna region, which dominates the total burning and they were made in the middle-late dry season when measured smoke levels in this region peak [*Eck et al.*, 2003]. In addition, we sampled as much of the lifetime of the plumes as possible, especially for the planned fires. Also, when samples from the same fire clearly reflected different relative amounts of flaming and smoldering, they were all included in the emission ratio plots, even if the R^2 of the plot was diminished. (In theory, the separate measurements of mostly flaming and mostly smoldering combustion could also be used to scale the measurements to other scenarios where different MCE are appropriate.)

[23] There are some fundamental limits to what our data can represent. One limitation is due to the timing of S2K. *Hoffa et al.* [1999] found that some early dry season fires in the humid savanna region can burn with lower MCE and thus they may have relatively higher emission factors for smoldering compounds. This suggests that the regression equations in Figure 3 should be used to calculate EF at lower MCE to explicitly estimate emissions from these fires.

[24] Another limitation involves smoke that is produced by a fire, but not entrained into a convection column where it can be sampled by an aircraft. This type of smoke results from "residual smoldering combustion" (RSC) [*Bertschi et al.*, 2003b]. Following Bertschi et al. we can estimate the correction due to RSC for the EF measured from an aircraft using the expression:

$$EF_{actual} = EF_{RSC} * F_{RSC} + EF_{AB} * F_{AB} \quad (1)$$

where EF_{actual} is the true fire-average emission factor, EF_{RSC} the emission factor during RSC, F_{RSC} the fraction of

Table 2. Initial Emission Ratios (ER) and Emission Factors (EF)[a] for Fires Investigated by AFTIR on the UW Convair-580 Aircraft During SAFARI 2000

UW Flight Number Date (2000) Fire Location/Name	1815 17 August Skukuza1, 2	1816 18 August Madikwe1	1819 20 August Madikwe2	1824 29 August Kruger	1825 31 August Beira	1825 31 August Lebombo[b]	1826 1 September Miombo	1831 5 September Dambo	1834 7 September Timbavati	Study Average	1σ	Humid Savanna Average[c]
CO_2 EF	1678	1715	1738	1688	1643	1675	1711	1779	1696	1703	39	1734
CO/CO_2 ER	0.0784	0.0590	0.0460	0.0726	0.0989	0.0845	0.0630	0.0264	0.0692	0.0664	0.0214	0.0508
CO EF	83.7	64.4	50.9	78.0	103.4	90.0	68.6	29.9	74.7	71.5	21.7	55.7
MCE	0.927	0.944	0.956	0.932	0.910	0.922	0.941	0.974	0.935	0.938	0.019	0.952
NO/CO_2 ER	0.0009	0.0019	0.0010	0.0011		0.0020	0.0010	0.0009	0.0008	0.0011	0.0004	0.0010
NO_2/CO_2 ER	0.0016	0.0020	0.0022	0.0019	0.0030	0.0015	0.0020	0.0011	0.0018	0.0020	0.0005	0.0017
NO_x as NO EF	2.86	4.56	3.79	3.45	3.36	3.97	3.50	2.43	3.01	3.37	0.64	3.14
CH_4/CO ER	0.0594	0.0541	0.0483	0.0704	0.0606	0.0141	0.0364	0.0375	0.0583	0.0531	0.0118	0.0368
CH_4 EF	2.84	1.99	1.40	3.14	3.58	0.73	1.43	0.64	2.49	2.19	1.00	1.16
C_2H_4/CO ER	0.0192	0.0151	0.0200	0.0156	0.0155	0.0174	0.0119	0.0231	0.0160	0.0171	0.0033	0.0156
C_2H_4 EF	1.61	0.97	1.02	1.22	1.60	1.57	0.82	0.69	1.19	1.19	0.35	0.77
C_2H_2/CO ER	0.0033	0.0037	0.0054	0.0043	0.0037		0.0037	0.0072	0.0034	0.0043	0.0013	0.0049
C_2H_2 EF	0.26	0.22	0.26	0.31	0.36		0.24	0.20	0.24	0.26	0.05	0.22
HCHO/CO ER	0.0158	0.0139	0.0225	0.0104	0.0126	0.0246	0.0102	0.0122	0.0187	0.0145	0.0043	0.0109
HCHO EF	1.42	0.96	1.23	0.87	1.40	2.37	0.75	0.39	1.50	1.06	0.39	0.63
CH_3OH/CO ER	0.0143	0.0156	0.0148	0.0202	0.0136	0.0071	0.0131	0.0093	0.0145	0.0144	0.0030	0.0118
CH_3OH EF	1.37	1.15	0.86	1.80	1.61		1.03	0.32	1.24	1.17	0.46	0.79
CH_3COOH/CO ER	0.0192	0.0168	0.0169	0.0169	0.0164	0.0132	0.0148	0.0125	0.0146	0.0160	0.0020	0.0140
CH_3COOH EF	3.44	2.32	1.84	2.82	3.64	2.55	2.18	0.80	2.34	2.42	0.90	1.72
HCOOH/CO ER	0.0021	0.0066	0.0087	0.0054	0.0045	0.0108	0.0051	0.0087	0.0064	0.0059	0.0022	0.0063
HCOOH EF	0.29	0.70	0.73	0.69	0.76	1.60	0.57	0.43	0.79	0.62	0.18	0.53
NH_3/CO ER	0.0076	0.0081	0.0122	0.0027			0.0097		0.0016	0.0070	0.0041	0.0065
NH_3 EF	0.39	0.32	0.38	0.13			0.40		0.07	0.28	0.14	0.27
HCN/CO ER	0.0094	0.0108	0.0131	0.0059	0.0055		0.0056	0.0108	0.0072	0.0085	0.0029	0.0073
HCN EF	0.76	0.67	0.64	0.44	0.55		0.37	0.31	0.52	0.53	0.15	0.35

[a]Emission factors are expressed as g/kg.

[b]Since for this fire, the vegetation is unknown, CH_4 is unreliable, and the NO_x and oxygenated compounds were influenced by cloud processing, the data for these compounds from this fire are not included in the study-average values.

[c]See section 3.2.6.

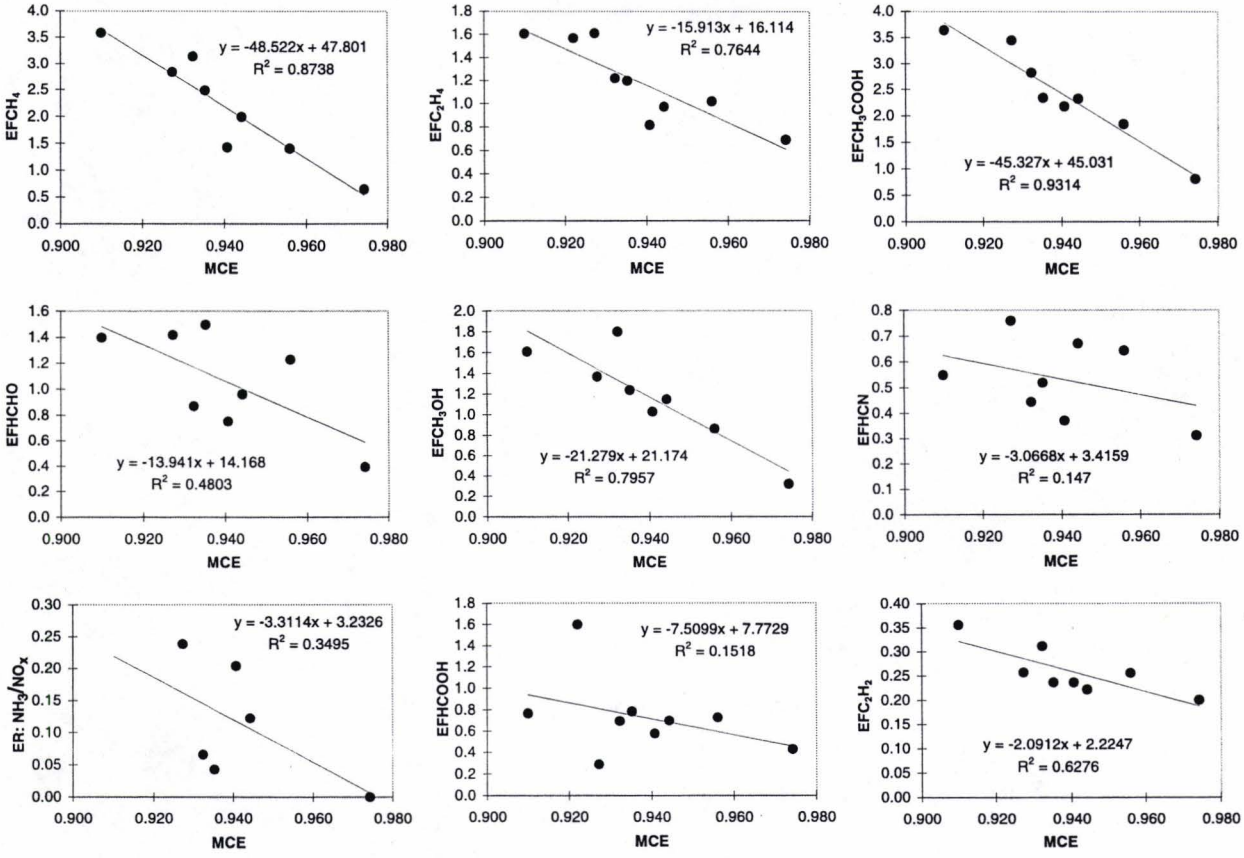

Figure 3. The fire-average initial emission ratios are used to derive fire-average initial emission factors (EF, g/kg dry fuel) and fire-average MCE as discussed in section 3.2.4. For the smoldering compounds measured in this study (except CO) we plot the initial EF for each fire versus fire-average MCE. The figure shows a range of fire-average EF and the dependence of EF on the different relative amount of flaming and smoldering that can occur during different fires. The plots are in order of molar abundance (from upper left). $EFNH_3$ ranged from zero to 0.4 g/kg, but we plot the emission ratio NH_3/NO_x instead to normalize the effects of varying fuel nitrogen content and to facilitate the discussion in section 3.2.6.

total fuel consumption during RSC, EF_{AB} the emission factor measured in-situ from an airborne platform, and F_{AB} the fraction of total fuel consumed for which the emissions are entrained in a convective plume. From equation (1) we expect a very small correction for pure grass fires since F_{RSC} is very small. However, a larger correction could occur in wooded savannas where large diameter, downed logs may be present (especially further from villages where such logs are harder to utilize as fuel). Ground-based fuel measurements for the planned fire in the miombo (UW Flight 1826) suggest that up to 10% of the total fuel consumption was due to logs that continued smoldering after strong convection from the fire had ceased (J. Pereira et al., personal communication, 2002). In addition, *Bertschi et al.* [2003b] found that the EF for smoldering logs in the miombo were very different from the miombo fire EF in this work. The net result is that if we assume 10% of fuel consumption by RSC (of logs) in equation (1) the emission factors for selected compounds are increased by the following factors: CH_4 (2.5), CH_3OH (1.7), NH_3 (1.4), HCHO (1.4), and CH_3COOH (1.3). The effects on MCE and other species are smaller [*Bertschi et al.*, 2003b].

[25] In summary, the assumption that all carbon emissions are detected causes a slight overestimate of EF as discussed in section 3.2.4. However, RSC probably increases the real EF for smoldering compounds toward the end of the dry season (especially in the wooded savannas as the large diameter fuels dry out). In addition, the tendency for some early dry season fires to have lower MCE [*Hoffa et al.*, 1999] could indicate that they have higher EF for smoldering compounds. Thus, the EF in Table 2 may mostly be conservative estimates. Clearly, more work is needed to quantify the influence of these important, complicating factors.

3.2.6. Comparison of ER and EF to Previous Work and Implications

[26] The emission factors and emission ratios presented here agree well with previous measurements in many cases. However, we also report a significant amount of improved or unique data for important fire emissions. *Andreae and Merlet* [2001, hereafter AM2001] reviewed previous emissions measurements for savanna fires. Therefore, we will

often compare our measurements to the values they reported. Fires can exhibit high variability so the comparisons should not be over interpreted. In addition, AM2001 often calculated EF assuming 45% carbon in the fuel, which would reduce the EF by 10% compared to ours. Thus, we deem agreement within 10% as excellent. Our average EF and ER for savanna fires are in Table 2.

[27] CO_2 and CO are the two most abundant emissions from biomass fires (excluding water). Our study-average EF for both these compounds are above the average values given by AM2001, but within their range. The ratio between CO_2 and CO, the combustion characteristics of fires, and equations for predicting EF for other trace gases are all related to the MCE. AM2001 reported an average MCE of 0.940 ($\Delta CO/\Delta CO_2$ = 0.063) for previous fire measurements in global tropical savannas. Their data set included mostly South African fires; 60% of the fires in our data set were also in South Africa, and we obtain a study-average MCE value of 0.938 ($\Delta CO/\Delta CO_2$ = 0.066). Despite this good agreement with AM2001, a different average MCE for African savanna fires can be computed that is based on our measurements for humid savanna fires. If we assume that the humid savanna region is 80% miombo and 20% dambo, that the miombo areas burn every two years, and the dambos burn annually [*Desanker et al.*, 1997], then the weighted average MCE is 0.952 (Table 2, last column). This "humid savanna" MCE value is only a little higher than our study-average MCE and the "real" average humid savanna MCE could be reduced by early season fires and RSC as discussed earlier.

[28] The major hydrocarbon emitted from fires is CH_4. *Ward et al.* [1992] developed a model for global methane emissions that predicts the EF of CH_4 ($EFCH_4$) as a function of combustion efficiency (CE, the fraction of burned fuel carbon released as CO_2). Our study-average $EFCH_4$ (2.2 g/kg) lies on their savanna-fire regression line at our estimated study-average CE of 0.927. The slope of our plot of $EFCH_4$ versus MCE is larger than their slope for $EFCH_4$ versus CE, but our slope is decreased if we plot versus CE and it is also based on a smaller range of values for the independent variable. Our average $\Delta CH_4/\Delta CO$ ER is 5.3%, which is lower than the AM2001 ER of 6.1%, but our average $EFCH_4$ (2.2 ± 1.0 g/kg) is very close to the AM2001 value for savanna fires of 2.3 ± 0.9 g/kg. We also measured EF for two C_2 hydrocarbons. The EF for C_2H_2 were not strongly dependent on MCE, in agreement with *Lobert et al.* [1991] who determined that C_2H_2 was produced by both flaming and smoldering combustion. Our EF for C_2H_4 and C_2H_2 are 150% and 90%, respectively, of the AM2001 values, but well within their large range. In deriving "preferred" EF values based on previous measurements, AM2001 may have included some data from aged smoke, which would have depleted levels of many reactive initial emissions such as C_2H_4 [e.g., *Blake et al.*, 1996; *Lee et al.*, 1997].

[29] In this work we report the first quantitative measurements of the emissions of oxygenated volatile organic compounds (OVOC) from African savanna fires. Earlier ground based and airborne FTIR studies showed that OVOC are major emissions from temperate and boreal fires [*Griffith et al.*, 1991; *Yokelson et al.*, 1996, 1997, 1999; *Worden et al.*, 1997; *Goode et al.*, 1999, 2000], but no quantitative measurements of OVOC were available for any African fires. *Koppmann et al.* [1997] had reported some "lower limits" for selected high molecular-weight, semi-volatile oxygenated organic compounds emitted by fires in sugar cane plantations and forests in South Africa. They concluded that these compounds were probably at least as common as "heavy" hydrocarbons. *Yokelson et al.* [1999] predicted both the identity and the average EF of the three main OVOC emitted by African savanna fires based on a linear fit of the EF versus MCE for fires in temperate regions. These predictions (in units of g/kg), followed by our study-average value in parentheses, are: HCHO, 1.6 (1.0); CH_3OH, 1.1 (1.2); and acetic acid 2.5 (2.4). The predictions are generally close and our African, fire-average EF lie tightly clustered about regression lines fit to EF versus MCE for fires in aboveground fine fuels from temperate, boreal, and tropical ecosystems [*Yokelson et al.*, 1999; *Goode et al.*, 2000; this work] (see Figure 4). This suggests that these plots are useful globally for predicting OVOC emissions from fires in aboveground fine fuels [*Bertschi et al.*, 2003b]. AM2001 also estimated EFs (in an unspecified manner) for the above oxygenates, which were close to our measurements for methanol, but factors of 2 and 3 lower than our measurements for acetic acid and formaldehyde.

[30] A major goal of our work in S2K was to determine if OVOC are important emissions from African savanna fires. In fact, the sum of the EF for the OVOC we measured is 5.30 g/kg, which is considerably larger than the sum of the EF for the hydrocarbons we detected (including methane) of 3.26 g/kg. The influence of tropical fire emissions has been studied with numerous atmospheric photochemical models [*Chatfield and Delaney*, 1990; *Fishman et al.*, 1991; *Richardson et al.*, 1991; *Keller et al.*, 1991; *Crutzen and Carmichael*, 1993; *Chatfield et al.*, 1996; *Thompson et al.*, 1996; *Jacob et al.*, 1996; *Koppmann et al.*, 1997; *Lelieveld et al.*, 1997; *Olson et al.*, 1997; *Mauzerall et al.*, 1998; *Lee et al.*, 1998], but none have included OVOC as initial emissions. However, *Mason et al.* [2001] showed that the OVOC we quantified in this work have a large effect on the production of ozone, HO_x, hydrogen peroxide, and the distribution of nitrogen reservoir species in smoke plume models. Their results and the measurements reported here show that OVOC should be included in future modeling studies of African fire emissions.

[31] We report several interesting observations regarding the emission of nitrogen-containing compounds from African savanna fires. HCN has significance both as a possible biomass-burning tracer [*Cicerone and Zellner*, 1983; *Rinsland et al.*, 2000; *Li et al.*, 2000], and as potential interference in measurements of NO_y [*Fahey et al.*, 1985; *Kliner et al.*, 1997]. Both *Lobert et al.* [1991] and *Yokelson et al.* [1997] reported that HCN was emitted in highly variable amounts by smoldering combustion of various types of biomass ($\Delta HCN/\Delta CO$ from ~0–5%). AM2001 recommended an EFHCN of 0.025–0.031 g/kg for savanna fires based on the only previous savanna-fire field measurements (in Australia) [*Hurst et al.*, 1994a, 1994b], which were near the low end of previous biomass-burning measurements. Our EFHCN (0.53 ± 0.14 g/kg) is ~20 times higher. Despite the variability noted above, in our savanna fire data EFHCN is not strongly dependent on MCE, and the average

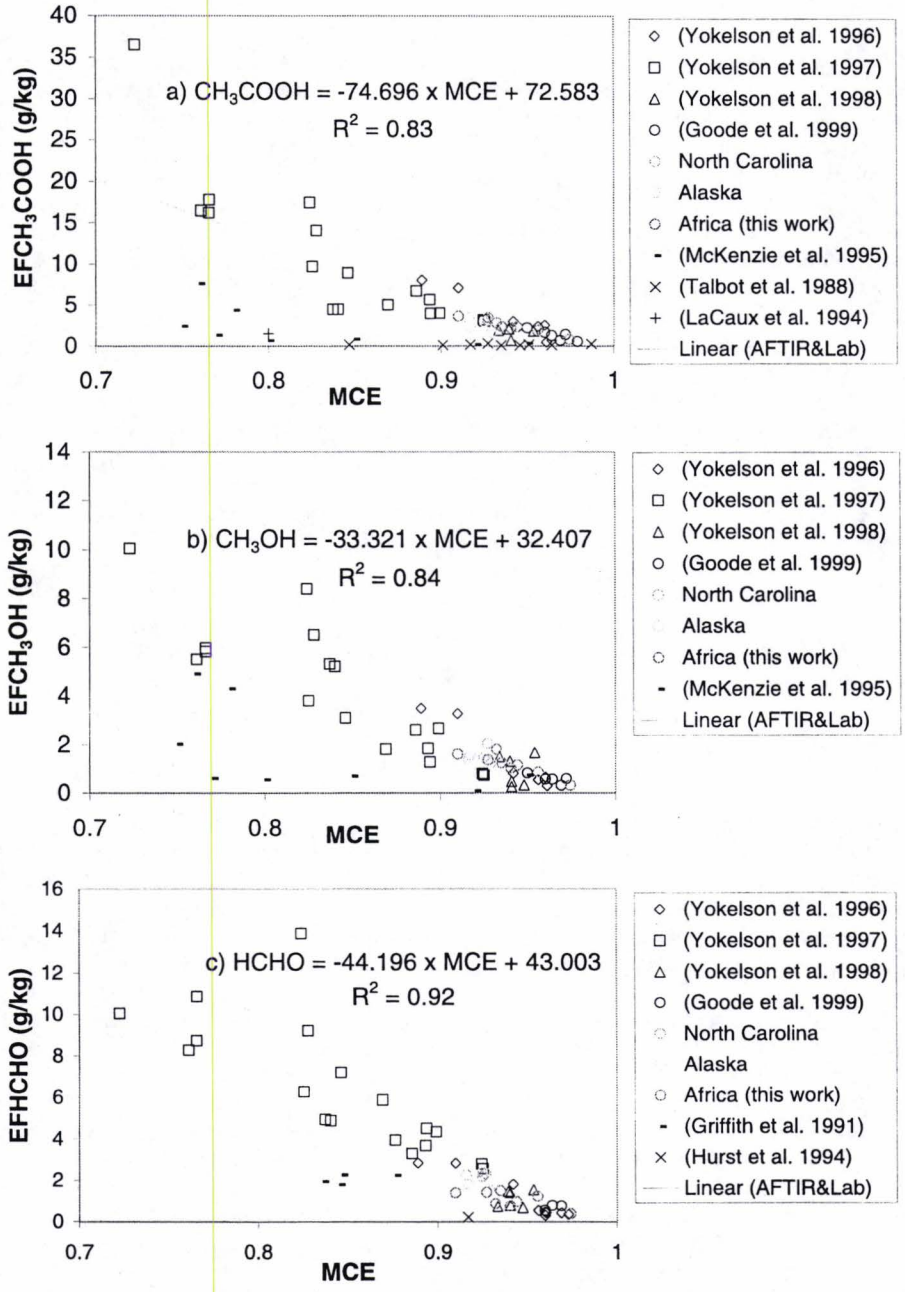

Figure 4. Emission factors plotted against MCE for (a) acetic acid, (b) methanol, and (c) formaldehyde; the major oxygenated organic compounds emitted by fires. The linear regression lines were fit to all the airborne FTIR results (colored symbols) from southern Africa [this work], Alaska [*Goode et al.*, 2000], and North Carolina [*Yokelson et al.*, 1999], and the open-path FTIR laboratory results (black, closed, unfilled symbols) for a wide variety of aboveground fine fuels. Some results from other techniques are also shown for comparison. The FTIR-based field and laboratory data are both close to the regression line for each compound. The regression equations (shown) can be used to estimate the initial emissions of these important compounds as discussed in section 3.2.6.

EF is a reasonable value for all our savanna fires. In addition, *Bertschi et al.* [2003a] saw no evidence of HCN emissions from the production and use of domestic biomass fuels. Column HCN can be monitored by automated, ground-based [*Rinsland et al.*, 2000] or space-based instrumentation [*Li et al.*, 2000]. These factors suggest that HCN may have value as a tracer for savanna fire emissions. However, the effect of seasonal variation in fuel moisture and nitrogen content on HCN emissions should be investigated. *Kliner et al.* [1997] made a detailed study of the influence of pressure, ozone, water, catalyst condition, and choice of reducing agent on HCN conversion in NO_y

instruments. Since HCN conversion was 100% under some conditions, some previous NO_y measurements in air impacted by biomass burning may be in error.

[32] Our study-average emission factor for NO_x (as NO) of 3.37 ± 0.64 g/kg is in reasonable agreement with the AM2001 recommendation of 3.9 ± 2.4 g/kg. There was a surprisingly large ER for $\Delta NO_x/\Delta CO$ for the dambo fire sampled on 5 September (UW Flight 1831), which can be deduced from Table 2. The ER was ~8%, which is closer to the values usually found for fossil fuel combustion (~10%) than for extratropical biomass burning (1–4%). This high ratio resulted from the very high flaming/smoldering ratio for this fire, as seen in the very low $\Delta CO/\Delta CO_2$ ER (2.64% or MCE = 0.974); the $\Delta NO_x/\Delta CO_2$ ER for this fire (0.2%) is within the usual range for biomass burning (AM2001).

[33] We measured variable ammonia emissions from savanna fires. The $\Delta NH_3/\Delta CO$ ER was very high (up to 4.5%) near the beginning and end of the miombo fire (UW Flight 1826, Table 1) when smoldering dominated. In contrast, there were never any detectable ammonia spectral signals during the dambo fire (UW Flight 1831, Table 1). Also, the $\Delta NH_3/\Delta CO$ ER measured with our artifact-free, open-path FTIR system at much higher smoke concentrations produced by fires in dambo grasses in both Zambia and 10 recent laboratory burns (T. J. Christian et al., manuscript in preparation, 2003) confirm that NH_3 was very likely below our detection limits in our airborne samples of the dambo fire. These low NH_3 emissions could be partly due to the high flaming/smoldering ratio or the low fuel nitrogen content since we measured an average N content for two samples of dambo grass (collected in the late dry season) of 0.22%, or about 1/5 of the average value for biomass. (The miombo litter samples averaged 1.2% N.) We conclude that NH_3 emissions from dambo fires are very small late in the dry season. (They could be higher earlier in the dry season when the grass has higher N content and fuel moisture.) Because of fuel nitrogen variability, *Goode et al.* [2000] plotted the ER $\Delta NH_3/\Delta NO_x$ versus MCE for fires mostly in temperate and boreal fuels. Our value of "zero" for this ER at the high MCE of the dambo fire is reasonably consistent with their model, but the $\Delta NH_3/\Delta NO_x$ ER for our other savanna fires at lower MCEs are less than half of what was measured with similar instrumentation for extratropical fires at similar MCEs (Figure 3) [see also *Goode et al.*, 2000, Figure 4]. If we correct our $\Delta NH_3/\Delta NO_x$ ER for the impact of residual smoldering combustion (see section 3.2.5) it raises the ER for our Miombo fire by 42%. Nevertheless, it seems that NH_3 emissions from late-season savanna fires are indeed lower, on the average, than from most extratropical fires. Finally, our study-average $EFNH_3$ for savanna fires (0.28 ± 0.14 g/kg) is ~10 times larger than the one previous NH_3 measurement for African savanna fires [*Delmas et al.*, 1995], but, it is 2–5 times lower than the values recommended by AM2001 based on the work of *Hurst et al.* [1994a, 1994b] in Australia. Thus, any uncertainty in our NH_3 measurements is small compared to the differences between our values and those reported previously.

[34] We conclude this section by coupling data in Table 2 with that of *Cofer et al.* [1996] for H_2, *Kuhlbusch et al.* [1991] for N_2, and *Sinha et al.* [2003a] for SO_2 to make a reasonably complete list of the top 15 trace gases directly emitted by African savanna fires (excluding water). The gases are listed next in the format: (rank in order of moles produced), chemical formula, and ER to CO_2 (ppb/ppm). (1) CO_2 1000, (2) CO 66.4, (3) H_2 12.6, (4) CH_4 3.53, (5) NO_x 3.10, (6) N_2 2.87 (7) C_2H_4 1.14, (8) CH_3COOH 1.06, (9) HCHO 0.97, (10) CH_3OH 0.96, (11) SO_2 0.85, (12) HCN 0.57, (13) NH_3 0.47, (14) HCOOH 0.39, (15) C_2H_2 0.29. This paper reports the first quantitative data obtained in Africa for 6 of the 15 most abundant trace gases produced by savanna fires.

3.3. Observations of Post Emission Smoke Processing

[35] Eleven of the fifteen most abundant trace gases emitted by savanna fires (listed above) are too reactive to become well mixed in the global troposphere. Photochemistry and other processes rapidly consume many of the initial emissions and produce new species. Determining the influence of biomass burning on local to global scales requires good emissions estimates, but also detailed understanding of the complex, postemission transformations, which can occur in smoke plumes that are very different from the "normal" atmosphere. We describe some significant postemission changes in the chemical composition of smoke due to photochemical or cloud processing. These observations also highlight the importance of using only nascent smoke samples for calculating initial emissions from biomass fires.

3.3.1. Rapid Photochemical Formation of Ozone and Acetic Acid

[36] Measuring the photochemical changes in plumes downwind of fires is complicated by the fact that the mixing ratios in a parcel of smoke change due to photochemistry, heterogeneous processes, and mixing. CO has a lifetime of about one month in the tropical troposphere and so, up to several days downwind from a fire, the CO mixing ratios can indicate the plume location and the rate of mixing. Photochemical transformations in a smoke parcel change the ratio of a compounds excess mixing ratio to that of CO. In particular, photochemistry involving NO_x, CO, and organic compounds produces O_3 and other products and therefore, the $\Delta O_3/\Delta CO$ ratio has often been used as an indicator of the degree of photochemical aging for smoke/haze samples [*Andreae et al.*, 1988, 1994; *Goode et al.*, 2000] and in modeling studies [e.g., *Chatfield and Delaney*, 1990; *Jacob et al.*, 1992, 1996; *Mauzerall et al.*, 1998].

[37] Our AFTIR spectra of minutes-old, African smoke show large, negative, excess ozone mixing ratios (Table 1), as found also for a fire in the Pacific Northwest by *Stith et al.* [1981]. This is due to destruction of O_3 by NO, HO_2, and particles. Multiplying these large, negative, excess O_3 values by −1 yields a lower limit for the ozone mixing ratios in the entrained background air, which, in Africa, were as high as 100 ppb (Table 1, Flights 1816, 1819, 1826, 1831, 1834). (These low-altitude results suggest that vast regions of southern Africa can have dry-season, surface ozone mixing ratios above 50 ppbv, which is the US EPA, 8-hour average, permissible exposure limit.)

[38] We sampled biomass-burning plumes both at their source and up to ~30 km downwind on three occasions during S2K: Flight 1825 (Beira Fire, 31 August), Flight 1826 (Miombo Fire, 1 September), and Flight 1834 (Timbavati Fire, 7 September). In all cases we observed an "O_3 hole" in nascent smoke followed by rapid production of

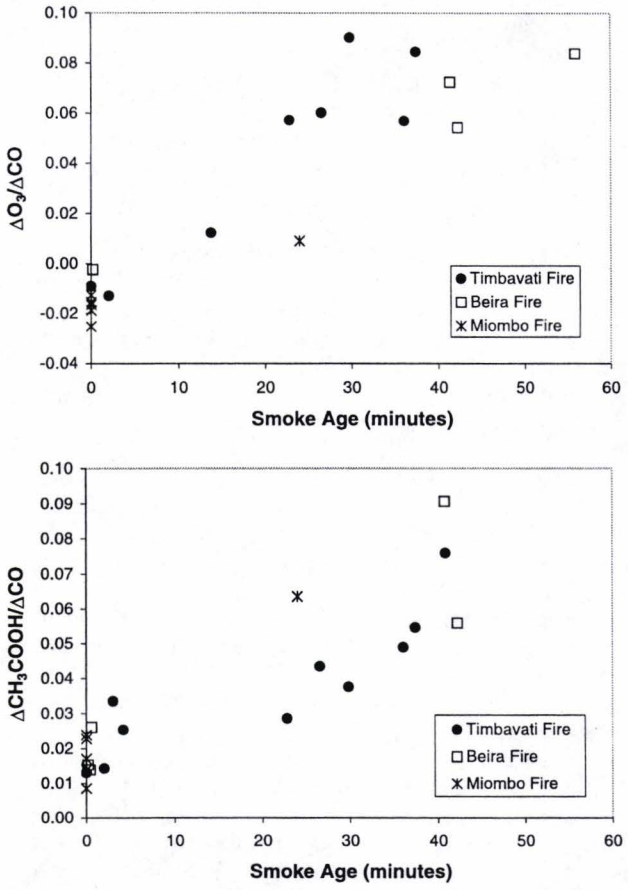

Figure 5. The rapid change in smoke composition due to photochemical processing is evident in the increasing ratios of excess O_3 and CH_3COOH (acetic acid) to excess CO as a function of smoke age. Excess O_3 and CH_3COOH rise to levels comparable to excess CH_4 in less than an hour. The average transport speed for the smoke (in m/s) was Timbavati 11.3, Beira 7.9, and Miombo 5.7.

both O_3 and acetic acid. In Figure 5 we illustrate the downwind changes in O_3 and acetic acid for these fires by plotting $\Delta O_3/\Delta CO$ and $\Delta CH_3COOH/\Delta CO$ versus smoke age. $\Delta O_3/\Delta CO$ increased to as much as 9% in less than 1 hour, which can be compared to the value of 22% we measured in biomass burning haze 2–4 days old off Namibia (UW Flight 1837) and 20–88% measured in biomass burning haze about 10 days transport time from Africa by *Andreae et al.* [1994]. $\Delta CH_3COOH/\Delta CO$ also rose to as much as 9% less than 1 hour downwind, which was more than 5 times the initial emission ratio (Beira Fire). Our measurements of the changing ratios in the downwind plumes could partly reflect changes in the source ratio since these were not Lagrangian experiments. However, on Flight 1834, we remeasured the source ratios ~1 h after our first source samples and the source variation was much smaller than the downwind variation. On Flight 1826 the downwind plume was intersected by younger smoke from another fire. Thus, for this fire only, the smoke age is not clearly defined. One possible explanation of the downwind data for this fire is that the injection of fresh emissions destroyed some O_3, but spurred CH_3COOH production.

[39] The initial emissions of acetic acid from savanna fires are much higher than previously thought [*Talbot et al.*, 1996] and additional, rapid secondary production occurs (as was also observed in Alaska [*Goode et al.*, 2000]). For example, on a mass basis, acetic acid is the most abundant organic initial emission from savanna fires and its ratio to CO more than triples after emission. The main sink of acetic acid is thought to be reaction with OH, but the products are unknown. *Jacob et al.* [1996] found that their photochemical model was sensitive to different assumptions about these products. Given the high levels of acetic acid that we observe, determining the products of its reaction with OH is of considerable importance. Finally, we did not see consistent, strong evidence of downwind production of formic acid in Africa as was observed in Alaska [*Goode et al.*, 2000].

[40] In summary, major changes in the chemistry of savanna-fire smoke during the first hour of aging include: (1) excess ozone and excess acetic acid rise to levels comparable to, or greater than, excess methane, and (2) NO_x is rapidly converted to reservoir species [*Mason et al.*, 2001]. *Hobbs et al.* [2003] compare the rates of production for O_3 and CH_3COOH reported here to those measured in other biomass-burning plumes by *Goode et al.* [2000] and *Hobbs et al.* [1996]. The changes in hydrocarbons and particle concentrations with smoke age are also discussed [*Hobbs et al.*, 2003]. *Jost et al.* [2003] describe photochemistry observed in a Namibian biomass-burning plume during S2K.

3.3.2. Cloud-Induced Changes in the Chemical Composition of Smoke

[41] During the planned fire at Madikwe Game Reserve on 18 August, a large cumulus cloud capped the vertical column of smoke ~3 km above the flame front (see photo at http://www.umt.edu/chemistry/faculty/yokelson/galleries/s2k/jpg_madikwe.htm). This provided an opportunity to compare a sample of nascent smoke below the cloud (Table 1, UW Flight 1816, altitude 1945 m) with two samples of increasingly cloud-processed smoke (altitude 3866 and 4166 m, respectively).

[42] Figure 6 shows the changes in $\Delta X/\Delta CO$ with increased cloud-processing for 6 gases (CO is used as a tracer). A dramatic "disappearance" of CH_3OH and NH_3 occurred in the cloud-processed smoke. The NO_2 and acetic acid ratios to CO also decreased markedly. In addition, the UW SO_2 analyzer indicated that SO_2 was removed from the plume at a rate similar to methanol. In contrast, $\Delta NO/\Delta CO$ and $\Delta HCHO/\Delta CO$ increased significantly and $\Delta CO/\Delta CO_2$ increased slightly (Table 1). The HCHO increase could be due to enhanced photochemistry in the cloud margins [*Madronich*, 1987] or heterogeneous conversion of CH_3OH to HCHO [*Singh et al.*, 2000]. The large decrease in $\Delta NO_2/\Delta NO$ could be due to enhanced photolysis of NO_2 or HONO (formed from NO_2 on particle surfaces). Other possibilities are discussed by *Ravishankara and Longfellow* [1999]. CH_3OH, NH_3, CH_3COOH, and SO_2 probably decreased because of their solubility. However, the relative rates of these decreases are not proportional to the Henry's Law constants for the gases [*Betterton*, 1992], which suggests that not all the gases reached equilibrium with the cloud water; possibly due to reactions of the dissolved gases in solution. If such reactions

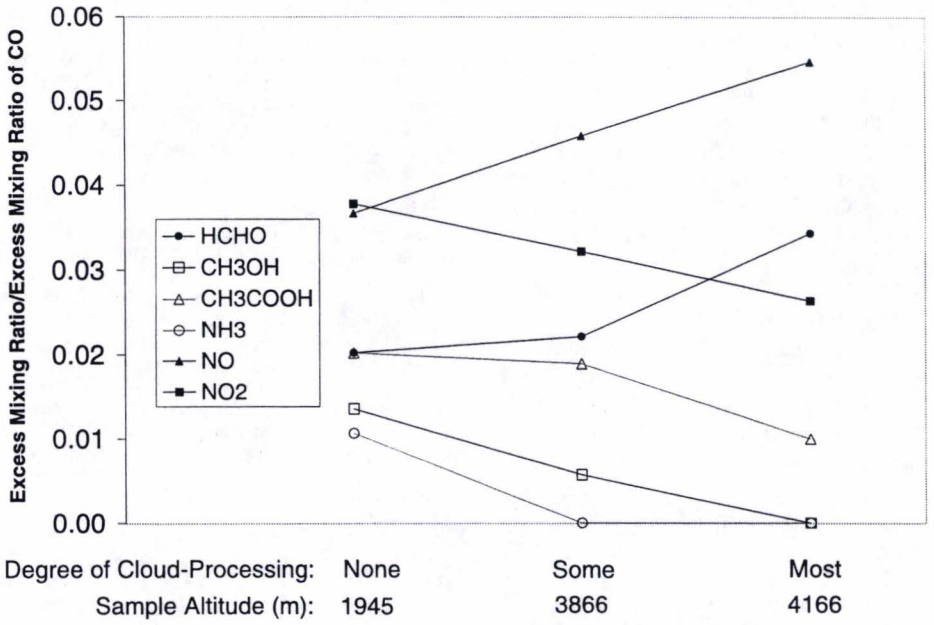

Figure 6. Excess mixing ratios of various species divided by the simultaneously measured excess mixing ratio of CO as a function of the degree of cloud processing. Cloud effects on the gases are decoupled from the effects of dilution by comparison to CO, which is an insoluble tracer. The observations are discussed in section 3.3.2.

occurred, the gases would not be released in their original concentrations if the cloud droplets evaporated [e.g., *Easter and Hobbs*, 1974]. Based on the size of the cloud and the wind speed, the cloud-processing effects probably occurred within a few minutes. The single sample obtained from the Lebombo Fire (Table 1, UW Flight 1825, altitude 3874 m) has characteristics consistent with moderate cloud processing since it showed lower than "normal" $\Delta CH_3OH/\Delta CO$, $\Delta CH_3COOH/\Delta CO$, and $\Delta NH_3/\Delta CO$, and higher than "normal" $\Delta HCHO/\Delta CO$ and $\Delta NO/\Delta NO_2$. Although clouds were not observed near this fire, it is possible that a capping cumulus cloud processed the smoke before we arrived since the smoke plume dynamics were similar to those observed during the Madikwe fire.

[43] The above observations justify omitting cloud-processed samples from the calculation of initial emission factors for many species. They also show that the transport of smoke in convective clouds is likely accompanied by fast, significant changes in smoke chemistry. The large influence of OVOC on smoke chemistry demonstrated by *Mason et al.* [2001] will be strongly altered if the concentrations of OVOC are changed by cloud-processing. The delay between emission and cloud-processing is important since photochemical processing of OVOC leads to high levels of H_2O_2 in hours-old smoke [*Mason et al.*, 2001]. On a broader scale, clouds (which cover 50% of the Earth on the average) could have similar effects on biogenic emissions, which include high levels of soluble oxygenates such as methanol [*Konig et al.*, 1995; *Kirstine et al.*, 1998]. In general, OVOC that are released or produced in the boundary layer and transported vertically by deep convection have a large influence on the HO_x budget of the upper troposphere [*Singh et al.*, 1995], but this influence may depend on cloud processes that are poorly understood.

[44] It is intriguing to estimate the amount of gases "scavenged" from the smoke by the capping cloud on UW Flight 1816. For example, based on the $\Delta CH_3OH/\Delta CO$ ratio below the cloud, and ΔCO in the most heavily cloud processed sample, a simple calculation suggests that 25 $\mu g/m^3$ of CH_3OH alone were removed from the smoke by the cloud. In contrast, *Decesari et al.* [2000] reported an average total dissolved matter content of 28 $\mu g/m^3$ (inorganic + organic) in polluted fog droplets in the Po River Valley. Comparison of these numbers suggests that clouds impacted by smoke can be extremely "dirty" and have high potential for intense multiphase chemistry and the generation of enriched new particles in the cloud detrainment zone [*Ravishankara and Longfellow*, 1999].

4. Conclusions

[45] We deployed an FTIR coupled to a multipass cell on the University of Washington's Convair-580 research aircraft to measure stable and reactive trace gases in southern Africa during the middle to late dry season (August–September 2000). This is a region and season of extensive biomass burning, which produced well-mixed haze layers that extended to 3.5 km in altitude south of most of the fires, and up to ~6 km in the humid savanna region where most of the burning occurs. We observed high CO, O_3, and water vapor in the haze layers. At the top of the haze layers there was usually a sharp transition to the much cleaner and drier free troposphere. Cumulus convection in nonprecipitating clouds played a potentially significant role in mixing these two different layers. We measured the vertical profiles of CO and other gases above instrumented ground sites and below the NASA ER-2 and overpasses by the TERRA satellite.

[46] The use of FTIR gave us the capability to measure most of the major trace gases emitted by 10 savanna fires that were representative of the fires that feed the haze layers (including two fires in the important humid savanna region). Measurements made in nascent smoke, throughout the course of the fires, and during peak, regional smoke levels were used to calculate initial emission factors. We report savanna fire emission factors for (in order of molar abundance) CO_2, CO, CH_4, NO_x (as NO), C_2H_4, CH_3COOH, HCHO, CH_3OH, HCN, NH_3, HCOOH, and C_2H_2. The initial emission factors for some smoldering compounds could be higher early in the dry season [*Hoffa et al.*, 1999] or where large-diameter fuels contribute to residual smoldering combustion [*Bertschi et al.*, 2003b]. These are the first quantitative measurements in Africa for 6 of the 15 most abundant trace gases emitted by savanna fires. Oxygenated organic compounds (which react photochemically to produce HO_x) accounted for 70% of the nonmethane organic compounds emitted by savanna fires. Since savanna fires are a major global source of trace gases, this has implications for the tropospheric HO_x budget [*Mason et al.*, 2001]. We measured a large emission factor for HCN from savanna fires, but observed no HCN emissions from the production and use of domestic biofuels in a separate study [*Bertschi et al.*, 2003a]. Thus, HCN may be useful as a tracer for savanna fires. The large HCN emissions may also mean that some NO_y measurements made in air impacted by fires are in error [*Kliner et al.*, 1997]. NH_3 emissions were found to be much higher than previously measured for African savanna fires, but lower than measured for Australian savanna fires [*Hurst et al.*, 1994a, 1994b].

[47] We observed significant, postemission production of acetic acid and ozone in smoke samples of measured ages from two fires. These are the first precise observations of photochemical rates in African smoke [*Hobbs et al.*, 2003]. $\Delta CH_3COOH/\Delta CO$ and $\Delta O_3/\Delta CO$ rose to levels as large as 9% ($>\Delta CH_4/\Delta CO$) in <1 h. Acetic acid was a major, initial organic emission and the major excess organic compound in ~1 hour-old smoke. Thus, the products of the reaction of acetic acid with OH need to be determined. We also observed fast, cloud-induced changes in smoke chemistry. Methanol, CH_3COOH, NO_2, and NH_3 were significantly reduced by exposure to clouds, but not at relative rates proportional to their Henry's Law constants. Cloud processing significantly increased HCHO and NO.

[48] Photochemical, cloud, and other processes rapidly and dramatically change smoke long before it becomes even locally mixed. Thus, many primary pollutants would be measured incorrectly in smoke more than a few minutes old. However, airborne measurements in nascent smoke compare well to laboratory smoke measurements (see Figure 4). The rapid evolution of smoke by cloud-processing and photochemistry occurs in an environment that is very different from "ambient" air. The timing between photochemical and cloud processing will also strongly affect the outcome. The postemission transformations critically influence the regional-global impact of biomass burning.

[49] **Acknowledgments.** This research was supported by funds provided by the National Science Foundation under grants ATM-9900494 and ATM-9901624, the Interagency Joint Fire Science Program, the Rocky Mountain Research Station, Forest Service, U.S. Department of Agriculture (INT-97082-RJVA and RMRS-99508-RJVA) and NASA grants NAGS-9022 and NAGS-7675. The authors thank Michael King, Bob Swap, Harold Annegarn, and Tim Suttles for their major role in SAFARI 2000 activities and NASA and the C-131 crew for logistical support. The UM personnel thank the UW Convair-580 crew and pilots for their support.

References

Andreae, M. O., Emissions of trace gases and aerosols from southern African savanna fires, in *Fire in Southern African Savannas: Ecological and Atmospheric Perspectives*, edited by B. W. van Wilgen, M. O. Andreae, J. G. Goldammer, and J. A. Lindesay, pp. 161–183, Witwatersrand Univ. Press, Johannesburg, South Africa, 1997.

Andreae, M. O., and P. Merlet, Emissions of trace gases and aerosols from biomass burning, *Global Biogeochem. Cycles*, *15*, 955–966, 2001.

Andreae, M. O., et al., Biomass-burning emissions and associated haze layers over Amazonia, *J. Geophys. Res.*, *93*, 1509–1527, 1988.

Andreae, M. O., B. E. Anderson, D. R. Blake, J. D. Bradshaw, J. E. Collins, G. L. Gregory, G. W. Sachse, and M. C. Shipham, Influence of plumes from biomass burning on atmospheric chemistry over the equatorial and tropical South Atlantic during CITE 3, *J. Geophys. Res.*, *99*, 12,793–12,808, 1994.

Andreae, M. O., E. Atlas, H. Cachier, W. R. Cofer III, G. W. Harris, G. Helas, R. Koppmann, J.-P. Lacaux, and D. E. Ward, Trace gas and aerosol emissions from savanna fires, in *Biomass Burning and Global Change*, edited by J. S. Levine, pp. 278–295, MIT Press, Cambridge, Mass., 1996.

Bertschi, I. T., R. J. Yokelson, D. E. Ward, T. J. Christian, and W. M. Hao, Trace gas emissions from the production and use of domestic biofuels in Zambia measured by open-path Fourier transform infrared spectroscopy, *J. Geophys. Res.*, *108*, doi:10.1029/2002JD002158, in press, 2003a.

Bertschi, I., R. J. Yokelson, D. E. Ward, J. G. Goode, R. Babbitt, R. A. Susott, and W. M. Hao, The trace gas and particle emissions from fires in large-diameter and belowground biomass fuels, *J. Geophys. Res.*, *108*, doi:10.1029/2002JD002100, in press, 2003b.

Betterton, E. A., Henry's law constants of soluble and moderately soluble organic gases: Effects on aqueous phase chemistry, in *Gaseous Pollutants: Characterization and Cycling*, edited by J. O. Nriagu, pp. 1–50, John Wiley, New York, 1992.

Blake, N. J., D. R. Blake, B. C. Sive, T. Y. Chen, F. S. Rowland, J. E. Collins, G. W. Sachse, and B. E. Anderson, Biomass burning emissions and vertical distribution of atmospheric methyl halides and other reduced carbon gases in the South Atlantic region, *J. Geophys. Res.*, *101*, 24,151–24,164, 1996.

Browell, E. V., et al., Ozone and aerosol distributions and air mass characteristics over the South Atlantic basin during the burning season, *J. Geophys. Res.*, *101*, 24,043–24,068, 1996.

Cahoon, D. R., Jr., B. J. Stocks, J. S. Levine, W. R. Cofer III, and K. P. O'Neill, Seasonal distribution of African savanna fires, *Nature*, *359*, 812–815, 1992.

Chatfield, R. B., and A. C. Delaney, Convection links biomass burning to increased tropical ozone: However, models will tend to overpredict O_3, *J. Geophys. Res.*, *95*, 18,473–18,488, 1990.

Chatfield, R. B., J. A. Vastano, H. B. Singh, and G. W. Sachse, A general model of how fire emissions and chemistry produce African/oceanic plumes (O_3, CO, PAN, smoke) in TRACE A, *J. Geophys. Res.*, *101*, 24,279–24,306, 1996.

Cicerone, R. J., and R. Zellner, The atmospheric chemistry of hydrogen cyanide (HCN), *J. Geophys. Res.*, *88*, 10,689–10,696, 1983.

Cofer, W. R., III, J. S. Levine, E. L. Winstead, D. R. Cahoon, D. I. Sebacher, J. P. Pinto, and B. J. Stocks, Source compositions of trace gases released during African savanna fires, *J. Geophys. Res.*, *101*, 23,597–23,602, 1996.

Crutzen, P. J., and M. O. Andreae, Biomass burning in the tropics: Impact on atmospheric chemistry and biogeochemical cycles, *Science*, *250*, 1669–1678, 1990.

Crutzen, P. J., and G. R. Carmichael, Modeling the influence of fires on atmospheric chemistry, in *Fire in the Environment: The Ecological, Atmospheric, and Climatic Importance of Vegetation Fires*, edited by P. J. Crutzen and J. G. Goldammer, pp. 89–105, John Wiley, New York, 1993.

Decesari, S., M. C. Facchini, E. Matta, and S. Fuzzi, Organic and inorganic solutes in fog droplets: A full characterization approach, paper presented at 13th International Conference on Clouds and Precipitation, Reno, NV, USA, 14–18 August, 2000.

Delmas, R., J. P. Lacaux, J. C. Menaut, L. Abbadie, X. Le Roux, G. Helas, and J. Lobert, Nitrogen compound emissions from biomass burning in tropical African savanna FOS/DECAFE 1991 experiment (Lamto, Ivory Coast), *J. Atmos. Chem.*, *22*, 175–193, 1995.

Desanker, P. V., , P. G. H. Frost, C. O. Justice, and R. J. Scholes (Eds.), *The Miombo Network: Framework for a Terrestrial Transect Study of Land-*

Use and Land-Cover Change in the Miombo Ecosystems of Central Africa, Conclusions of the Miombo Network Workshop Zomba, Malawi, December 1995, *IGBP Rep. 41*, 109 pp., IGBP, Stockholm, 1997.

Easter, R. C., and P. V. Hobbs, The formation of sulfates and the enhancement of cloud condensation nuclei in clouds, *J. Atmos. Sci.*, *35*, 1586–1594, 1974.

Eck, T. F., et al., Variability of biomass burning aerosol optical characteristics in southern Africa during the SAFARI 2000 dry season campaign and a comparison of single scattering albedo estimates from radiometric measurements, *J. Geophys. Res.*, *108*, doi:10.1029/2002JD002321, in press, 2003.

Fahey, D. W., C. S. Eubank, G. Hubler, and F. C. Fehsenfeld, Evaluation of a catalytic reduction technique for the measurement of total reactive odd-nitrogen NO_y in the atmosphere, *J. Atmos. Chem.*, *3*, 435–468, 1985.

Fishman, J., K. Fakhruzzaman, B. Cros, and D. Nganga, Identification of widespread pollution in the Southern Hemisphere deduced from satellite analyses, *Science*, *252*, 1693–1696, 1991.

Fishman, J., J. H. Hoell Jr., R. D. Bendura, R. J. McNeal, and V. W. J. H. Kirchoff, NASA GTE TRACE A Experiment (September–October 1992): Overview, *J. Geophys. Res.*, *101*, 23,865–23,880, 1996.

Goode, J. G., R. J. Yokelson, R. A. Susott, and D. E. Ward, Trace gas emissions from laboratory biomass fires measured by open-path Fourier transform infrared spectroscopy: Fires in grass and surface fuels, *J. Geophys. Res.*, *104*, 21,237–21,245, 1999.

Goode, J. G., R. J. Yokelson, D. E. Ward, R. A. Susott, R. E. Babbitt, M. A. Davies, and W. M. Hao, Measurements of excess O_3, CO_2, CO, CH_4, C_2H_4, C_2H_2, HCN, NO, NH_3, HCOOH, CH_3COOH, HCHO, and CH_3OH in 1997 Alaskan biomass burning plumes by airborne Fourier transform infrared spectroscopy (AFTIR), *J. Geophys. Res.*, *105*, 22,147–22,166, 2000.

Griffith, D. W. T., Synthetic calibration and quantitative analysis of gas-phase FTIR spectra, *Appl. Spectrosc.*, *50*, 59–70, 1996.

Griffith, D. W. T., W. G. Mankin, M. T. Coffey, D. E. Ward, and A. Riebau, FTIR remote sensing of biomass burning emissions of CO_2, CO, CH_4, CH_2O, NO, NO_2, NH_3 and N_2O, in *Global Biomass Burning: Atmospheric, Climatic, and Biospheric Implications*, edited by J. S. Levine, pp. 230–239, MIT Press, Cambridge, Mass., 1991.

Hao, W. M., D. E. Ward, G. Olbu, and S. P. Baker, Emissions of CO_2, CO, and hydrocarbons from fires in diverse African savanna ecosystems, *J. Geophys. Res.*, *101*, 23,577–23,584, 1996.

Hobbs, P. V., Clean air slots amid dense atmospheric pollution in southern Africa, *J. Geophys. Res.*, *108*, doi:10.1029/2002JD002156, in press, 2003.

Hobbs, P. V., J. S. Reid, J. A. Herring, J. D. Nance, R. E. Weiss, J. L. Ross, D. A. Hegg, R. D. Ottmar, and C. Liousse, Particle and trace-gas measurements in the smoke from prescribed burns of forest products in the Pacific Northwest, in *Biomass Burning and Global Change*, edited by J. S. Levine, pp. 697–715, MIT Press, Cambridge, Mass., 1996.

Hobbs, P. V., P. Sinha, R. J. Yokelson, T. J. Christian, D. R. Blake, S. Gao, T. W. Kirchstetter, T. Novakov, and P. Pilewskie, Evolution of particle and gas emissions from a savanna fire in South Africa, *J. Geophys. Res.*, *J. Geophys. Res.*, *108*, doi:10.1029/2002JD002352, in press, 2003.

Hoffa, E. A., D. E. Ward, W. M. Hao, R. A. Susott, and R. H. Wakimoto, Seasonality of carbon emissions from biomass burning in a Zambian savanna, *J. Geophys. Res.*, *104*, 13,841–13,853, 1999.

Holzinger, R., C. Warneke, A. Hansel, A. Jordan, W. Lindinger, D. H. Scharffe, G. Schade, and P. J. Crutzen, Biomass burning as a source of formaldehyde, acetaldehyde, methanol, acetone, acetonitrile, and hydrogen cyanide, *Geophys. Res. Lett.*, *26*, 1161–1164, 1999.

Hurst, D. F., D. W. T. Griffith, and G. D. Cook, Trace gas emissions from biomass burning in tropical Australian savannas, *J. Geophys. Res.*, *99*, 16,441–16,456, 1994a.

Hurst, D. F., D. W. T. Griffith, J. N. Carras, D. J. Williams, and P. J. Fraser, Measurements of trace gases emitted by Australian savanna fires during the 1990 dry season, *J. Atmos. Chem.*, *18*, 33–56, 1994b.

Jacob, D. J., et al., Summertime photochemistry of the troposphere at high northern latitudes, *J. Geophys. Res.*, *97*, 16,421–16,431, 1992.

Jacob, D. J., et al., Origin of ozone and NO_x in the tropical troposphere: A photochemical analysis of aircraft observations over the South Atlantic basin, *J. Geophys. Res.*, *101*, 24,235–24,250, 1996.

Jost, C., J. Trentmann, D. Sprung, M. O. Andreae, J. B. McQuaid, and H. Barjat, Trace gas chemistry in a young biomass burning plume over Namibia: Observations and model simulations, *J. Geophys. Res.*, *108*, doi:10.1029/2002JD002431, in press, 2003.

Justice, C. O., J. D. Kendall, P. R. Dowty, and R. J. Scholes, Satellite remote sensing of fires during the SAFARI campaign using NOAA advanced very high resolution radiometer data, *J. Geophys. Res.*, *101*, 23,597–23,602, 1996.

Keller, M., D. J. Jacob, S. C. Wofsy, and R. C. Harriss, Effects of tropical deforestation on global and regional atmospheric chemistry, *Clim. Change*, *19*, 139–158, 1991.

Kirstine, W., I. Galbally, Y. Ye, and M. Hooper, Emissions of volatile organic compounds (primarily oxygenated species) from pasture, *J. Geophys. Res.*, *103*, 10,605–10,619, 1998.

Kliner, D. A. V., B. C. Daube, J. D. Burley, and S. C. Wofsy, Laboratory investigation of the catalytic reduction technique for measurement of atmospheric NO_y, *J. Geophys. Res.*, *102*, 10,759–10,776, 1997.

Konig, G., M. Brunda, H. Puxbaum, C. N. Hewitt, S. C. Duckham, and J. Rudolph, Relative contribution of oxygenated hydrocarbons to the total biogenic VOC emissions of selected mid-European agricultural and natural plant species, *Atmos. Environ.*, *29*, 861–874, 1995.

Koppmann, R., A. Khedim, J. Rudolph, D. Poppe, M. O. Andreae, G. Helas, M. Welling, and T. Zenker, Emissions of organic trace gases from savanna fires in southern Africa during the 1992 Southern Africa Fire Atmosphere Research Initiative and their impact on the formation of tropospheric ozone, *J. Geophys. Res.*, *102*, 18,879–18,888, 1997.

Kuhlbusch, T. A., J. M. Lobert, P. J. Crutzen, and P. Warneck, Molecular nitrogen emissions from denitrification during biomass burning, *Nature*, *351*, 135–137, 1991.

Lacaux, J. P., D. Brocard, C. Lacaux, R. Delmas, B. Ajoua, V. Yoboué, and M. Koffi, Traditional charcoal making: An important source of atmospheric pollution in the African tropics, *Atmos. Res.*, *35*, 71–76, 1994.

Lacaux, J. P., J. M. Brustet, R. Delmas, J. C. Menaut, L. Abbadie, B. Bonsang, H. Cachier, J. Baudet, M. O. Andreae, and G. Helas, Biomass burning in the tropical savannas of Ivory Coast: An overview of the field experiment Fire of Savannas (FOS/DECAFE 91), *J. Atmos. Chem.*, *22*, 195–216, 1995.

Lacaux, J. P., R. Delmas, C. Jambert, and T. A. J. Kuhlbusch, NO_x emissions from African savanna fires, *J. Geophys. Res.*, *101*, 23,585–23,596, 1996.

Lee, M., B. G. Heikes, D. J. Jacob, G. Sachse, and B. Anderson, Hydrogen peroxide, organic hydroperoxide, and formaldehyde as primary pollutants from biomass burning, *J. Geophys. Res.*, *102*, 1301–1309, 1997.

Lee, M., B. G. Heikes, and D. J. Jacob, Enhancements of hydroperoxides and formaldehyde in biomass burning impacted air and their effect on atmospheric oxidant cycles, *J. Geophys. Res.*, *103*, 13,201–13,212, 1998.

Lelieveld, J., P. J. Crutzen, D. J. Jacob, and A. M. Thompson, Modeling of biomass burning influences on tropospheric ozone, in *Fire in Southern African Savannas: Ecological and Atmospheric Perspectives*, edited by B. W. van Wilgen et al., pp. 217–238, Witwatersrand Univ. Press, Johannesburg, South Africa, 1997.

Li, Q. B., D. J. Jacob, I. Bey, R. M. Yantosca, Y. J. Zhao, Y. Kondo, and J. Notholt, Atmospheric hydrogen cyanide (HCN): Biomass burning source, ocean sink?, *Geophys. Res. Lett.*, *27*, 357–360, 2000.

Lindesay, J. A., M. O. Andreae, J. G. Goldammer, G. Harris, H. J. Annegarn, M. Garstang, R. J. Scholes, and B. W. van Wilgen, International Geosphere-Biosphere Programme/International Global Atmospheric Chemistry SAFARI-92 field experiment: Background and overview, *J. Geophys. Res.*, *101*, 23,521–23,530, 1996.

Lobert, J. M., D. H. Scharffe, W. M. Hao, T. A. Kuhlbusch, R. Seuwen, P. Warneck, and P. J. Crutzen, Experimental evaluation of biomass burning emissions: Nitrogen and carbon containing compounds, in *Global Biomass Burning: Atmospheric, Climatic, and Biospheric Implications*, edited by J. S. Levine, pp. 289–304, MIT Press, Cambridge, Mass., 1991.

Madronich, S., Photodissociation in the atmosphere, 1, Actinic flux and the effects of ground reflection and clouds, *J. Geophys. Res.*, *92*, 9740–9752, 1987.

Mason, S. A., R. J. Field, R. J. Yokelson, M. A. Kochivar, M. R. Tinsley, D. E. Ward, and W. M. Hao, Complex effects arising in smoke plume simulations due to inclusion of direct emissions of oxygenated organic species from biomass combustion, *J. Geophys. Res.*, *106*, 12,527–12,539, 2001.

Mauzerall, D. L., J. A. Logan, D. J. Jacob, B. E. Anderson, D. R. Blake, J. D. Bradshaw, B. Heikes, G. W. Sachse, H. Singh, and R. Talbot, Photochemistry in biomass burning plumes and implications for tropospheric ozone over the tropical South Atlantic, *J. Geophys. Res.*, *103*, 8401–8423, 1998.

McKenzie, L. M., W. M. Hao, G. N. Richards, and D. E. Ward, Measurement and modeling of air toxins from smoldering combustion of biomass, *Environ. Sci. Technol.*, *29*, 2047–2054, 1995.

McMillan, W. W., et al., Tropospheric carbon monoxide measurements from the Scanning High-Resolution Interferometer Sounder on 7 September 2002 in southern Africa during SAFARI 2000, *J. Geophys. Res.*, *108*, doi:10.1029/2002JD002335, in press, 2003.

Olson, J., et al., Results from the Intergovernmental Panel on Climatic Change photochemical model intercomparison (PhotoComp), *J. Geophys. Res.*, *102*, 5979–5991, 1997.

Ravishankara, A. R., and C. A. Longfellow, Reactions on tropospheric condensed matter, *Phys. Chem. Chem. Phys.*, *1*, 5433–5441, 1999.

Reid, J. S., P. V. Hobbs, R. F. Ferek, D. Blake, J. V. Martins, M. R. Dunlop, and C. Lioussc, Physical, chemical, and optical properties of regional hazes dominated by smoke in Brazil, *J. Geophys. Res.*, *103*, 32,059–32,080, 1998.

Richardson, J. L., J. Fishman, and G. L. Gregory, Ozone budget over the Amazon: Regional effects from biomass burning emissions, *J. Geophys. Res.*, *96*, 13,073–13,087, 1991.

Rinsland, C. P., E. Mahieu, R. Zander, P. Demoulin, J. Forrer, and B. Buchmann, Free tropospheric CO, C_2H_6, and HCN above central Europe: Recent measurements from the Jungfraujoch station including the detection of elevated columns during 1998, *J. Geophys. Res.*, *105*, 24,235–24,249, 2000.

Schmid, B., et al., Coordinated airborne, space borne, and ground-based measurements of massive, thick aerosol layers during the dry season in South Africa, *J. Geophys. Res.*, *108*, doi:10.1029/2002JD002297, in press, 2003.

Shea, R. W., B. W. Shea, J. B. Kauffman, D. E. Ward, C. I. Haskins, and M. C. Scholes, Fuel biomass and combustion factors associated with fires in savanna ecosystems of South Africa and Zambia, *J. Geophys. Res.*, *101*, 23,551–23,568, 1996.

Singh, H. B., M. Kanakidou, P. J. Crutzen, and D. J. Jacob, High concentrations and photochemical fate of oxygenated hydrocarbons in the global troposphere, *Nature*, *378*, 50–54, 1995.

Singh, H. B., et al., Impact of biomass burning emissions on the composition of the South Atlantic troposphere: Reactive nitrogen and ozone, *J. Geophys. Res.*, *101*, 24,203–24,220, 1996.

Singh, H. B., et al., Distribution and fate of selected oxygenated organic species in the troposphere and lower stratosphere over the Atlantic, *J. Geophys. Res.*, *103*, 3795–3805, 2000.

Sinha, P., P. V. Hobbs, R. J. Yokelson, I. T. Bertschi, D. R. Blake, I. J. Simpson, S. Gao, T. W. Kirchstetter, and T. Novakov, Emissions of trace gases and particles from savanna fires in southern Africa, *J. Geophys. Res.*, *108*, doi:10.1029/2002JD002325, in press, 2003a.

Sinha, P., P. V. Hobbs, R. J. Yokelson, T. J. Christian, T. W. Kirchstetter, and R. Bruintjes, Emissions of trace gases and particles from two ships in the southern Atlantic Ocean, *Atmos. Environ.*, in press, 2003b.

Stith, J. L., L. F. Radke, and P. V. Hobbs, Particle emissions and the production of ozone and nitrogen oxides from the burning of forest slash, *Atmos. Environ.*, *15*, 73–82, 1981.

Stocks, B. J., B. W. van Wilgen, W. S. W. Trollope, D. J. McRae, J. A. Mason, F. Weirich, and A. L. F. Potgieter, Fuels and fire behavior dynamics on large-scale savanna fires in Kruger National Park, South Africa, *J. Geophys. Res.*, *101*, 23,541–23,550, 1996.

Susott, R. A., G. J. Olbu, S. P. Baker, D. E. Ward, J. B. Kauffman, and R. Shea, Carbon, hydrogen, nitrogen, and thermogravimetric analysis of tropical ecosystem biomass, in *Biomass Burning and Global Change*, edited by J. S. Levine, pp. 350–360, MIT Press, Cambridge, Mass., 1996.

Swap, R., M. Garstang, S. A. Macko, P. D. Tyson, W. Maenhaut, P. Artaxo, P. Kallberg, and R. Talbot, The long-range transport of southern African aerosols to the tropical South Atlantic, *J. Geophys. Res.*, *101*, 23,777–23,792, 1996.

Talbot, R. W., K. M. Beecher, R. C. Harriss, and W. R. Cofer III, Atmospheric geochemistry of formic and acetic acids at a mid-latitude temperate site, *J. Geophys. Res.*, *93*, 1638–1652, 1988.

Talbot, R. W., et al., Chemical characteristics of continental outflow over the tropical South Atlantic Ocean from Brazil and Africa, *J. Geophys. Res.*, *101*, 24,187–24,202, 1996.

Thompson, A. M., K. E. Pickering, D. P. McNamara, M. R. Schoeberl, R. D. Hudson, J. H. Kim, E. V. Browell, V. W. J. H. Kirchhoff, and D. Nganga, Where did tropospheric ozone over southern Africa and the tropical Atlantic come from in October 1992? Insights from TOMS, GTE TRACE A, and SAFARI 1992, *J. Geophys. Res.*, *101*, 24,251–24,278, 1996.

Trollope, W. S. W., L. A. Trollope, A. L. F. Potgieter, and N. Zambatis, SAFARI-92 characterization of biomass and fire behavior in the small experimental burns in the Kruger National Park, *J. Geophys. Res.*, *101*, 23,531–23,540, 1996.

Ward, D. E., and L. F. Radke, Emissions measurements from vegetation fires: A comparative evaluation of methods and results, in *Fire in the Environment: The Ecological, Atmospheric and Climatic Importance of Vegetation Fires*, edited by P. J. Crutzen and J. G. Goldammer, pp. 53–76, John Wiley, New York, 1993.

Ward, D. E., R. A. Susott, J. B. Kauffman, R. E. Babbitt, D. L. Cummings, B. Dias, B. N. Holben, Y. J. Kaufman, R. A. Rasmussen, and A. W. Setzer, Smoke and fire characteristics for cerrado and deforestation burns in Brazil: BASE-B Experiment, *J. Geophys. Res.*, *97*, 14,601–14,619, 1992.

Ward, D. E., W. M. Hao, R. A. Susott, R. A. Babbitt, R. W. Shea, J. B. Kauffman, and C. O. Justice, Effect of fuel composition on combustion efficiency and emission factors for African savanna ecosystems, *J. Geophys. Res.*, *101*, 23,569–23,576, 1996.

Webster, C. R., R. D. May, C. A. Trimble, R. G. Chave, and J. Kendall, Aircraft (ER-2) laser infrared absorption spectrometer (ALIAS) for in situ stratospheric measurements of HCl, N_2O, CH_4, NO_2, and HNO_3, *Appl. Opt.*, *33*, 454–472, 1994.

Worden, H., R. Beer, and C. P. Rinsland, Airborne infrared spectroscopy of 1994 western wildfires, *J. Geophys. Res.*, *102*, 1287–1299, 1997.

Yokelson, R. J., and I. T. Bertschi, Vibrational spectroscopy in the study of fires, in *Handbook of Vibrational Spectroscopy*, vol. 4, edited by J. M. Chalmers, and P. R. Griffiths, pp. 2879–2886, John Wiley, New York, 2002.

Yokelson, R. J., D. W. T. Griffith, and D. E. Ward, Open-path Fourier transform infrared studies of large-scale laboratory biomass fires, *J. Geophys. Res.*, *101*, 21,067–21,080, 1996.

Yokelson, R. J., D. E. Ward, R. A. Susott, J. Reardon, and D. W. T. Griffith, Emissions from smoldering combustion of biomass measured by open-path Fourier transform infrared spectroscopy, *J. Geophys. Res.*, *102*, 18,865–18,877, 1997.

Yokelson, R. J., D. W. T. Griffith, R. A. Susott, and D. E. Ward, Spectroscopic studies of biomass fire emissions, in *Proceedings of the 13th Conference on Fire and Forest Meteorology*, vol. 1, pp. 183–196, Int. Assoc. of Wildland Fire, Fairfield, Wash., 1998.

Yokelson, R. J., J. G. Goode, I. Bertschi, R. A. Susott, R. E. Babbitt, D. E. Ward, W. M. Hao, D. D. Wade, and D. W. T. Griffith, Emissions of formaldehyde, acetic acid, methanol, and other trace gases from biomass fires in North Carolina measured by airborne Fourier transform infrared spectroscopy (AFTIR), *J. Geophys. Res.*, *104*, 30,109–30,125, 1999.

I. T. Bertschi, Interdisciplinary Arts and Sciences, University of Washington-Bothell, Bothell, WA 59812, USA.

T. J. Christian and R. J. Yokelson (corresponding author), Department of Chemistry, University of Montana, Missoula, MT 59807, USA. (byok@selway.umt.edu)

W. M. Hao, Fire Sciences Laboratory, USDA Forest Service, Missoula, MT 59807, USA.

P. V. Hobbs, Department of Atmospheric Sciences, University of Washington, Seattle, WA 98195, USA.

D. E. Ward, Enviropyronics, LLC, P.O. Box 968, White Salmon, WA 59807, USA.